



# UPDATED REGIONAL TECHNOLOGY IMPLEMENTATION PLAN FOR ZAMA

## Plains CO<sub>2</sub> Reduction (PCOR) Partnership Phase III Task 15 – Deliverable D86

*Prepared for:*

Andrea M. Dunn

National Energy Technology Laboratory  
U.S. Department of Energy  
626 Cochrans Mill Road  
PO Box 10940  
Pittsburgh, PA 15236-0940

DOE Cooperative Agreement No. DE-FC26-05NT42592

*Prepared by:*

Panqing Gao  
James A. Sorensen  
Jason R. Braunberger  
Thomas E. Doll  
Steven A. Smith  
Charles D. Gorecki  
Steven B. Hawthorne  
Edward N. Steadman  
John A. Harju

Energy & Environmental Research Center  
University of North Dakota  
15 North 23rd Street, Stop 9018  
Grand Forks, ND 58202-9018

2014-EERC-05-14

February 2014  
Approved

## **EERC DISCLAIMER**

LEGAL NOTICE This research report was prepared by the Energy & Environmental Research Center (EERC), an agency of the University of North Dakota, as an account of work sponsored by the U.S. Department of Energy (DOE) National Energy Technology Laboratory (NETL). Because of the research nature of the work performed, neither the EERC nor any of its employees makes any warranty, express or implied, or assumes any legal liability or responsibility for the accuracy, completeness, or usefulness of any information, apparatus, product, or process disclosed or represents that its use would not infringe privately owned rights. Reference herein to any specific commercial product, process, or service by trade name, trademark, manufacturer, or otherwise does not necessarily constitute or imply its endorsement or recommendation by the EERC.

## **ACKNOWLEDGMENT**

This material is based upon work supported by DOE NETL under Award Number DE-FC26-05NT42592.

## **DOE DISCLAIMER**

This report was prepared as an account of work sponsored by an agency of the United States Government. Neither the United States Government, nor any agency thereof, nor any of their employees, makes any warranty, express or implied, or assumes any legal liability or responsibility for the accuracy, completeness, or usefulness of any information, apparatus, product, or process disclosed, or represents that its use would not infringe privately owned rights. Reference herein to any specific commercial product, process, or service by trade name, trademark, manufacturer, or otherwise does not necessarily constitute or imply its endorsement, recommendation, or favoring by the United States Government or any agency thereof. The views and opinions of authors expressed herein do not necessarily state or reflect those of the United States Government or any agency thereof.

## **NDIC DISCLAIMER**

This report was prepared by the EERC pursuant to an agreement partially funded by the Industrial Commission of North Dakota, and neither the EERC nor any of its subcontractors nor the North Dakota Industrial Commission (NDIC) nor any person acting on behalf of either:

(A) Makes any warranty or representation, express or implied, with respect to the accuracy, completeness, or usefulness of the information contained in this report or that the use of any information, apparatus, method, or process disclosed in this report may not infringe privately owned rights; or



(B) Assumes any liabilities with respect to the use of, or for damages resulting from the use of, any information, apparatus, method, or process disclosed in this report.

Reference herein to any specific commercial product, process, or service by trade name, trademark, manufacturer, or otherwise does not necessarily constitute or imply its endorsement, recommendation, or favoring by the North Dakota Industrial Commission. The views and opinions of authors expressed herein do not necessarily state or reflect those of the North Dakota Industrial Commission.

## TABLE OF CONTENTS

LIST OF FIGURES .....	iii
LIST OF TABLES .....	vii
EXECUTIVE SUMMARY .....	viii
INTRODUCTION .....	1
Background Discussion of Zama .....	2
Nature of the Data Used for Zama Modeling.....	4
Overview of the Geology of the Zama Oil Field .....	5
WORK TO ADDRESS WELLBORE INTEGRITY ISSUES .....	7
Reaction Experiments on Zama Reservoir Rock .....	11
Sample Description and Methods of Analysis .....	12
Discussion of Results from Geochemical Reaction Experiments .....	14
Rock Sample Analysis Results .....	14
Brine Sample Analysis Results.....	14
Discussion of the Rock-Based Geochemical Reaction Experimental Results .....	16
Reaction Experiments on Wellbore Cement.....	18
Discussion of Cement Studies .....	19
Cement Studies Conclusions .....	21
BASIC CASING CORROSION-TESTING EXPERIMENTS .....	21
Sample Description and Methods of Analysis .....	21
Steel Casing Reaction Studies .....	23
Discussion of Results from Casing Corrosion-Testing Experiments.....	23
Summary of Key Findings of Casing Corrosion-Testing Experiments .....	25
RESERVOIR MODELING FOR EOR AND STORAGE PURPOSES .....	25
Geologic Modeling.....	27
Stratigraphic Framework .....	31
Petrophysical Analysis.....	32
Structural Model .....	37
Facies Modeling.....	38
Petrophysical Property Modeling .....	39
Volumetrics.....	39
Production Analysis .....	41
F Pool Production .....	41
Muskeg L.....	49
G2G Production.....	50
PVT Modeling.....	51

Continued. . .

## TABLE OF CONTENTS (continue)

Simulator and EOS .....	51
Minimum Miscibility Pressure .....	54
Effect of H <sub>2</sub> S on MMP .....	56
Effect of Pressure Depletion on MMP.....	56
History-Matching Process .....	58
Approaches .....	58
Results.....	58
F Pool Prediction .....	61
Formation Water Extraction Assisted by Acid Gas Injection .....	61
Future EOR and Storage Capacity Potential .....	65
Current EOR Configuration with Bottom Water Extraction Well .....	66
G2G and Muskeg L Prediction.....	69
Case Design .....	69
Results and Discussion .....	70
CO <sub>2</sub> STORAGE EFFICIENCY IN ZAMA REEFS .....	72
Real-Time Injection.....	72
Simulation Prospections .....	72
F Pool.....	72
G2G Pool .....	73
Muskeg L Pool.....	74
Sensitivity Analysis.....	74
Storage Capacity and Efficiency Evaluation.....	75
KEY OBSERVATIONS AND CONCLUSIONS .....	76
ACKNOWLEDGMENTS .....	79
REFERENCES .....	79
MINERALOGICAL COMPOSITION AND FLUID ANALYSIS DATA FROM ROCK REACTIVITY EXPERIMENTS.....	Appendix A
ZAMA STEEL CASING HIGH-PRESSURE AND -TEMPERATURE BATCH REACTOR EXPERIMENTAL RESULTS.....	Appendix B

## LIST OF FIGURES

1	AGS ERCB Zama geological and hydrogeological study area.....	6
2	AGS ERCB simplified paleogeography of the Keg River carbonate .....	7
3	AGS ERCB Zama subbasin field area .....	8
4	AGS ERCB northeastern Alberta stratigraphic and hydrostratigraphic section .....	9
5	AGS ERCB Zama and Shekilie Basin stratigraphic cross section.....	10
6	Zama and Shekilie Basin schematic diagram.....	11
7	Examples of Zama core plug samples used in the rock experiments.....	13
8	Photographs and schematic of a batch reactor used to test the reactivity of rock, cement, and steel samples exposed to CO <sub>2</sub> and a mixture of CO <sub>2</sub> –H <sub>2</sub> S under Zama reservoir conditions .....	13
9	Examples of mineralogy based on XRD for Zama rock samples before and after exposure to CO <sub>2</sub> .....	15
10	Cation concentrations by fluid sample, showing higher reactivity with CO <sub>2</sub> and brine .....	16
11	TDS of brine solutions after rocks (Plugs 1–6) and brine were exposed to CO <sub>2</sub> and CO <sub>2</sub> –H <sub>2</sub> S for 28 days at Zama reservoir temperature and pressure .....	17
12	Optical images of Class H neat cement submerged in a solution saturated with CO <sub>2</sub> only (a and b) and CO <sub>2</sub> –H <sub>2</sub> S (c and d) at 122°F and 2176 psi for 28 days .....	20
13	SEM BSE images showing pyrite (bright spots) within the carbonated region of cement exposed to CO <sub>2</sub> –H <sub>2</sub> S.....	22
14	Optical microscopy (400×) images of steel coupons after exposure to CO <sub>2</sub> and CO <sub>2</sub> –H <sub>2</sub> S in brine and low-TDS water.....	23
15	Steel coupons after exposure to CO <sub>2</sub> in brine and CO <sub>2</sub> –H <sub>2</sub> S in brine .....	24
16	Mass differences between casing material coupons as measured before and after exposure to pure CO <sub>2</sub> and CO <sub>2</sub> combined with H <sub>2</sub> S under both water and brine .....	26

Continued. . .

## LIST OF FIGURES (continued)

17	Concentrations of manganese in water and brine for each of the seven studied casing metals and a control for each of the exposure conditions .....	26
18	Concentrations of iron in water and brine for each of the seven studied casing metals and a control for each of the exposure conditions .....	27
19	Coupon of 5LX65 steel before and after exposure to CO <sub>2</sub> and tap water .....	28
20	Structural surfaces for the G2G model.....	31
21	Structural surfaces for the Muskeg L model .....	32
22	Generic structural framework for the models .....	33
23	Depth shift of the core data to match with wireline logs.....	34
24	Porosity derived from the neural network approach .....	35
25	QC of the neural network-derived porosity.....	36
26	Histogram showing bimodal distribution of porosity due to interparticle and vuggy/fractured porosity .....	37
27	Presence of the vuggy component in the reservoir porosity .....	38
28	Vuggy reefal carbonate of North Dakota Devonian Winnipegosis Formation .....	39
29	Resulting permeability log .....	40
30	Crossplot between core porosity and core permeability to identify microfacies within the reef.....	41
31	Petrophysical logs that were populated into each static model .....	42
32	Well section example showing calculated petrophysical logs as correlated to the upscaled logs .....	43
33	Conceptual geology of a pinnacle reef, training image from the conceptual geology and microfacies model of Muskeg L reef.....	44

Continued. . .

## LIST OF FIGURES (continued)

34	Regression equation for good-quality reservoir and poor-quality reservoir used as trend in petrophysical modeling of the permeability property .....	45
35	Petrophysical models of pinnacle Muskeg L for porosity, permeability, and water saturation .....	46
36	F pool geology and development schematic .....	47
37	Keg River F pool, Phase 1, Apache Canada .....	47
38	Production rate of oil, gas, and water from the G2G pool .....	50
39	Cumulative production of oil, gas, and water from the G2G pool .....	51
40	Regression on GOR and oil formation volume factor for G2G pool .....	55
41	Regression on GOR and oil formation volume factor for Muskeg L pool .....	55
42	H <sub>2</sub> S effect on CO <sub>2</sub> MMP .....	57
43	History match of cumulative oil production for the G2G pool .....	59
44	History match of liquid rate for the G2G pool .....	59
45	History match of oil rate for the G2G pool .....	60
46	History match of water cut for the G2G pool .....	60
47	History match of cumulative liquid production for the Muskeg L pool .....	61
48	History match of cumulative oil production for the Muskeg L pool .....	62
49	History match of oil production rate for the Muskeg L pool .....	62
50	History match of water cut for the Muskeg L pool .....	63
51	History match of cumulative production for the F pool .....	63
52	History match of BHP for the F pool .....	64

Continued. . .

## **LIST OF FIGURES (continued)**

53	History-matching results for cumulative oil, gas, and water production and simulated and measured well BHP .....	67
54	Field oil recovery (current EOR configuration with bottom water extraction well) and cumulative amounts of injected and produced CO <sub>2</sub> (current EOR configuration with bottom water extraction well) .....	68
55	Reservoir pressure behavior (current EOR configuration with bottom water extraction well) and cross-sectional view of gas saturation (current EOR configuration with bottom water extraction well) .....	69
56	Injected acid gas composition over time for six pinnacles.....	73

## LIST OF TABLES

1	OOIP Estimates of Six Pools .....	5
2	Zama Reservoir-Modeling Workflow .....	29
3	Static Model Parameters.....	42
4	Base-Case Volumetrics .....	47
5	F Pool Properties .....	49
6	Summary of Production and Injection for Five Pools.....	52
7	Compositional Data of All Five Pinnacles .....	54
8	Predictive Simulation Results .....	68
9	Case Design for G2G and Muskeg L .....	70
10	Average Compositions of Four Components .....	73
11	Injected CO <sub>2</sub> in All Six Pools.....	73
12	CO <sub>2</sub> Utilization Factor and Recovery Contribution Based on Simulation Predictions .....	76
13	Estimates on CO <sub>2</sub> Storage Capacities for Three Extra Pools .....	76





## **UPDATED REGIONAL TECHNOLOGY IMPLEMENTATION PLAN FOR ZAMA**

### **EXECUTIVE SUMMARY**

Since December 2006, the Zama oil field in northwestern Alberta, Canada, has been the site of acid gas (approximately 70% carbon dioxide (CO<sub>2</sub>) and 30% hydrogen sulfide [H<sub>2</sub>S]) injection for the simultaneous purpose of enhanced oil recovery (EOR), acid gas disposal, and CO<sub>2</sub> storage. Plains CO<sub>2</sub> Reduction (PCOR) Partnership Phase III activities were designed and conducted to build upon knowledge gained in Phase II, including laboratory studies of the effects of acid gas on storage integrity and modeling efforts to develop improved predictions of both oil recovery and CO<sub>2</sub> storage capacity at Zama.

Previous geochemical modeling work conducted under Phase II indicated that reactions between Zama-type acid gas and typical Zama reservoir rocks can lead to varying degrees of both dissolution and precipitation. The Phase III program included laboratory experimental activities to directly examine geochemical interactions between Zama reservoir rocks, brine, pure CO<sub>2</sub>, and CO<sub>2</sub>-H<sub>2</sub>S under Zama reservoir pressure and temperature conditions. No clear differences were observed between the preexposure and postexposure mineralogy. However, the applicability of these results may be limited because the rock samples that were available for these efforts were all limestones and there can be significant quantities of dolomite in the Zama pinnacle reefs. Also, the experiments were of a short duration (28 days) and static. Longer-duration experiments that incorporate more variables may be more appropriate for assessing the interactions between acid gas and a carbonate reservoir.

While the rock analysis data may have limited applicability, some insight may be gained from the evaluation of changes in the composition of the fluids in which the rocks were immersed during the experiments. A clear decrease in the reactivity of both calcium and sulfate was observed in the samples exposed to the H<sub>2</sub>S-rich gas stream. Also, measurements of total dissolved solids (TDS) data indicate that CO<sub>2</sub>-H<sub>2</sub>S dissolved a lesser quantity of total mineral content. From the perspective of storage integrity, this lower mineral loss will presumably correspond to minimal loss of structural integrity of the formation. These results suggest that the presence of H<sub>2</sub>S may actually reduce the reactivity of some carbonate rocks, thereby possibly serving to maintain reservoir and wellbore integrity rather than degrade it.

The effects that acid gas streams may have on wellbore cement were examined by exposing cement cores to pure CO<sub>2</sub> and CO<sub>2</sub>-H<sub>2</sub>S mixtures under Zama reservoir conditions. The

studies used Class H portland cement, which is typically used on acid gas injection/production wells. The addition of  $\text{H}_2\text{S}$  to the  $\text{CO}_2$  storage system resulted in the formation of ettringite throughout the cement and precipitation of pyrite in the carbonated rim. Both phenomena can potentially lead to degradation of cement integrity. However, the experimental results also indicated that  $\text{CO}_2$  in the system may dissolve the ettringite and reprecipitate calcium carbonates that may help improve the overall cement integrity.

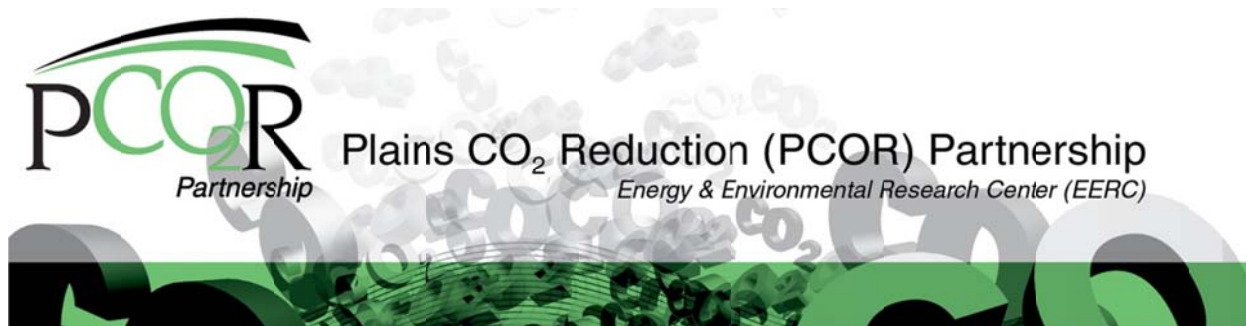
The effects of corrosion on seven well casing steels, when exposed to  $\text{CO}_2$  and acid gas under typical Zama reservoir conditions, were evaluated. The highest level of corrosion was observed in steels that were submerged in high-TDS water and exposed to pure  $\text{CO}_2$ . Corrosion rates from tests that included  $\text{H}_2\text{S}$  were consistently lower than those that included pure  $\text{CO}_2$ , with higher corrosive mass loss appearing in all samples reacted with pure  $\text{CO}_2$ . However, a significant amount of sulfur was found on the surfaces of samples exposed to  $\text{CO}_2$ – $\text{H}_2\text{S}$  mixtures. While pitting was observed in all of the samples, it was more severe in cases of pure  $\text{CO}_2$  exposure as compared to  $\text{CO}_2$ – $\text{H}_2\text{S}$ . As with the rock studies, these results appear to suggest that, in some circumstances, the presence of  $\text{H}_2\text{S}$  may actually serve to counteract the effects of  $\text{CO}_2$ , helping to maintain wellbore integrity rather than contributing to its degradation.

PVT (pressure–volume–temperature) modeling work was performed to investigate the effect of  $\text{H}_2\text{S}$  and varying gas–oil ratios (GOR) on minimum miscible pressure (MMP). The results indicate that MMP decreased nearly linearly with increasing levels of  $\text{H}_2\text{S}$  in the injection gas dropping from 2660 psi with pure  $\text{CO}_2$  to 2020 psi with 20 mol%  $\text{H}_2\text{S}$  in the G2G pool. Likewise, when the GOR was reduced from 414 to 200 scf/bbl, the simulated MMP dropped from 2660 psi to 1950 psi. These results indicate that it is important to consider both the components of the injected gas and the GOR of the current oil when estimating the MMP.

Modeling-based investigations of different operational scenarios yielded insight regarding the  $\text{CO}_2$  sweep efficiency, possible injection and production schemes, EOR potential, and  $\text{CO}_2$  storage capacity for Zama pinnacles. Static models of three of the six additional pinnacles were used to conduct dynamic simulations of various combinations of acid gas injection, EOR, and water extraction. The predicted storage capacity from simulation of the three individual pinnacles ranged from 0.18 million tons (MMt) to 1.22 MMt of  $\text{CO}_2$ , with the average storage capacity of the three pinnacles being nearly 0.4 MMt. Assuming the 840 other pinnacle reefs in the Zama Field have similar storage capacity, the  $\text{CO}_2$  storage capacity may be nearly 334 MMt. With respect to EOR potential, results indicate acid gas EOR may yield an additional 6.2% to 15.6% of the original oil in place. The simulated  $\text{CO}_2$  utilization factor results for the modeled Zama pools averaged approximately 0.62 tons/bbl or 11 Mscf/bbl.

Overall, the laboratory results indicate that the injection of a  $\text{CO}_2$ – $\text{H}_2\text{S}$  mixed-gas stream into a carbonate formation for EOR and  $\text{CO}_2$  storage is not likely to be more deleterious to wellbore integrity than the injection of pure  $\text{CO}_2$ . In fact, it appears that under some circumstances, the presence of  $\text{H}_2\text{S}$  may actually help maintain wellbore integrity against degradation from  $\text{CO}_2$ . These observations are supported by the fact that industrial-scale acid gas injection projects have been conducted in Alberta for over 20 years with no reported breaches in the wellbore integrity of acid gas injection wells. The modeling results confirm that miscible flooding with sour acid gas is an excellent means of storing large volumes of  $\text{CO}_2$  while improving oil recovery. There are hundreds of pinnacle reefs throughout the world that hold in

excess of 1 million barrels of oil each. The results of the PCOR Partnership research activities at Zama indicate that, globally, pinnacle reef structures represent an excellent opportunity to recover millions of barrels of incremental oil through CO<sub>2</sub>-based EOR and also have a great potential to perhaps store billions of tons of CO<sub>2</sub>. The results also indicate that CO<sub>2</sub> streams do not have to be “pure” to be considered for use in carbon capture, utilization, and storage projects and that some impurities may even be desirable under certain circumstances.



## **UPDATED REGIONAL TECHNOLOGY IMPLEMENTATION PLAN FOR ZAMA**

### **INTRODUCTION**

Since December 2006, the Zama oil field in northwestern Alberta, Canada, has been the site of acid gas (approximately 70% carbon dioxide [CO<sub>2</sub>] and 30% hydrogen sulfide [H<sub>2</sub>S]) injection for the simultaneous purpose of enhanced oil recovery (EOR), H<sub>2</sub>S disposal, and CO<sub>2</sub> storage. Apache Canada Ltd. (Apache Canada) is the owner/operator of the oil field and the nearby natural gas-processing plant that supplies the acid gas and, as such, has conducted the injection and hydrocarbon recovery processes at Zama. In close cooperation with Apache Canada, the Plains CO<sub>2</sub> Reduction (PCOR) Partnership has conducted site characterization, modeling, and monitoring, verification, and accounting (MVA) activities at the site throughout this period. This project has been conducted as part of the U.S. Department of Energy (DOE) National Energy Technology Laboratory (NETL) Regional Carbon Sequestration Partnership Program and has been recognized by the Carbon Sequestration Leadership Forum as being uniquely able to fill technological gaps with regard to geological storage of CO<sub>2</sub>.

The PCOR Partnership Program has been conducted over the course of three distinct phases. Phase I was a 2-year effort initiated in late 2003, primarily focused on regional-scale characterization of industrial CO<sub>2</sub> sources and potential geological and terrestrial storage opportunities. One of the key findings of Phase I was that natural gas-processing plants in close proximity to oil fields would be good candidate locations for carbon capture and storage (CCS) projects. Phase II was a 4-year effort conducted from 2005 to 2009 that included several field-based projects to evaluate CCS approaches, including the injection of CO<sub>2</sub>-rich acid gas from a gas-processing plant into an oil reservoir near Zama, Alberta, Canada. One of the primary products of the Phase II efforts was a Regional Technology Implementation Plan (RTIP) that presented and discussed the results of the site characterization and MVA efforts at Zama (Smith and others, 2009). Although Phase II of the PCOR Partnership ended in 2009, Apache Canada continued the injection operations at Zama as part of its commercial operations of the gas-processing plant and oil field and, in fact, expanded the injection operations to include additional reservoirs in the Zama Field. Phase III of the PCOR Partnership, which began in 2007 and is scheduled to run until 2017, is focused on large-scale commercial demonstrations of storage in geologic sinks. With Apache Canada planning to continue its commercial injection operations beyond 2017, the opportunity existed for the PCOR Partnership to include Zama-related activities as part of its Phase III program. Phase III activities were designed to build upon the results presented in the Phase II RTIP (Smith and others, 2009), including laboratory studies of the effects of acid gas on storage integrity and modeling efforts to develop improved predictions

of both oil recovery and CO<sub>2</sub> storage capacity at Zama. This report presents and discusses the primary Zama-related PCOR Partnership Phase III activities and the key results and lessons learned from those activities.

## **Background Discussion of Zama**

In the implementation of CCS initiatives, it is important to ensure that other gaseous components common to emission streams in addition to CO<sub>2</sub> are not overlooked. The majority of CO<sub>2</sub> sources contain other hydrocarbon gas components because it is technically difficult and expensive to isolate CO<sub>2</sub> from typical emission streams. A common term for multicomponent gas streams containing sulfur dioxide (SO<sub>2</sub>), CO<sub>2</sub>, and H<sub>2</sub>S is acid gas. In Alberta and elsewhere, operators have been disposing of acid gas in depleted oil and natural gas reservoirs for at least 20 years. Operations at Zama are currently focused on the injection of acid gas into several oil reservoirs, which at Zama occur as distinct, typically isolated, carbonate pinnacle reef structures capped by a thick layer of impermeable anhydrite. Apache Canada commercially operates the injection activities for the purposes of EOR, acid gas disposal, and CO<sub>2</sub> storage. Acid gas has been obtained from a nearby gas-processing plant as a by-product of oil and gas production in the Zama oil field. After the separation process, oil and gas are sent to market, while acid gas is redirected back to the field for utilization in EOR operations.

The overarching goals of both the Phase II and Phase III PCOR Partnership Zama activities have been to address three primary issues: 1) determination of CO<sub>2</sub> and/or H<sub>2</sub>S vertical migration, or lack thereof, from the pinnacle; 2) development of reliable predictions regarding the long-term fate of injected acid gas; and 3) generation of data sets that will support the development and monetization of carbon credits associated with the geologic storage of CO<sub>2</sub> at the Zama oil field.

To address these issues, in Phase II, a variety of research activities were conducted at multiple scales of investigation in an effort to fully understand the ultimate fate of the injected gas. The results of geological, geomechanical, geochemical, and engineering work have been used to fully describe the injection zone and adjacent strata in an effort to predict the long-term storage potential of this site. Through these activities, confidence in the ability of the Zama oil field to provide long-term containment of injected gas has been achieved (Smith and others, 2009).

Although the Zama oil field includes hundreds of individual pinnacle reef reservoirs, Phase II MVA activities at Zama were focused on injection at a single pinnacle reef reservoir, referred to operationally as the F pool. Monitoring the F pool site has been (and continues to be) conducted primarily through fluid sampling and pressure monitoring in both the target pinnacle reef and overlying strata. A gas-phase perfluorocarbon tracer, designed to mimic the injected gas, has been used in an effort to identify any leakage into overlying stratigraphic horizons. Pressure is also being measured at the injection zone and overlying productive zones to ensure that 1) overpressurization of the target is not occurring and causing undue stress on the overlying cap rock that could potentially lead to failure and 2) out-of-zone migration along wellbore pathways is not occurring. Certifying the integrity of the system has been a critical focus area, with tests being completed on the cap rock and injection zone to determine the nature of potential

geochemical and geomechanical changes that may occur as a result of acid gas exposure under supercritical pressures and temperatures (Smith and others, 2009).

Geological investigations were conducted on the reservoir, local, and regional (subbasinal) scales. Results of these investigations indicate that natural out-of-zone migration of CO<sub>2</sub> from this system is unlikely and regional flow is extremely slow, on the order of thousands to tens of thousands of years to migrate out of the basin. The potential for leakage through existing wellbores was also evaluated and found to be very low. Geomechanical evaluations, including 3-D modeling, were completed on the injection zone and adjacent stratigraphy. This series of tests confirms that the geologic structures that are being utilized are excellent candidates for sequestration. The cap rock is considered to be extremely stable, has extremely low permeability, and is not likely to fracture when subjected to injection pressures well beyond the maximum allowed. Geochemical modeling aids in the understanding of the long-term fate of acid gas injected into carbonate rocks. Evaluations of the Zama system indicate that the impact of mineralization on the overall storage capacity of the system is negligible and will occur very slowly over geologic time scales (Smith and others, 2009).

Continuous injection at the F pool has taken place at a depth of 4900 feet into the carbonate pinnacle reef structure since December 2006. As of September 30, 2009, approximately 58,000 tons of acid gas had been injected into the pinnacle reef, of which approximately 40,000 tons was CO<sub>2</sub>. Incremental oil production from the pinnacle reef over the course of the project, as of September 30, 2009, was approximately 25,000 barrels.

Phase II results indicated that a robust, yet practical, MVA program can be developed. Given the proper geologic setting, MVA activities can be relatively inexpensive and not adversely affect commercial EOR operations. However, there were still questions about the effects of the Zama acid gas stream on wellbore integrity and the ultimate EOR potential and storage capacity of the Zama Field as a whole. Wellbore integrity issues were examined through a series of laboratory-based experiments on the effects of Zama-type acid gas on steels commonly used for well casing, wellbore cements, and Zama reservoir rocks. Static and dynamic simulation modeling efforts were based on data from six pinnacle reefs in the Zama oil field that are currently under acid gas injection for EOR. Those pinnacle reefs (a.k.a. “pools”) are referred to in this report by their Apache Canada operational designations as follows: 1) F, 2) G2G, 3) Muskeg L, 4) NNN, 5) RRR, and 6) Z3Z. While data from all six pinnacles were applied to the Phase III PCOR Partnership activities and storage capacity estimates were generated for all six, three (F, G2G, and Muskeg L) served as the primary focal points of the Phase III efforts. As a part of this evaluation, complex fluid behaviors were studied for both EOR efficiency and long-term storage purposes. A high-resolution heterogeneous geocellular model was constructed for the three primary pinnacles under investigation. Each of these models was run through a high-resolution history-matching exercise, and predictions were developed for EOR potential. Modeling-based investigations of different operational scenarios for using these pinnacles for CO<sub>2</sub> storage were also conducted. These modeling activities yield previously unavailable insight regarding the CO<sub>2</sub> sweep efficiency, possible injection and production schemes, EOR potential, and CO<sub>2</sub> storage capacity for each pinnacle.

## **Nature of the Data Used for Zama Modeling**

Gaps in data, whether they are related to geologic characteristics or operational parameters over time, will introduce uncertainty to a model and possibly lead to unreliable results. The quality of data is also important, as poor-quality data can skew the understanding of a reservoir, thereby leading to additional uncertainty. With this in mind, substantial efforts were made to acquire as many high-quality data as possible with respect to both the geology and operations of the Zama reservoir pinnacles. A wide variety of data were obtained to support the Phase III Zama modeling efforts. Apache Canada was the primary source of the data, although some were obtained from publicly available sources such as published literature and the Alberta Geological Survey (AGS) Energy Resources Conservation Board (ERCB). All data provided by Apache Canada were considered to be confidential. The general types of data that were obtained and applied to the Phase III activities can be categorized according to those that were used for static modeling and those that were used for dynamic modeling.

The static modeling data included the following:

- Well log
- Well deviation
- Raw 3-D seismic SEG-Y data
- Pressure transient study data or reports
- Core analysis data (porosity, permeability, relative permeability, capillary pressure, mineralogy)
- Seismic survey data
- Downhole logs (e.g., formation microimaging, gamma ray, resistivity, neutron density, etc.)
- Drilling and completion data, including workover and formation pressure-testing records

Dynamic modeling of additional pinnacles required the following data:

- Production and injection history
- Completion, perforation, stimulation, and workover records
- Reservoir fluid pressure, volume, temperature (PVT) data
- Relative permeability and capillary pressure data
- Average reservoir pressure
- Reservoir water chemistry
- Injection gas composition data

- Produced gas analysis
- Injection wellhead/bottomhole pressure (BHP)
- Separator operating conditions
- Previous simulation reports
- Tracer data

Seismic survey data were essential to determining the dimensions and general shapes of each of the Zama pinnacles. Apache Canada provided processed and interpreted Keg River seismic depth maps for each of the six study pinnacles, which yielded a 3-D understanding of pinnacle geometry that was applied to the development of accurate static models.

Data related to original-oil-in-place (OOIP), recovery estimates, and production and injection activities were particularly valuable to the modeling activities. In previous research activities, the reserves and reservoir size of Zama pinnacles have been evaluated using volumetric and production approaches. The initial approach was to determine reservoir size volumetrically from seismic mapping, simulation and analogue studies, and initial well-drilling results. Analysis of the production decline data and material balance methods was later used to provide additional estimates of the reservoir volumetric size, OOIP, and oil recovery estimates and to calibrate the volumetric results. The quality of the material balance estimates and production decline analysis is generally considered to be most accurate after roughly 20% of the estimated recoverable reserves have been produced, which is a threshold that appears to have been crossed for all six pinnacles evaluated during this project. The OOIP on the basis of volumetric estimates for each of six pinnacles are listed in Table 1.

Injection and production records are most important to dynamically estimate reservoir and production behavior. For this project, detailed records of injection and production beginning with initial production data for each well were collected for the F, NNN, Muskeg L, Z3Z, G2G, and RRR pinnacles. With regard to acid gas injection, the monthly compositional injectant and productant data were also collected. The analysis of injection and production data for each pinnacle is provided in the Production Analysis section of this report. The data have been formatted for simulation purposes.

### **Overview of the Geology of the Zama Oil Field**

Understanding the geologic characteristics of a reservoir is critical to accurately predicting its ability to safely and securely inject and store large volumes of CO<sub>2</sub> for long periods of time. While the characterization of the Zama pinnacles and their overlying cap rocks are described in detail in the Phase II RTIP (Smith and others, 2009), the results of those characterization activities played a prominent role in conducting the Phase III activities. With that in mind, it is useful to provide a brief overview of the geology of the Zama oil field.

**Table 1. OOIP Estimates of Six Pools**

Pinnacle	Keg River Z3Z	Keg River RRR	Keg River NNN	Keg River G2G	Muskeg L	Keg River F
OOIP, MMStb	2.380	4.700	3.530	3.710	2.700	4.300



The geology of the pinnacle reef structures in the Zama area has become well defined and understood through the process of drilling and completing in excess of 1500 wells within over 860 pinnacles over 40+ years of oil and gas production operations. This significant amount of activity is very advantageous in defining the geologic and reservoir parameters, and it has been concluded that acid gas injection and storage within the Zama Keg River pinnacles is a safe operation and that out-of-zone migration from the reservoirs is unlikely. Balancing this, the large number of vintage well penetrations can be viewed as a significant number of potential leak paths; this wellbore integrity issue is discussed later in this report.

In order to evaluate the potential for long-term containment of the injected acid gas, an in-depth knowledge of the target injection zone and surrounding area is critical. It is important to define the direction and rate of any acid gas or CO<sub>2</sub> movement that may take place within the reservoir and the bounding formations. The Keg River reefs provide high-quality oil production and storage reservoirs, as they contain a high percentage of good to very good permeability (100 to 1000 mD). However, significant variations can occur both vertically and laterally. These reefs are good candidates for CO<sub>2</sub> miscible flooding as they are compact and contain reservoirs with porous sections of up to 300 ft (100 m) in thickness. Based on available data, it seems there is no potential for acid gas leakage through faults and fractures (Burke, 2009).

Figure 1 presents the regional-scale geology and hydrology of the Zama subbasin as compiled by the AGS ERCB on behalf of the PCOR Partnership (Buschkuehle and others, 2007). Figure 2 illustrates the simplified paleogeography of the Keg River carbonate sequence within the Middle Devonian Elk Point Basin in western Canada; open marine shales lie to the northwest

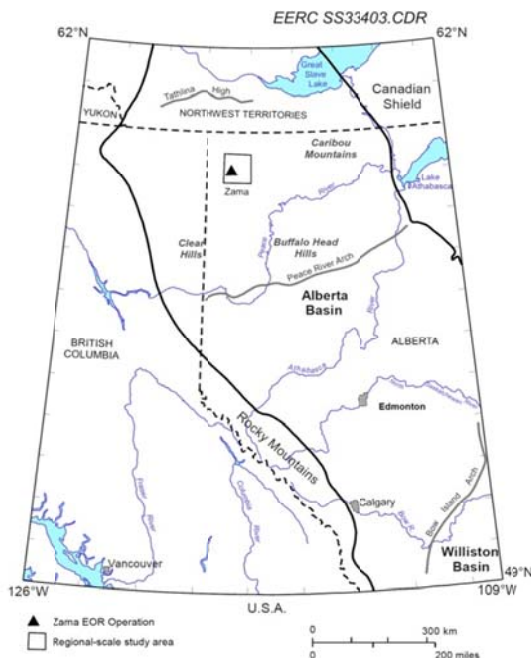


Figure 1. AGS ERCB Zama geological and hydrogeological study area.

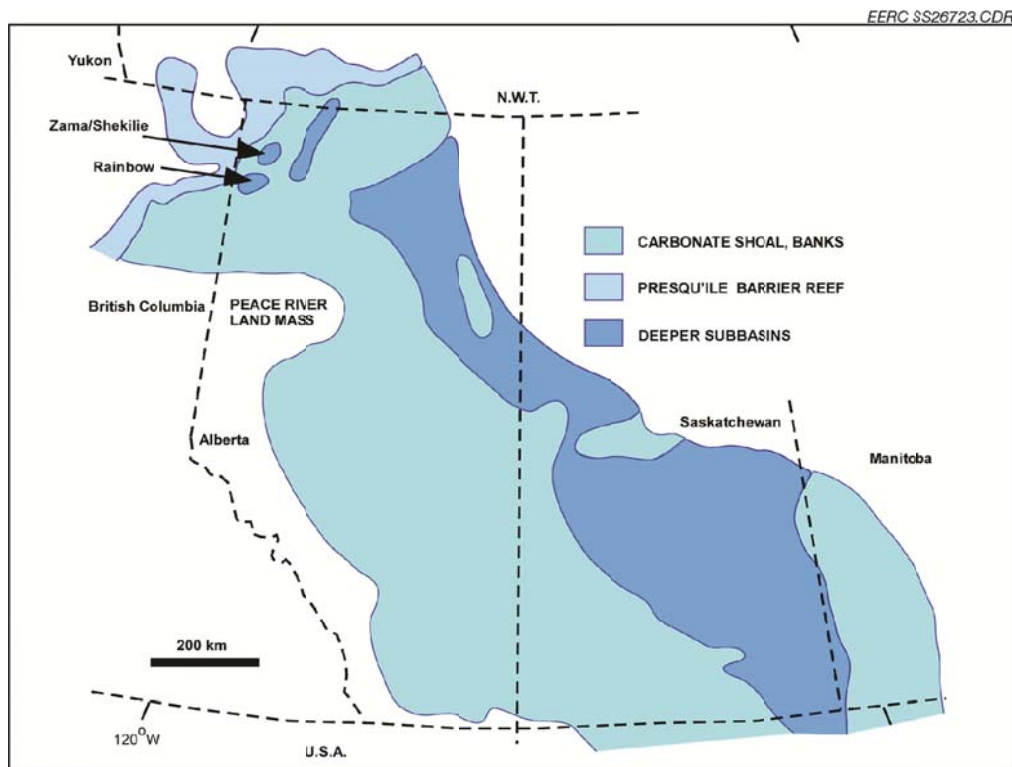


Figure 2. AGS ERCB simplified paleogeography of the Keg River carbonate.

of the Presqu'ile Barrier reef area. Figure 3 locates the Apache acid gas injection sites within the Zama subbasin, and Figure 4 details the stratigraphic and hydrostratigraphic delineation and nomenclature of the northeastern Alberta (Zama) area lithologic section. The sedimentary succession in ascending order from the Precambrian crystalline basement to the surface consists of the Middle and Upper Devonian carbonates, evaporites, and shales; Mississippian carbonates; and Lower Cretaceous shales overlain by Quaternary glacial drift unconsolidated sediments (Buschkuehle and others, 2007).



The Keg River reef buildups were formed in a lagoon partially surrounded by carbonate banks and fronted by the Presqu'ile Barrier to the west; this is illustrated by Figure 5, which is a schematic representation of the Zama Basin pinnacle reef development. To date, over 840 pinnacles have been discovered in the Zama subbasin. On average, these pinnacles cover roughly 40 acres (0.16 km<sup>2</sup>) at the base and are roughly 400 ft (120 m) high, as shown in Figure 6.

## WORK TO ADDRESS WELLBORE INTEGRITY ISSUES

Demonstrating wellbore integrity for CO<sub>2</sub> injection wells is not only important from the standpoint of maintaining cost-effective CCS operations but is also a critical component of showing regulators and the public that drinking water sources and the environment in general can be protected from impacts. This concept is even more important when one of the components of

∞

### Legend

-  Acid Gas Injection
-  Zama EOR Sites
-  Subbasin Boundary
-  Zama Oil Pool Outlines
-  Zama Gas Pool Outlines

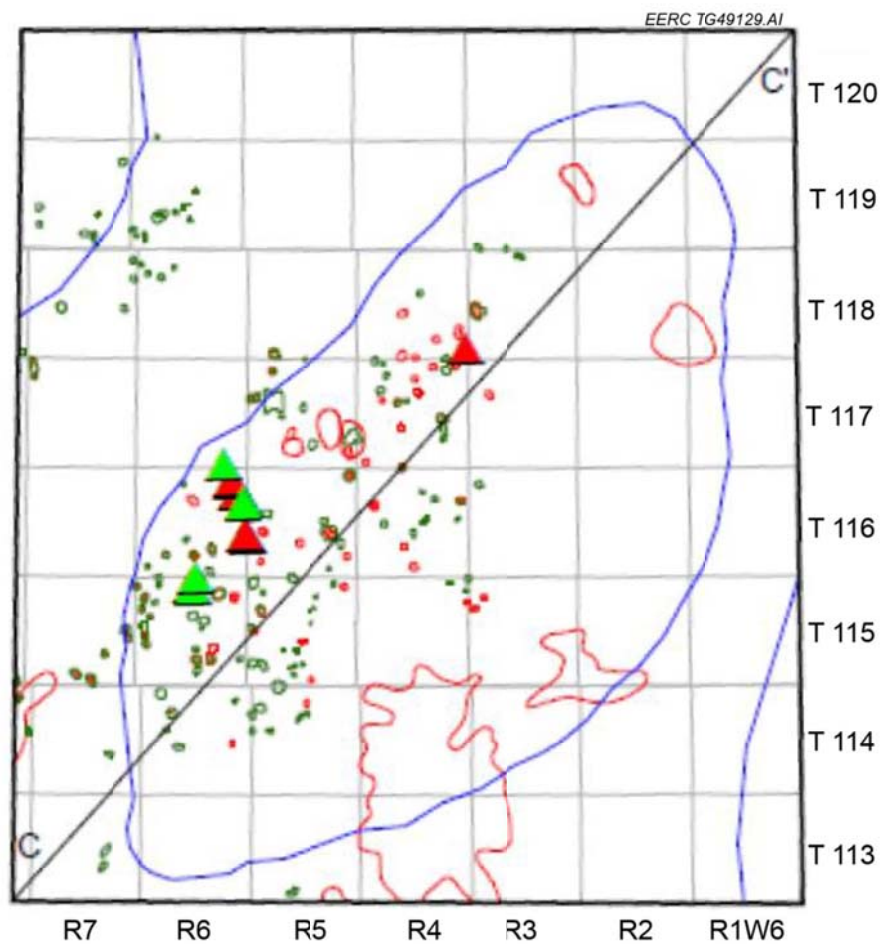
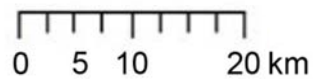


Figure 3. AGS ERCB Zama subbasin field area.

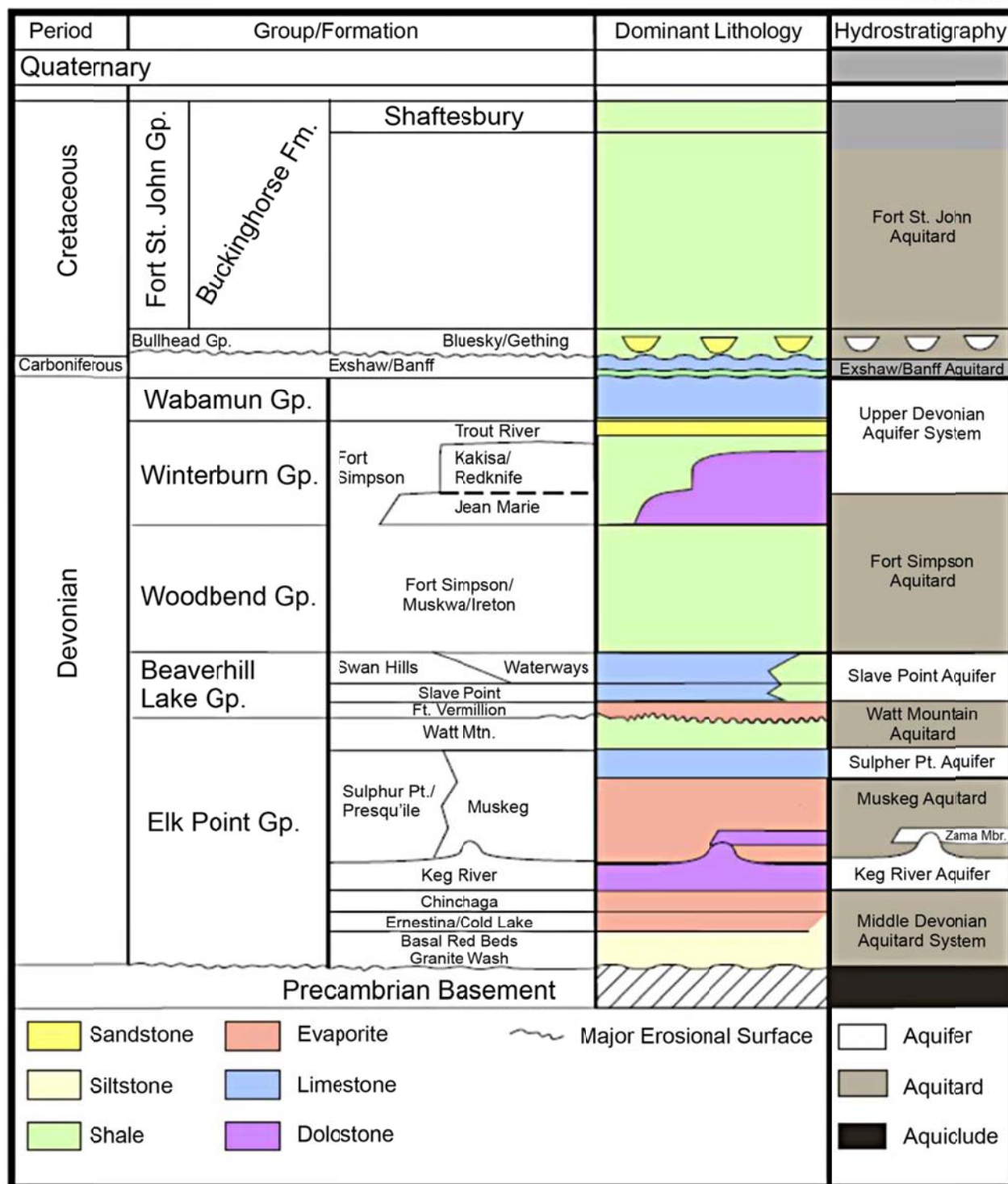
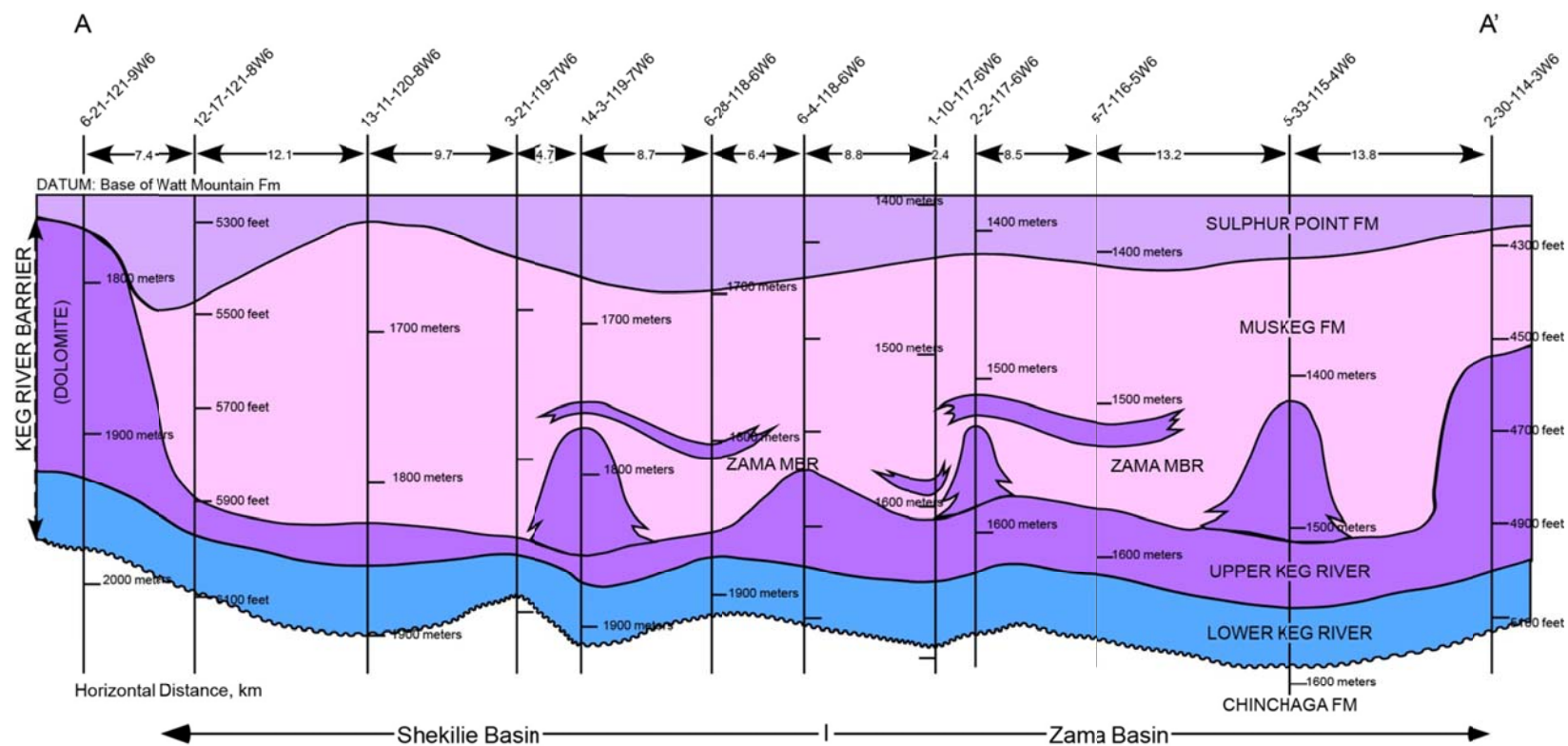


Figure 4. AGS ERCB northeastern Alberta stratigraphic and hydrostratigraphic section.



EERC TG49131.AI

Figure 5. AGS ERCB Zama and Shekilie Basin stratigraphic cross section.



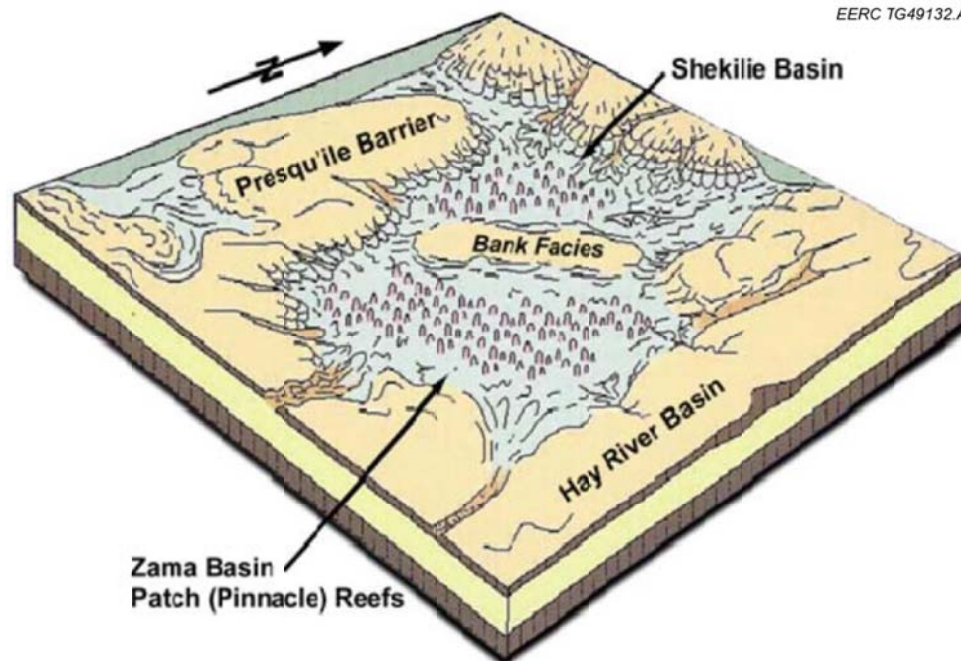


Figure 6. Zama and Shekilie Basin schematic diagram.

the injection stream is  $\text{H}_2\text{S}$ , a highly toxic and corrosive gas. Because the acid gas stream at Zama includes an average of 30%  $\text{H}_2\text{S}$ , a series of laboratory-based activities were conducted to examine the effects of a typical Zama acid gas stream on the three materials that comprise the wellbore in a Zama pinnacle: reservoir rock, cement, and steel casing. The approaches and results of those experimental activities are presented as follows.

### Reaction Experiments on Zama Reservoir Rock

When  $\text{CO}_2$  is injected into deep geologic media (e.g., petroleum reservoirs, non-hydrocarbon-bearing saline formations, etc.) it can interact both physically and chemically with reservoir fluids and rocks. In the literature, these interactions are often referred to as physical and chemical trapping of  $\text{CO}_2$  (Gunter and others, 2004). During physical trapping,  $\text{CO}_2$  retains its physical and chemical structure while in stratigraphic, structural, and capillary traps. Chemical trapping includes solubility, ionic, and mineral trapping whereby  $\text{CO}_2$  changes its physical and chemical structure. Solubility trapping involves acid-generating reactions (Kaszuba and Janecky, 2009) as  $\text{CO}_2$  dissolves in formation water to form carbonic acid ( $\text{HCO}_3^-[\text{aq}]$ ). The interaction of  $\text{HCO}_3^-(\text{aq})$  with alkaline aluminosilicate and carbonate minerals may result in the formation of dissolved alkali carbonates and bicarbonates, thereby enhancing solubility trapping. During mineral trapping,  $\text{CO}_2$  reacts directly or indirectly with minerals in the aquifer rocks and dissolves in formation water, causing selective dissolution and precipitation of rock-forming minerals. The complexities of these effects are compounded when  $\text{H}_2\text{S}$  is included in the injectant stream, as it is in the Zama Field. The potential for dissolution of the reservoir rock is relevant to the issue of wellbore integrity. Dissolution of reservoir rock along its interface with wellbore cement can cause a weakening of the bond between the rock and the cement. This can result in areas of higher vertical permeability and also reduce the mechanical integrity of the

wellbore, thereby causing cracks to form. The occurrence of any of these phenomena can result in vertical migration of injected gas along the wellbore and out of the storage reservoir into overlying strata.

The geochemical interactions within CO<sub>2</sub>–H<sub>2</sub>S–water–rock systems are complex under static reservoir conditions and even more so under the dynamic pressure and temperature conditions that occur within an operating oil reservoir such as Zama that is undergoing injection and production operations. Information on CO<sub>2</sub>–brine–reservoir interactions in the literature is generally indirect and mostly based on the analysis of gas or fluid samples recovered from observation wells. When one also considers the inherent heterogeneity of geologic systems, particularly carbonate systems, it becomes clear that such geochemical interactions are highly reservoir-specific and cannot be generalized. As part of the PCOR Partnership Phase II Zama activities, the Alberta Research Council (ARC) performed numerical simulations to examine the potential behavior of the CO<sub>2</sub> and H<sub>2</sub>S components of the acid gas after its injection into a typical Zama pinnacle. A more detailed discussion of the Phase II Zama geochemical modeling study is presented in Smith and others (2009), but generally speaking, the ARC results indicate that reactions between Zama-type acid gas mixtures and typical Zama carbonate mineral assemblages are complex. Those reactions can lead to varying degrees of both dissolution and precipitation, depending on specific brine chemistry, temperature, and pressure conditions. While the Phase II geochemical modeling provided previously unavailable insight regarding potential reactions between Zama acid gas and Zama rocks, there were no laboratory geochemical experimental data to support or refute those results. With this in mind, laboratory activities were conducted as part of the PCOR Partnership Phase III Program to directly examine the geochemical interactions between Zama reservoir rocks, brine, CO<sub>2</sub>, and H<sub>2</sub>S under Zama reservoir pressure and temperature conditions. The following sections detail those examinations.

### **Sample Description and Methods of Analysis**

Experimental activities were conducted involving six ¾-inch-diameter, 1½-inch-long Zama core plugs (Figure 7) representing depths ranging from 4656 to 4715 ft. Average local porosity for the formation is about 10%, and permeability ranges from 100 to 1000 mD. These plugs were sectioned into two lengths that were then cut axially into four pieces each, providing four matching sample pairs to be subjected to four experimental conditions replicated in two exposures. Understanding the mineralogical composition of a rock is necessary to understand its potential reactivity to CO<sub>2</sub> and CO<sub>2</sub>–H<sub>2</sub>S gas streams; therefore, some material from each original core plug was subjected to analysis using x-ray diffraction (XRD) to determine bulk mineralogical composition (Appendix A). Study samples were all limestone plugs from the Muskeg, Zama, and Keg River Formations composed of, on average, 80%–92% calcite, 5%–16% dolomite, and quartz, typically minor but perhaps as high as 8%.

Samples from each plug were inserted into vials and completely submerged in a brine or low-total dissolved solids (TDS) (<1000 ppm) water for batch reaction studies. Brine was composed of 16 wt% or 100,000 ppm Cl<sup>-</sup>. Two 16-cell batch reactor vessels (Figure 8) were pressurized to 2100 psi and equilibrated to a temperature of 140°F. One reactor was pressurized with a reactant of 100% CO<sub>2</sub>, while another was maintained at 30 mol% H<sub>2</sub>S in CO<sub>2</sub>. These conditions were maintained for 28 days in the reaction studies.

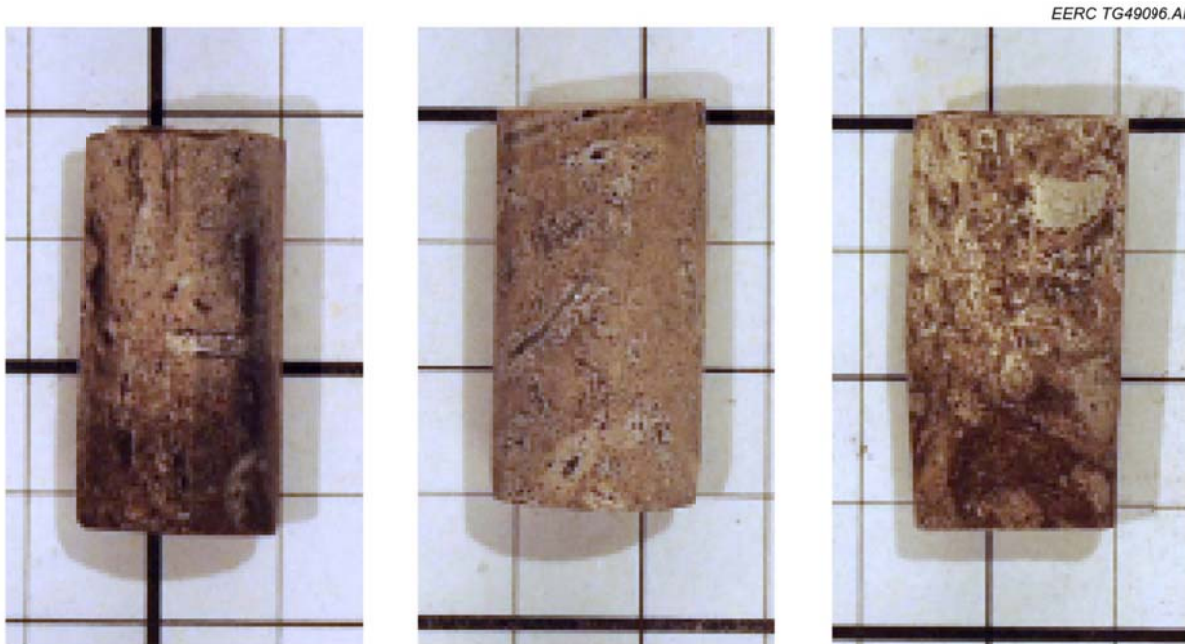


Figure 7. Examples of Zama core plug samples used in the rock experiments.

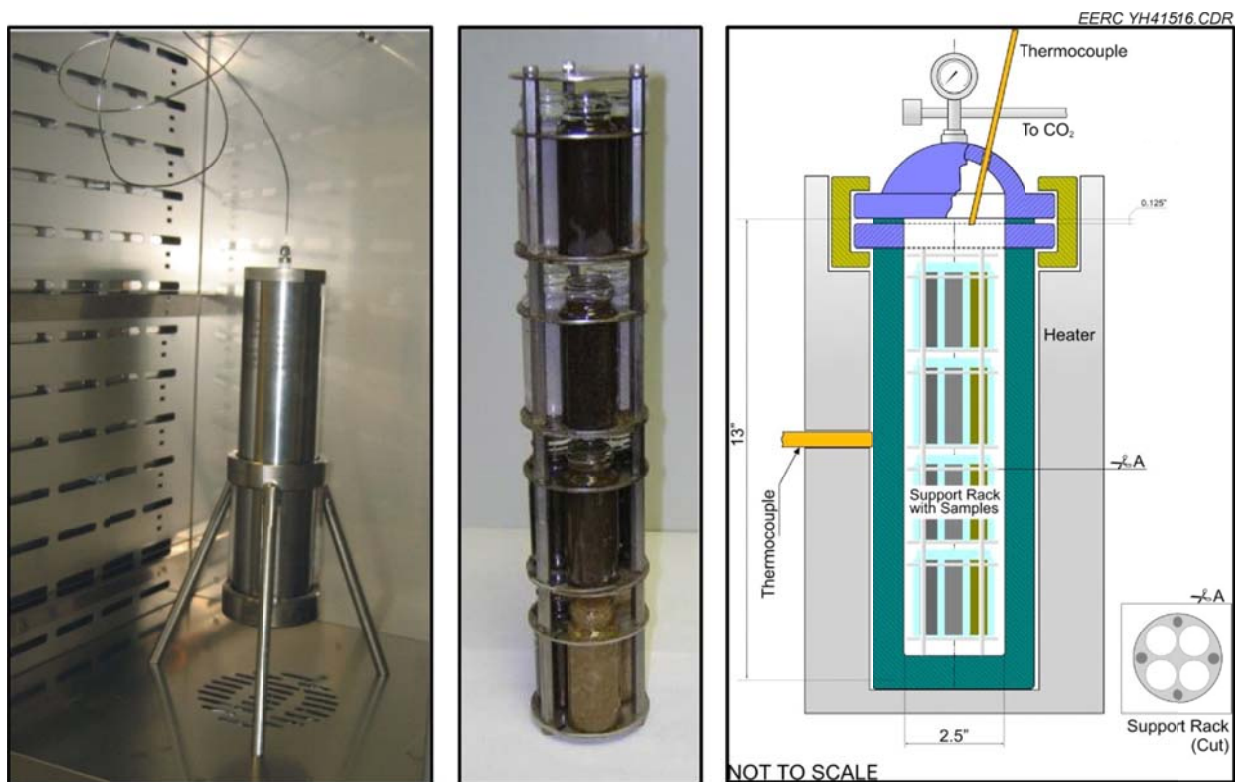


Figure 8. Photographs and schematic of a batch reactor used to test the reactivity of rock, cement, and steel samples exposed to  $\text{CO}_2$  and a mixture of  $\text{CO}_2\text{--H}_2\text{S}$  under Zama reservoir conditions.



After exposure, rock samples representing each original core were analyzed using XRD. These data were compared to the preexposure analytical data to look for changes in mineralogy that might be indicative of dissolution or precipitation. In addition, the fluid that each sample had been submerged in during reaction was analyzed for several ions and TDS. Blank vials containing both brine and pure water were reacted along with samples and analyzed as a baseline for the fluid in which the samples were submerged.

## **Discussion of Results from Geochemical Reaction Experiments**

### ***Rock Sample Analysis Results***

No clear differences were observed between the preexposure and postexposure mineralogy analysis data (Figure 9). This is not entirely surprising considering the rock samples used in these studies were so predominantly calcite. Unfortunately, the applicability of these results to the operations at Zama may be limited. The samples provided by Apache Canada for this Phase II study were all limestones, which is worth noting because previous mineralogical characterization efforts involving other Zama core samples (Smith and others, 2009) indicated that some facies within a typical Zama pinnacle are dominated by dolomite and often include sulfate cement and trace amounts of pyrite. The Phase II geochemical modeling suggested that dolomite and iron-bearing minerals such as pyrite may be the source for much of the precipitation that was predicted to occur in a Zama pinnacle undergoing acid gas injection. The lack of dolomite and pyrite in the Phase III plug samples precludes a direct comparison of the Phase III rock reaction experimental results to the Phase II geochemical modeling results.

### ***Brine Sample Analysis Results***

While the rock analytical results showed little change, some additional insight may be gained from the evaluation of changes in the composition of the fluids in which the rocks were immersed during the experiments. A proxy for understanding changes in oxide composition of the samples is to examine the solids dissolved in those fluids after exposure to pure CO<sub>2</sub> and the Zama CO<sub>2</sub>-H<sub>2</sub>S mixture. Figure 10 shows cation concentrations in the fluids after exposure, and Figure 11 shows TDS after exposure. Examination of these data reveals trends in the tendencies of various minerals to react under the experimental conditions. For instance:

1. Calcium is the dominant cation in the carbonate minerals being studied. Its relative abundance in fluid samples shows that it more readily dissolves with low-TDS water as a solvent and with pure CO<sub>2</sub> as a reactant.
2. Sulfate appears to be significantly less soluble in the presence of H<sub>2</sub>S, as its concentrations were consistently lower in the fluids from the vials that were exposed to CO<sub>2</sub>-H<sub>2</sub>S as compared to those exposed to pure CO<sub>2</sub>.
3. TDS are almost uniformly higher in the fluid baths of samples exposed to pure CO<sub>2</sub> as opposed to CO<sub>2</sub>-H<sub>2</sub>S gas.

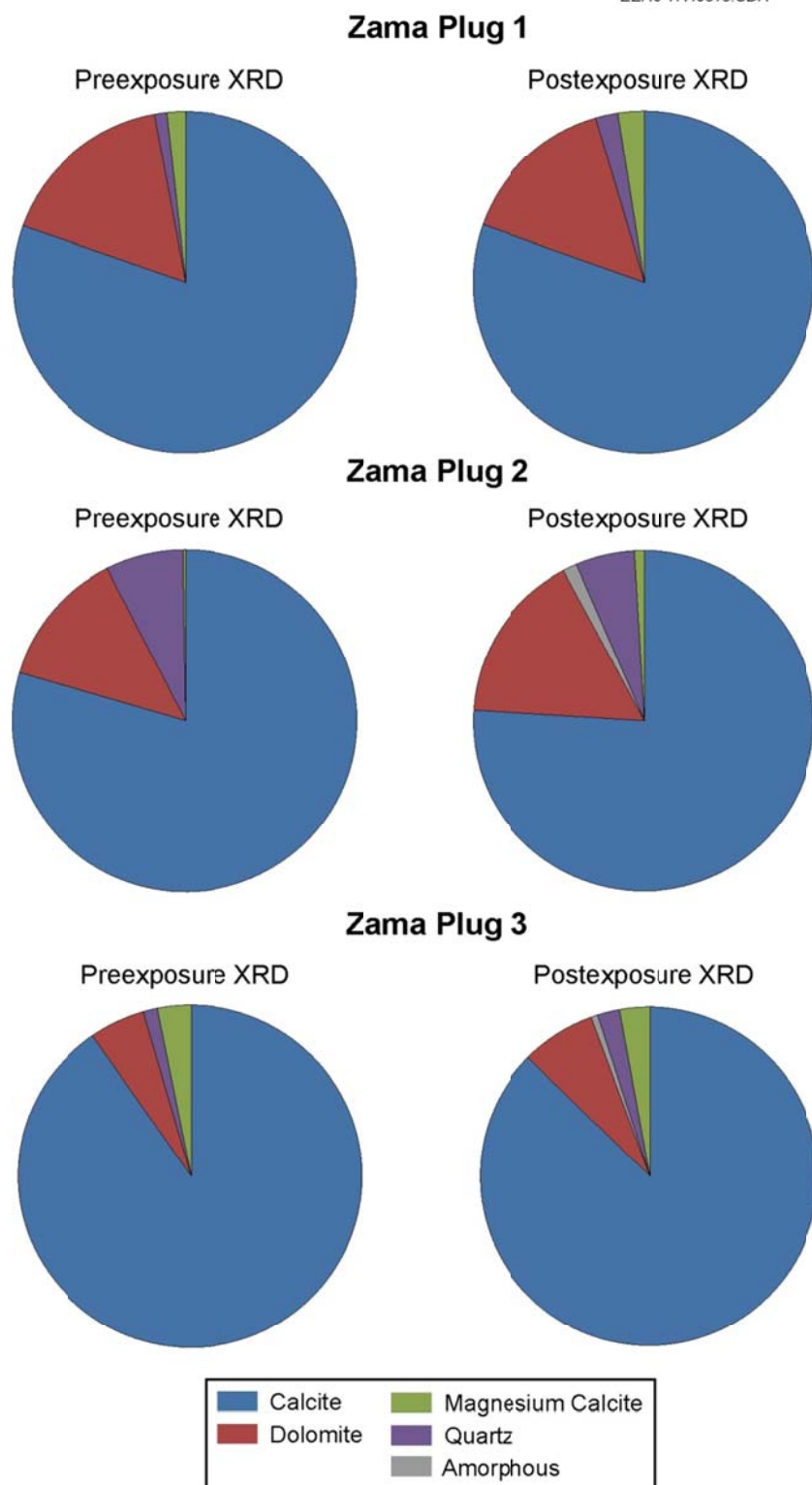


Figure 9. Examples of mineralogy based on XRD for Zama rock samples before and after exposure to CO<sub>2</sub>.

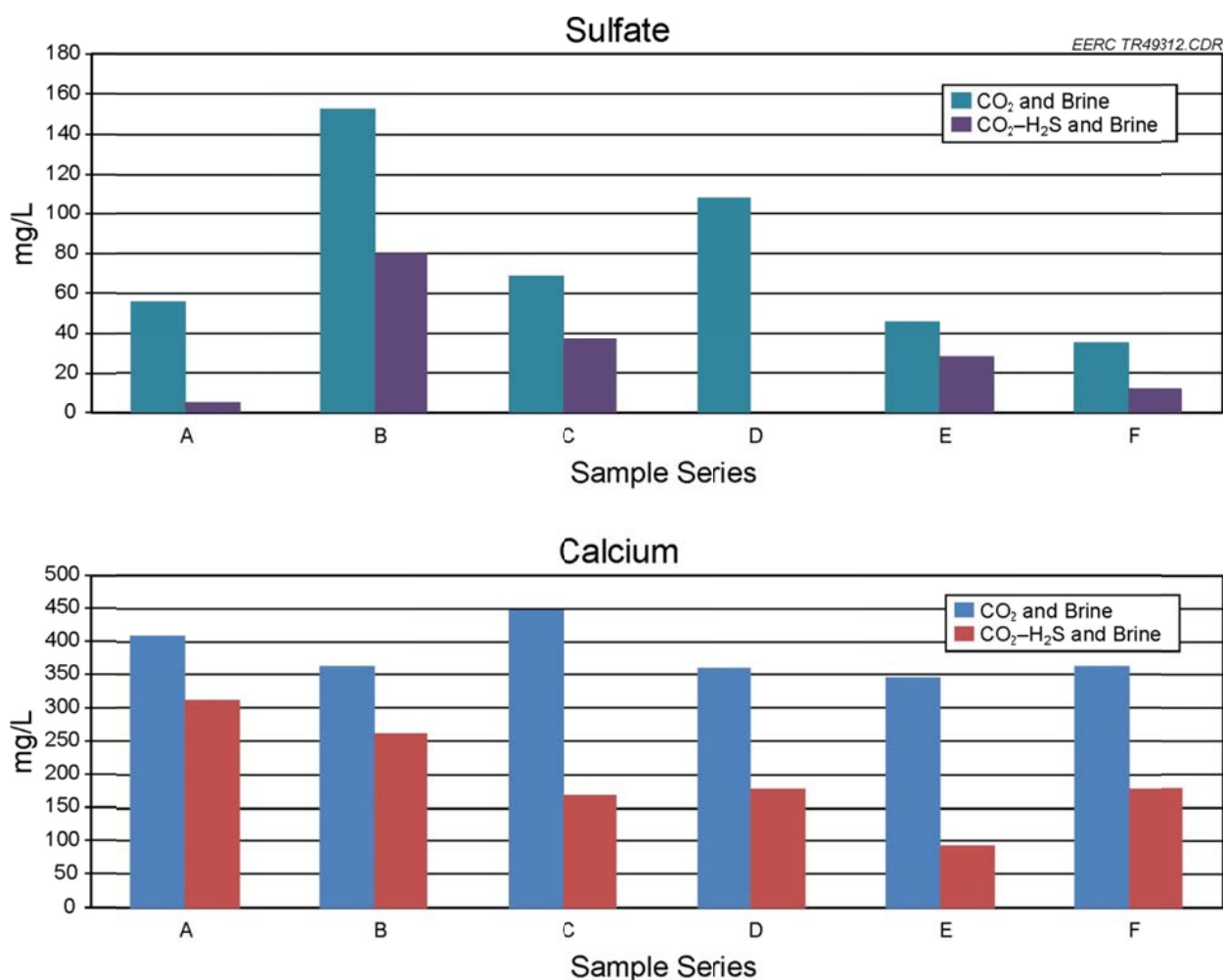


Figure 10. Cation concentrations by fluid sample, showing higher reactivity with CO<sub>2</sub> and brine.

### ***Discussion of the Rock-Based Geochemical Reaction Experimental Results***

Some of the experimental results suggest that a gas stream that includes H<sub>2</sub>S, as opposed to a pure CO<sub>2</sub> stream, may be less reactive with a carbonate reservoir. This statement is based on the clear decrease in the reactivity of both calcium and sulfate that was observed in the samples exposed to the H<sub>2</sub>S-rich gas stream. Measurements of TDS from sample fluids indicate that in the saline reservoir environment CO<sub>2</sub>-H<sub>2</sub>S will dissolve a lesser quantity of total mineral content. Presumably this lower mineral loss will correspond to minimal loss of structural integrity of the formation. This suggests that despite the reputation of H<sub>2</sub>S behaving as an extremely corrosive agent, under some conditions, the presence of H<sub>2</sub>S in the system may actually reduce the reactivity of some carbonate rocks, thereby possibly serving to maintain wellbore integrity rather than degrade it.

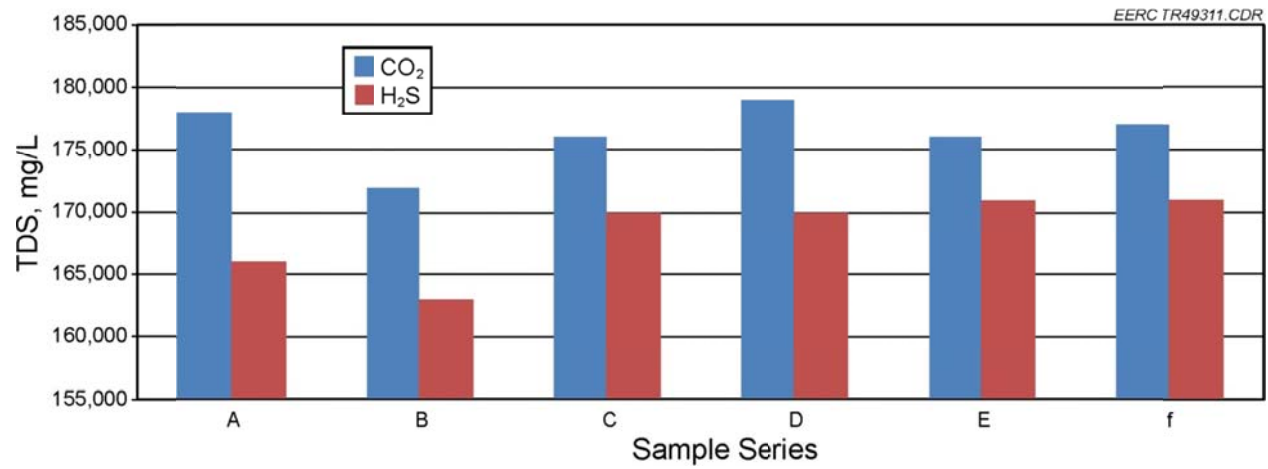


Figure 11. TDS of brine solutions after rocks (Plugs 1–6) and brine were exposed to CO<sub>2</sub> and CO<sub>2</sub>–H<sub>2</sub>S for 28 days at Zama reservoir temperature and pressure.

While the pre- and postexposure XRD data and visual examination of the rock samples indicate that little to no dissolution of minerals occurred during the 28-day test, it is important to note that this was a short-term exposure test. The observed stronger effect of CO<sub>2</sub> toward the dissolution of carbonate minerals suggests that, over a long period of time, some increase in pore space and permeability may occur, thus possibly facilitating the development of leakage pathways along the rock–cement interface of wellbores. This potential phenomenon is particularly important to keep in mind because the Phase II geochemical modeling suggested that over time (years to decades) a segregation of CO<sub>2</sub> and H<sub>2</sub>S may occur in the Zama pinnacles, with H<sub>2</sub>S preferentially dissolving into the water and the gas phase in the pinnacle becoming more CO<sub>2</sub>-rich (Smith and others, 2009). If this predicted behavior occurs, then wellbore integrity along the rock–cement interface may still be affected years after injection begins.

Finally, while the results of these experimental activities provide new insight regarding the potential effects of a typical Zama acid gas stream on a predominantly limestone Zama pinnacle rock, it is important to note that these results are limited in their applicability for several reasons. Foremost is that the samples used in these studies are not representative of a significant portion of most Zama pinnacles. Previous core studies of Zama pinnacles indicate that dolomite-dominated facies can be just as prevalent as limestone-dominated facies, if not more so in some cases. Also, some facies can have significant amounts of sulfate-bearing minerals such as gypsum and iron-bearing minerals such as pyrite, both of which are known to be more reactive with H<sub>2</sub>S. Other factors that limit the applicability of these results are the effects that changes in reservoir pressure, temperature, and fluid chemistry may have on geochemical reactions. As an operating oil field, history suggests that those parameters will likely undergo both minor and major fluctuations over time. Replicating such changes in conditions, and their potential effects, were beyond the scope of these experimental efforts.

### ***Reaction Experiments on Wellbore Cement***

The ability of wellbore cements to maintain stability and competence over long periods of exposure to CO<sub>2</sub> and H<sub>2</sub>S is a critical component of wellbore integrity. Chemical reactions between portland-based wellbore cements, CO<sub>2</sub>, and brine have been studied extensively. However, there is limited information on the physical and chemical characteristics of wellbore cement exposed to acid gas (e.g., CO<sub>2</sub>–H<sub>2</sub>S mixtures, such as occur at Zama) under geological storage conditions. Previous studies focused primarily on mechanical properties of cement exposed to hydrocarbons and did not discuss chemical alteration under geological storage conditions. The Phase III Zama study builds upon these former studies in that it uses intact cement cores and exposes them to CO<sub>2</sub>–H<sub>2</sub>S and brines under typical geological storage scenarios, including temperature and pressure conditions observed in Zama pinnacles. These efforts characterize the diffusive chemical alteration of the various cement phases. This study is important for gaining a better understanding of storage permanence and wellbore integrity in environments where the CO<sub>2</sub> injection stream is not pure. The wellbore cement studies presented in this report were conducted in close collaboration with researchers at DOE NETL in Pittsburgh, Pennsylvania. A detailed presentation of the methods and results can also be found in Kutcho and others (2011).

### *Cement Studies Experimental Procedure*

Cement slurry samples were mixed using Class H portland cement. This is a class of cement that is typically used on wells that are expected to be exposed to acid gas, either through injection or production activities, and is representative of cements used at Zama. Samples were cast in the form of cylindrical rods measuring 0.47 in. in diameter  $\times$  5.12 in. (12 mm in diameter  $\times$  122°F 130 mm long) and submerged in a 1% NaCl–brine solution for curing. The cement was allowed to cure for a total of 28 days at a temperature of 122°F and a water pressure of 2176 psi to simulate a geological sequestration depth of approximately 4265 ft.

Upon completion of the curing process, the cements were exposed to the CO<sub>2</sub>–H<sub>2</sub>S mixtures. Cement samples were placed in glass vials, which were placed in a rack with a top deflector plate to prevent the CO<sub>2</sub> and H<sub>2</sub>S from blowing directly onto the sample vials during filling. Water (or brine) was added to each vial to cover one-half of the cement samples, which allowed for simultaneous exposures with supercritical CO<sub>2</sub>–H<sub>2</sub>S (or pure CO<sub>2</sub>) saturated with water and water saturated with the CO<sub>2</sub>–H<sub>2</sub>S (or pure CO<sub>2</sub>). An operating pressure of 2204 psi (152 bar) was used for cement exposure, and pump temperatures were stabilized to 122°F. By following a stepwise fill/equilibrate procedure for the CO<sub>2</sub>, the pump volume could then be accurately read and the mass of CO<sub>2</sub> delivered to the vessel calculated based on the liquid CO<sub>2</sub> density of 0.89 g/mL in the pump. For the mixed CO<sub>2</sub>–H<sub>2</sub>S experiments, known mixtures were produced by alternating CO<sub>2</sub> and H<sub>2</sub>S additions to the reactor.

Four primary exposure conditions were considered in this study: 1) humid CO<sub>2</sub> supercritical phase, 2) solution with dissolved CO<sub>2</sub>, 3) humid CO<sub>2</sub> supercritical phase with 21 mol% H<sub>2</sub>S, and 4) solutions with dissolved CO<sub>2</sub>–H<sub>2</sub>S. Aqueous-phase conditions consisting of 0%, 1%, and 10% by mass NaCl were used. All cement samples were exposed at 122°F for 28 days.

### *Analysis of Cement Samples*

After exposure, the cement samples were sectioned and polished for both optical microscopy and scanning electron microscopy (SEM). Changes in cement chemistry and microstructure were determined using SEM equipped with backscattered electron imaging (BSE), coupled with energy-dispersive spectroscopy. Cement cores were also ground and placed on glass holders for XRD analysis in order to identify crystalline phases within the cement.

### *Discussion of Cement Studies*

As seen in Figure 12, the outer rim of the submerged cement exposed to the CO<sub>2</sub>–H<sub>2</sub>S-saturated solution appeared black rather than orange, as was the case with CO<sub>2</sub> exposure. The orange rim is typical of CO<sub>2</sub>-exposed cement and is likely a result of decalcification, which allows the iron-rich ferrite and its hydration products to show through.

The interior of the CO<sub>2</sub>–H<sub>2</sub>S cement samples appeared darker than the interior of the CO<sub>2</sub>-only samples. The submerged portion showed typical signs of acid attack by carbonic acid in that

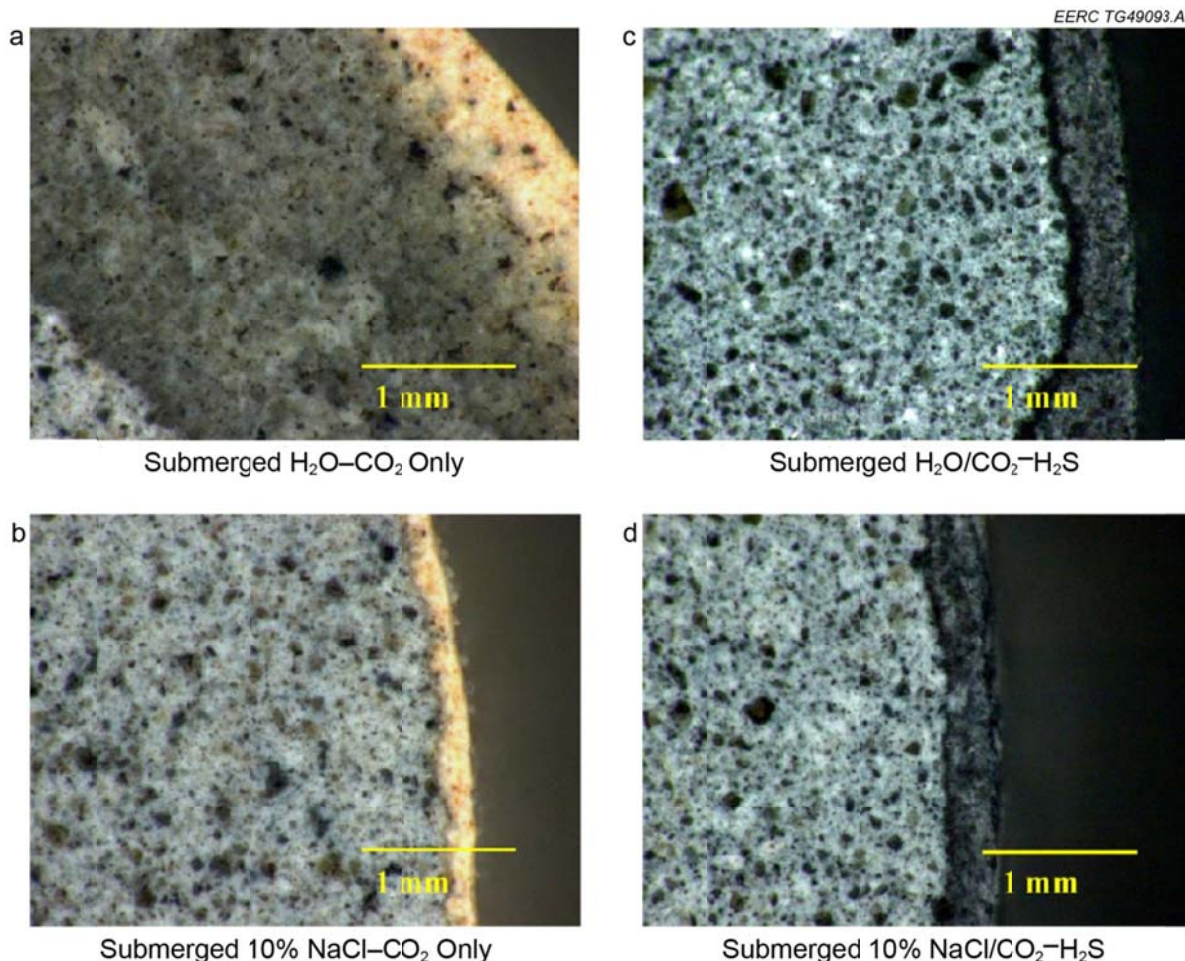


Figure 12. Optical images of Class H neat cement submerged in a solution saturated with  $\text{CO}_2$  only (a and b) and  $\text{CO}_2-\text{H}_2\text{S}$  (c and d) at  $122^\circ\text{F}$  and 2176 psi for 28 days. Samples depicted in “a” and “c” were submerged in  $\text{H}_2\text{O}$ -only, and samples depicted in b and d were submerged in a 10%  $\text{NaCl}$  solution. These images highlight the difference in alteration depth with respect to the solubility of  $\text{CO}_2$  with salinity. Sample size is approximately 0.47 in. in diameter. Optical images were taken at  $100\times$ .

there was an outer porous zone, an intermediate zone of calcium carbonate precipitation, and an inner zone leached of calcium hydroxide. The headspace portion did not develop the individual distinct alteration zones, likely because of a lack of water to diffuse ions out of (and away from) the cement matrix. There were no observable differences between the submerged and headspace portions of the samples with regard to the  $\text{H}_2\text{S}$ -cement interaction. Differences in carbonation depth (exterior alteration zone) were observed among all the cement samples and experimental conditions and correlated to the compositions of the various aqueous solutions. The water-only solution enabled the deepest carbonation penetration, and the 10%  $\text{NaCl}$  solution had the least carbonation penetration, as expected, because of the higher solubility of  $\text{CO}_2$  in lower-ion-strength solutions.

### ***Cement Studies Conclusions***

The addition of  $\text{H}_2\text{S}$  to the  $\text{CO}_2$  storage system resulted in two main mineralogical differences in portland Class H cement: 1) the precipitation of significant amounts of ettringite (possibly secondary ettringite) and 2) the precipitation of pyrite in the carbonated rim of the cement (Figure 13). Secondary ettringite formation subsequent to the hardening of cement can lead to cracking, spalling, strength loss, and degradation. In the presence of oxygen and moisture, pyrite will potentially oxidize to ferrous sulfate and sulfuric acid. The free sulfuric acid will typically react on any calcite present to produce gypsum, which can potentially increase molecular volume by 103% and lead to expansion cracks.

$\text{CO}_2$  may dissolve the ettringite and reprecipitate calcium compounds (such as calcium carbonates) and may potentially help improve the overall cement integrity. Further studies are needed to determine what effect pyrite formation and secondary ettringite formation would have on the long-term integrity of the wellbore under these conditions. Specific studies are needed to focus on the potential for pyrite oxidation and its effect on wellbore cement as well as the impact of secondary ettringite formation on the mechanical integrity of the cement.

### **BASIC CASING CORROSION-TESTING EXPERIMENTS**

In an injection well, the steel casing of that well is the first wellbore material to be exposed to  $\text{CO}_2$ , and it is exposed to that injection stream for the entire operational life of that well. The steel casing also serves as the last barrier between a  $\text{CO}_2$ -saturated formation and a potential fast vertical leakage pathway through an abandoned or suspended well. As such, the ability of the casing to maintain its competence after prolonged exposure to  $\text{CO}_2$  and/or acid gas is a vital component of wellbore integrity. The introduction of the new U.S. Environmental Protection Agency policies for the “Class VI” injector wells used for CCS and new standards for geological storage by the Canadian Standards Association as well as increasing demand for  $\text{CO}_2$  EOR operations place further value on understanding the corrosion mechanisms of steel pipes and well casing associated with transportation and injection of supercritical  $\text{CO}_2$  and mixtures of  $\text{CO}_2$  and  $\text{H}_2\text{S}$ .

Corrosion already represents a significant problem in oilfield operations. While steel corrosion in the presence of water has been studied extensively, corrosion of steel equipment in  $\text{CO}_2$  and mixtures of  $\text{CO}_2$  and  $\text{H}_2\text{S}$  have only begun to draw attention in recent years. In the interest of further understanding these processes, the Zama Phase III efforts included examinations of corrosion processes in a variety of steels used in oilfield applications when exposed to  $\text{CO}_2$  and acid gas under conditions that are representative of Zama reservoirs.

#### **Sample Description and Methods of Analysis**

For casing corrosion experiments, seven types of steel (5LX65, J55, N80, C90, C95, K55, and P110) commonly used to manufacture oilfield casing were evaluated in this work. Coupons of these steels were cut into two equal parts, and each half was placed into a separate vial, one containing a low-TDS water and the other containing a 16.5% (100,000 mg/L) NaCl brine



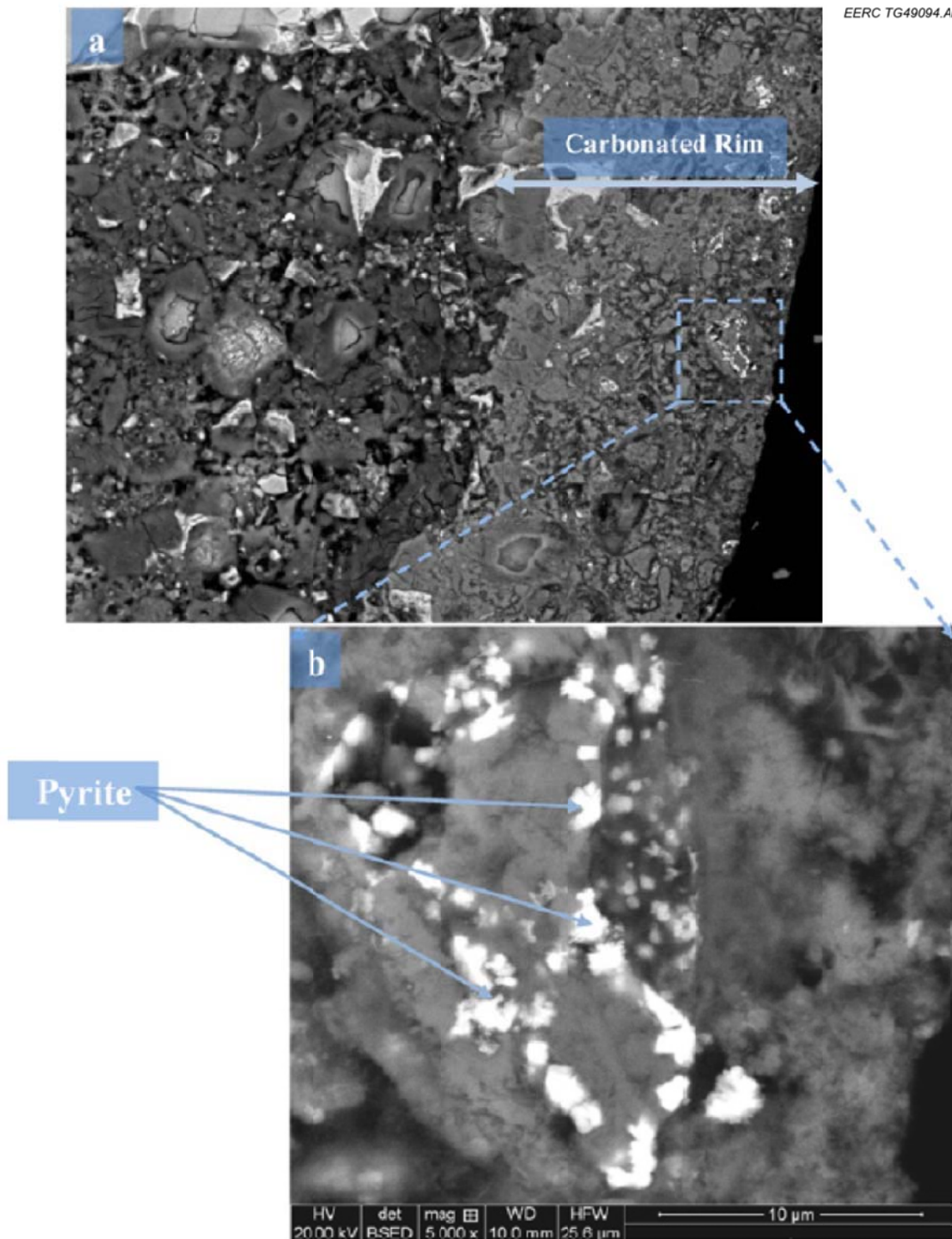


Figure 13. SEM BSE images showing pyrite (bright spots) within the carbonated region of cement exposed to  $\text{CO}_2\text{--H}_2\text{S}$ : a) low-magnification view of the cement showing the carbonated rim and b) high-magnification view of the region located in the box. Pyrite was identified by elemental spectra and confirmed by XRD.

solution similar to the formation water typical of the Keg River Formation. In all, two sample sets of 14 (seven low-TDS water and seven brine solution) were placed into two sealed autoclaves and brought to temperature and pressure conditions representative of the reservoir, 140°F and 2100 psi, respectively.

### *Steel Casing Reaction Studies*

One sample set was continuously exposed for a period of 28 days to pure CO<sub>2</sub>, while the other was exposed to a mixture similar to that of the EOR injection stream (70% CO<sub>2</sub>, 30% H<sub>2</sub>S) for the same time period.

### **Discussion of Results from Casing Corrosion-Testing Experiments**

Prior to undergoing reaction, samples were cleaned and weighed. The surfaces of the samples were then mapped using an optical profiler capable of detecting surface deformation down to the nanometer scale. After exposure to CO<sub>2</sub> and/or acid gas, the samples were weighed again and studied using optical microscopy (Figure 14) as well as the optical profiler. Figure 15 shows the variations in steel coupons after exposure. The reacted brine and water were also analyzed for dissolved metals and compared with control blanks which had been reacted without coupons in them. Results for each steel are presented in Appendix B.

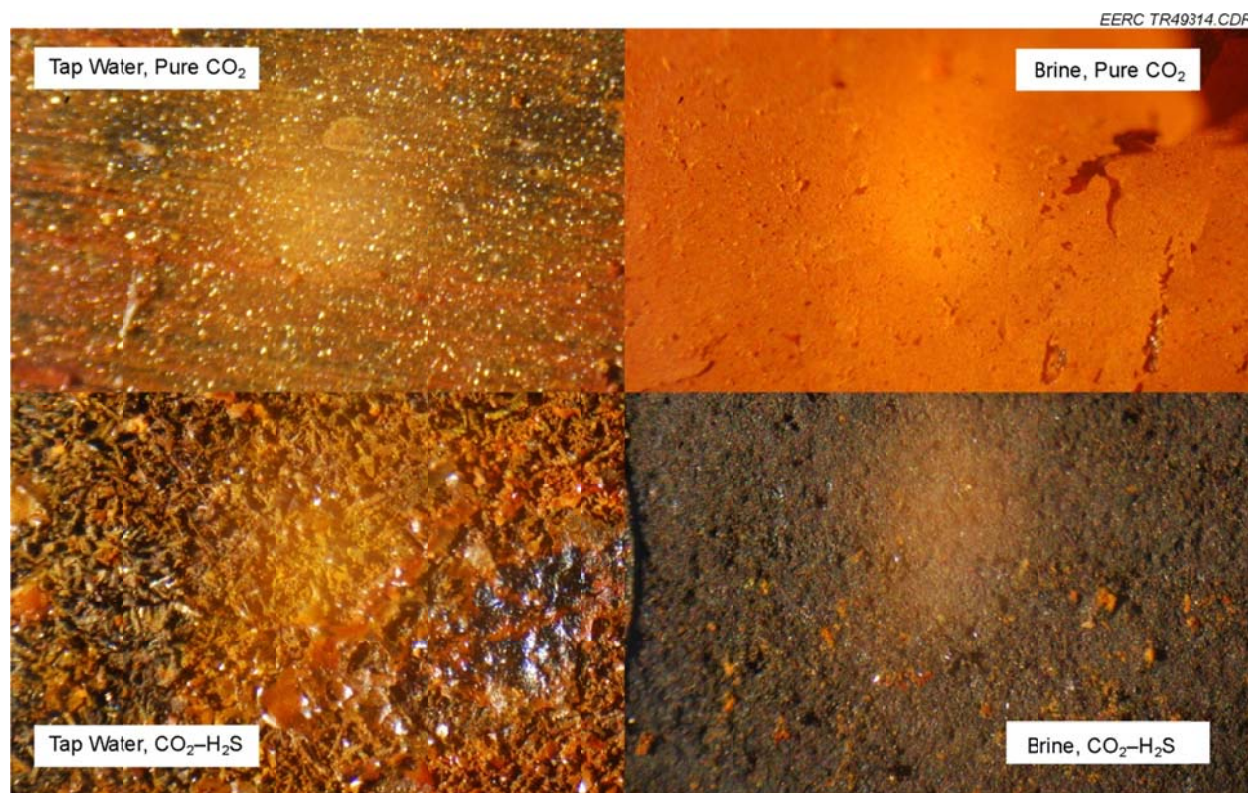


Figure 14. Optical microscopy (400×) images of steel coupons after exposure to CO<sub>2</sub> and CO<sub>2</sub>–H<sub>2</sub>S in brine and low-TDS water.



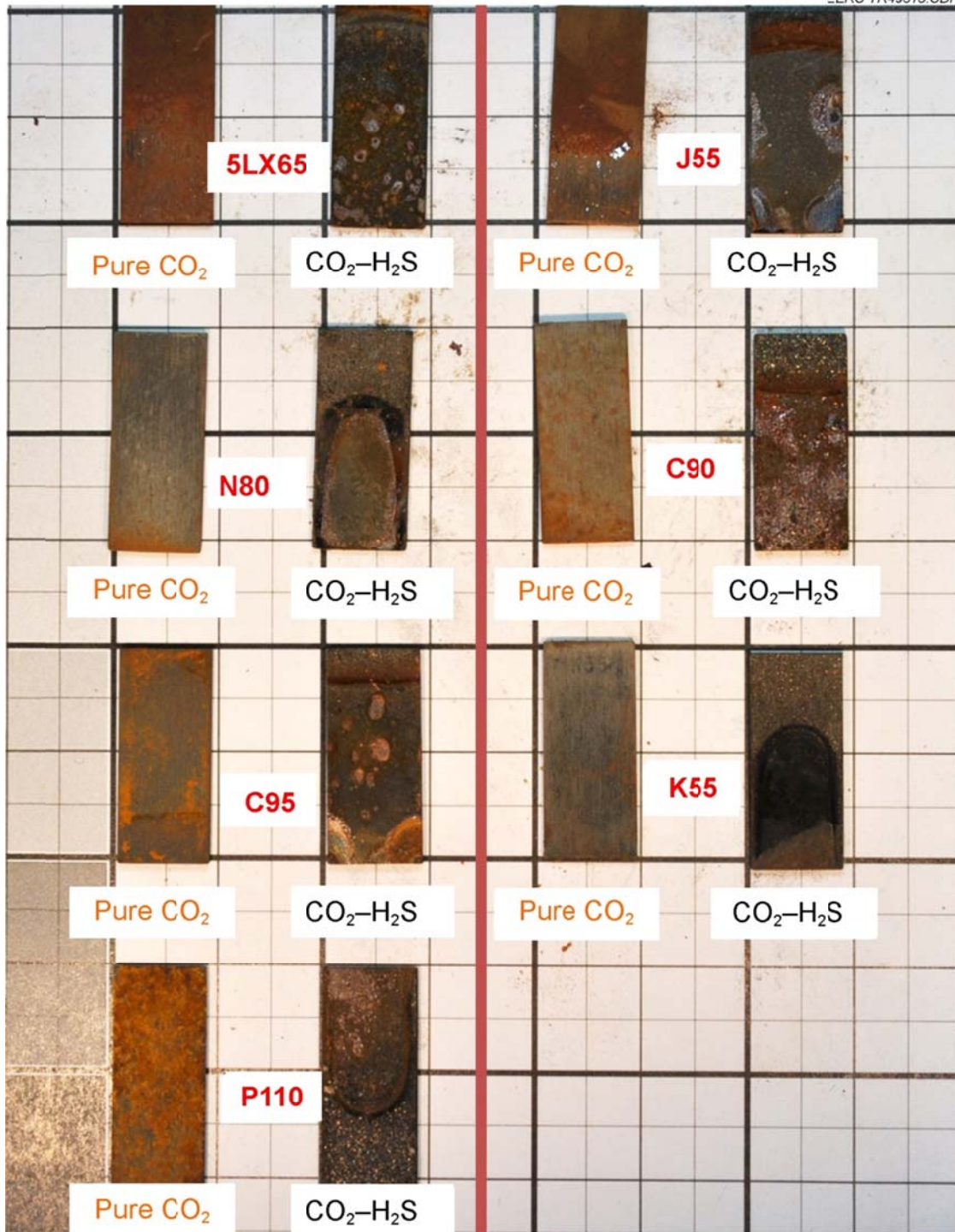


Figure 15. Steel coupons after exposure to CO<sub>2</sub> in brine and CO<sub>2</sub>-H<sub>2</sub>S in brine.

Based on before-and-after comparison of profiler data as well as SEM and fluid analysis data, several observations can be made to characterize the reactions of the evaluated steel alloys with CO<sub>2</sub> and H<sub>2</sub>S in brine and tap water solutions:

1. The highest level of corrosion was observed in brine solutions under a pure CO<sub>2</sub> atmosphere; this assessment is based on broad agreement between weight measurements (Figure 16), fluid analysis (Figure 17), optical microscopy, and optical profiler data.
2. In the presence of H<sub>2</sub>S in brine, the corrosion rate was lower if compared to pure CO<sub>2</sub>, less iron was introduced to the study fluid containing these samples, and samples gained rather than lost mass (Figures 17 and 18).
3. After exposure to acid gas, a significant amount of sulfur was found on the exposed surfaces by SEM, which also accounts for some of the observed increase in mass.
4. Corrosive mass loss appears to take place in all samples reacted with pure CO<sub>2</sub>. However, for samples submerged in brine, this is masked by the deposition of solution solids.
5. J55 and N80 steels are slightly more resistant to both pure CO<sub>2</sub> and the acid gas mixture than K55 steel.
6. Pitting effects were observed by the profiler on all samples (Figure 19).

### **Summary of Key Findings of Casing Corrosion-Testing Experiments**

While pitting took place in all exposures, it was more severe in cases where H<sub>2</sub>S was not employed. In contrast to the mass leaching of iron that was seen in pure CO<sub>2</sub> exposures, the H<sub>2</sub>S exposures demonstrated significant deposition of sulfur. This deposition, if it correlates with sulfur inclusion in the steel's crystalline matrix, may cause sulfur embrittlement, an effect compounding any possible masked corrosive mass loss.

Both J55 and N80 steels show a lower rate of mass loss and pitting than K55 steel while maintaining a similar rate of sulfur deposition. Thus they are likely to exhibit similar sulfur embrittlement as well as a lower incidence of failure due to corrosion.

## **RESERVOIR MODELING FOR EOR AND STORAGE PURPOSES**

The static geologic models of the pinnacles were used to conduct dynamic simulation modeling of potential operational scenarios, including various combinations of acid gas injection, EOR, and water extraction. History matching was used to improve the reliability of the simulation results. Because data for the F pool had already been gathered as part of the PCOR Partnership Phase II activities, simulation efforts were first conducted on the F pool. Based on the results of F pool modeling, subsequent dynamic simulations on the G2G and Muskeg L pools were modified to include more emphasis on the effects of equation of state (EOS), changes in minimum miscibility pressure (MMP), and pressure depletion on the results of the potential



Figure 16. Mass differences between casing material coupons as measured before and after exposure to pure  $\text{CO}_2$  (below) and  $\text{CO}_2$  combined with  $\text{H}_2\text{S}$  (above) under both water (blue) and brine (red).

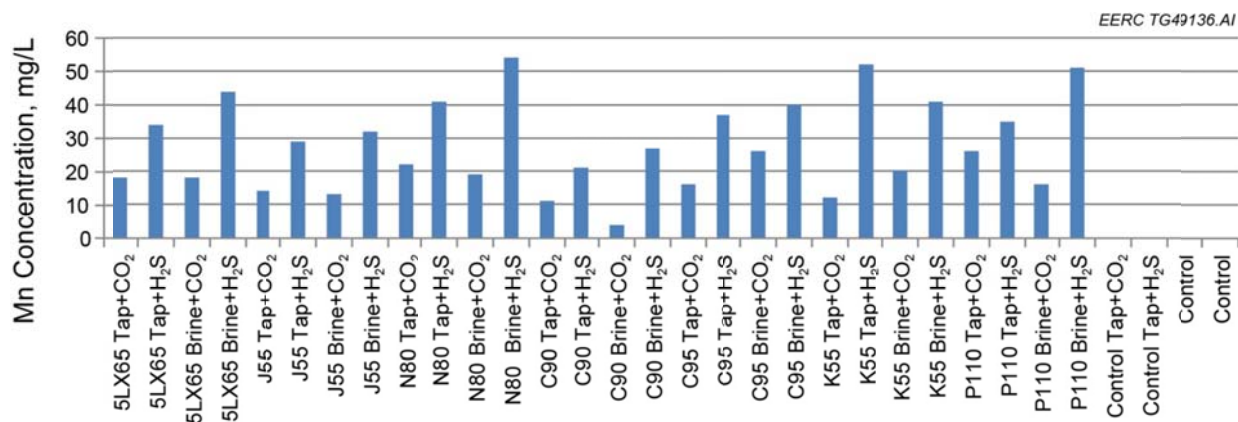


Figure 17. Concentrations of manganese in water and brine for each of the seven studied casing metals and a control for each of the exposure conditions.

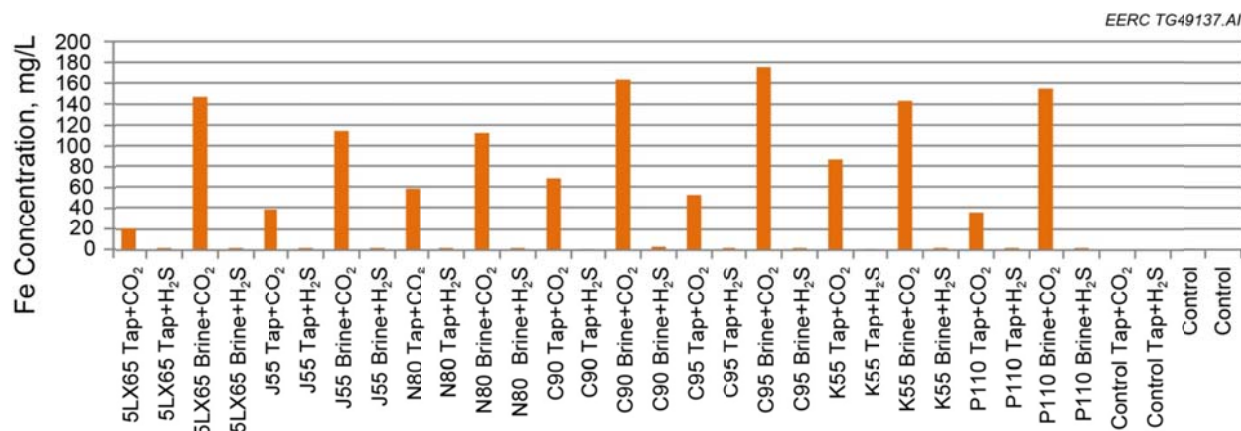


Figure 18. Concentrations of iron in water and brine for each of the seven studied casing metals and a control for each of the exposure conditions.

operational scenarios. The knowledge gained from the more detailed F, G2G, and Muskeg L modeling was then applied to develop predictions of EOR potential and storage capacity for the other pinnacles (NNN, RRR, and Z3Z). The following sections describe the approaches and results of the dynamic simulation modeling activities for the Zama pinnacles. The modeling workflow can be seen in Table 2.

### Geologic Modeling

Static geocellular models were built for the F, G2G, and Muskeg L pinnacle reefs with available data. A robust workflow consisting of a literature review, analog core analysis, building a stratigraphic framework, petrophysical analysis, structural modeling, facies modeling, petrophysical modeling by multiple-point statistics, and volumetric calculations was followed for all three pinnacles.

McCamis and Griffith (1968) reported several internal structures for the pinnacle reefs found in the Zama area. Core photos and descriptions of each facies were provided. This allowed for a proper understanding of the complex factors that comprise good and poor reservoir facies. A multiple-point statistical analysis was performed in order to more closely replicate the facies as described in the McCamis and Griffith report.

Since Zama pinnacle core was unavailable to view for this study, an analog core from another Devonian pinnacle reef of the Winnipegosis Formation in the Williston Basin was described. The North Dakota pinnacle reefs are a direct analog to Zama pinnacle reefs. Both reefs are Devonian carbonate reservoirs and exhibit the same type of facies and structural framework. The core from North Dakota Industrial Commission (NDIC) Well 6535 provided useful information in resolving the porosity types found in the pinnacle reefs. Thus a bimodal distribution is expected in the petrophysical analysis, which can be resolved based on this core analysis exercise.

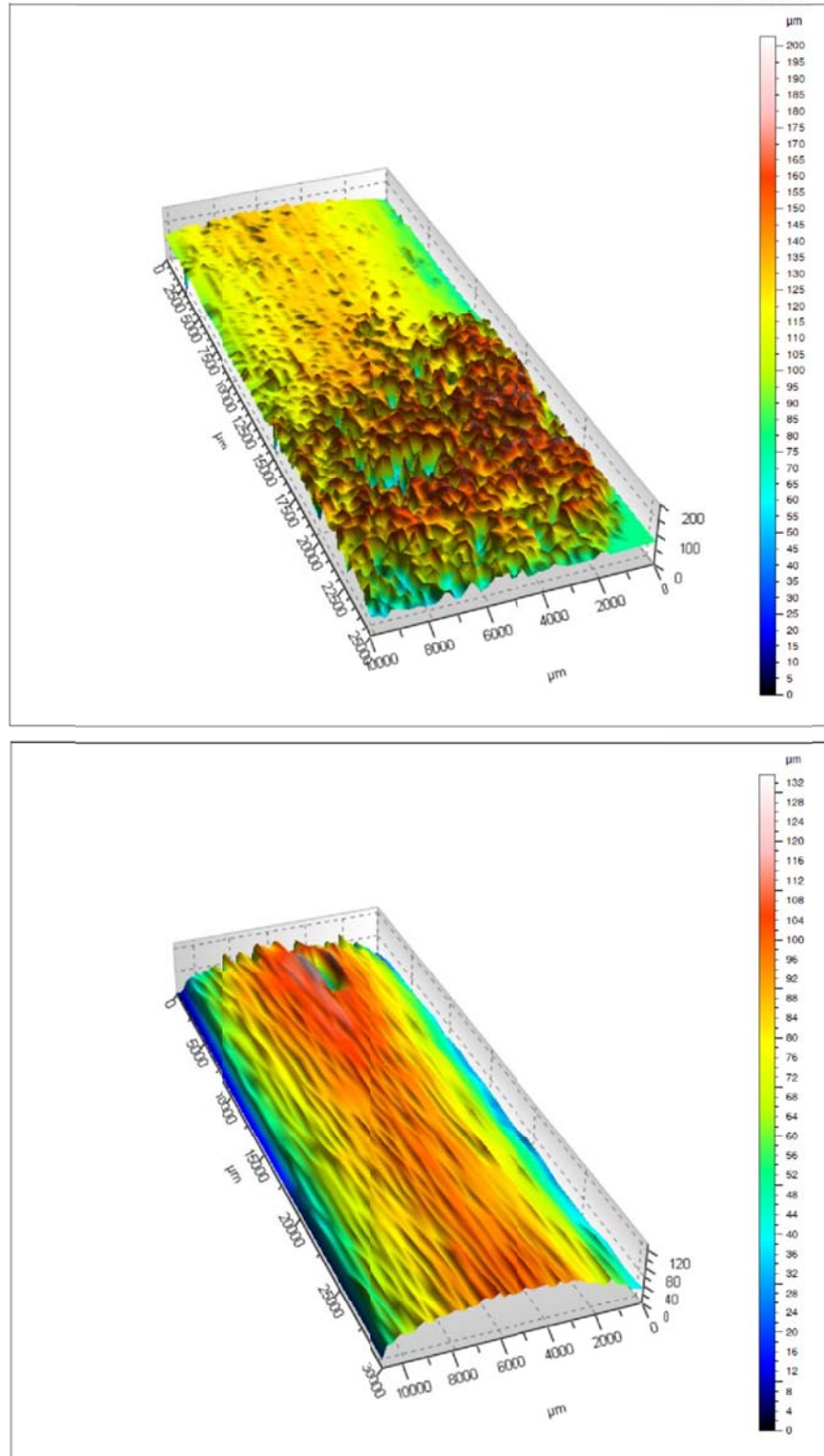


Figure 19. Coupon of 5LX65 steel before (below) and after (above) exposure to CO<sub>2</sub> and tap water.



**Table 2. Zama Reservoir-Modeling Workflow**

Developed Static Geologic Reservoir Model for F Pool – Version 1 Scoping Model (March 2011)	<ul style="list-style-type: none"> <li>• Structural model was developed using multipoint geostatistics and generic reservoir properties; such as permeability and porosity; water saturation was distributed homogeneously by model zone, and layers were populated.</li> </ul>
Performed History Match (May 2011)	<ul style="list-style-type: none"> <li>• Geologic model was imported into Computer Modelling Group Ltd. (CMG) generalized EOS model (GEM) simulator for history match.</li> <li>• Matched indices included water cut, production rate, injection rate, and pressure tendency.</li> </ul>
Performed Initial Simulations	<ul style="list-style-type: none"> <li>• With a base case of gas injection only, a maximum injection pressure constraint of 3300 psi was used.</li> <li>• For simultaneous acid gas injection and formation water extraction, a water extraction well was placed in the bottom portion, Rg/w (ratio of acid gas injected to extracted water at reservoir conditions).</li> </ul>
Updated Static Geologic Reservoir Model for F Pool – Version 2 (March 2011)	<ul style="list-style-type: none"> <li>• Developed more rigorous understanding of structure reef edge, facies, and reservoir and cap rock properties.</li> <li>• Incorporated reasonable variations of reservoir parameters, including level of communication between different formations and horizons and influence of production activities on gas pools.</li> </ul>
Performed History Match (May 2011)	<ul style="list-style-type: none"> <li>• Geologic model was imported into CMG’s GEM simulator for history match.</li> <li>• Matched indices included water cut, production rate, injection rate, and pressure tendency.</li> </ul>
Performed Additional Simulations (Spring 2012)	<ul style="list-style-type: none"> <li>• Geologic model was imported into CMG’s GEM simulator for predictive simulations.</li> <li>• Numerical aquifer setting.</li> <li>• Processes for 1) modeling multiphase flow of water (brine) and gas (methane, CO<sub>2</sub>, and H<sub>2</sub>S) and 2) modeling mass transfer between water and gas phases, with a special focus on CO<sub>2</sub> and H<sub>2</sub>S dissolution into formation brine.</li> <li>• Scenarios: 1) bottomhole pressure (BHP) constraints of 300 psi at production well, 2) constraints of 2100 psi, and 3) constraints of 300 psi at production well and 2100 psi at water extraction well.</li> <li>• Modeling simulation results were analyzed.</li> </ul>
Collected Additional Data (2009–2012)	<ul style="list-style-type: none"> <li>• Acquired additional seismic data from Apache for five more pinnacles.</li> <li>• More detailed analyses of well logs within the modeling area were completed.</li> <li>• Acquired additional production data from Apache for five more pinnacles.</li> </ul>
Developed PVT for G2G and Muskeg L Pools (January 2013)	<ul style="list-style-type: none"> <li>• Chose EOS for PVT modeling.</li> <li>• Regression work on experimental test obtained from operator.</li> <li>• Investigated H<sub>2</sub>S effect on solvent/MMP; different CO<sub>2</sub>–H<sub>2</sub>S ratio cases were simulated.</li> <li>• Investigated pressure depletion effect on solvent/MMP; an approach was developed to numerically simulate MMP with depleted procedure.</li> </ul>
Performed Static Geologic Modeling for G2G and Muskeg L Pools (Spring 2013)	<ul style="list-style-type: none"> <li>• Conducted more detailed log analyses and added reprocessed seismic map data.</li> <li>• Modeled pool structure, which included a better definition of the reef edge, formation boundaries, and features that create a structural trap by digitizing depth structure maps of the Zama Member top surface and correlated with the tops from production and injection wells within the pinnacles.</li> <li>• A petrophysical analysis was conducted on lithology, porosity, permeability, and water saturation.</li> <li>• Multipoint statistics (MPS) method was used to create a facies model.</li> <li>• Calculated volumetrics of each pinnacle for various scenarios.</li> </ul>
History-Matched Dynamic Model (Summer 2013)	<ul style="list-style-type: none"> <li>• Numerical tuning.</li> <li>• Properties/parameters sensitivity analysis.</li> <li>• Liquid production rates were used as primary constraints; BHPs were used as the secondary constraints.</li> <li>• Matched indices included water cut, production rate, injection rate, and pressure tendency.</li> </ul>

Continued. . .



**Table 2. Zama Reservoir-Modeling Workflow (continued)**

Performed Predictions (Summer 2013)	<ul style="list-style-type: none"><li>• Analyzed flooding efficiency of current injection and production system.</li><li>• The six cases were designed:<ul style="list-style-type: none"><li>– G2G_1) – Base case parameters, current injection mode, and BHP constraint.</li><li>– G2G_2) – Current injection and production system, water-alternating gas (WAG) injection of 1:1 water/gas ratio and cyclic period of 1 year.</li><li>– G2G_3) – Infill drilling case. Based on the analysis of all above cases, a pseudo-production well is configured in the center of the pinnacle.</li><li>– Muskeg L_1) – Base case parameters, current injection mode, and BHP constraint.</li><li>– Muskeg L_2) – Based on the analysis of history match and Case 1, the early breakthrough ends up in the EOR process if no action is taken on Well 102/05-01-116-06W6/00. In this case, the well is shut in and other wells keep using BHP constraints.</li><li>– Muskeg L_3) – Infill drilling case. Based on the analysis of all above cases, a pseudo-production well is configured in the center of the pinnacle.</li></ul></li></ul>
Performed CO <sub>2</sub> Storage Analysis of Multiple Scenarios (June 2013)	<ul style="list-style-type: none"><li>• Real-time injection.</li><li>• Using the two best history-matched models, six test cases were simulated for CO<sub>2</sub> injection at F, G2G, and Muskeg L for injection periods of 30 years.</li><li>• Sensitivities of CO<sub>2</sub> storage in pinnacle reefs are analyzed on the basis of simulation results by effective storage bulk, displacement mechanisms, vertical connectivity, and aquifer.</li><li>• Parameters for storage capacity and efficiency evaluation were generated, and a quick estimate equation is used to predict the storage capacity in the Z3Z, NNN, and RRR pools.</li></ul>

Pinnacle reefs have very complex geologic and facies relationships, and as a result, a thorough understanding of the geology is necessary in order to properly predict oil in place, CO<sub>2</sub> storage capacity, and fluid movement in the reservoir. Borehole image logs were used to more accurately identify the different facies and determine each facies' properties along the wellbores. Seismic attribute data interpretations were used to identify the reef vs. nonreef facies to aid in the distribution of facies in the reservoir. These properties were then spatially distributed throughout the theoretical reservoir model using a combination of MPS and object-modeling workflow to produce equiprobable reef facies, structure, and volumetric realizations. Multipoint geostatistics offer a way to map the complex pinnacle geology in the modeling of the F, G2G, and Muskeg L pools. The resulting maps are not unique; rather, many alternative maps are created, each conforming to known geology and the expected shape of the geologic unit. The maps incorporate important geologic characteristics, including lithology, porosity, and permeability. The alternative 3-D geologic maps, when viewed together, provide estimates of the geologic variability of the reef and can lead directly to estimates of uncertainty for process models that are built upon the 3-D geology, such as flow and transport models (Phelps and Boucher, 2009). For the modeling of the F pool, two model versions were developed.

### ***Stratigraphic Framework***

The structural surfaces for the F (Figures 20 and 21), G2G, and Muskeg L models were created by digitizing depth structure maps of the Zama Member top surface correlated with the

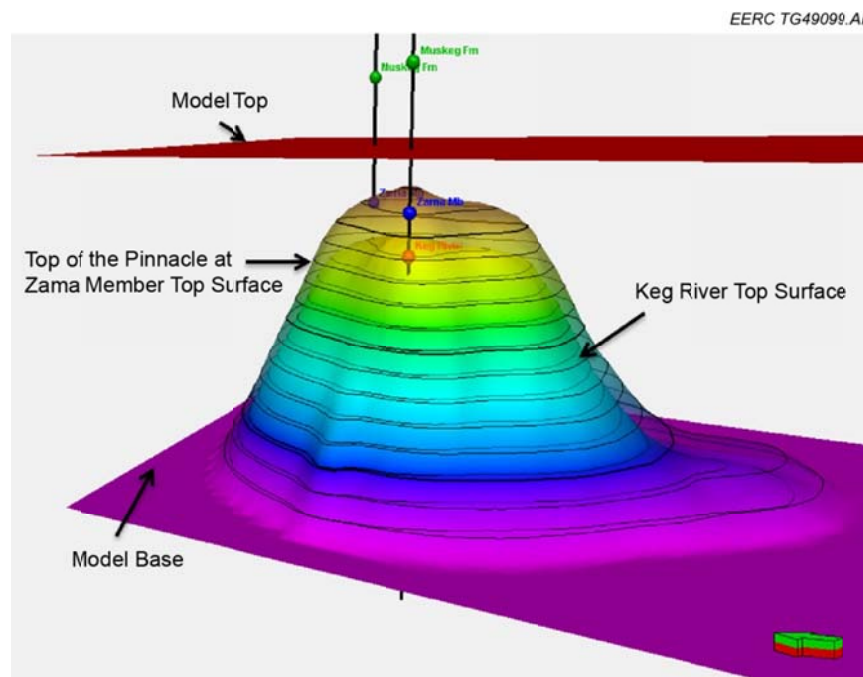


Figure 20. Structural surfaces for the G2G model.

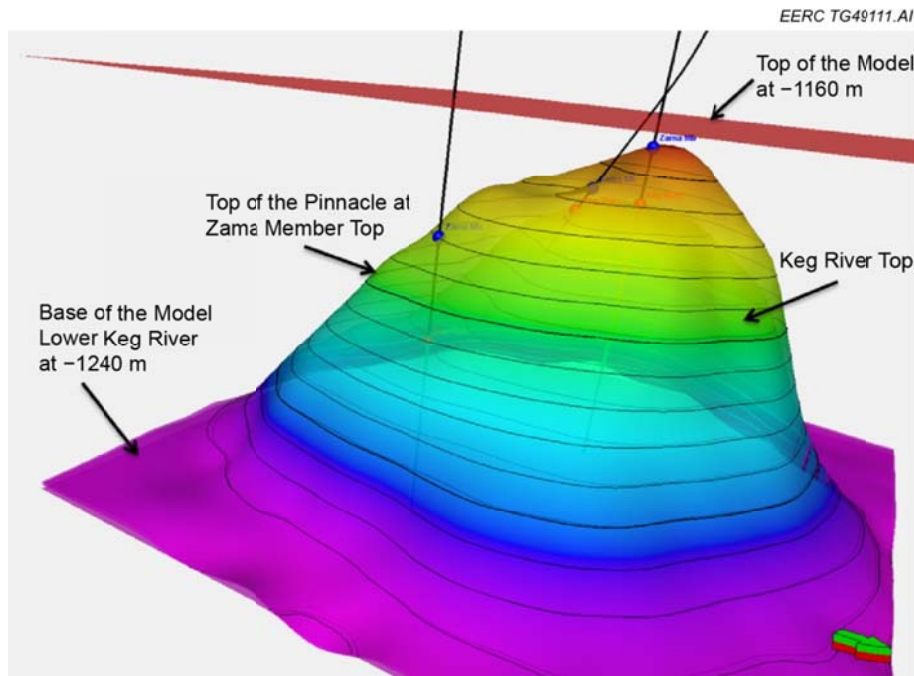


Figure 21. Structural surfaces for the Muskeg L model.

tops from production and injection wells within the pinnacles. The Upper Keg River Formation was picked from tops and followed the same trend as the Zama top in order to minimize surface crossover and keep the internal structure of the reef realistic based on literature review. The surfaces were constrained laterally using polygons around the pinnacle based on the limits of the provided structure maps, which included the outer limits of the reef. A zone was created between the uppermost Zama Member and an arbitrary surface 30 meters above to represent the volume of anhydrite that represents the overlying Muskeg Formation. The base of the model was picked 30 meters below the top of the Mound Zone, again to capture the pinnacle geometry but not add a significant amount of cells to the final model. Additionally, layering was set for each zone to optimize heterogeneity of the petrophysical properties (Figure 22).

### ***Petrophysical Analysis***

A petrophysical analysis was conducted to determine the reservoir properties before geostatistically populating them into the model. Logs derived from petrophysical analysis include lithology, porosity, permeability, and water saturation. Openhole logs were used in combination with a neural network approach when data were lacking. Each process underwent a quality check (QC) utilizing crossplots and a sensitivity analysis to fine-tune the base case static model.

Prior to the petrophysical analysis, core depths did not match the same depth of the logs and needed to be depth-shifted in some wells. A depth mismatch typically is caused by core mislabeling, or fractured, broken, or lost core. The mismatched depth makes it difficult to give

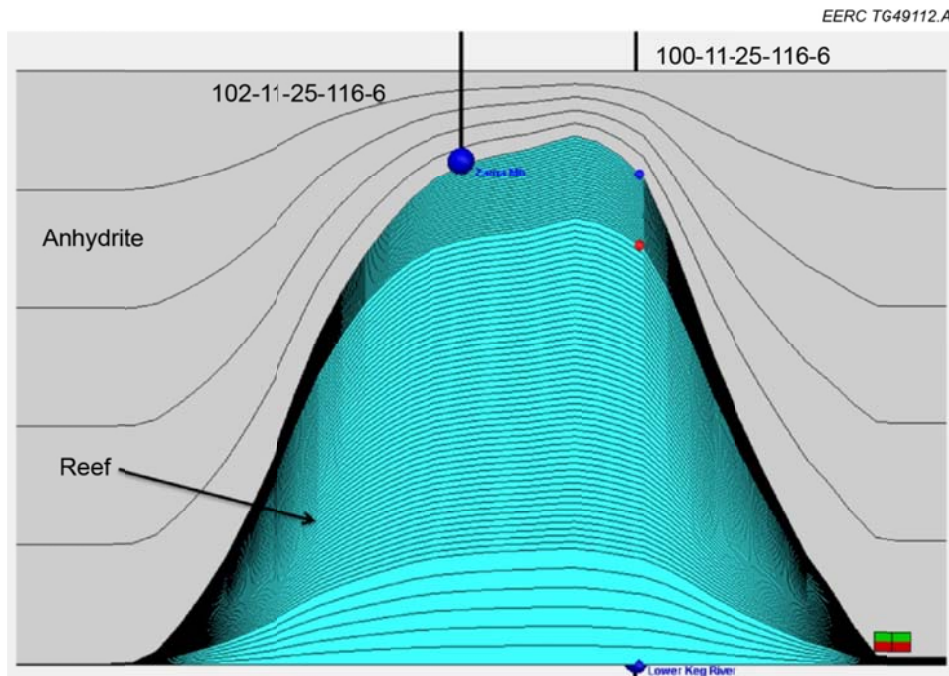


Figure 22. Generic structural framework for the models. A reef structure divided into layers to capture heterogeneity capped by extensive anhydrite.

the confidence factor needed when quality-checking the logs calculated from the petrophysical analysis. Grain density data from lab analysis on the core allowed for the core to be depth-shifted to match the wireline bulk density (Figure 23).

Porosity and permeability in the model were both analyzed in Techlog, utilizing the neural network process to create a synthetic log. A neural network utilizes an algorithm with core data and their relationship to the wireline logs (Figure 24). The neural network learns by example, that is, the portion of the well that has the core data, to create a continuous synthetic log. The synthetic log then undergoes a QC in comparison to the core data. In the Muskeg L pinnacle, sonic log porosity was substituted for the two wells—50111606W600 and 102050111606W600—which had no core data, whereas the neural network approach was used for the other well—40111606W600—and Well 112511606W600, the only well penetrating the G2G pinnacle, as the core data were available to guide the resulting log. The input logs for the neural networking were spontaneous potential, calliper, gamma ray, neutron porosity, density, and acoustic velocity. Porosity generated from the cores is used to supervise the resulting porosity log.

The synthetic log QC process identified data outliers for the synthetic porosity log, deviating between the 1:1 regression line of the core data (Figure 25). However, these data points in the core create unusual spikes, most likely resulting from vugs or fractures in the matrix.

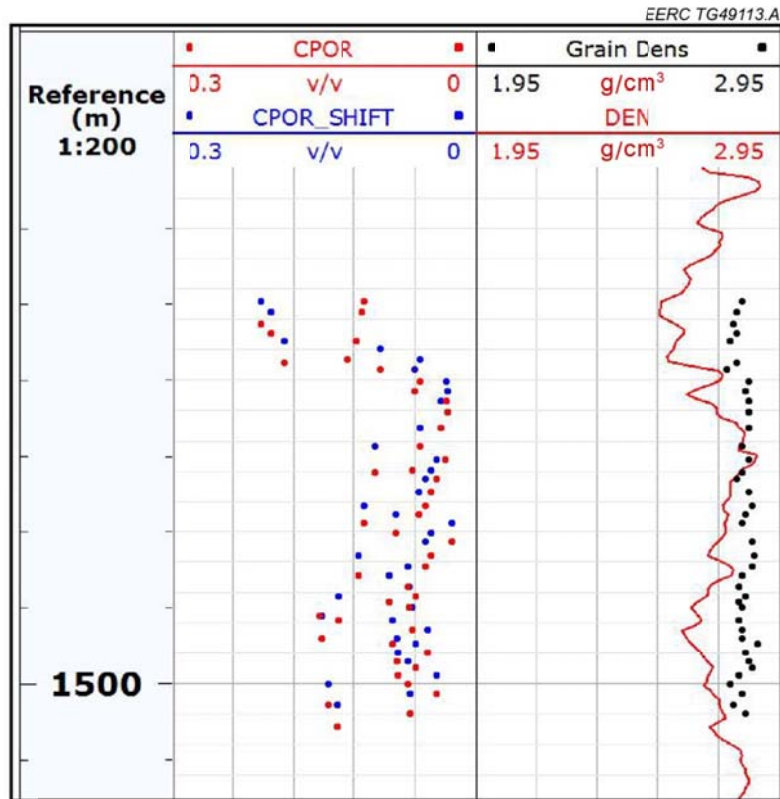


Figure 23. Depth shift of the core data to match with wireline logs. Well 100-11-25-116-6 in G2G pinnacle. Depth shift was 0.6 meters.

Porosity generated from neutron density logs and acoustic logs have been compared to understand the vuggy component present in the reservoir (Figure 26). The vuggy component, which can be derived by subtracting acoustic porosity from the neutron density porosity (Kerans and Tinkler, 1997), gives negative values, showing the presence of vugs in the reservoir (Figure 27). Because of the presence of vugs or fractures in the carbonate reservoir, the porosity property was also fine-tuned during the sensitivity analysis and multiplied by a factor ranging between 0.9 and 2 to match the OOIP of the reservoir calculated from production data and account for fractured or vuggy porosity.

As mentioned above, the North Dakota pinnacle reefs are a direct analog to Zama pinnacle reefs. Core photos taken from one of the North Dakota pinnacles show the presence of vuggy porosity in the reef (Figure 28). A similar approach as described above was applied for generation of a synthetic permeability log as well. The input logs for the neural networking were spontaneous potential, gamma ray, deep resistivity, neutron porosity, bulk density, and acoustic velocity. Permeability from the core analysis data was used to supervise the resulting permeability log (Figure 29).



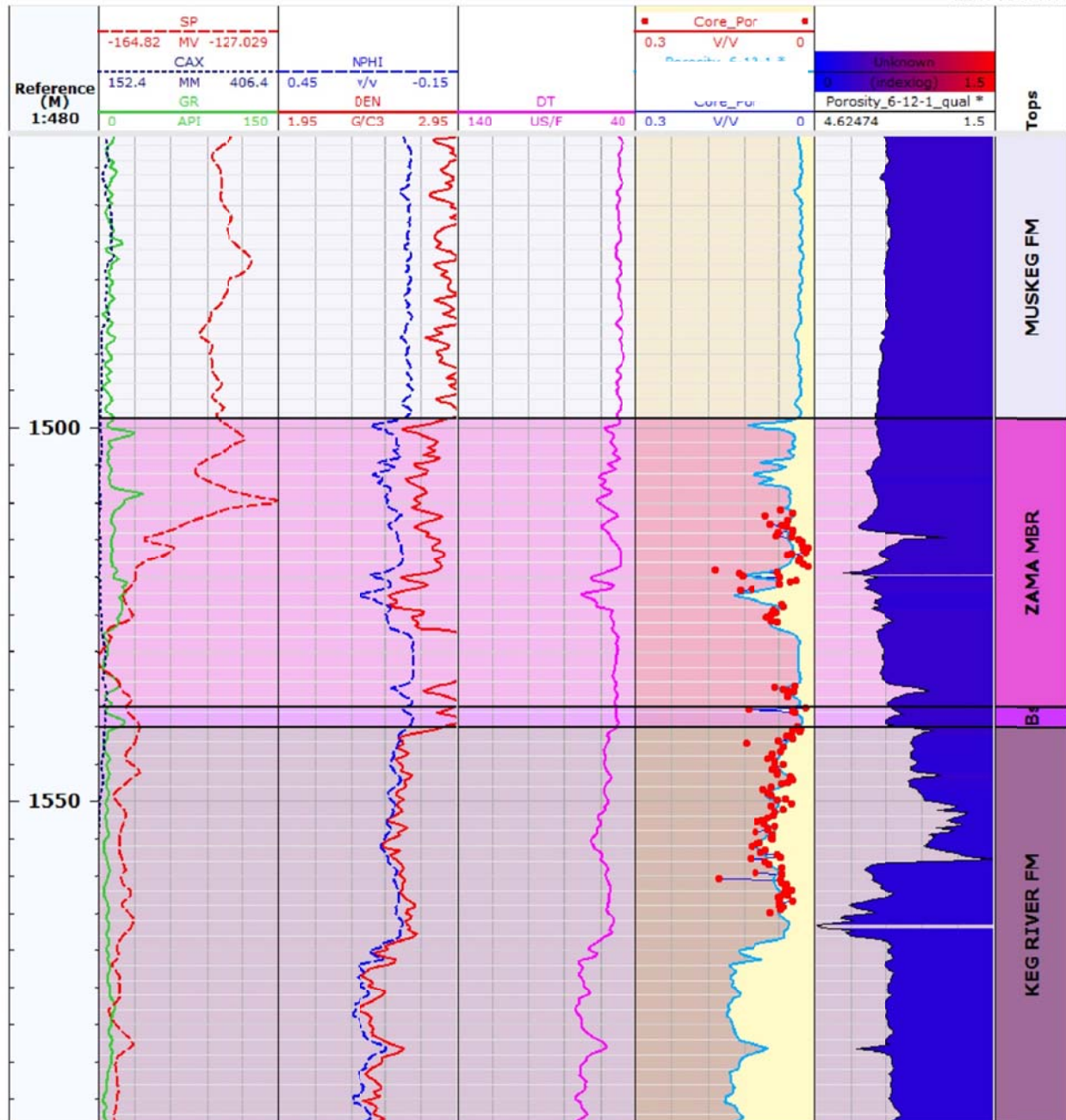


Figure 24. Porosity derived from the neural network approach. Input logs are shown in the first three tracks, the derived porosity and the core porosity in the fourth track, and the quality/accuracy of the generated log in the fifth track, followed by formation tops in the sixth track.

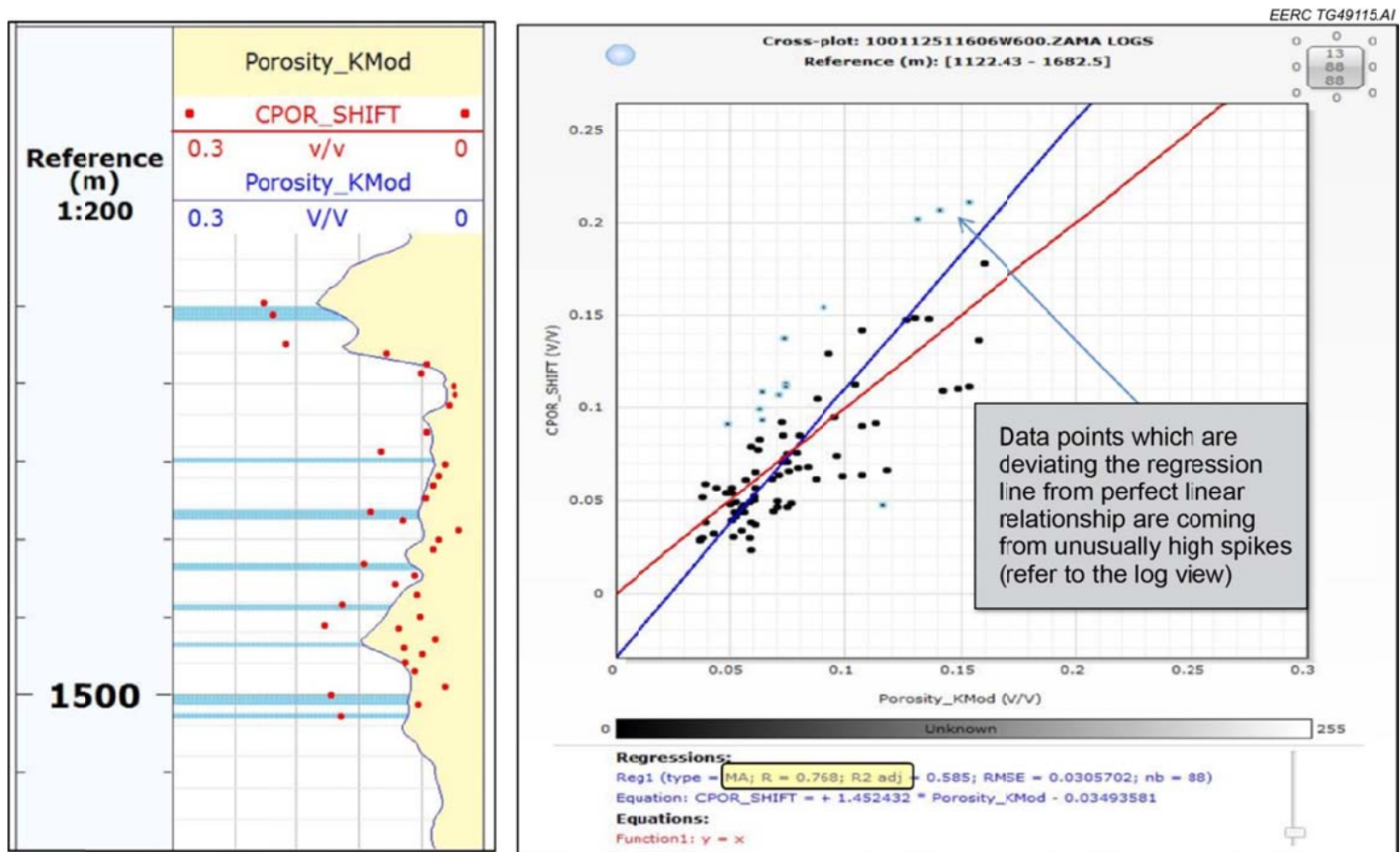


Figure 25. QC of the neural network-derived porosity.

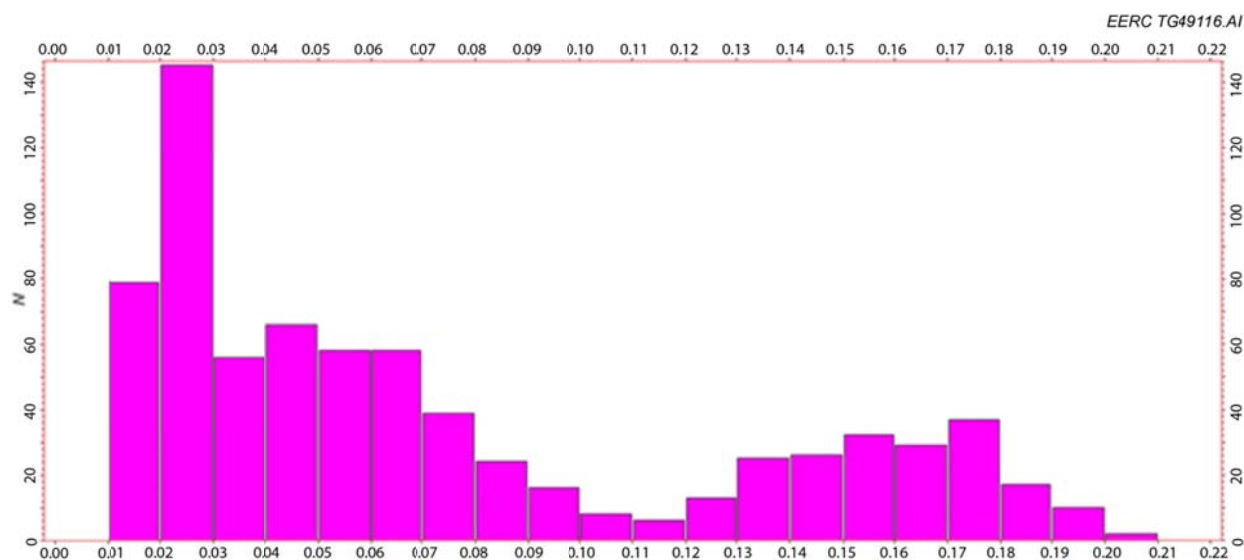


Figure 26. Histogram showing bimodal distribution of porosity due to interparticle and vuggy/fractured porosity.

The lithology of the model is designed in a hierarchical fashion. The model has two macrofacies: 1) reef which makes the pinnacle structural and 2) anhydrite, which is postdepositional to the pinnacle formation. The reef facies was further divided into good and poor reservoir microfacies utilizing the permeability and porosity crossplot to determine good or poor reservoir within the pinnacle (Figure 30). The following petrophysical properties will be geostatistically populated into the reservoir model: macrofacies, microfacies, porosity, permeability, and water saturation (Figure 31).

Figure 31 shows the permeability generated by the neural network approach. Input logs are shown in the first four tracks, the derived permeability and the core permeability in the fifth track, and the quality/accuracy of the generated log in the sixth track, followed by formation tops in the last track.

### ***Structural Model***

A 3-D grid was generated following the stratigraphic framework to build a structural model utilizing surfaces derived from seismic-based structural maps and well tops. The horizontal I, J grid spacing is 10 meters for G2G and 20 meters for Muskeg L. There are four different zones above the pinnacle in each model: 1) Anhydrite zone (and within pinnacle), 2) Zama Member zone, 3) Keg River zone, and 4) Mound zone. Zones are further divided by layers. The layer thickness is based on vertical variogram analysis, aiming at capturing heterogeneity with the smallest number of layers. The model parameters are shown in Table 3.

After building the structural model, logs were upscaled along the cells penetrated by the well trajectory. Macrofacies, microfacies, porosity, permeability, and water saturation logs that were generated during petrophysical analysis were upscaled into the structural model. Figure 32 shows different petrophysical logs correlated to the upscaled logs.



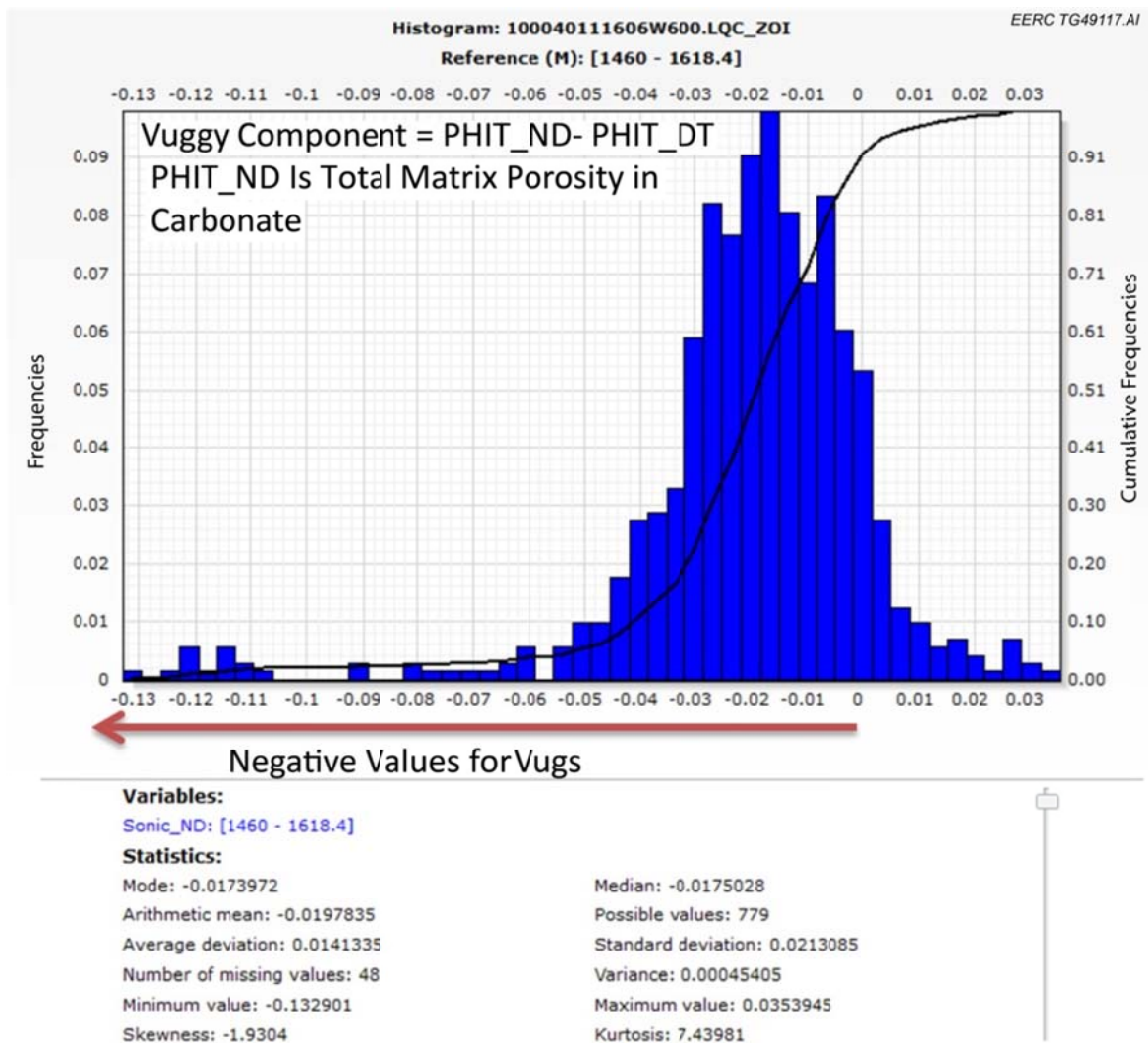


Figure 27. Presence of the vuggy component in the reservoir porosity.

### *Facies Modeling*

The MPS method was used to create a facies model for the pinnacle and assist in geostatistically populating the structural model with the data determined from the petrophysical analysis. The MPS method utilizes a training image or a representation of a pinnacle reef and creates a facies model similar to that of the training image (Figure 33). Along with the training image, the MPS will also acknowledge hard data (in this instance the microfacies well data) to help statistically populate the facies and guide the training image at the same time. This process helps when there are limitations in terms of data; few wells; limited seismic data; and complex carbonate geology.

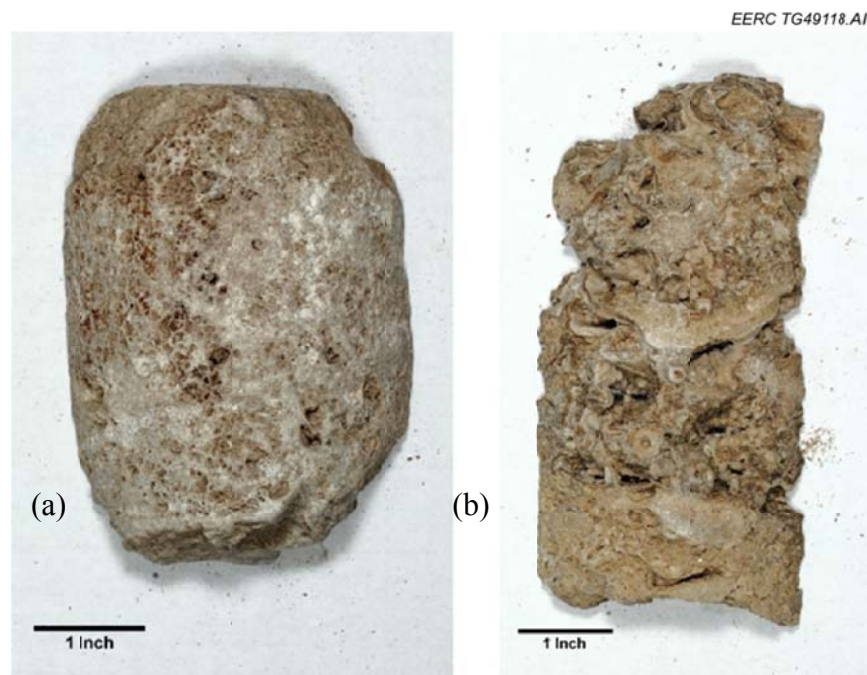


Figure 28. Vuggy reefal carbonate of North Dakota Devonian Winnipegosis Formation. Cores belong to Well 6535 (NDIC) from depths of a) 6515 ft and b) 6603 ft.

### ***Petrophysical Property Modeling***

Properties derived from the petrophysical analysis were populated geostatistically using the sequential Gaussian simulation (SGS) method. The SGS modeling method honors well data, input distributions, variograms, and trends. A random seed value is assigned, distributing the property stochastically. Because of minimal well data, variogram ranges were difficult to define, and hard data are limited. Running a sensitivity analysis on the variogram determined that the variogram range does not highly affect the overall volumetric properties of the reservoir. This made the variogram a statistical parameter that needed no fine-tuning. Additionally, the properties were conditioned by the poor and good reservoir microfacies. The ranges of each property are dependent on the upscaled log statistics and general statistical distribution for each zone. The permeability model has been conditioned with functional trends for both good and poor reef facies, based on the core porosity–permeability relationship (Figure 34).

Cross sections of the porosity, permeability, and water saturation petrophysical models for the Muskeg L pinnacle are shown in Figure 35. As the models are conditioned by the facies, they show notable similarity between all the petrophysical models.

### ***Volumetrics***

The volumetrics of each pinnacle were calculated for various scenarios. The results have been analyzed by varying the oil–water contact and a standard deviation of porosity. The

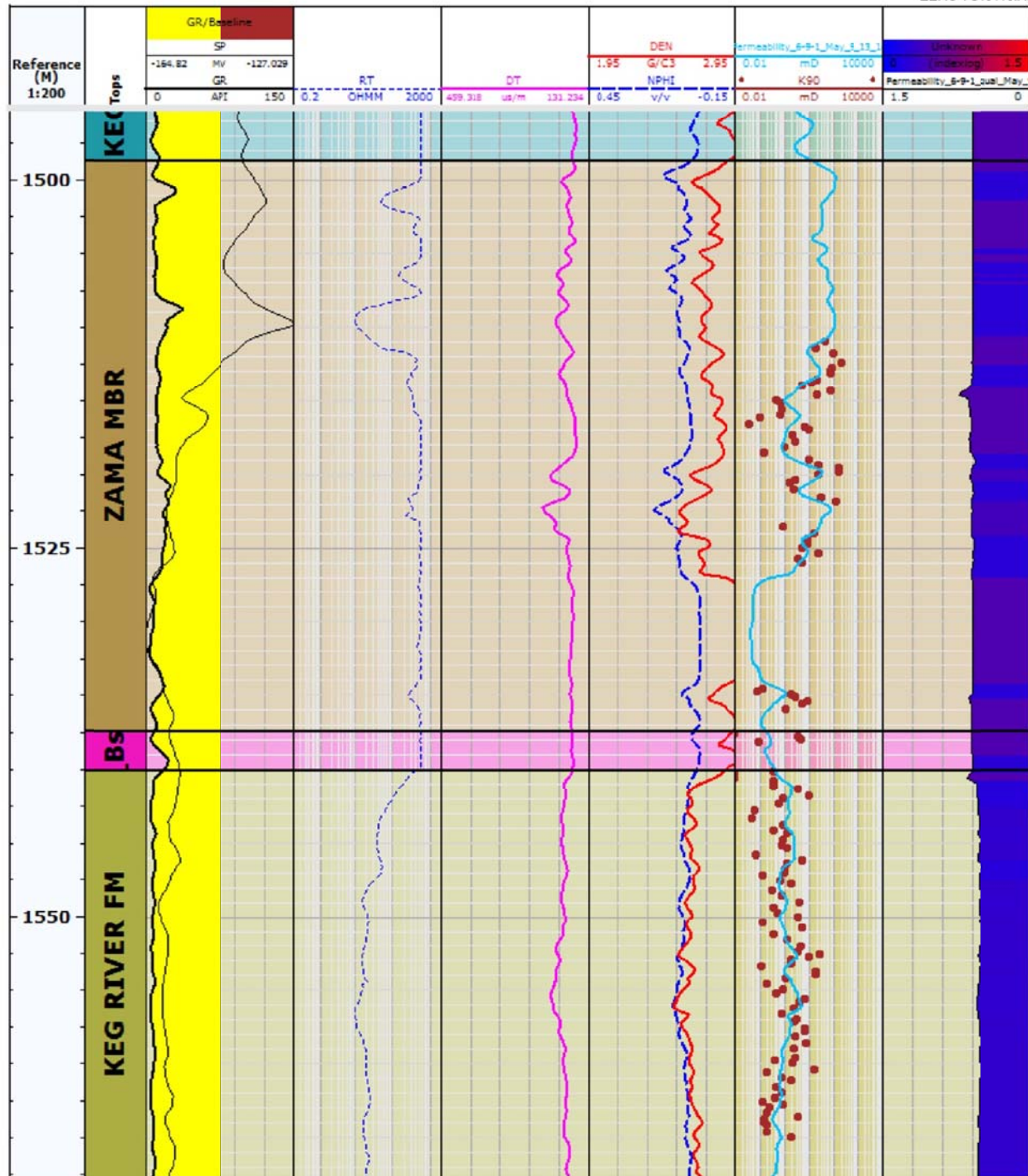


Figure 29. Resulting permeability log.

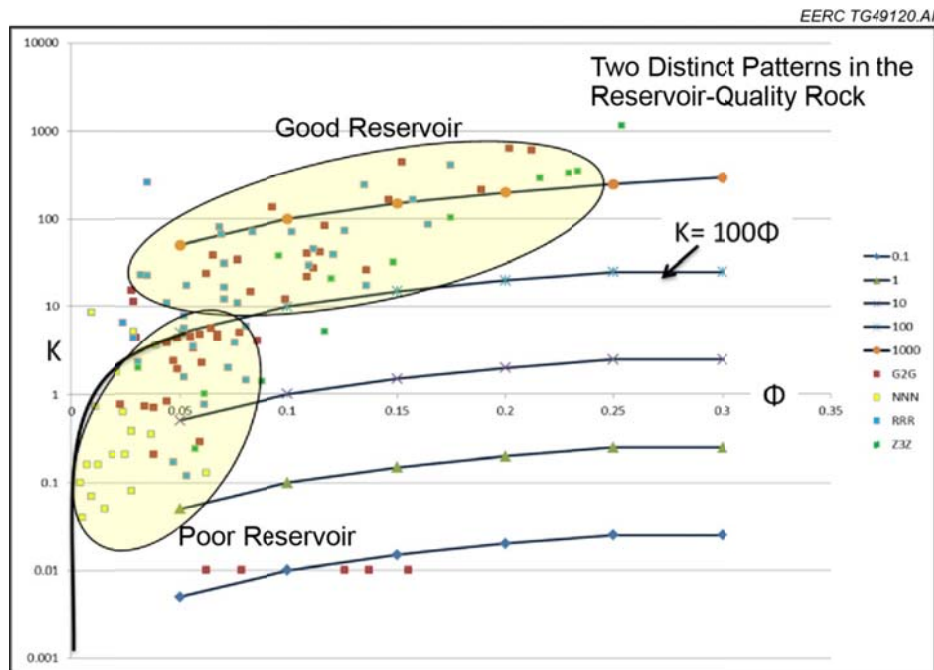


Figure 30. Crossplot between core porosity and core permeability to identify microfacies within the reef.

porosity and oil–water contact are the most uncertain variables, as only one well may not represent the oil–water contact in the entire reservoir and vuggy and fractured porosity are present in the carbonate reservoir, but in uncertain amounts. Table 4 shows the base case volumetrics, which are similar to reported OOIP from the AGS ERCB Annual Reserves Report (2012), thus validating the model to be passed on to dynamic simulation.

## Production Analysis

### *F Pool Production*

The F pool was discovered in 1967, and 1.1 MMstb of oil, which is 28% of OOIP (material balance calculation), was produced during a 20-year production period (1967–1987) with only one well (discovery well). F pool production is from a pinnacle reef in the carbonate Keg River Formation. A thick anhydrite of the Muskeg Formation overlies the Keg River Formation and serves as a cap rock for all of the pinnacle reefs in the Zama oil field. The F pool oil is of API (American Petroleum Institute) 35.2° gravity. The initial reservoir pressure and temperature were 2095 psi and 160°F, respectively. The initial gas/oil ratio (GOR) was 282 scf/bbl, and the saturation pressure was 1275 psi. The reservoir initially produced under depletion drive, and the pressure and production behaviors were indicative of poor aquifer support at the later production stage. The pinnacle schematic can be seen in Figure 36. The location of the F pool relative to other acid gas EOR candidates can be seen in Figure 37.



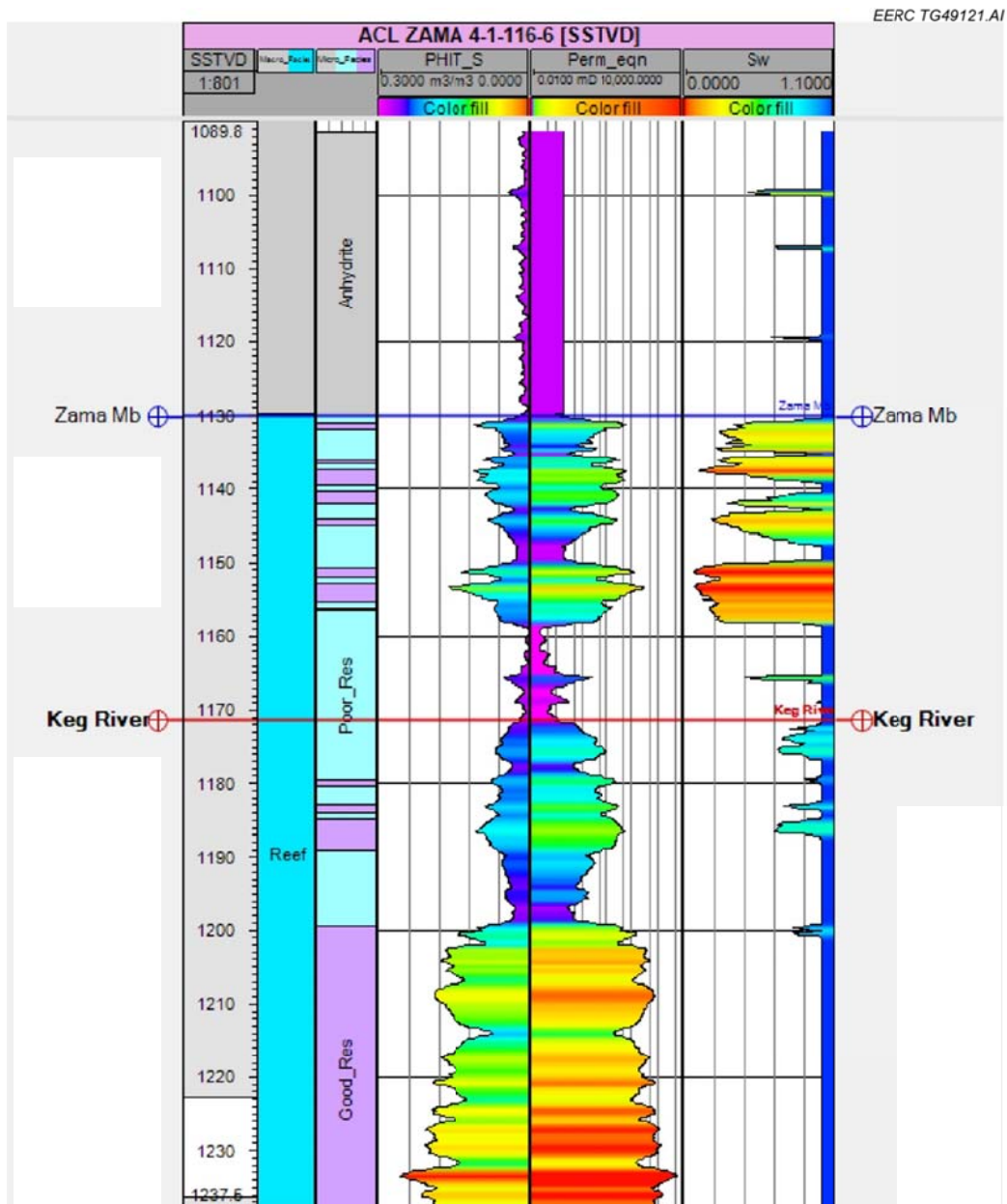
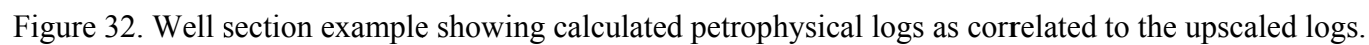


Figure 31. Petrophysical logs that were populated into each static model.

**Table 3. Static Model Parameters**

Model	(I, J) Grid Spacing	Zones	Total (K) Layers	Total Cells
G2G	32.8 ft. (10 meters)	4	86	185,760
Muskeg L	65.6 ft. (20 meters)	4	101	333,300



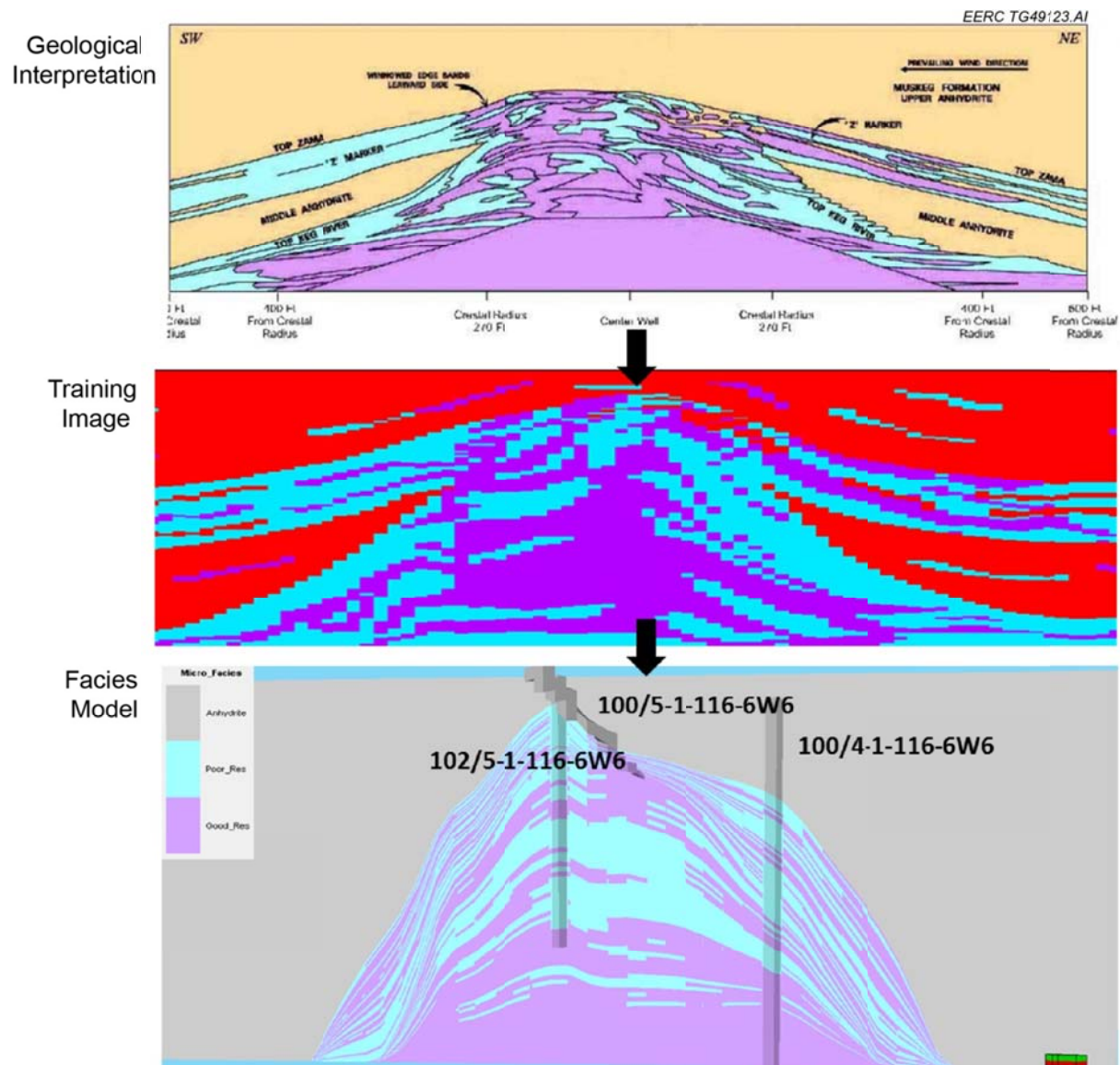


Figure 33. Conceptual geology of a pinnacle reef (top), training image from the conceptual geology (middle) and microfacies model of Muskeg L reef (bottom).

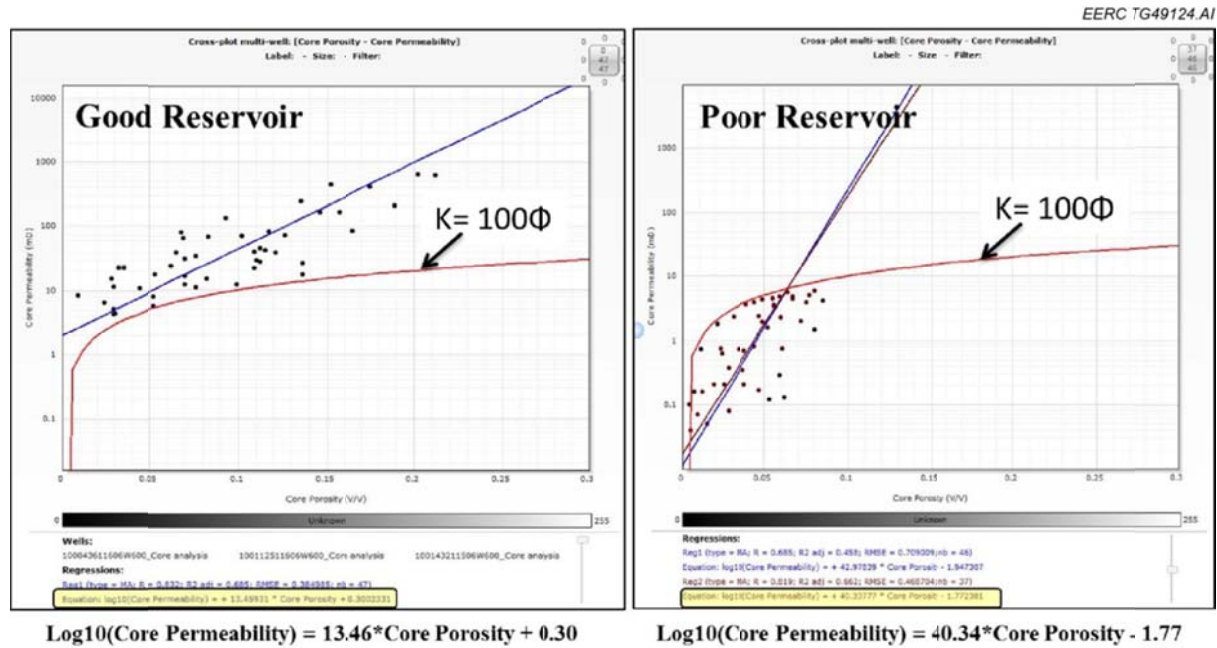


Figure 34. Regression equation for good-quality reservoir (left) and poor-quality reservoir (right) used as trend in petrophysical modeling of the permeability property.



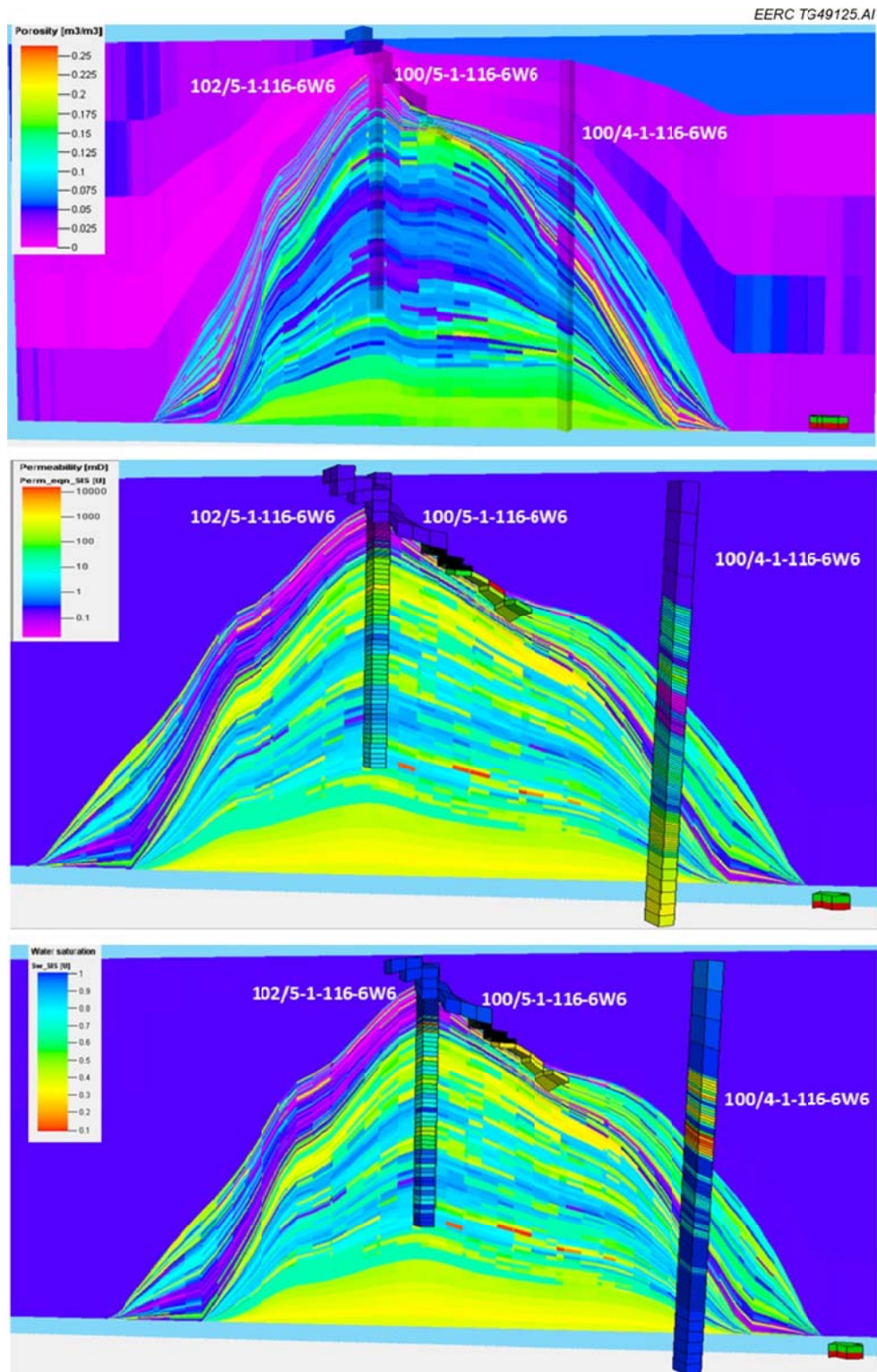
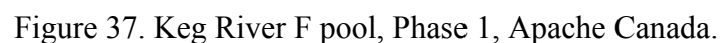
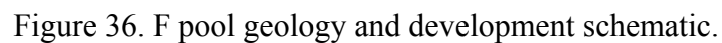


Figure 35. Petrophysical models of pinnacle Muskeg L for porosity (top), permeability (middle), and water saturation (bottom).

Results	Zama G2G	Zama Muskeg L
Area of the Pinnacle, ft <sup>2</sup>	3,637,341	2,435,776
Average Pay Thickness, ft	180	295
Bulk Volume, 10 <sup>3</sup> ft <sup>3</sup>	73,440	43,152
Pore Volume, 10 <sup>3</sup> Rft <sup>3</sup>	3747	3292
OOIP, 10 <sup>3</sup> bbl	3415	2698



The F pool discovery well (100/08-13-116-06-6W6) was placed on production in February 1967. Oil and associated gas were originally produced from the pool under primary depletion, with a peak oil rate of 945 bbl/d in 1968. In late 1986, Keg River oil production was shut in, and the well was completed as a saltwater disposal well in October 1987 by Dome Petroleum. The original reservoir pressure in the F pool was 2095 psig at datum depth of 3605.3 ft MSL (mean sea level). Reservoir pressures depleted with primary production through to the end of the 1980s. When oil production was suspended in October 1986, the reservoir pressure was 613 psia. This significant observed pressure depletion is the first indication of the reservoir having poor aquifer support. The F pool was then used for produced water disposal into the Keg River Formation until water injection operations were suspended in October 1991. Cumulative water injection was about 1.8 MMbbl. At that time, the F pool pressure had been increased to 3494 psi. This was 1.67 times the original pressure, with no evidence of leakage from the structure. This is direct evidence of the formation and cap rock strength and integrity far in excess of the EOR operating pressures. In 1992, Co-Enerco attempted unsuccessfully to produce Keg River oil from this location, with little incremental oil being produced. Waterflooding of small pinnacles in the area, such as the Zama Keg River F pool, was found to be challenging because of their small size and heterogeneity. In June 1997, the Keg River completion in the F pool was abandoned by Gulf Canada, and the well was completed as a gas-producing well in the Slave Point Formation (which directly overlies the Muskeg Formation), at which point it was redesignated as the FFF gas well. The gas completion watered out and was suspended in November 2006. The FFF completion is suspended at the surface and is now utilized as a monitoring well for potential leakage of injected acid gas from the Keg River F pool (Smith and others, 2009).

Apache Canada purchased the Zama Field from Phillips Petroleum in December 2000 and drilled a second well in the Keg River F pool in January 2002 at Well Location 100/01-13-116-06W6. This well encountered oil at the top and center of the F pool pinnacle. It was completed open and placed on production in March 2002. It was suspended in early 2004 after producing just 34,220 bbl of oil. This was another indication that the repressuring of the pool with water had failed to support and sweep by-passed primary oil production into the upper portion of the pinnacle. The fluid production from this production period lowered the Keg River F pool pressure to 16,500 kPa. A third F pool production well, at Location 103/01-13-116-06W6, was drilled and completed in September 2004. This third well targeted the south flank of the pool opposite the 100/08-13 discovery well. The well was placed on production in August 2005. Perforated low in the formation, it was a poor producer, with a cumulative oil production of about 470 bbl between August 2005 and May 2006. Beginning in November 2006, Well 103/01-13 was then utilized to draw water off the lower portion of the pinnacle to lower the average reservoir pressure down to the original ERCB-approved range of 13,700 to 14,450 kPa(g). This objective was accomplished by May 2006, but injection was not started until December 2006 when the Zama Keg River F pool was the third pool to be placed on acid gas EOR. The 100/01-13-116-06W6 well was recompleted in 2004 as the F pool acid gas injector but was not placed on injection until December 2006, following the depressuring period. The fourth and newest well in the pool, 102/08-13-116-6W6, was drilled in August 2008 to intersect the top of the pinnacle near the original 100/08-13 well. The well was designed to provide drainage of the upper part of the reef, which was not accessed by the discovery well but was first perforated near the original oil–water contact at –3566 ft. Table 5 shows the basic properties of the F pool.

**Table 5. F Pool Properties**

Play Type	Keg River Pinnacle Reef
Initial Reservoir Pressure	2095 psi (14,447 kPa)
Reservoir Temperature	160°F (71°C)
Initial Water Saturation	15% (from logs)
Porosity	10% (from logs)
Initial GOR	292.13 scf/bbl (52 m <sup>3</sup> /m <sup>3</sup> )
Initial Formation Volume Factor	1.183 rvol/stdvol
Bubble Point Pressure	11,275 psi (8791 kPa)
Oil gravity	35.2° API

### ***Muskeg L***

The Muskeg L pool was discovered in 1967 with an estimated OOIP of 2.7 MMstb. The pool had produced 754,740 barrels of oil during a 45-year production period (1967–2012) with two production wells. Production is from the Keg River Formation. Similar to the F Pool, the Muskeg Formation anhydrite overlies the Keg River Formation and serves as a cap rock. The Muskeg L pool oil has an oil gravity of 33.5° API. The initial reservoir pressure and temperature were 1988 psi and 170°F respectively. The initial GOR was 375 scf/bbl, and the saturation pressure was 1326 psi. The reservoir initially produced under depletion drive, and the pressure and production behaviors were indicative of poor aquifer support at the later production stage. The location of the Muskeg L pool relative to other acid gas EOR candidates can be seen in Figure 37.

The Muskeg L pool discovery well (100/04-01-116-06W6/00) was placed on production in April 1967. Oil and associated gas were originally produced from the pool under primary depletion, with a peak oil rate of 286 bbl/d in May 1973. In late 1986, Keg River oil production was shut in, and the well was completed as a saltwater disposal well in October 1987 by Dome Petroleum. The original reservoir pressure in the Muskeg L pool was 1988 psig at datum depth of 4938 ft MD (measured depth). Reservoir pressures depleted with primary production through to the end of the 1980s. The Muskeg L pool was then used for produced water disposal into the Keg River Formation until water injection operations were suspended in 2004. Cumulative water injection was about 1.26 MMbbl.

Similar to the F pool, after the Apache Canada purchased the Zama Field from Phillips Petroleum in December 2000, the second well was drilled in the Muskeg L in January 2002 at Well Location 100/05-01-116-06W6/00. This well encountered oil at the top and center of the Muskeg L. It was completed and placed on production in February 2002. It was suspended in early 2008 after producing 95,811 bbl of oil. In May 2010, it was converted to a gas injection well. A third production well 102\_05-01-116-06W6\_00 was drilled and completed in 2010. This third well targeted the south flank of the pool opposite the 100/08-13 discovery well. The well was placed on production in August 2010. Perforated low in the formation, it was a poor producer, with a cumulative oil production of about 30,257 bbl between August 2010 and May 2012. At the early beginning of the production, the bottom of the discovery well was used to inject produced water.

## G2G Production

The G2G pool was discovered in 1968 with a 3.71 MMstb of OOIP. During a 34-year production period (1968–2012), 1.27 MMstb of oil was produced with one production well. Production is from the Keg River Formation. Similar to both the F and Muskeg L Pools, the Muskeg Formation anhydrite overlies the Keg River Formation and serves as a cap rock. The G2G pool oil is 32.9° API gravity. The initial reservoir pressure and temperature were 2026 psi and 160°F respectively. The initial GOR was 414 scf/bbl, and the saturation pressure was 1615 psi. The reservoir initially produced under depletion drive, and the pressure and production behaviors were indicative of poor aquifer support at the later production stage. The location of the G2G pool relative to other acid gas EOR candidates can be seen in Figure 37.

The G2G pool discovery well (100/11-25-116-06W6/00) was put into production in April 1968. Oil and associated gas were originally produced from the pool under primary depletion, with a peak oil rate of 569 bbl/d in May 1970. In late 1986, Keg River oil production was shut in until 2006. There was a short production (January–August 1993) in this time span with an average oil rate of 50 scf/bbl. The original reservoir pressure in the G2G pool was 1988 psig at datum depth of 5515 ft MD. Reservoir pressures depleted with primary production through to the end of the 1980s.

After the Apache Canada purchased the Zama Field from Phillips Petroleum in December 2000, the second well (102/11-25-116-06W6/00) was drilled in the G2G in early 2002. This well encountered oil at the top of the Zama Member. It was completed and placed on production in

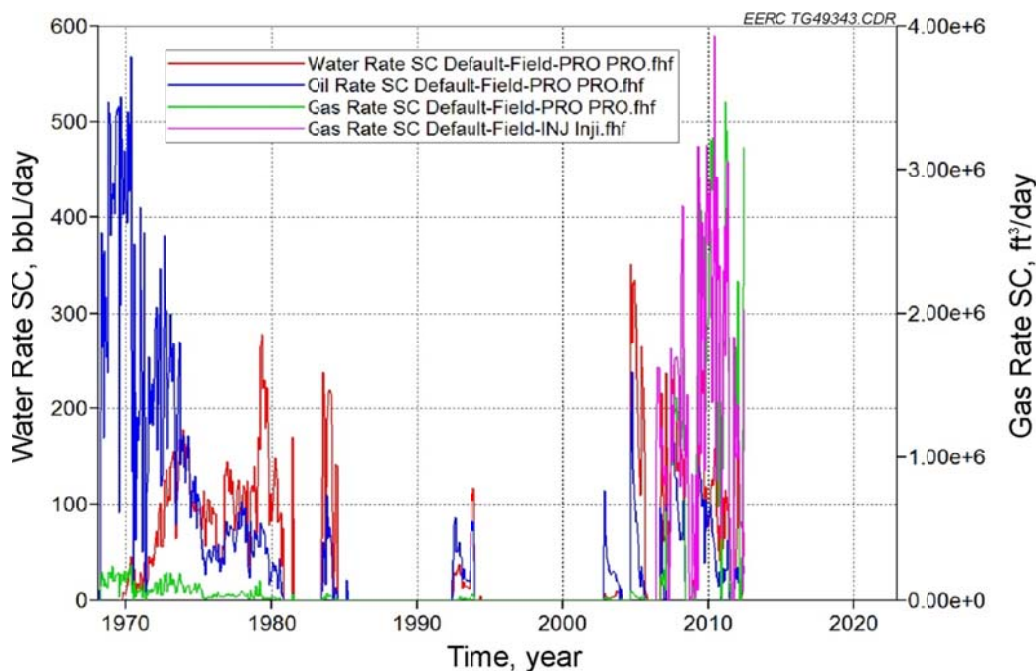


Figure 38. Production rate of oil, gas, and water from the G2G pool (SC refers to standard conditions).



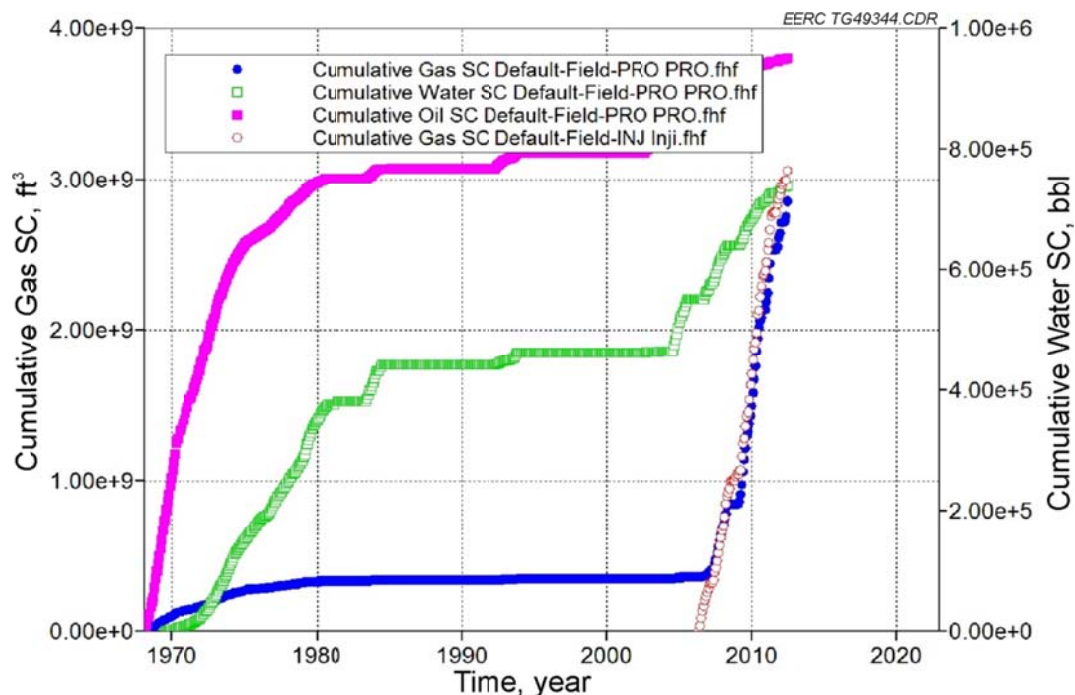


Figure 39. Cumulative production of oil, gas, and water from the G2G pool.

October 2002. It was suspended in June 2005 after producing 44,484 bbl of oil. In May 2006, it was converted to a gas injection well. The pool's production history is detailed in Figures 38 and 39.

The production information is summarized by pool in Table 6, which is collected by well, start date of production, current status, cumulative oil production, OOIP, primary recovery factor, and EOR recovery to date.

## PVT Modeling

### *Simulator and EOS*

Development of accurate EOS models is an integral part of the compositional reservoir simulation process, as they are necessary input for a dynamic model to accurately define fluid properties and phase behaviors at varying reservoir conditions. The PVT data for crude oil samples from each pinnacle are available and were used to define PVT relationships under reservoir conditions of each pool. Constant composition expansion, differential liberation (DL) analysis, separator, and fluid compositional analysis data were also available for oil samples. A seven-component Peng–Robinson EOS model was developed and tuned based on the available experimental PVT data using WinProp™, a phase property program developed by CMG. CMG WinProp uses cubic EOS to perform phase equilibrium and property calculations.

In efforts to reliably predict the phase behavior of different fluids, two models were set for G2G and Muskeg L, respectively. Tuned EOS models were further validated by predicting MMPs for pure CO<sub>2</sub> and acid gas (different proportions) mixtures.

**Table 6. Summary of Production and Injection for Five Pools**

Pool	Well	Production Start	Production End	Current Status	Cum, Oil Prod. Well (pre-acid gas injection), bbl	Cum, Oil Prod. Well, bbl
Z3Z	100/05-34-115-06W6/00	1969-11	1992-10	Converted into acid gas injector 1998-04	1,205,478	1,205,478
	1W0/05-34-115-06W6/00	2004-06		Oil producer	0	424,915
	100/08-33-115-06W6/00	2009-04		Oil producer	0	98,691
	TOTAL				1,205,478	1,729,084
RRR	100/14-32-115-06W6/00	1967-11		Oil producer	1,059,715	1,107,958
	100/11-32-115-06W6/00	1982-04	1994-12		472,626	472,626
	102/14-32-115-06W6/02	2001-06	2006-01	Converted into acid gas injector 2007-06	86,910	86,910
	TOTAL				1,619,250	1,667,494
NNN	100/04-36-116-06W6/00	1967-11		Oil producer (shut in 1987-08 to 2011-02)	1,230,564	1,253,607
	102/04-36-116-06W6/00	2001-12	2005-10	Converted into acid gas injector 2006-11	165,885	165,885
	100/04-36-116-06W6/04	2008-12		Oil Producer	0	60,778
	TOTAL				1,396,449	1,480,271
G2G	100/11-25-116-06W6/00	1968-03		Oil producer (shut in 1984-07 to 1992-04 and 1994-01 to 2006-09)	1,059,057	1,207,406
	102/11-25-116-06W6/00	2002-10	2005-10	Converted into acid gas injector 2006-06	59,309	59,309
	TOTAL				1,118,366	1,266,715

Continued. . .

**Table 6. Summary of Production and Injection for Five Pools (continued)**

Pool	Well	Production Start	Production End	Current Status	Cum, Oil Prod. Well (pre-acid gas injection), bbl	Cum, Oil Prod. Well, bbl
Muskeg L	100/04-01-116-06W6/00	1967-04		Oil producer (shut in 1983-08 to 1985-09 and 1987-12 to 2012-01)	69,176	594,684
	100/04-01-116-06W6/02			Acid gas injector (injection started 1969-10), CURRENTLY NO GAS INJECTION	0	0
	100/05-01-116-06W6/00	2002-02		Oil producer (under shut in conditions since 2008-03)	0	119,927
	102/05-01-116-06W6/00	2010-08			0	40,341
	TOTAL				69,176	754,952
F	100/08-13-116-06W6/00	1967-02		Oil producer (shut in during 1987-10 to now)	1,431,889	1,431,889
	103/01-13-116-06W6/00	2005-8		Oil Producer	625	3,581
	100/08-13-116-06W6/00	1987-10		Water injection (under shut-in conditions between 1991-1 and 1997-12 )	0	0
	100/01-13-116-06W6/00	2006-12		Acid gas injection (stopped injection in 2009-6)	0	0
	TOTAL				1,432,514	1,435,470



The mole fractions of all six pinnacles (G2G, Muskeg L, NNN, RRR, Z3Z, and F) are listed in Table 7. In this study, the G2G and Muskeg L pools have been given more attention. Compositional analyses of G2G and Muskeg L provided by Apache Canada show that the reservoir produces acidic, black crude oil with a mole fraction of liquid hydrocarbons (C<sub>7+</sub>) for all samples greater than 25%. Both G2G and Muskeg L pools have seven pseudo components after grouping. The components include H<sub>2</sub>S, CO<sub>2</sub>, N<sub>2</sub>-C<sub>2</sub>H, C<sub>3</sub>H-NC<sub>4</sub>, IC<sub>5</sub>-C<sub>6</sub>, C<sub>7</sub>-C<sub>17</sub>, and C<sub>18+</sub>. The regression models are tuned to meet the accuracy requirement. The model showed less than a 5% variance between experimental data and calculated results of EOS after tuning.

Comparative results between the EOR-tuned simulation results and the PVT experimental data are presented in Figures 40 (G2G) and 41 (Muskeg L).

### ***Minimum Miscibility Pressure***

Injection processes are most effective to enhance recovery when the injected acid gas is nearly or completely miscible with the oil in the reservoir. It is well-known that the behavior of gas miscibility is highly pressure-dependent and is expressed as MMP, which defines the pressure at which miscibility is achieved. By determining MMP in context with the study area, miscibility between each pinnacle crude oil and injected acid gas can be better understood.

Injected acid gases interact with reservoir fluids in either a miscible or an immiscible process. The fashion and efficiency of this system is highly dependent on reservoir conditions (pressure and temperature) but also is a function of gas and oil composition. For instance, high-molecular-weight oil and oils already containing dissolved gas such as methane and nitrogen tend to have higher MMPs. Therefore, it is necessary that the EOS model developed to perform phase equilibrium and property calculations should also be able to reasonably predict the MMP for better representation of compositional changes occurring in the reservoir during an acid gas injection displacement process.

**Table 7. Compositional Data of All Five Pinnacles**

Components	Mole Fraction, %					
	G2G	NNN	RRR	Muskeg L	Z3Z	F
H <sub>2</sub> S	1.61	2.06	19.33	2.52	6.68	2.39
CO <sub>2</sub>	2.17	2.26	1.42	0.65	0.68	1.25
N <sub>2</sub>	1.12	0.5	0.32	0.53	0.33	0.54
CH <sub>4</sub>	23.47	26.19	25.76	21.56	27.27	20.95
C <sub>2</sub>	6.79	6.32	5.93	6.89	6.90	5.90
C <sub>3</sub>	5.16	4.97	3.80	5.61	5.02	4.61
i-C <sub>4</sub>	0.95	1.14	0.98	1.32	1.28	1.18
n-C <sub>4</sub>	3.01	2.69	2.52	3.16	3.39	2.88
i-C <sub>5</sub>	1.16	2.01	1.59	2.51	1.69	1.81
n-C <sub>5</sub>	1.59	1.78	1.59	2.53	1.84	1.96
C <sub>6</sub>	3.42	3.83	3.14	4.40	3.61	4.30
C <sub>7+</sub>	49.55	46.05	33.62	48.32	41.31	52.23

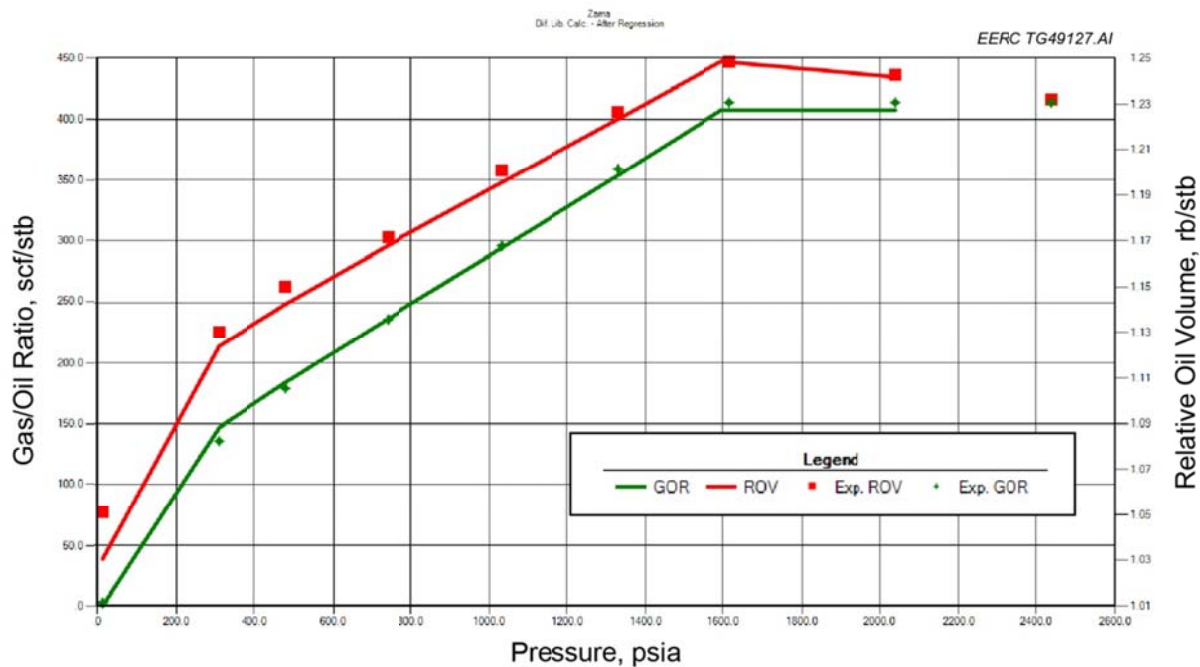


Figure 40. Regression on GOR and oil formation volume factor for G2G pool (ROV is relative oil volume).

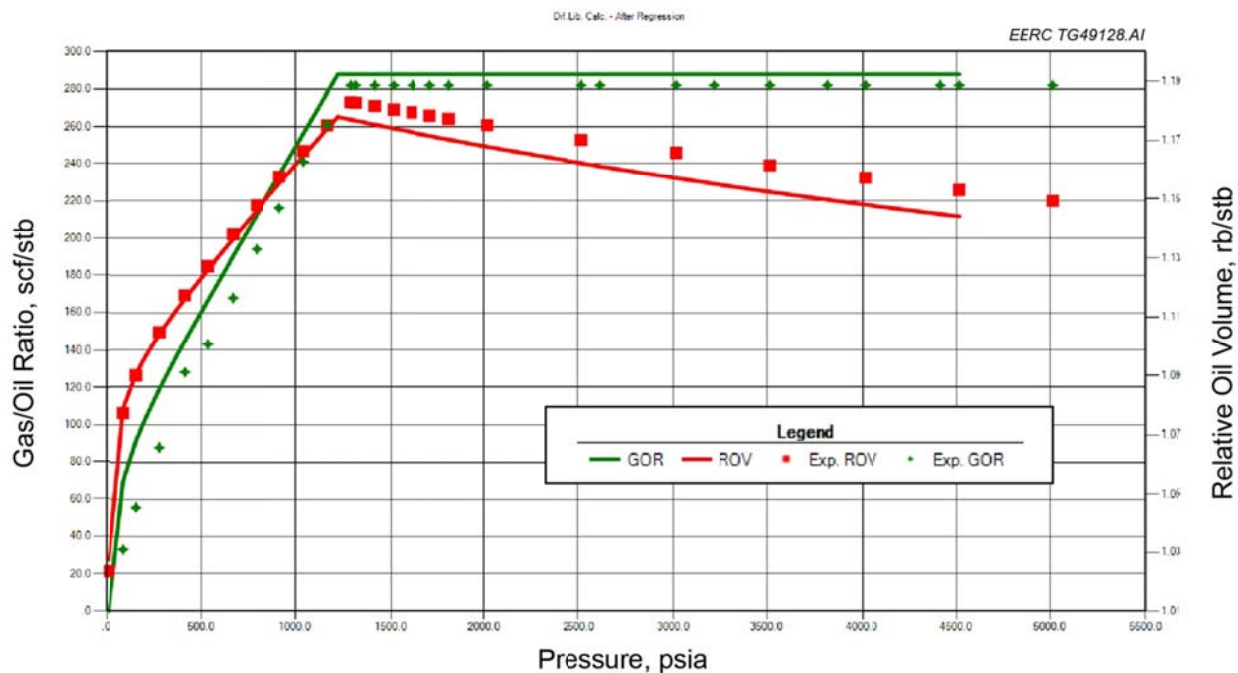


Figure 41. Regression on GOR and oil formation volume factor for Muskeg L pool.

On the basis of collected experimental data, the initial solution GOR of 414 scf/bbl as a function of pressure was determined from the DL experiment. After the regression of PVT tests, the predicted MMP of pure CO<sub>2</sub> for original oil of the G2G pool was 2660 psia. MMP of pure CO<sub>2</sub> for original oil of Muskeg L pool was 2780 psia.

### ***Effect of H<sub>2</sub>S on MMP***

The injection solvent supplied from a nearby gas plant is expected to produce CO<sub>2</sub>–H<sub>2</sub>S streams with a range of compositions because of a number of operational factors. H<sub>2</sub>S makes up a large portion of the injectant. Simulation work to better understand the effect of H<sub>2</sub>S on the phase behavior and MMP was carried out. The results can be used to evaluate the potential of applying miscible CO<sub>2</sub>–H<sub>2</sub>S flooding in G2G and Muskeg L in further work. The measurements were simulated via the two simulators discussed previously in the modeling process, six scenarios of different CO<sub>2</sub>–H<sub>2</sub>S gas ratios were considered: pure CO<sub>2</sub>, and CO<sub>2</sub> containing 20 and 40 mol% H<sub>2</sub>).

According to the simulation model, the MMP decreased almost linearly with the amount of H<sub>2</sub>S in the injection gas in the range of compositions studied. The trends of MMP change from two simulators showed consistency. The results show that miscible flooding with sour acid gas is feasible in the Zama pools and could provide an excellent means of storing/sequestering these gases while improving oil recovery. The simulated MMPs were found to be 4.1% higher and 5.5% lower than the measured values for pure CO<sub>2</sub> and the tested acid gas mixture, respectively.

The CO<sub>2</sub> MMP of the Muskeg L oil at 160°F was 2780 psia, while that of the G2G oil was 2660 psia at its reservoir temperature of 169°F. These results are in line with the common observation that the CO<sub>2</sub> MMP increases with increasing temperature, although in this case, the two recombined reservoir fluids have somewhat different compositions.

Addition of 20 mol% H<sub>2</sub>S to the CO<sub>2</sub> had the effect of reducing the MMP for both oils to 2150 psia for the Muskeg L oil and 2020 psia for the G2G oil at their respective reservoir temperatures. Injection of 40 mol% 60 mol% CO<sub>2</sub> gas further reduced the MMP to 1700 psia for the Muskeg L oil and 1650 psia for the G2G oil. From the data summary presented in Figure 42, it is observed that the MMP drops almost linearly with the mole fraction of H<sub>2</sub>S in the injection gas.

### ***Effect of Pressure Depletion on MMP***

Because of the mobility difference of the single component of reservoir fluid, the composition of produced fluid varies by production stages. A clear clue is the change in GOR during depletion, which reflects the reservoir fluid phase variations due to change in reservoir pressure. During primary depletion and secondary waterflood processes, the monitoring of dissolved gas is one of the important indices in production management since the reservoir pressure and GOR data provide essential value in the design of tertiary development, especially with a solvent injection project.

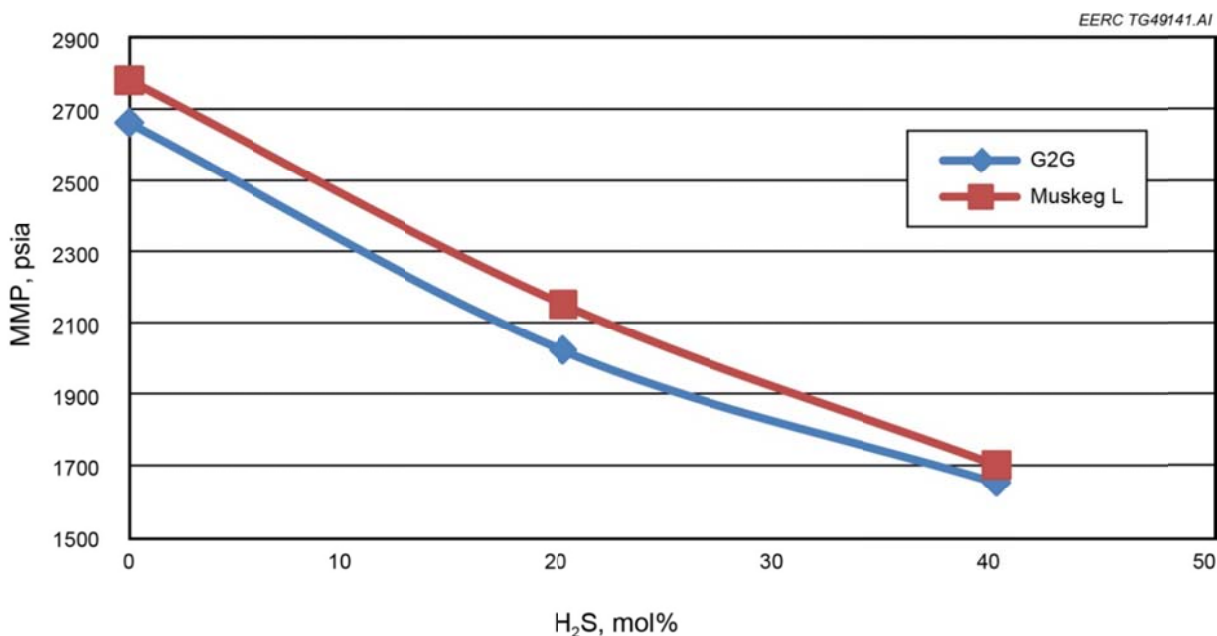


Figure 42. H<sub>2</sub>S effect on CO<sub>2</sub> MMP.

According to the model, the compositions of the Zama G2G pool significantly changed because of a long term of depletion. Typical PVT studies are performed on the initial recombined oil, representative of the composition at the time of early development. A simulation-based investigation of the phase behavior aspects of injected acid gas and liberated oil, representative of the composition at a given depletion pressure, will be used for developing more robust EOS PVT models. The use of robust PVT models in compositional simulations will greatly assist in determining optimum production and injection pressure schemes, thus maximizing both oil recovery and CO<sub>2</sub> storage volumes. The main objective of this part of the modeling investigation is to aid in pool pressure depletion and repressurization to effectively utilize previously stored acid gas for EOR purposes at other depleted pools.

A significant change in the oil composition, especially the production of light hydrocarbon components because of depletion, greatly affects the MMP between the residual oil and solvent (acid gas [CO<sub>2</sub>–H<sub>2</sub>S]). The following procedures were utilized to investigate this aspect of PVT modeling in the efficient EOR design of the Zama pools. The modeling procedures are as following:

1. The model was tuned to meet the regression accuracy, as achieved above.
2. The oil was numerically flashed to ambient pressure at reservoir temperature conditions (low pressure, incremental to reduce error).
3. The pressure value was picked as the system reading showed a current GOR of 200 scf/bbl.

4. The model fraction of Step 3 residual oil was generated.
5. The tuned model was refilled with the mole fraction of residual oil to predict new MMP at current reservoir conditions.

While GOR and the required reservoir pressure are complicated in terms of reservoir heterogeneity and past and future management, this value should be a target to reach, exceed, and maintain to maximize production. In the event that compartmentalized blocks have been shown to produce low gas or dead oil, miscibility may be significantly lower, as predicted, and may be reasonably managed as such if lower pressures are determined to be practical.

The simulation results show that the MMP between pure CO<sub>2</sub> and G2G oil is dropped from 2660 to 1950 psia when the GOR dropped from 414 to 200 scf/bbl. The MMP of Muskeg L was dropped from 2780 to 1700 psia when the GOR dropped from 375 to 200 scf/bbl.

## **History-Matching Process**

### ***Approaches***

In order to get reliable simulation results, history matching is performed on the basis of integral data collection, which is beyond a simple process of parameter adjustment in the G2G and Muskeg L pool modeling. History matching, which reduces the geologic uncertainties, which will allow for more accurate prediction of future reservoir performance during primary depletion and gas injection, was run using the dynamic reservoir model described previously. The history match was performed utilizing production and injection rates from the field dates spanning from 1968 to 2012.

The reason behind simulating the full history was to provide an estimate of fluid saturation and reservoir pressure for acid gas injection and to provide an accurate representation of the current reservoir conditions. During the history match period, oil production rates were used as primary constraints, and BHPs were used as the secondary constraints. Historical oil production and water rates of each well were used to compare with the simulation results for the effectiveness of the model and to determine the parameters that need to be adjusted. After a number of simulation runs, which included adding all the stimulations during the production period, modifying the geologic model, and tuning the PVT models with the special core analysis data and simulator numerical setting. An analytical bottom water is used in the history match process to dynamically reflect the oil–water contact change.

### ***Results***

An agreeable match of the production history was obtained. The matched indices of the G2G pool are shown graphically in Figures 43–46 and briefly discussed here. The simulated and actual water cut of the field is shown in Figure 46; the symbols represent the field data, while the curves represent the simulation results. This figure shows a good match between the actual water cut and the simulated water cut. The resultant oil production rate and real production rate are

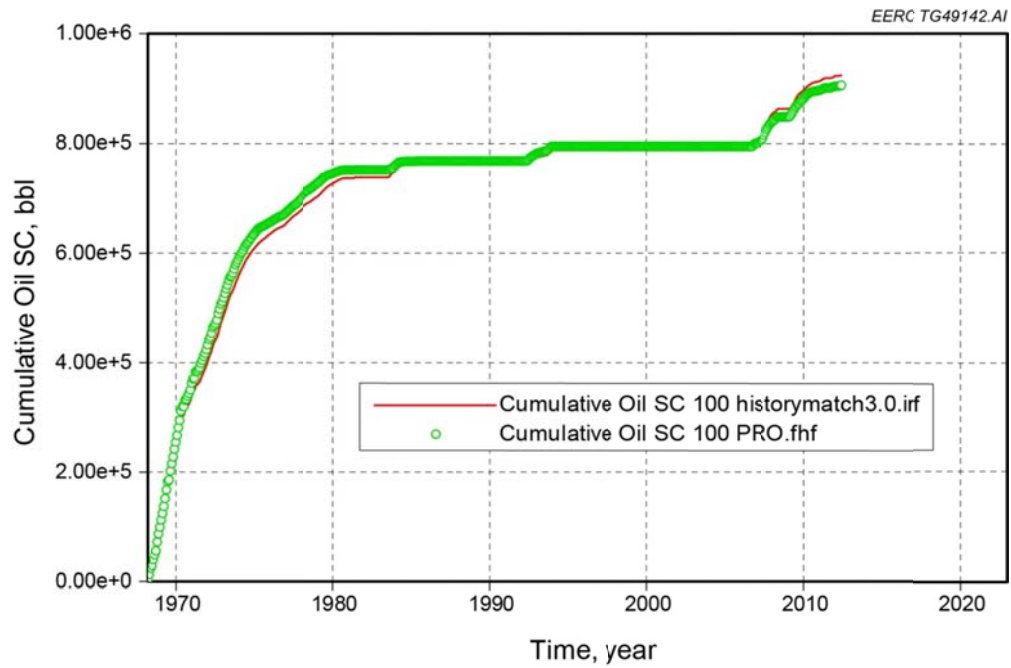


Figure 43. History match of cumulative oil production for the G2G pool.

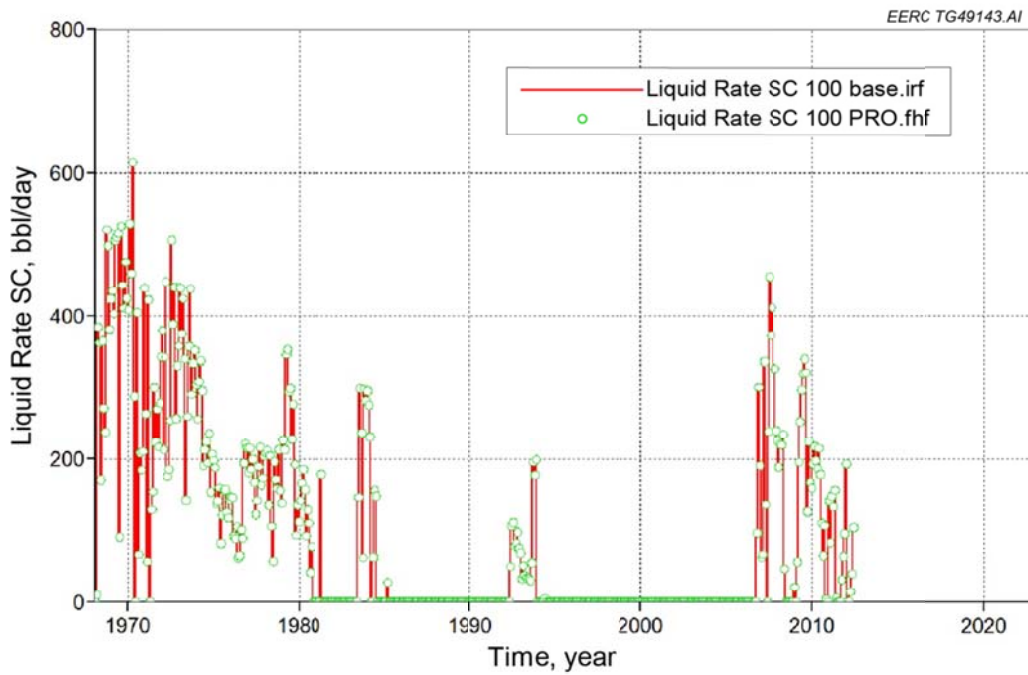


Figure 44. History match of liquid rate for the G2G pool.

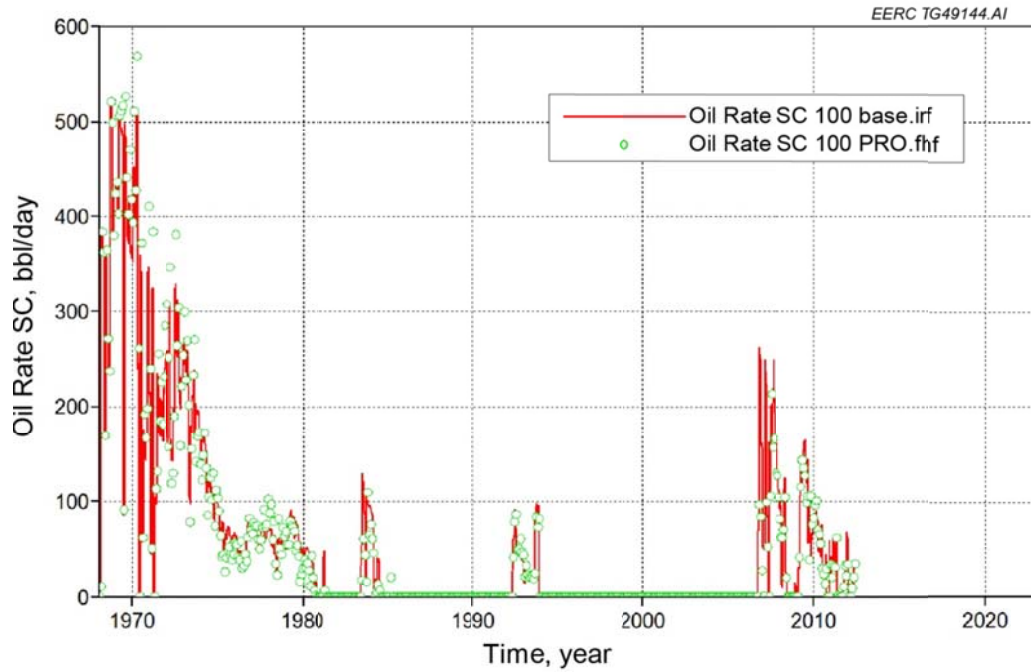


Figure 45. History match of oil rate for the G2G pool.

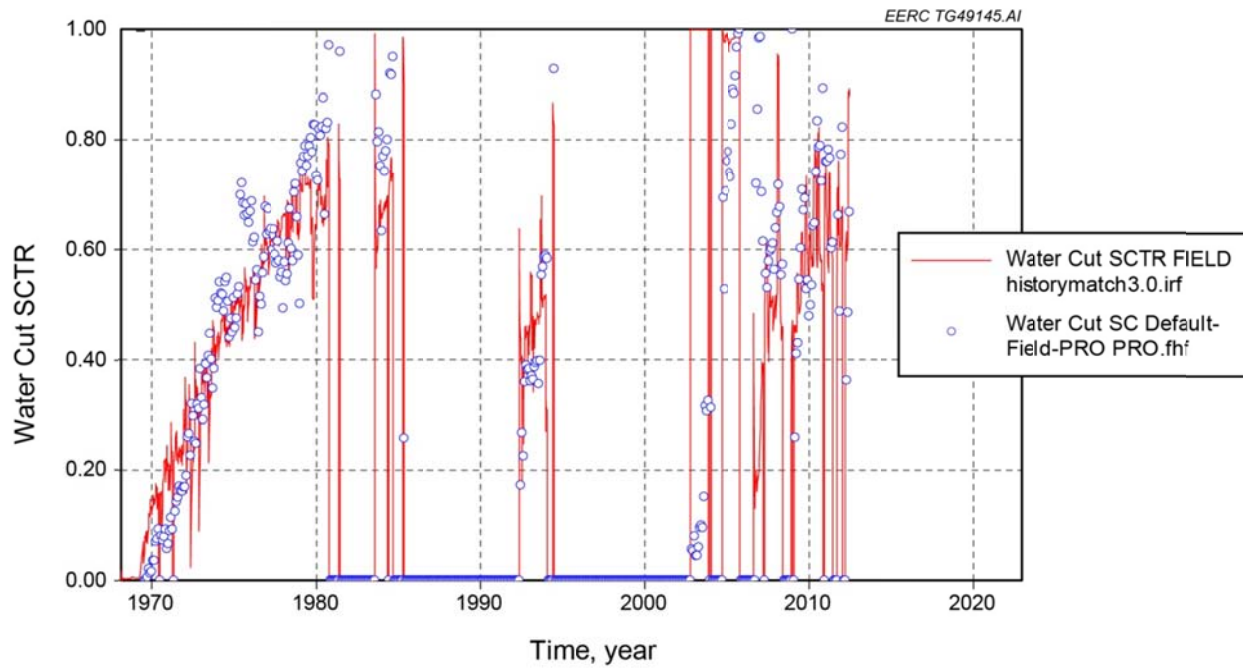


Figure 46. History match of water cut for the G2G pool (SCTR refers to sector).



plotted versus time in Figure 45. The actual production rate and the simulated production rate have a good match because the oil production rate is specified as input based on the actual production record. Similarly, the history-matching results of the Muskeg L pool are shown in Figures 47–50, and the history-matching results of the F pool are shown in Figures 51 and 52.

## F Pool Prediction

### *Formation Water Extraction Assisted by Acid Gas Injection (no oil production)*

This modeling used Version 1 static and dynamic models. The Version 1 static model consists of an oil zone (Zama and Keg River Formations) at the top portion of the reef and lower Keg River aquifer (below oil–water contact). This static geologic model had 616,512 ( $104 \times 104 \times 57$ ) cells. The cells were 50 ft  $\times$  50 ft in the I and J directions, with varying thickness (the K direction) ranging from 3 ft for the zone above the oil–water contact to 19 ft for the zone below the oil–water contact. One of the equiprobable realizations of the constructed static geologic model was then exported to CMG GEM for performing dynamic simulations to evaluate the viability of formation water extraction through acid gas injection (no oil production) in general and at  $R_{g/w}$  (ratio of acid gas injected to extracted water at reservoir conditions) near to 1:1 in particular.

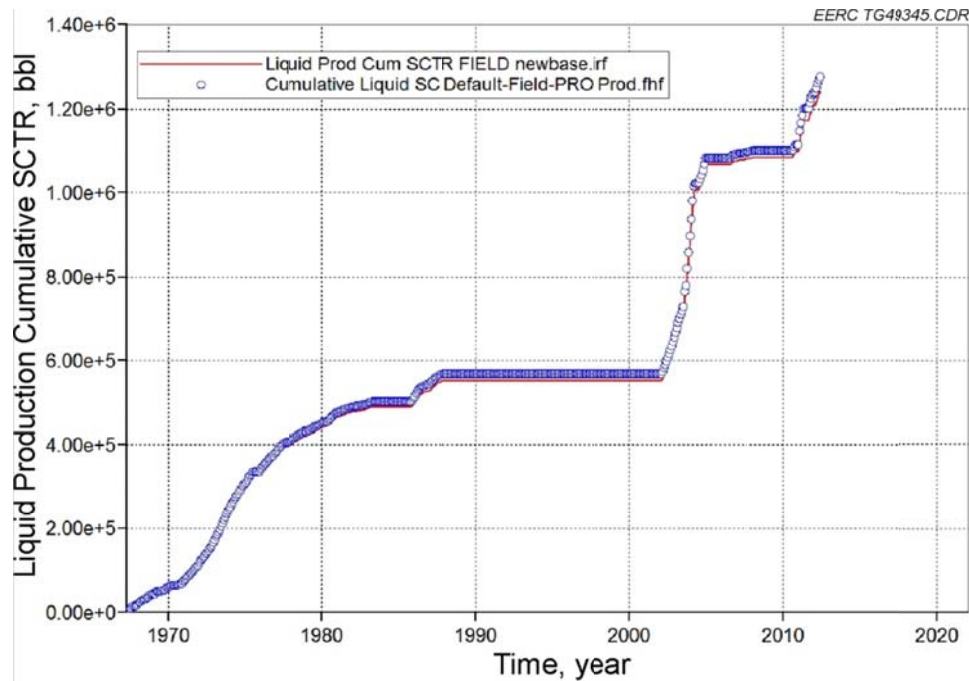


Figure 47. History match of cumulative liquid production for the Muskeg L pool.

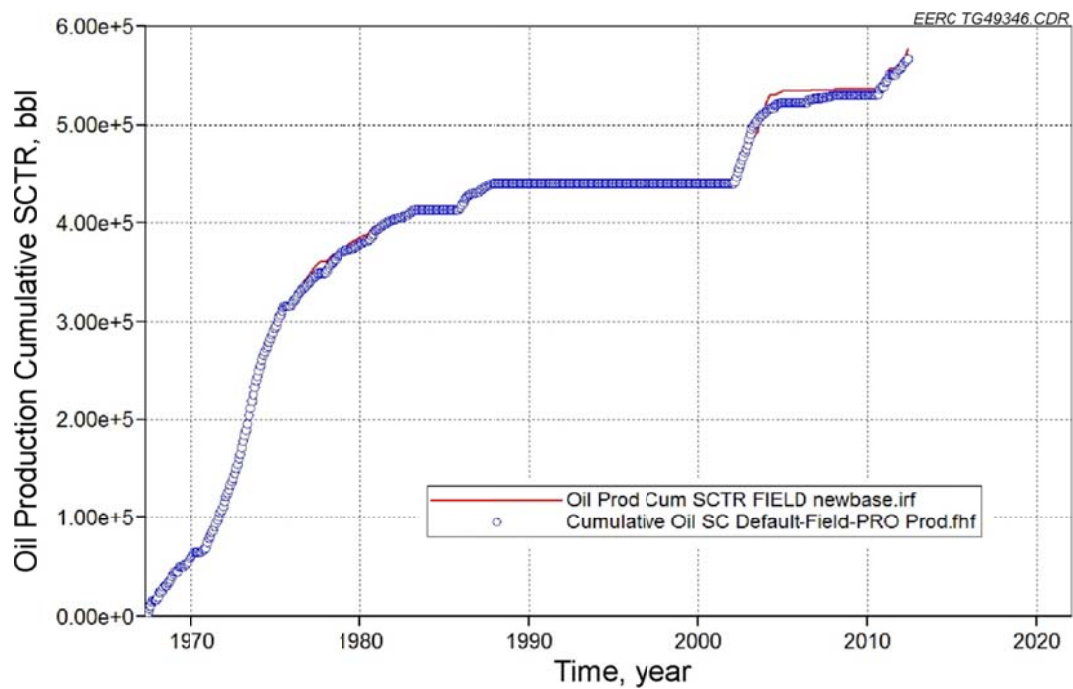


Figure 48. History match of cumulative oil production for the Muskeg L pool.

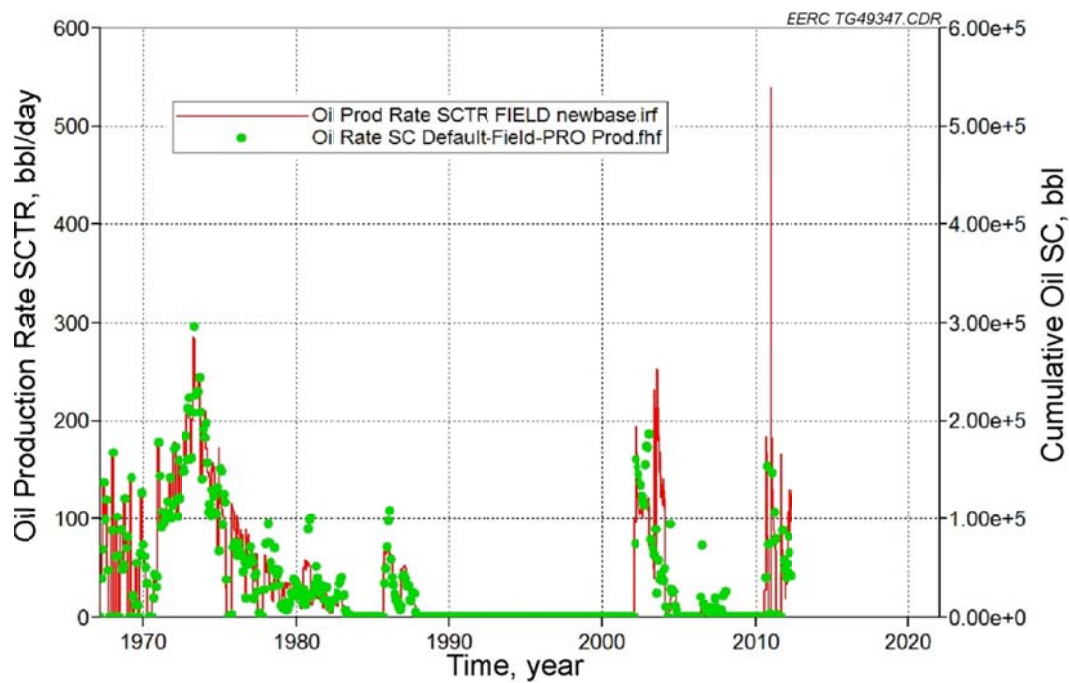


Figure 49. History match of oil production rate for the Muskeg L pool.

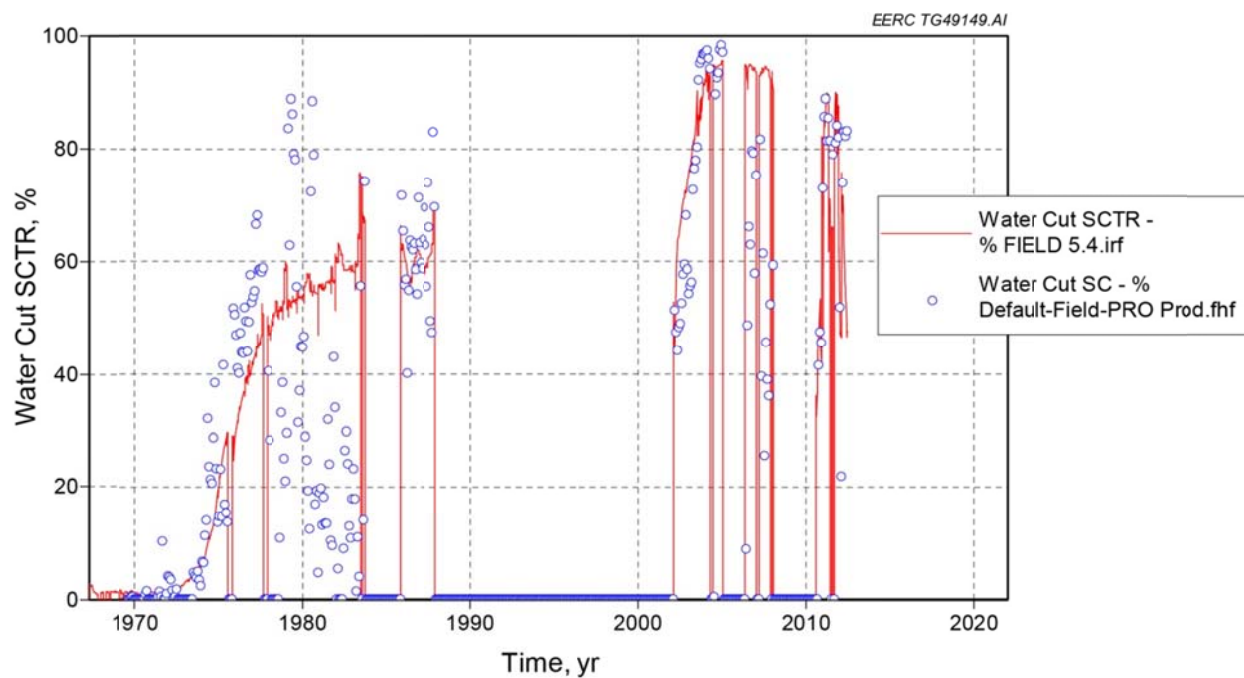


Figure 50. History match of water cut for the Muskeg L pool.

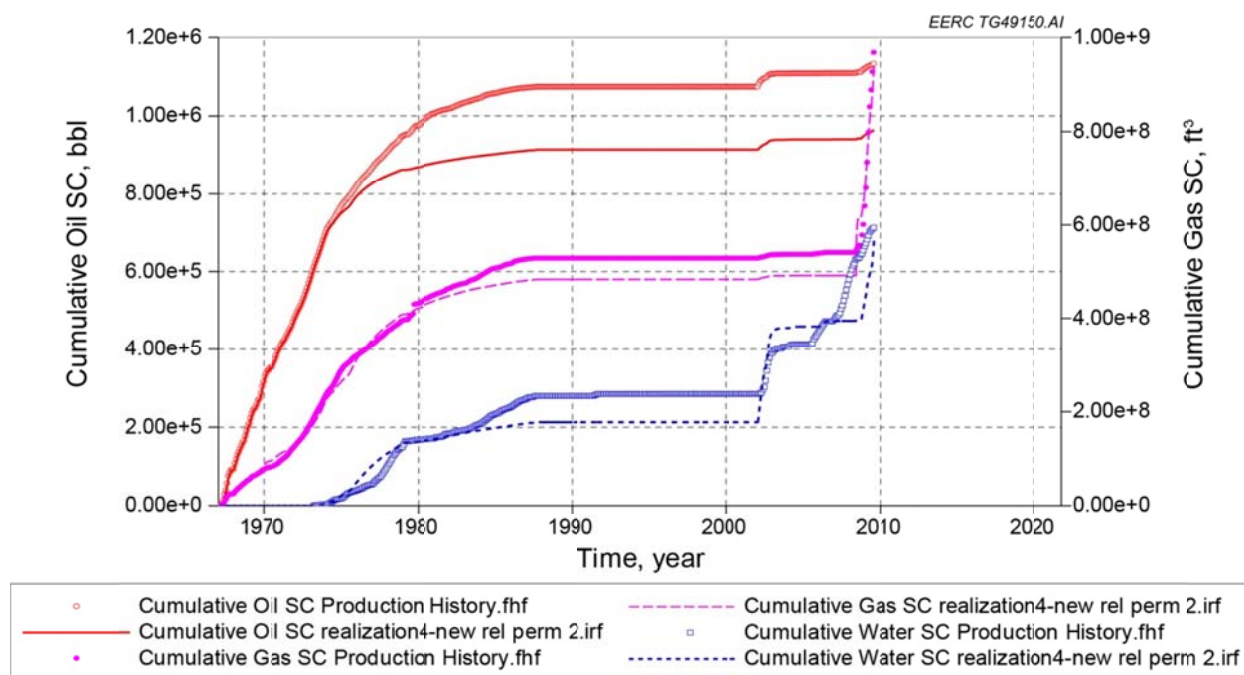


Figure 51. History match of cumulative production for the F pool.

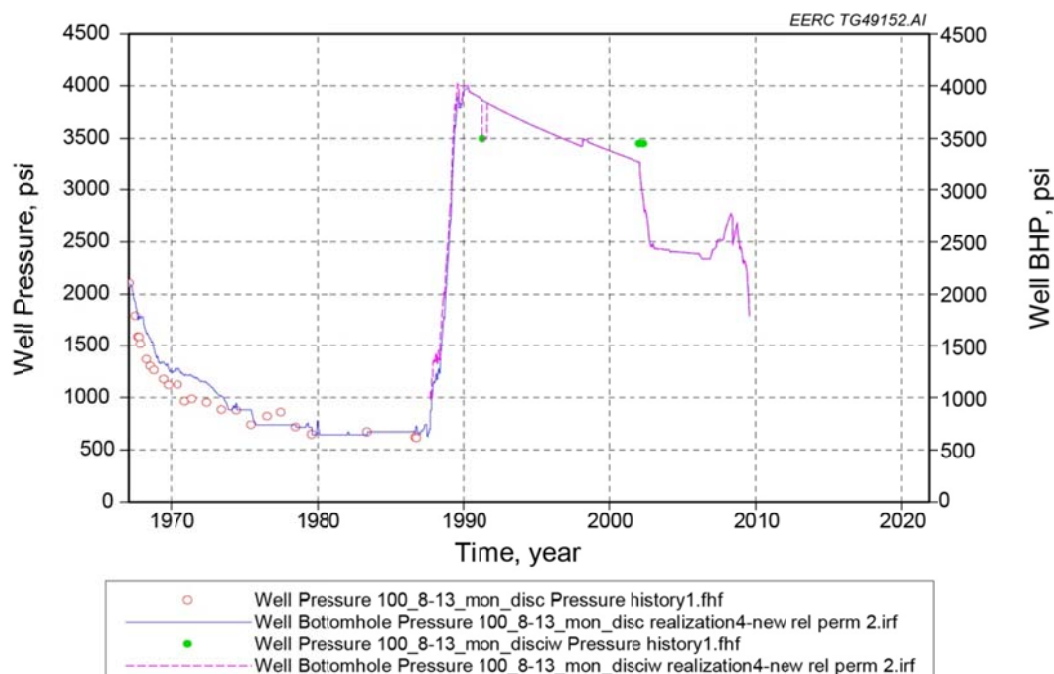


Figure 52. History match of BHP for the F pool.

To speed up the dynamic simulations, the surrounding cap rock (Muskeg Formation) included in the static geologic model was assigned as inactive (null) blocks in the dynamic model. In view of the significantly high formation water salinity (~180,000 ppm), solubility of acid gas in the aqueous phase was neglected. To further simplify the dynamic modeling efforts, no capillary pressure effects were considered in the Version 1 dynamic model, and a constant initial water saturation of 15% for an oil zone and 45% for a modeled transition zone (15 ft) between the oil zone and oil–water contact were used. The availability of detailed production histories allowed for a preliminary history match for cumulative oil, gas, and water production and reservoir pressure (Knudsen and others, 2012).

In addition to the modeled water zone below the oil–water contact, a small numerical aquifer with no leakage option was added at the bottom of the structure for improving simulated pressure response. In view of the nonavailability of experimental relative permeability curves (oil–water and gas–oil) for the F pool, available experimental relative permeability curves from another oil pool were used for good reservoir and tight reservoir rocks in the dynamic model. The experimental relative permeability curves were adjusted during the history match, and no relative permeability hysteresis was considered. The exercise of attaining a reasonable history match for cumulative production and injection volumes through August 2009 was done to have a representative distribution of reservoir fluids and material balance prior to brine extraction/pressure relief modeling.

Six different cases (Cases 2–7) of simultaneous acid gas injection and formation water extraction along with a base case of gas injection only (Case 1) were tested in predictive simulation runs. These cases include acid gas injection through an injector well (Gas Inj-1)

placed in a selected high-permeability zone of the oil zone situated in the top portion of the structure (Saini and others, 2013).

In all of the cases, a maximum injection pressure constraint of 3300 psi was used, which is less than the maximum permissible bottomhole injection pressure of 3400 psi. In the base case (Case 1), acid gas at the injection rate of 1 MMt a year was injected without the extraction of formation water. In Cases 2 and 3, a water extraction well was placed in the bottom portion (the water zone below the oil–water contact) of the reef structure. The gas injection rate similar to that of the base case was used. The water extraction was stopped as soon as gas breakthrough was observed at a water extraction well. However, acid gas injection was continued until the reservoir pressure reached the set maximum pressure limit of 3300 psi. For Cases 2 and 3, Rg/w was found to be near 1.30:1. Compared to a storage capacity of 0.05 MMt in the base case, storage capacity was increased to 0.47 and 0.62 MMt in Cases 2 and 3, respectively. To optimize the gas injection and water extraction ratio, two different extraction well production rates (standard conditions of 60°F and 14.7 psi) of 429 and 397 bbl/day were tested (Cases 4 and 5). The Rg/w was decreased to 1.16:1 (Case 4) and 1.11:1 (Case 5) compared to the observed value of 1.28:1 in Case 3. For these cases, an increase in excess of 1300% was observed in the storage capacity compared to the base case. The gas breakthrough times varied from 4.5 (Case 3) to 6.5 years (Case 5).

A blowdown scenario (i.e., an increase in both gas injection and water extraction rates) was also evaluated (Cases 6 and 7). For this, both acid gas and water extraction rates were doubled compared to Cases 2–5. This resulted in a tenfold increase in storage capacity compared to Case 1. For these cases, Rg/w values were 1.18:1 (Case 6) and 1.22:1 (Case 7). Because of reservoir heterogeneity and higher injection/extraction rates, early gas breakthrough (~1.8 years) was observed at one of the extraction wells. Detailed results for all of the simulation scenarios (Cases 1–7) can be found elsewhere.

An achievement of near 1:1 Rg/w in these cases suggests that gas injection can potentially be used to extract formation water while achieving a significant increase in storage capacity. Overall, controlled extraction of formation water assisted by acid gas injection using a suitably located injection and extraction well pair results in maximum storage capacity at the Zama F pool.

### ***Future EOR and Storage Capacity Potential***

For evaluating the future EOR potential of the F pool, the second iteration of the static geologic model, i.e., the Version 2 model, was used. Based on the initial history-matching efforts with the Version 1 static model, the initially constructed static model was further conditioned, and a new static model (Version 2) was constructed. This version consists of 349,920 ( $104 \times 104 \times 30$ ) cells. The cells were sized 50 ft  $\times$  50 ft in the I and J directions with varying thickness (the K direction), ranging from 10 ft (3.05 m) to 15 ft (4.57 m) for the zone above the oil–water contact and 50 ft below the oil–water contact. The Version 2 model has a heterogeneous distribution of initial water saturation and end point saturation values for oil, gas, and water phases. One of the equiprobable static realizations (P10 OOIP) was chosen for performing detailed history-matching and predictive simulations. In the case of the Version 2 dynamic

model, the trace component (methane with a mole fraction of 0.0001) option was included in the EOS model developed for simulating an acid gas–water system (i.e., water zone below oil–water contact). The solubility of CO<sub>2</sub> and H<sub>2</sub>S components in the aqueous phase was modeled using one of the available options (Henry’s law constants by Harvey’s method). The available correlations, namely Rowe–Chou and Kestin, were used for modeling aqueous-phase density and viscosity, respectively. This time, hysteresis effects for both relative permeability (gas–oil) and capillary pressures (oil–water and gas–oil) were also considered.

A detailed history matching was performed to match cumulative production (oil, gas, and water) and gas injection volumes and reservoir pressure response through May 2012. The individual well performance was also history-matched. The results are shown in Figure 53.

A good match for oil, gas, and water production volumes and injected acid gas volumes was achieved. For a satisfactory pressure response match, only 49% of total injected water had to enter into the reservoir. In addition to the modeled reef structure below the oil–water contact, a numerical aquifer (thickness = 1.3 ft, porosity = 10%, permeability = 15 mD, and radius = 2700 ft) with no leakage option was added at the bottom of the structure for improving simulated water production and pressure response. Oil–water and gas–oil relative permeability curves for both high- and low-permeability rocks were adjusted for satisfactory results. Other adjusted parameters include vertical permeability, well productivity indices, and volume modifier for reef structure below the oil–water contact.

The history-matched (through May 2012) model was then used to run predictive simulations to evaluate future EOR and storage capacity potential in two scenarios of continuing the current EOR configuration for the next 20 years with and without bottom water extraction. The results are summarized in Table 8.

#### ***Current EOR Configuration with Bottom Water Extraction Well***

In this scenario, current EOR configuration, i.e., acid gas injection through one injector and oil production through two existing producer wells with a water extraction well, was continued for the next 20 years. The water extraction well was perforated at the bottom of the structure to manage reservoir pressure through water extraction from the water zone below the oil–water contact. It was located away from the current producers and gas injector. An acid gas injection rate similar to previous scenarios was used. This time, minimum BHP constraints of 300 psi (2068 kPa) at the production wells and 2100 psi at the water extraction well were used. Another well constraint was to shut down the producer wells if oil production went below 30 bbl/day. This scheme shows a 5% increase in incremental oil recovery (16.2% to 22.1%) compared to the case with no bottom water extraction well. This also results in an additional storage capacity gain of 1.01 MMt, which is 4.8 times more compared to the case with no water extraction well. Plots of field oil recovery and amounts of cumulative CO<sub>2</sub> (injected and produced) are shown in Figure 54. These gains in oil recovery and CO<sub>2</sub> storage capacity may be attributed to two conditions. Better sweep may be attained by further movement of injected gas into unswept regions of the reservoir. Also, the availability of additional pore space in the water zone below the oil–water contact may increase capacity. Although the primary purpose of a

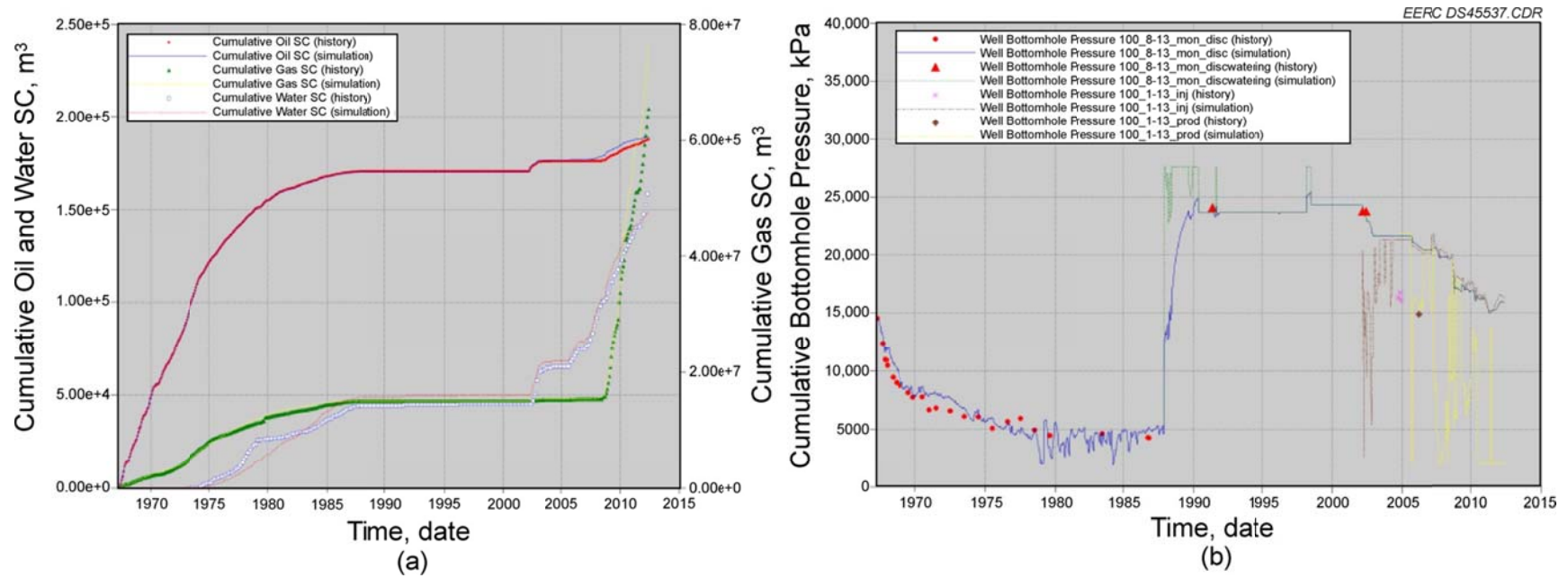


Figure 53. a) History-matching results for cumulative oil, gas, and water production and b) simulated and measured well BHP.



**Table 8. Predictive Simulation Results, future EOR and storage capacity potential**

Variable	Current EOR Configuration with Bottom Water Extraction Well (completed [perforation at the bottom of the structure] in the water zone below oil–water contact)		
	Continuing Current EOR Configuration	Minimum BHP Constraint of 2100 psi (14,478 kPa) at Production Wells	Minimum BHP Constraints of 2068 kPa (300 psi) at Production Wells and 14,478 kPa (2100 psi) at Water Extraction Well
Incremental Oil Recovery, %	16.2	12.6	22.1
Injection/Production Duration, years	20	20	20
Cumulative CO <sub>2</sub> Injected (70% of total acid gas injection), MMt	14.58	9.15	11.52
Cumulative CO <sub>2</sub> Produced, MMt	14.37	8.85	10.30
Net CO <sub>2</sub> Stored, MMt	0.21	0.30	1.22
Oil Produced, MMstb (m <sup>3</sup> )	0.70 (1.98e4)	0.55 (1.55e4)	0.95 (2.69e4)
Water Produced, MMstb (m <sup>3</sup> )	3.07 (8.69e4)	1.17 (3.31e4)	7.86 (2.223e5)

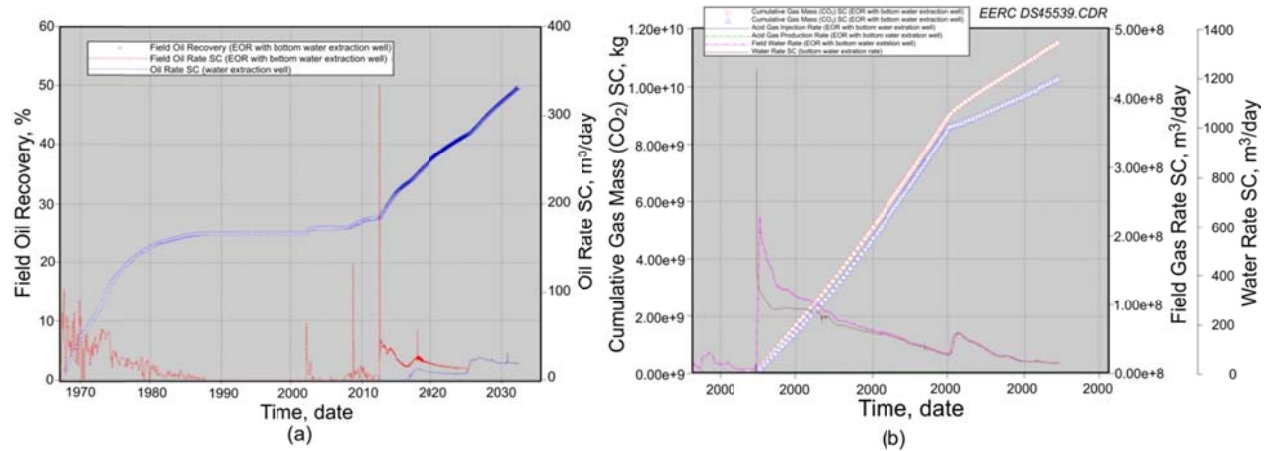


Figure 54. a) Field oil recovery (current EOR configuration with bottom water extraction well) and b) cumulative amounts of injected and produced CO<sub>2</sub> (current EOR configuration with bottom water extraction well).

water extraction well was to manage reservoir pressure through water extraction for additional storage capacity gain, oil production at a significant rate of 120 bbl/day was continued from this well until acid gas injection was stopped. The reason for this was the downstructure movement of residual oil from both swept and unswept regions of the oil-producing zone.

The long-term fate (50-year postinjection period) of injected acid gas was also evaluated. As can be seen in Figure 55 (a), average reservoir pressure stays constant at 2965 psi, which is significantly lower than the 90% of the formation fracture extension pressure of 3654 psi.

## G2G and Muskeg L Prediction

### *Case Design*

Predictive simulation cases were developed based in the current production system to estimate the potential incremental recovery and CO<sub>2</sub> storage potential of the other five pinnacle reefs with acid gas injection. The prediction cases for the G2G and Muskeg L pools are slightly different than those used in the F Pool. The results of history match discussed in the previous section were used as the initial condition for the predictive simulation model to develop the reservoir management strategies. The base case is to operate under the current production mode and to predict the production to July 2042. Then different recovery processes were simulated such as continuous acid gas injection, WAG injection to evaluate these different (EOR) recovery processes, and a detailed description after the prediction. Based on the distribution of residual oil with above the cases, infill-drilling scenarios were designed for G2G and Muskeg L, respectively. The critical importance of a thorough understanding of reservoir geology and rock properties for miscible gas injection schemes has been confirmed by the experiences of gas breakthrough and override in a number of reservoirs in other pinnacles. A summary of case design for G2G and Muskeg L can be found in Table 9.

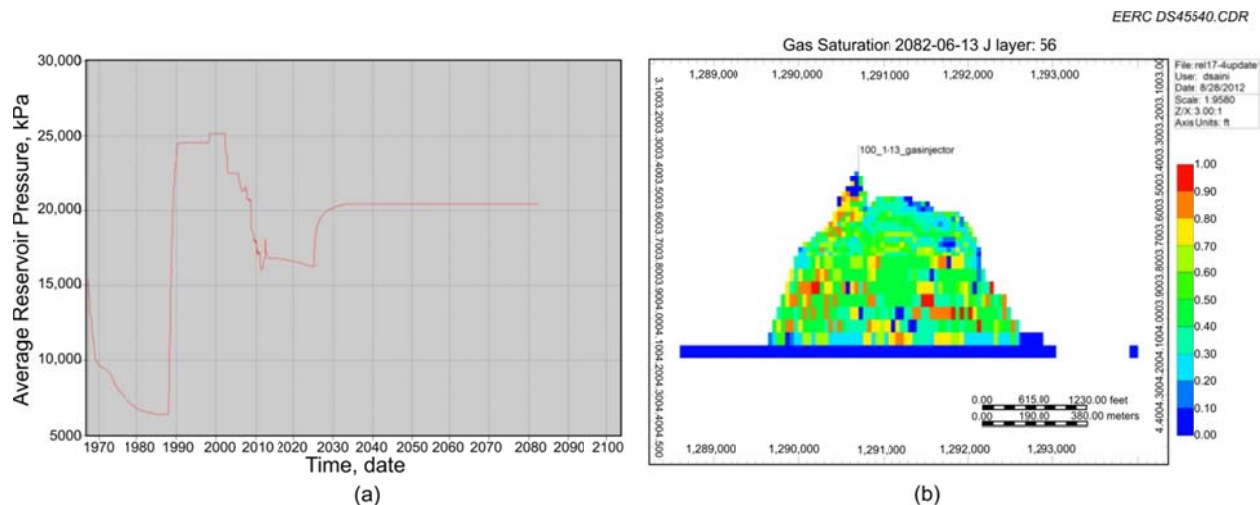


Figure 55. a) Reservoir pressure behavior (current EOR configuration with bottom water extraction well) and b) cross-sectional view of gas saturation (current EOR configuration with bottom water extraction well).

**Table 9. Case Design for G2G and Muskeg L**

Case No.	Type of Injection	Production and Injection Control	Termination of Prediction	Case Description
G2G_1	Continuous injection	BHP	July 2042	Continuously inject acid gas with current production and injection system
G2G_2	WAG	BHP	July 2042	Water alternating acid gas injection
G2G_3	Infill drilling	BHP	July 2042	Infill producer configured on the basis of analysis of prediction
Muskeg L_1	Continuous injection	BHP	July 2042	Continuously inject acid gas with current production and injection system
Muskeg L_2	Current producer shut-in	BHP	July 2042	One of the current producers shut in because of low sweep efficiency and early breakthrough
Muskeg L_3	Infill drilling	BHP	July 2042	Infill producer configured on the basis of analysis of prediction

### ***Results and Discussion***

The simulation study shows that miscible acid gas injection is the preferred recovery mechanism for part of the reservoir under study. This is a result of several key factors, including the favorable miscibility with the native oil (lower miscibility pressure with reservoir crude), better solvent, a more favorable mobility ratio because of high acid gas viscosity and density, and availability of large quantities of acid gas from the underlying formation. Acid gas is, therefore, an attractive and miscible EOR agent in the Zama pools.

#### ***G2G Pool Case 1: Continuous CO<sub>2</sub> Injection with Constant BHP Constraints***

In this case, the injection and production modes are all set as BHP control to ensure a MMP could be reached during the whole injection process. Early on, the daily CO<sub>2</sub> injection rate was significantly higher than later time periods because the BHP increased, resulting in a decrease in the injectivity. The prediction ends in July 1, 2042, a 30-year prediction. An incremental recovery from this scenario is 1.11% of OOIP. The high-permeability channels in the Zama Member of the Muskeg Formation result in very low sweep efficiency.

#### ***G2G Pool Case 2: WAG Process***

The WAG (1:1 ratio) process was simulated to evaluate the reservoir response to WAG. The cyclic period is 1 year. Compared with continuous injection, the use of injectant was dropped significantly. The prediction ends in July 1, 2042, a 30-year prediction. A comparison of sweep efficiency is also made, as the main purpose of WAG is to improve the sweep efficiency of injected gas. The results show that the completion of G2G is designed for gas-assisted gravity drainage in which a vertical flow dominates the recovery mechanism. Thus the contribution from the WAG process is limited in such a situation. The incremental recovery from this scenario is 1.11% of OOIP, which is the same as the continuous CO<sub>2</sub> injection case.

### *G2G Pool Case 3: Infill Drilling*

Based on the analysis of the previous G2G cases, the current injection and production system is not favourable to form an effective flow path for EOR and storage. An additional synthetic well was added to the simulation model at the beginning of the prediction to investigate the effect that infill drilling may have on production. The well is completed at the center of the G2G pool, above the original oil–water contact where the saturation of residual oil is relatively high after primary production in the above scenarios. The prediction also spans 30 years. The ultimate recovery from this scenario was up to 11.75% of OOIP, with significant incremental CO<sub>2</sub> storage as well. The cumulative oil production in this case increased to 0.410 MMstb. With a current oil price of \$90/bbl and assuming an infill-drilling cost of \$15 million (one production well), the raw profit of this scenario can reach as high as \$22 million.

### *Muskeg L Pool Case 1: Continuous CO<sub>2</sub> Injection with Constant BHP Constraints*

In this case, the injection and production modes are all set as BHP control to ensure a MMP could be reached during the whole injection process. Early on, the daily CO<sub>2</sub> injection rate was significantly higher than later time periods because the BHP increased, resulting in a decrease in the injectivity. The prediction ends in July 1, 2042, a 30-year prediction. The total injection volume of acid gas is 267 MMscf in this scenario. The average pressure remained above 2500 psi to ensure miscibility was obtained. An ultimate recovery from this scenario was 3.65%. The high-permeability channels in the Zama Member of Muskeg Formation result in very low sweep efficiency for this case.

### *Muskeg L Pool Case 2: Well 102/05-01-116-06W6/00 Shut-In*

Based on the analysis of history match and Case 1, early breakthrough ends the EOR process if no action is taken on Well 102/05-01-116-06W6/00 to improve the sweep efficiency of injected gas. In this case, the well is shut in and other wells keep working under BHP constraints. The prediction ends July 1, 2042, a 30-year prediction. The result shows that the productivity of the whole reservoir drops as a result of shutting in Well 102/05-01-116-06W6/00. The oil rate of 100/04-01-116-06W6/00 did not improve as predicted. By tracking the distribution of CO<sub>2</sub> mole fraction, the CO<sub>2</sub> migrated smoothly to the whole reservoir with the injection continuing. There was no effective pressure gradient between producer and gas injector, indicating that there was no connectivity between the injector–producer pair, resulting in virtually no incremental recovery. The recovery contribution from the CO<sub>2</sub> injection is only 1.60%. The volume stored in the reservoir is much more than that of Case 1, which indicates a low utilization efficiency.

### *Muskeg L Pool Case 3: Infill Drilling*

Based on the analysis of the previous Muskeg L cases, the current injection and production system is not favorable to form an effective flow path for EOR and storage. A pseudo-production well is configured in the model at the beginning of the prediction. To reduce the hypothetical drilling cost, the new well is designed as a vertical production well. The well is completed above the original oil–water contact in an area with high predicted residual oil saturation. The prediction case covers a 30-year production and injection timeframe. The incremental oil recovery from this scenario is 11.80% of OOIP. With more production, the usage of gas is

increased by 45.4%. The cumulative CO<sub>2</sub> injection in Case 3 is 0.176 MMt. The oil production contributed by CO<sub>2</sub> injection is up to 0.22 MMstb.

## **CO<sub>2</sub> STORAGE EFFICIENCY IN ZAMA REEFS**

There are hundreds of pinnacle reefs throughout the world that hold in excess of 1 million barrels of oil each. These pinnacles represent an excellent opportunity to recover incremental oil through EOR and have a great potential to store CO<sub>2</sub>. With all detailed investigations presented above, more efforts were put into developing a methodology to evaluate the CO<sub>2</sub> storage in other pinnacle reefs of the Zama. Three more pinnacle reefs (NNN, RRR, and Z3Z) in the Zama oil field, currently under acid gas EOR, are evaluated in this section. Based on the similarity of pinnacle reefs in the same deposit, the methodology introduced here is to use high-resolution simulation in pools of sufficient data to calibrate the quick estimates of similar pools.

### **Real-Time Injection**

According to the literature, the original solution gas produced from Keg River oil pools contained approximately 5% CO<sub>2</sub> and 3% H<sub>2</sub>S. The Zama gas-processing plant also processes nonassociated gas, which contains approximately 13% H<sub>2</sub>S and 8% CO<sub>2</sub>. An amine extraction system generates an effluent stream that is approximately 4% methane, 66% CO<sub>2</sub>, and 30% H<sub>2</sub>S. This stream is injected as the acid gas miscible flood solvent. A summary of the injected acid gas composition for all six pools over time is shown in Figure 56.

The acid gas injection in the G2G pool started in June 2006, as one of the production wells was converted into an injector. By the end of May 2012, the cumulative acid gas injection in the G2G pool is 3.06 Bscf. Table 10 presents the average composition of four components since the acid gas injection started in the six-pool area. Table 11 counted the injected CO<sub>2</sub> volume for each of the six pools (to June 2012).

### **Simulation Prospections**

Each of the three simulated pinnacles is analyzed in this section regarding its use for CO<sub>2</sub> storage.

#### ***F Pool***

In the first two scenarios, the simulation model keeps the current EOR injection and production system, that is, acid gas injection through one injector and oil production through two existing producers, and continues for the next 30 years with BHPs of 300 and 2100 psi in the producer in the two scenarios. With the BHP control of 300 psi, 0.21 MMt CO<sub>2</sub> can be stored in the F pool. With the minimum production BHP constraint of 2100 psi, 0.30 MMt CO<sub>2</sub> can be stored. In the scenario of configuring a water extraction well at the bottom of the pool, the CO<sub>2</sub> storage capacity of the F pool is predicted as high as 1.22 MMt.

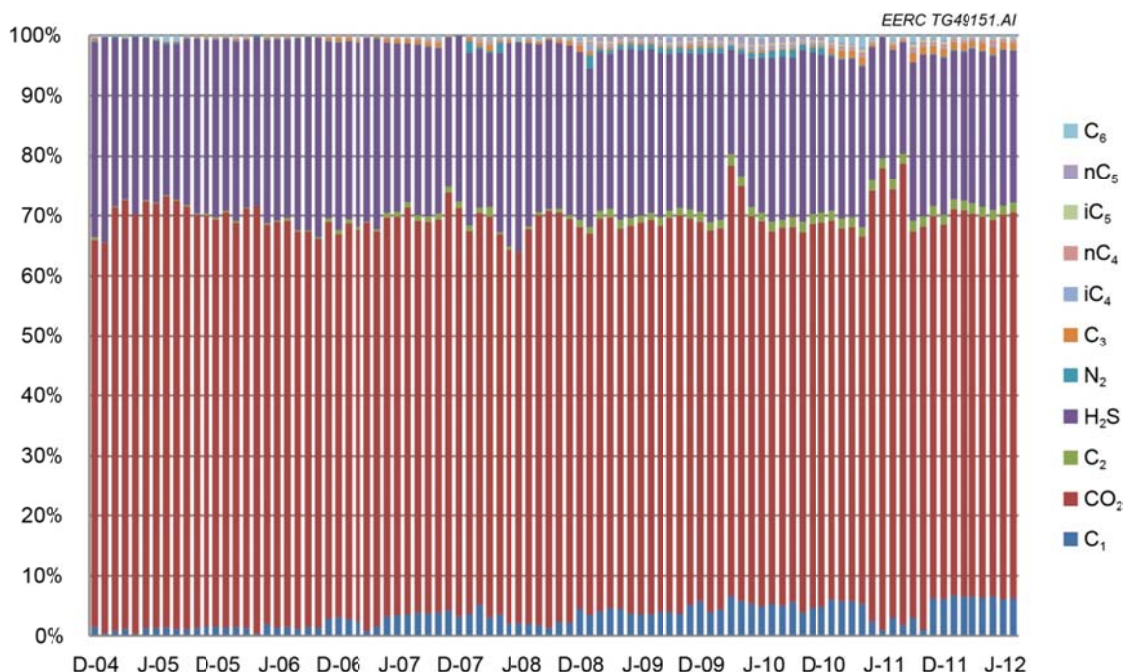


Figure 56. Injected acid gas composition over time for six pinnacles.

**Table 10. Average Compositions of Four Components**

Component	CH <sub>4</sub>	CO <sub>2</sub>	C <sub>2</sub> H <sub>6</sub>	H <sub>2</sub> S
Fraction, mol%	5.08	67.32	1.70	25.90

**Table 11. Injected CO<sub>2</sub> in All Six Pools, to June 2012**

Pool	F	G2G	NNN	RRR	Z3Z	Muskeg L
Injected CO <sub>2</sub> Volume, MMt	0.086	0.109	0.091	0.094	0.198	0.059

### ***G2G Pool***

According to the predictive results, the change of injection and production mode would barely have an effect on the CO<sub>2</sub> storage because of the existing of high-permeability channel. The injectant of high mobility is forced to the producer with a very low pressure gradient. The scenario of the current production and injection mode has a storage capacity of 0.035 MMt of CO<sub>2</sub> in G2G pool. The case of shutting in the high-permeability perforation would not change the situation because of the high mobility of the acid gas and a mature vertical flow system in the pinnacle. On the basis of analysis of displacement efficiency, the infill well configured in the model would contribute to both oil recovery and volume of CO<sub>2</sub> storage, which has a storage capacity of 0.174 MMt.



### ***Muskeg L Pool***

The gas injection well is close to the production well. A significant EOR effect can be seen at the early stage of the injection. Once breakthrough happens, it is difficult for the injectant to spread out and increase the sweep efficiency. According to the prediction, the current production mode would keep 32,000 tons of CO<sub>2</sub> underground after 30 years of the EOR process. The CO<sub>2</sub> utilization factor is as much as 13.14 Mscf/bbl. Similar to the G2G pool, the WAG process, which is very successful in a conventional and integral reservoir, could not work functionally in pinnacles because of the complex structure. The CO<sub>2</sub> storage capacity after a WAG process is very close to the case of the current production mode. The infill drilling dramatically lowers the residual oil saturation and brings the pinnacle another 9.74% of OOIP in production. Meanwhile, the CO<sub>2</sub> utilization factor is also dropped to 3.98 Mscf/bbl, and the CO<sub>2</sub> storage capacity of Muskeg L can be as high as 59,000 tons.

### **Sensitivity Analysis**

A key point in evaluation of CO<sub>2</sub> storage capacity in a hydrocarbon reservoir is the volume of hydrocarbon. In such a case, the fundamental assumption is that the volume previously occupied by the produced hydrocarbons becomes, by and large, available for CO<sub>2</sub> storage. The storage capacity can be calculated on the basis of reservoir properties such as original OOIP, recovery factor, temperature, and pressure, which are related to in situ CO<sub>2</sub> characteristics such as phase behavior and density.

Compared with existing research on conventional hydrocarbon reservoirs, the gas storage in reefs is more complex. According to this research, a few uncertainties and sensitive parameters that affect the CO<sub>2</sub> storage efficiency are found as following:

*Effective Storage Bulk* – The first uncertainty is to fix the effective pore volume which relates to the storage capacity directly. The lack of consistent methodologies and guidelines for capacity estimations is the problem that all the gas storage efforts in hydrocarbon reservoirs are facing. As a rule of thumb, high-resolution geologic modeling is the key to estimating pore volume. Without sufficient time and tools to develop a geologic model, a few key parameters should be considered in a quick estimation of effective pore volume, like pinnacle shape, porosity, capillary pressure, etc.

*Displacement Mechanisms* – Gravity difference dominates the displacement in the first depletion stage. Later in the gas injection process, vertical flow contributes more to long-term injection.

*Vertical Connectivity* – Compared with large-scale deposition, the vertical connectivity of pinnacles takes more weight in both oil displacement and CO<sub>2</sub>/acid gas migration. The recognition of internal barriers is the key to evaluating vertical flowability.

*Aquifers* – Different from conventional reservoirs, aquifers in the production of pinnacles are usually more active. According to the analysis on the Zama F and G2G pools, the bottom water moves frequently during production. With the reservoir pressure

fluctuating, mainly decreasing after being put into production, the oil–water contact increases, which has been interpreted in production logging. Since the storage mechanisms are different between aquifers and hydrocarbon, oil–water contact must be fixed in long-term storage.

### Storage Capacity and Efficiency Evaluation

The volumetric-based CO<sub>2</sub> storage resource estimate is based on the standard industry method to calculate OOIP (Litynski and others, 2010). In this section, a semi-production-based process for CO<sub>2</sub> storage resource estimate in pinnacle pools is discussed. Production-based CO<sub>2</sub> storage resource estimates are generally preferred over volumetric-based CO<sub>2</sub> storage resource estimates because production data contain detailed information collected from the formation. If no production data are available, then volumetric-based CO<sub>2</sub> storage resource estimates may be applied. In the Zama research, the quick volumetric-based CO<sub>2</sub> storage resource estimate was developed on the basis of reservoir simulation, which provided evidence of mechanisms of displacement and the ranges of important parameters.

With the condition that storage volume methodology for oil and gas reservoirs was based on quantifying the volume of oil and gas that has been or could be produced, and assuming that it could be replaced by a similar volume of CO<sub>2</sub> under certain CO<sub>2</sub> utilization factors, both oil/gas and CO<sub>2</sub> volumes are calculated at initial formation pressure or a pressure that is considered a maximum CO<sub>2</sub> storage pressure.

A simple form of the volumetric equation to calculate the capacity of acid gas storage in hydrocarbon pinnacle reefs is as follows (Litynski and others, 2010):

$$G = A \cdot h_n \cdot \phi_e (1 - S_{wi}) B \cdot \rho_{co2} \cdot E \quad [\text{Eq. 1}]$$

The variables include the product area (A), net thickness (h<sub>n</sub>), average effective porosity (φ<sub>e</sub>), original hydrocarbon saturation (1-initial water saturation, expressed as a fraction [S<sub>wi</sub>]), and initial oil (or gas) formation volume factor (B) yield (OOIP or organic gas in place). The storage efficiency factor (E) is derived from local CO<sub>2</sub> EOR experience or reservoir simulation as a standard volume of CO<sub>2</sub> per volume of OOIP. The standard CO<sub>2</sub> density (ρ<sub>co2</sub>) converts standard CO<sub>2</sub> volume to mass.

The expression of storage capacity can be simplified as:

$$G = \text{OOIP} \cdot E_u \cdot E_{rCO2} \cdot \rho_{co2} \quad [\text{Eq. 2}]$$

The simplified variables include OOIP (bbl), the CO<sub>2</sub> utilization factor -E<sub>u</sub> (Mscf/bbl), and the hydrocarbon recovery factor contributed by CO<sub>2</sub>-E<sub>rCO2</sub> (%).

Based on the simulation results for the F, G2G, and Muskeg L pools, the ranges of the above parameters are fixed and listed in Table 12. The average CO<sub>2</sub> utilization factor for all three pools is 10.02 Mscf/bbl. The recovery contribution by CO<sub>2</sub> was also averaged. In a pessimistic estimate, the Zama pools would have another 6.20% of OOIP in recovery once acid gas is employed. All the infill-drilling cases show a good opportunity to boost the contribution to 15.60% of OOIP. Quick estimates of storage capacity are made for the NNN, RRR, and Z3Z pools with both optimistic and pessimistic results, which can be seen in Table 13. The average optimistic storage capacity of all six pools is 0.397 MMt. Assuming the 840 pools in Zama have similar storage capacity, the CO<sub>2</sub> that can be stored in this area is up to as much as 334 MMt.

## KEY OBSERVATIONS AND CONCLUSIONS

Since December 2006, the Zama oil field in northwestern Alberta, Canada, has been the site of acid gas injection for the simultaneous purpose of EOR, acid gas disposal, and CO<sub>2</sub> storage. PCOR Partnership Phase III activities included laboratory studies of the effects of acid gas on storage integrity and modeling efforts to develop improved predictions of both oil recovery and CO<sub>2</sub> storage capacity at Zama. The results of these research activities are not only directly applicable to ongoing and future acid gas injection activities at Zama but also offer insights that can be applied to future CO<sub>2</sub> storage and EOR operations in the thousands of pinnacle reef reservoirs that exist in sedimentary basins around the world. Key observations and conclusions from the PCOR Partnership Zama activities are presented below.

**Table 12. CO<sub>2</sub> Utilization Factor and Recovery Contribution Based on Simulation Predictions**

Pool	E <sub>u</sub> , Mscf/bbl		E <sub>rCO<sub>2</sub></sub> , %	
	Pessimistic	Optimistic	Pessimistic	Optimistic
Keg River F	22.9	9.73	12.60	22.00
Keg River G2G	5.6	4.77	4.40	15.00
Muskeg L	13.15	3.98	1.60	9.80
Average	10.02		6.20	15.60

**Table 13. Estimates on CO<sub>2</sub> Storage Capacities for Three Extra Pools**

Pool	OOIP, MMstb	CO <sub>2</sub> Utilization (E <sub>u</sub> ), MMscf/bbl	Recovery Contributed by CO <sub>2</sub> (E <sub>rCO<sub>2</sub></sub> ), %		Storage Capacity G, MMt	
			Pessimistic	Optimistic	Pessimistic	Optimistic
Keg River Z3Z	2.380	10.02	6.20	15.60	0.083	0.209
Keg River RRR	4.700	10.02	6.20	15.60	0.164	0.412
Keg River NNN	3.530	10.02	6.20	15.60	0.123	0.310

The laboratory experimental examinations of geochemical interactions between Zama reservoir rocks, brine, pure CO<sub>2</sub>, and CO<sub>2</sub>-H<sub>2</sub>S under Zama reservoir pressure and temperature conditions showed no clear differences between the preexposure and postexposure mineralogy. It should be noted that the applicability of these results may be limited because the rock samples that were available for these efforts were all limestones (i.e., predominantly calcite) while more mineralogically complex dolomite-dominated facies are common in the Zama pinnacle reefs. This is an important caveat to bear in mind when considering these results, because the Phase II modeling results (Smith and others, 2009) indicated that dolomite and iron-bearing minerals such as pyrite may be the source for much of the dissolution and precipitation that was predicted to occur in a Zama pinnacle undergoing acid gas injection. It is also important to note that the experiments were of a short duration (28 days) and static. Longer-duration experiments that incorporate dynamic variables representing the pressure, temperature, and hydrogeochemistry changes that would occur in an operating injection and production scenario are necessary. Such long-term experiments would more accurately assess the geochemical interactions that may occur between acid gas and a carbonate reservoir.

While the rock analysis data may have limited applicability, some insight may be gained from the evaluation of changes in the composition of the fluids in which the rocks were immersed during the experiments. Some of the experimental results suggest that a gas stream that includes H<sub>2</sub>S may be less reactive with a carbonate reservoir than a stream of pure CO<sub>2</sub>. This is based on the clear decrease in the reactivity of both calcium and sulfate that was observed in the samples exposed to the H<sub>2</sub>S-rich gas stream. Also, measurements of TDS data indicate that a CO<sub>2</sub>-H<sub>2</sub>S mixture will dissolve a lesser quantity of total mineral content. From the perspective of storage integrity, this lower mineral loss will presumably correspond to a minimal loss of structural integrity of the reservoir formation. This suggests that, under some conditions, the presence of H<sub>2</sub>S may actually reduce the reactivity of some carbonate rocks, in turn possibly serving to maintain reservoir and wellbore integrity rather than degrading it.

The results of the Class H portland cement exposure experiments indicated that the addition of H<sub>2</sub>S to the CO<sub>2</sub> storage system resulted in 1) the precipitation of significant amounts of ettringite and 2) the precipitation of pyrite in the carbonated rim of the cement. Ettringite formation subsequent to the hardening of cement can lead to cracking, spalling, strength loss, and degradation. Pyrite precipitation can also potentially lead to degradation of cement integrity. However, the experimental results indicated that CO<sub>2</sub> in the system may dissolve the ettringite and reprecipitate calcium carbonates that may potentially help improve the overall cement integrity.

Laboratory experimental studies on the effects of corrosion on seven well casing steels when exposed to CO<sub>2</sub> and acid gas under typical Zama reservoir conditions showed that the highest level of corrosion was observed in steels that were submerged in high-TDS water and exposed to pure CO<sub>2</sub>. Corrosion rates from experiments that included H<sub>2</sub>S were consistently lower than those that include pure CO<sub>2</sub>, with higher corrosive mass loss appearing in all samples reacted with pure CO<sub>2</sub>. However, a significant amount of sulfur was found on the surfaces of samples exposed to CO<sub>2</sub>-H<sub>2</sub>S mixtures. While pitting was observed in all of the exposed samples, it was more severe in cases of pure CO<sub>2</sub> exposure as compared to cases where H<sub>2</sub>S was present. As with the rock studies, these results appear to suggest that, in some circumstances, the

presence of H<sub>2</sub>S may actually serve to counteract the effects of CO<sub>2</sub>, helping to maintain wellbore integrity rather than contributing to its degradation.

Overall, the laboratory results indicate that the injection of a CO<sub>2</sub>–H<sub>2</sub>S mixed-gas stream into a carbonate formation for EOR and CO<sub>2</sub> storage is not likely to be more deleterious to wellbore integrity than the injection of pure CO<sub>2</sub>. In fact, it appears that, under some circumstances, the presence of H<sub>2</sub>S may actually help maintain wellbore integrity against degradation from CO<sub>2</sub>. These observations are supported by the fact that industrial-scale acid gas injection projects have been conducted in Alberta for over 20 years with no reported breaches in the wellbore integrity of acid gas injection wells. The results of the PCOR Partnership Phase II Zama activities indicated that the implementation of an MVA plan that is based on the current Alberta regulations for acid gas disposal is an effective approach to ensuring the long-term, safe storage of CO<sub>2</sub> and/or CO<sub>2</sub>–H<sub>2</sub>S in deep carbonate pinnacle reef formations. The results of the Phase III efforts offer no evidence to counter that previous conclusion. In fact, while the toxicity of H<sub>2</sub>S will require specialized monitoring at surface facilities, the results indicate that the presence of H<sub>2</sub>S in the system does not necessarily require any additional or extraordinary MVA technologies to be applied in the deep subsurface.

PVT modeling work was performed to investigate the effect of H<sub>2</sub>S and varying GOR on MMP. The results indicate that MMP decreased nearly linearly with increasing levels of H<sub>2</sub>S in the injection gas, dropping from 2780 psi with pure CO<sub>2</sub> to 2020 psi with 20 mol% H<sub>2</sub>S in the G2G pool. Likewise, when the GOR was reduced from 414 to 200 scf/bbl, the simulated MMP dropped from 2780 psi to 1950 psi. These results indicate that it is important to consider both the components of the injected gas and the GOR of the current oil when estimating the MMP.

Static models of six pinnacles were created and used to conduct dynamic simulation modeling of potential operational scenarios, including various combinations of acid gas injection, EOR, and water extraction. The integration of seismic data was critical to the development of static models that accurately represent the geometry of the pinnacles, and, correspondingly, their volumetric parameters. Well log data that could be correlated to core analysis data were also highly valuable in the development of the static model. Such data are particularly important with respect to the realistic distribution of porosity and permeability properties within the many facies that are present in a typical carbonate pinnacle reef. Future carbon capture, utilization, and storage (CCUS) projects that target pinnacle reefs should include core collection and analysis, a robust well-logging program, and seismic survey data acquisition as part of the site characterization phase. History matching was used to improve the reliability of the simulation results.

The storage capacity of the six examined Zama pinnacles ranged from a minimum of 175,000 tons of CO<sub>2</sub> to a maximum of 1,220,000 tons of CO<sub>2</sub>, with the average storage capacity of the six pinnacles being nearly 400,000 tons. Assuming the 840 pinnacles in the Zama area have similar storage capacity, the CO<sub>2</sub> storage capacity of the entire Zama area may be nearly 334 million tons. With respect to EOR potential, conservative estimates indicate that the Zama pools would recover an additional 6.2% of OOIP through the injection of acid gas. The use of infill-drilling schemes as part of an acid gas EOR operation may boost that productivity to as

high as 15.6% of OOIP. The simulated CO<sub>2</sub> utilization factor results for the modeled Zama pools averaged approximately 0.62 tons/bbl or 11 Mscf/bbl.

While the laboratory results speak to the integrity of CO<sub>2</sub> storage containment, the modeling results confirm that miscible flooding with sour acid gas is an excellent means of storing large volumes of CO<sub>2</sub> while improving oil recovery. There are hundreds of pinnacle reefs throughout the world that hold in excess of 1 million barrels of oil each. The results of the PCOR Partnership research activities at Zama indicate that, globally, pinnacle reef structures represent an excellent opportunity to recover millions of barrels of incremental oil through CO<sub>2</sub>-based EOR and also have a great potential to perhaps store billions of tons of CO<sub>2</sub>. Also, the success of the ongoing Zama injection activities combined with the results of the PCOR Partnership research clearly demonstrate that CO<sub>2</sub> streams do not have to be “pure” to be considered for use in CCUS projects and that some impurities may even be desirable under certain circumstances.

## **ACKNOWLEDGMENTS**

The authors thank Apache Canada Ltd. for its extraordinarily generous support for the PCOR Partnership efforts at Zama. The access that Apache Canada Ltd. provided with respect to its operational and seismic survey data were essential to the successful execution of this research program. In particular, the authors want to thank Bill Jackson and Doug Nimchuk for their steadfast support and guidance over the many years of this project. The collaborative efforts of Barbara Kutcho, Brian Strazisar, Christina Lopano, and George Guthrie of DOE NETL, which were essential to the wellbore cement studies, are also greatly appreciated. The authors also thank Schlumberger Carbon Services for providing the Petrel and Techlog software packages and Computer Modelling Group Ltd. for providing simulation software packages for use in this research. We also want to acknowledge the efforts made by David Ryan of Natural Resources Canada and Stefan Bachu of Alberta Innovates – Technology Futures, who provided invaluable guidance and support. Finally the authors want to thank former EERC employees Yevhen (Eugene) Holubnyak and Alexey Ignatchenko for their contributions to the geochemistry and steel corrosion experimental activities.

## **REFERENCES**

- Burke, L., 2009, PCOR project Apache Zama F Pool acid gas EOR & CO<sub>2</sub> storage: Report prepared by RPS Energy Canada for the Energy & Environmental Research Center.
- Buschkuehle, M., Haug, K., Michael, K., and Berhane, M., 2007, Regional-scale geology and hydrogeology of acid gas enhanced oil recovery in the Zama oil field in northwestern Alberta: Report prepared by Alberta Energy and Utilities Board and Alberta Geological Survey, Canada, for the Plains CO<sub>2</sub> Reduction Partnership, Energy & Environmental Research Center.



- Gunter, W.D., Bachu, S., and Benson, S., 2004, The role of hydrogeological and geochemical trapping in sedimentary basins for secure geological storage of carbon dioxide: Geological Society, London, Special Publications, v. 233, no. 1, p. 129–145.
- Kaszuba, J. P., and Janecky, D.R., 2009, Geochemical impacts of sequestering carbon dioxide in brine formations: Geophysical Monograph Series, v. 183, p. 239–247.
- Kerans, C., and Tinker, S.W., 1997, Sequence stratigraphy and characterization of carbonate reservoirs: Society of Economic Paleontologists and Mineralogists Short Course Notes 40, 130 p.
- Knudsen, D.J., Saini, D., Gorecki, C.D., Peck, W.D., Sorensen, J.A., Steadman, E.N., and Harju, J.A., 2012, Using multiple-point statistics for conditioning a Zama pinnacle reef facies model to production history: Poster presented at the American Association of Petroleum Geologists (AAPG) Annual Conference and Exhibition, Long Beach, California.
- Kutchko, B.G. Strazisar, B.R., Hawthorne, S.B., Lopano, C.L., Miller, D.J., Hakala, J.A., and Guthrie, G.D., 2011, H<sub>2</sub>S–CO<sub>2</sub> reaction with hydrated Class H well cement—acid gas injection and CO<sub>2</sub> cosequestration: International Journal of Greenhouse Gas Control, v. 5, p. 880–888.
- Litynski, J., Deel, D., Rodosta, T., Guthrie, G., Goodman, A., Hakala, A., Bromhal, G., and Frailey, S., 2010, Summary of the methodology for development of geologic storage estimates for carbon dioxide: U.S. Department of Energy, National Energy Technology Laboratory Carbon Storage Program report, September, p. 6.
- McCamis, J.,G. and Griffith, L.S., 1968, Middle Devonian facies relations Zama Area: Alberta. AAPG Bulletin, v. 52, no. 10, p. 1899–1924.
- Phelps, G., and Boucher, A., 2009, Mapping locally complex geologic units in three dimensions—the multi-point geostatistical approach: Workshop presented at the 2009 Annual Meeting of the Geological Society of America, Portland, Oregon, October 17.
- Saini D., Gorecki C.D., Knudsen D.J., Sorensen J.A., and Steadman E.N., 2013, A simulation study of simultaneous acid gas EOR and CO<sub>2</sub> storage at Apache’s Zama F Pool: Energy Procedia, in press.
- Smith, S.A., McLellan, P., Hawkes, C., Steadman, E.N., and Harju, J.A., 2009, Geomechanical testing and modeling of reservoir and cap rock integrity in an acid gas EOR/sequestration project, Zama, Alberta, Canada: Energy Procedia, v. 1, no. 1, p. 2169–2176.

## **APPENDIX A**

# **MINERALOGICAL COMPOSITION AND FLUID ANALYSIS DATA FROM ROCK REACTIVITY EXPERIMENTS**

**Table A-1. Mineralogical Composition**

Sample Name	EERC Sample ID	Rock Type	Formation	Calcite	Dolomite	Magnesium Calcite	Quartz	Amorphous
Plug 1-A	1598-031-1-IS	Limestone	Keg River					
	Preexposure			85.75	8.46	0.00	0.65	5.14
	Postexposure CO <sub>2</sub>			84.52	9.78	0.00	1.45	4.21
Plug 1-B	1598-031-2 IS	Limestone	Keg River					
	Preexposure			87.81	7.88	0.00	0.66	3.65
	Postexposure CO <sub>2</sub> +H <sub>2</sub> S			84.23	9.76	0.25	1.87	3.22
Plug 2-A	1598-031-3 IS	Limestone	Muskeg					
	Preexposure			86.39	0.00	0.00	0.00	13.61
	Postexposure CO <sub>2</sub>			86.45	0.00	0.00	0.00	13.23
Plug 3-A	1598-031-4-IS	Limestone	Keg River					
	Preexposure			90.05	6.09	0.00	1.47	2.38
	Postexposure CO <sub>2</sub>			92.25	5.62	0.00	2.13	1.98
Plug 3-B	1598-031-5-IS	Limestone	Keg River					
	Preexposure			90.33	5.19	0.00	1.33	3.15
	Postexposure CO <sub>2</sub> +H <sub>2</sub> S			89.25	7.20	0.65	2.13	2.92
Plug 4-A	1598-031-6-IS	Dolomitic Limestone	Keg River					
	Preexposure			79.59	12.92	0.00	7.23	0.26
	Postexposure CO <sub>2</sub>			77.63	16.59	1.36	5.62	0.96
Plug 4-B	1598-031-7-IS	Dolomitic Limestone	Keg River					
	Preexposure			80.36	16.74	0.00	1.15	1.76
	Postexposure CO <sub>2</sub>			81.79	15.26	0.00	2.12	2.51
Plug 5-A	1598-031-8-IS	Limestone	Zama					
	Preexposure			80.84	0.56	5.63	0.99	11.98
	Postexposure CO <sub>2</sub>			82.35	0.42	6.12	0.63	13.42
Plug 6-A	1598-031-9-IS	Limestone	Keg River					
	Preexposure			87.46	0.75	2.30	0.73	8.75
	Postexposure CO <sub>2</sub>			87.46	0.75	2.30	0.73	8.75
Plug 6-B	1598-031-10-IS	Limestone	Keg River					
	Preexposure			94.85	1.02	0.00	0.38	3.75
	Postexposure CO <sub>2</sub> +H <sub>2</sub> S			94.85	1.02	0.00	0.38	3.75

## **APPENDIX B**

# **ZAMA STEEL CASING HIGH-PRESSURE AND -TEMPERATURE BATCH REACTOR EXPERIMENTAL RESULTS**

# ***Zama Steel Casing High-Pressure and -Temperature Batch Reactor Experimental Results***



**EERC**

Energy & Environmental Research Center®  
Putting Research into Practice

**Energy & Environmental Research Center (EERC)...**

The International Center for Applied Energy Technology®

INDUSTRY, GOVERNMENT, AND THE  
RESEARCH COMMUNITY

RESEARCH COMMUNITY



# Experimental Setup

- Seven types of steel coupons
- Two types of fluid presaturation:
  - Tap water
  - 16.5 wt% NaCl brine
- Two acid gas injection scenarios:
  - Pure CO<sub>2</sub>
  - 30 mole% H<sub>2</sub>S + 70 mole% CO<sub>2</sub>
- Zama oilfield conditions:
  - 2100 psi exposure pressure
  - 71°C temperature

Pressure: 2100 psi

CO<sub>2</sub> Content: 100 and 70 mol%

H<sub>2</sub>S Content: 0 and 30 mol%

Temperature: 71°C (140°F)

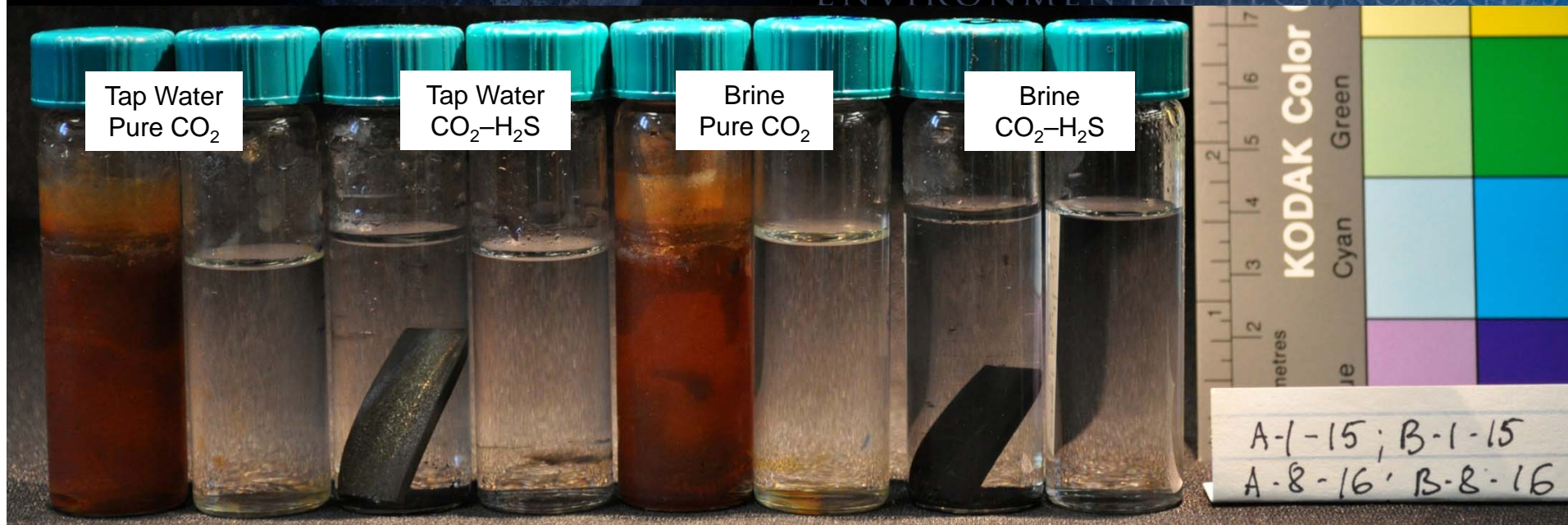
Saturation Conditions:  
1. Tap water  
2. NaCl, 100,000 mg/L

Time of Exposure: 28 days

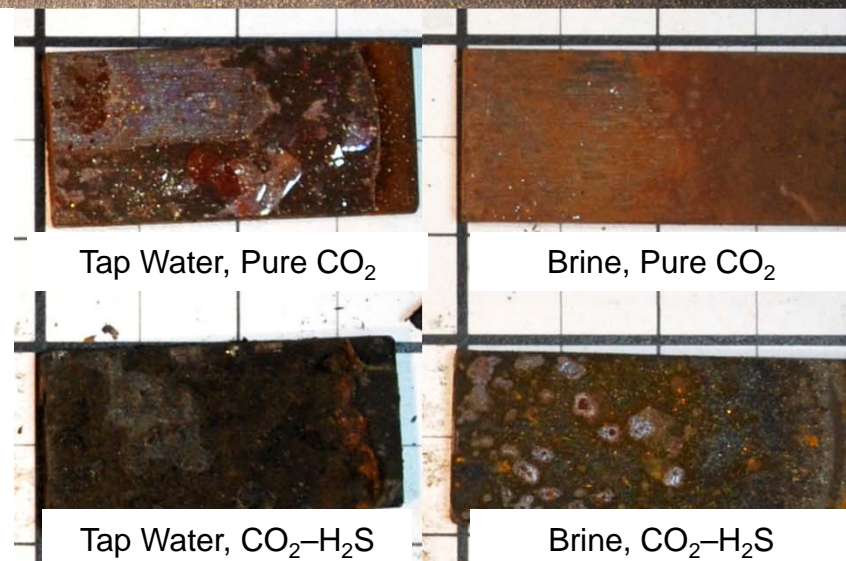
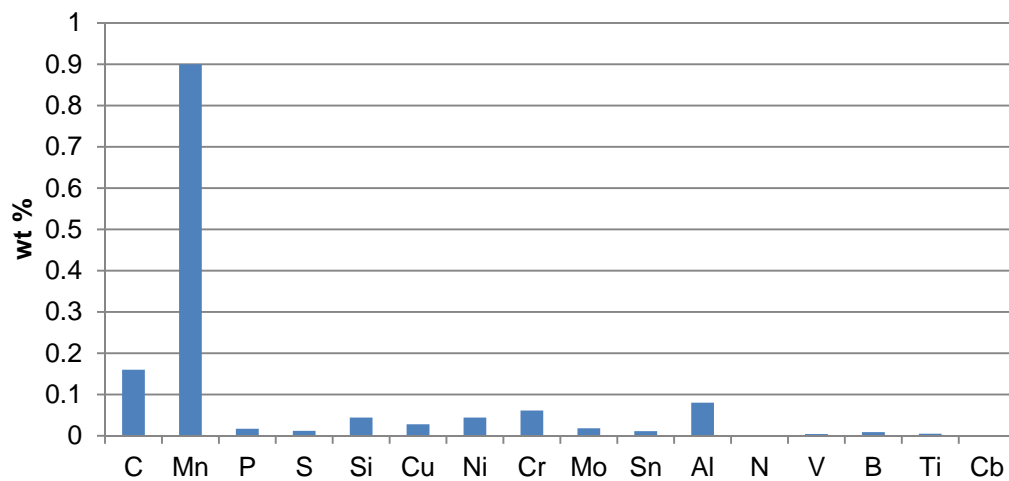
Number of Steel Coupon Types: 7



# Steel 5LX65



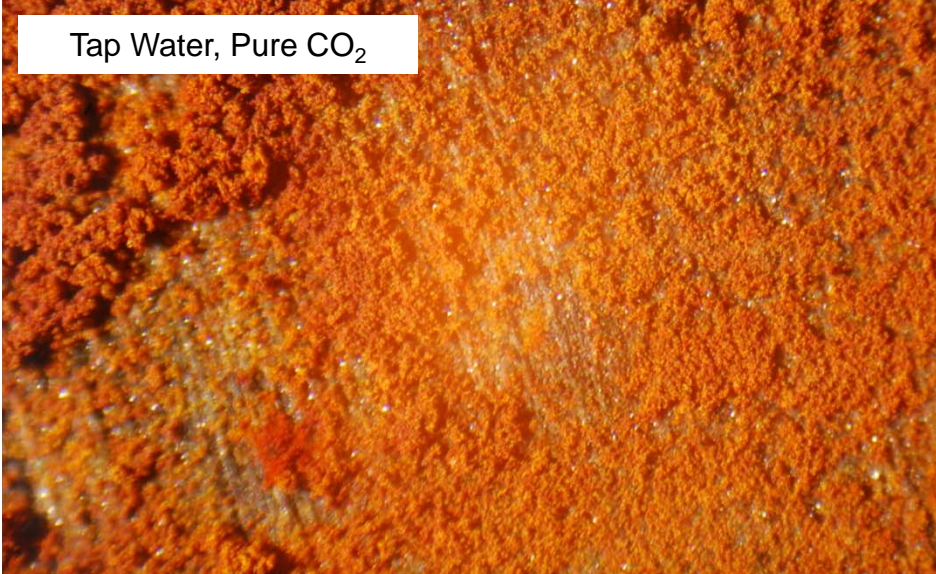
Original Chemical Composition of 5LX65 Steel (Fe is in balance)



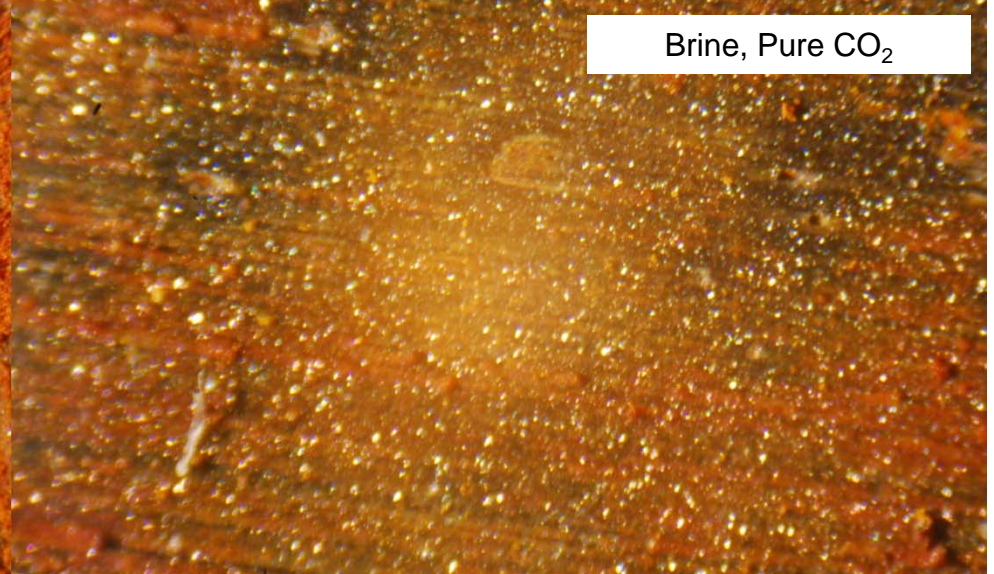


# Steel 5LX65 (x400) after Exposure

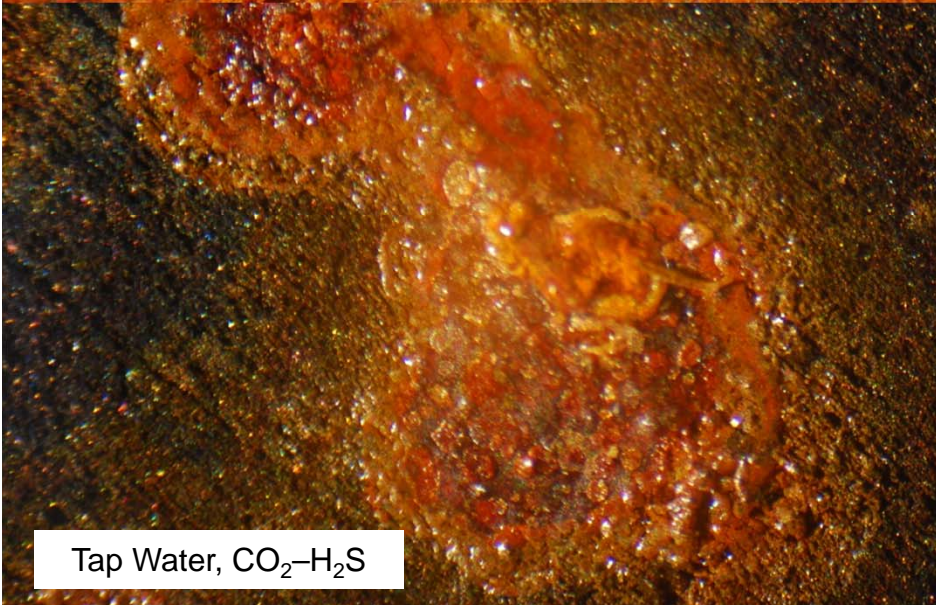
Tap Water, Pure CO<sub>2</sub>



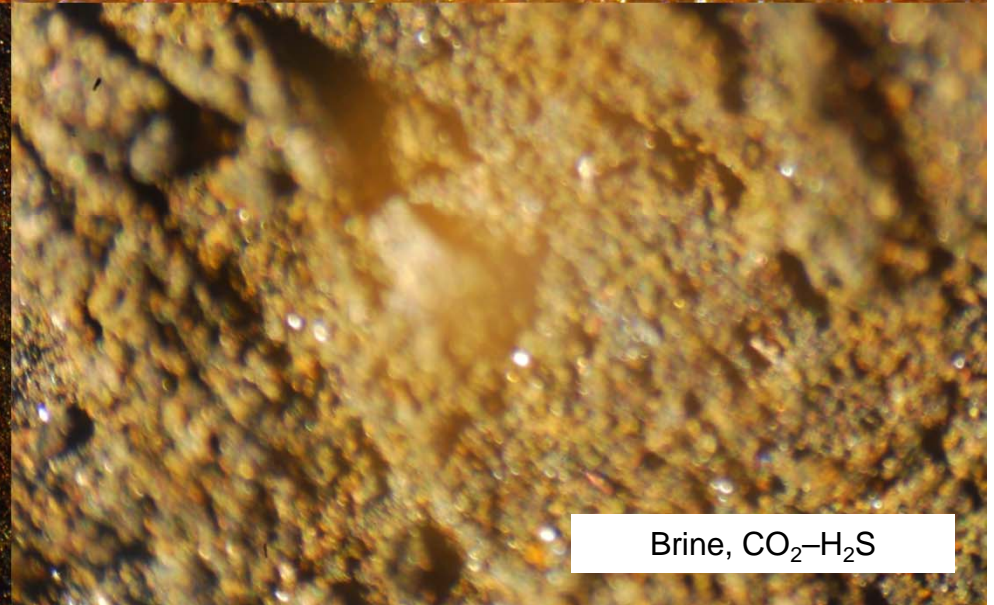
Brine, Pure CO<sub>2</sub>



Tap Water, CO<sub>2</sub>-H<sub>2</sub>S



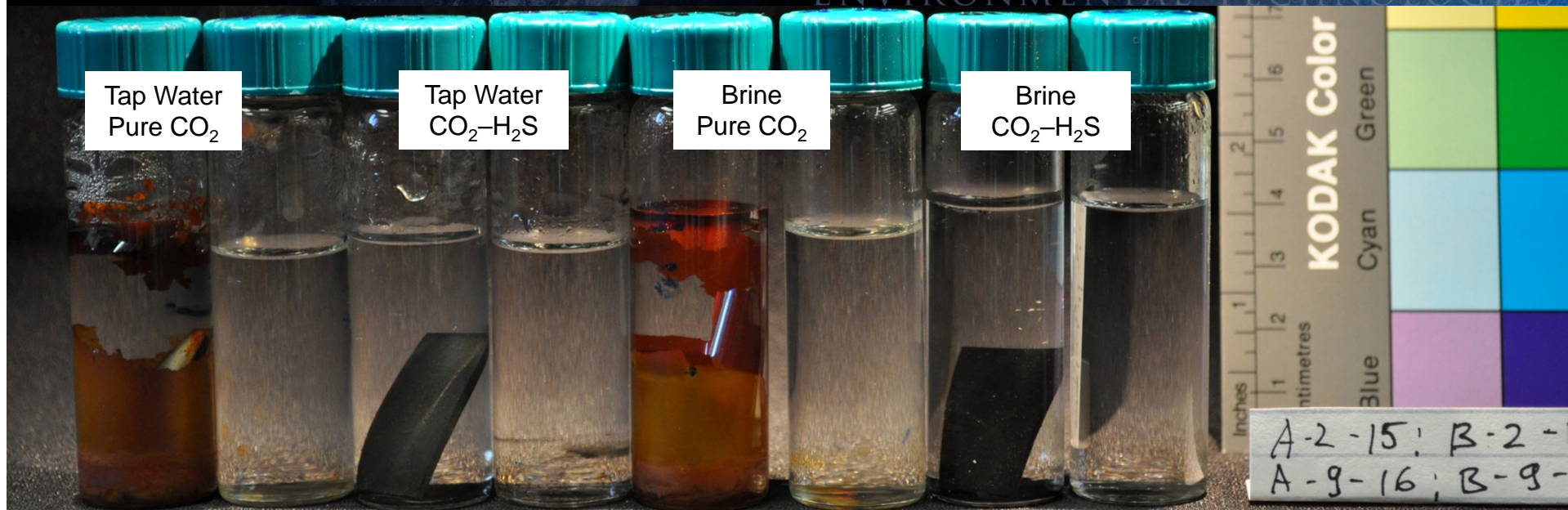
Brine, CO<sub>2</sub>-H<sub>2</sub>S



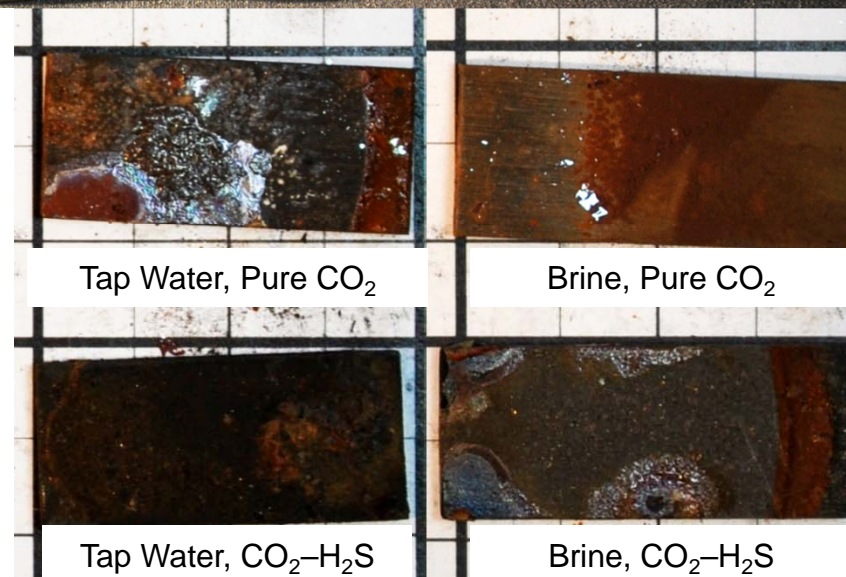
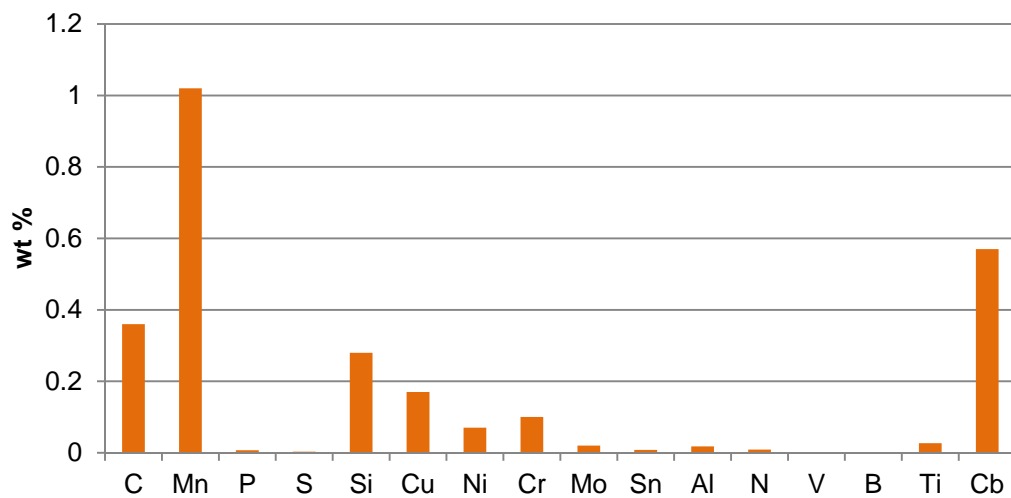


# Steel J55

RESEARCH AND DEVELOPMENT PROGRAMS, OPPORTUNITIES FOR TECHNOLOGY COMMERCIALIZATION  
WORLD-CLASS CENTERS OF EXCELLENCE  
ENVIRONMENTAL TECHNOLOGIES



Original Chemical Composition of 5LX65 Steel (Fe is in balance)



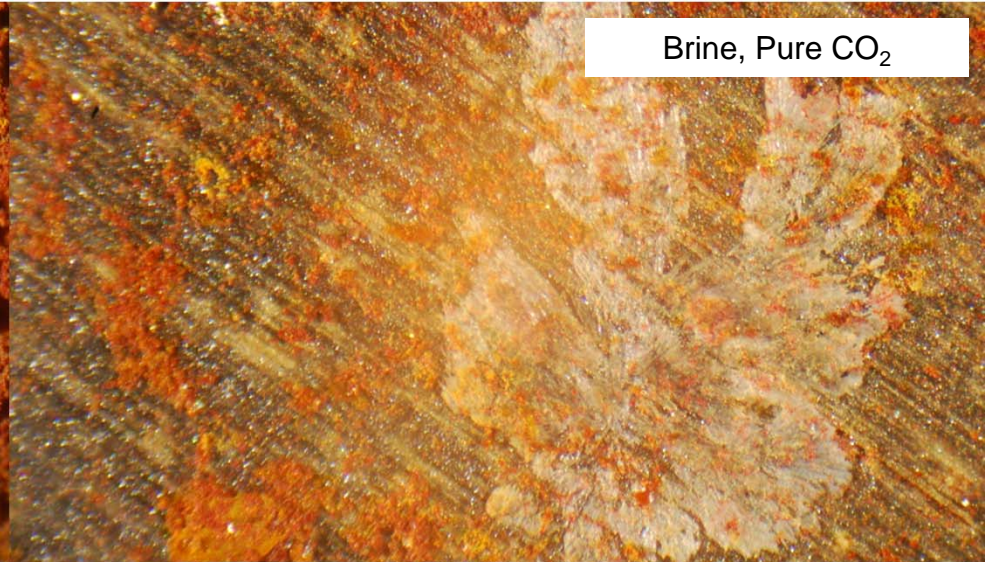


# Steel J55 (x400) after Exposure

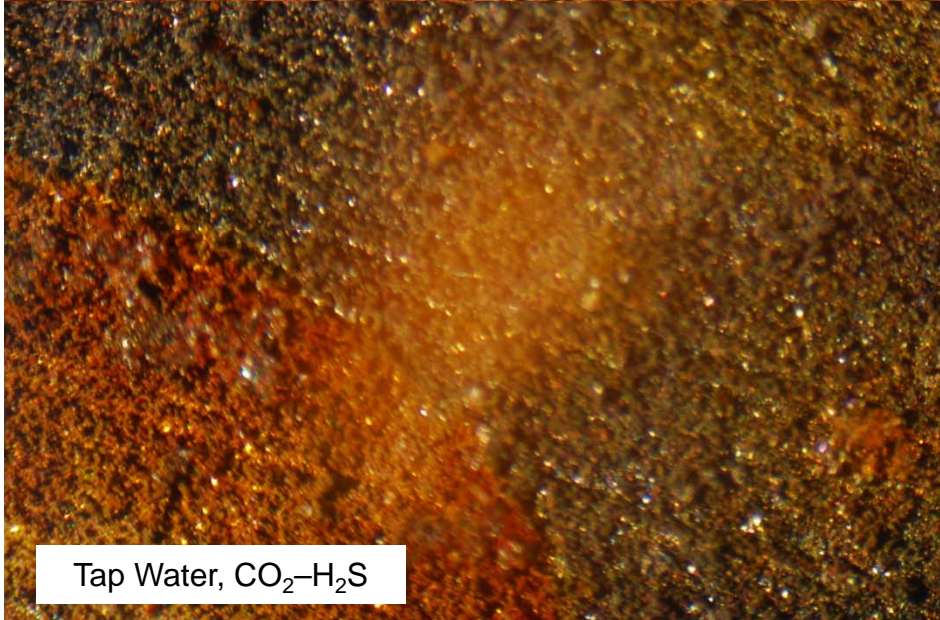
Tap Water, Pure CO<sub>2</sub>



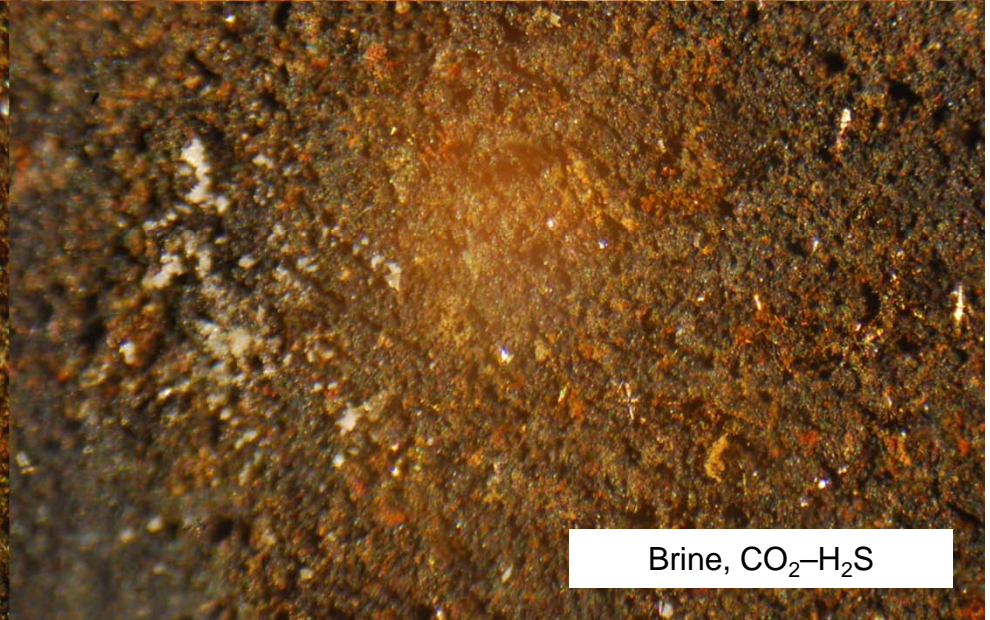
Brine, Pure CO<sub>2</sub>



Tap Water, CO<sub>2</sub>-H<sub>2</sub>S

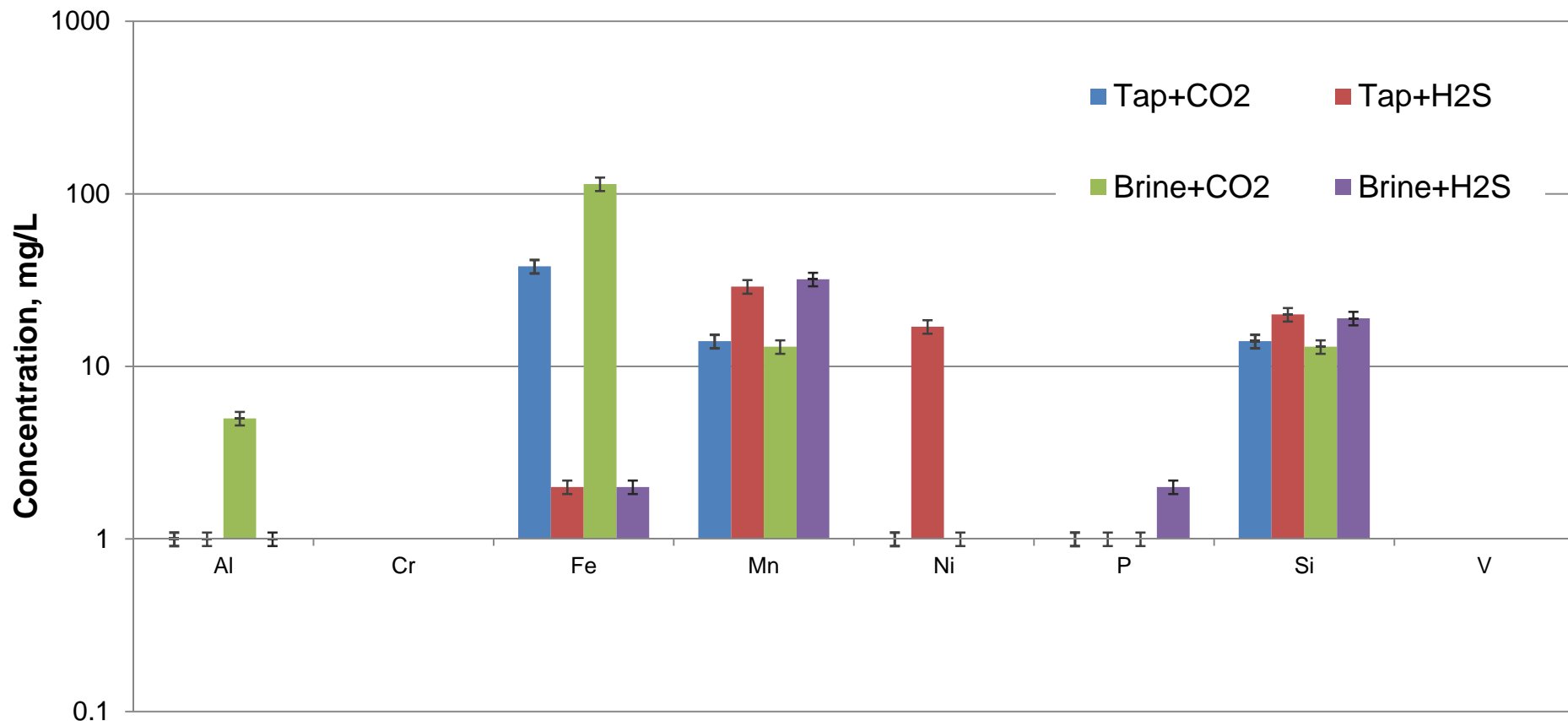


Brine, CO<sub>2</sub>-H<sub>2</sub>S



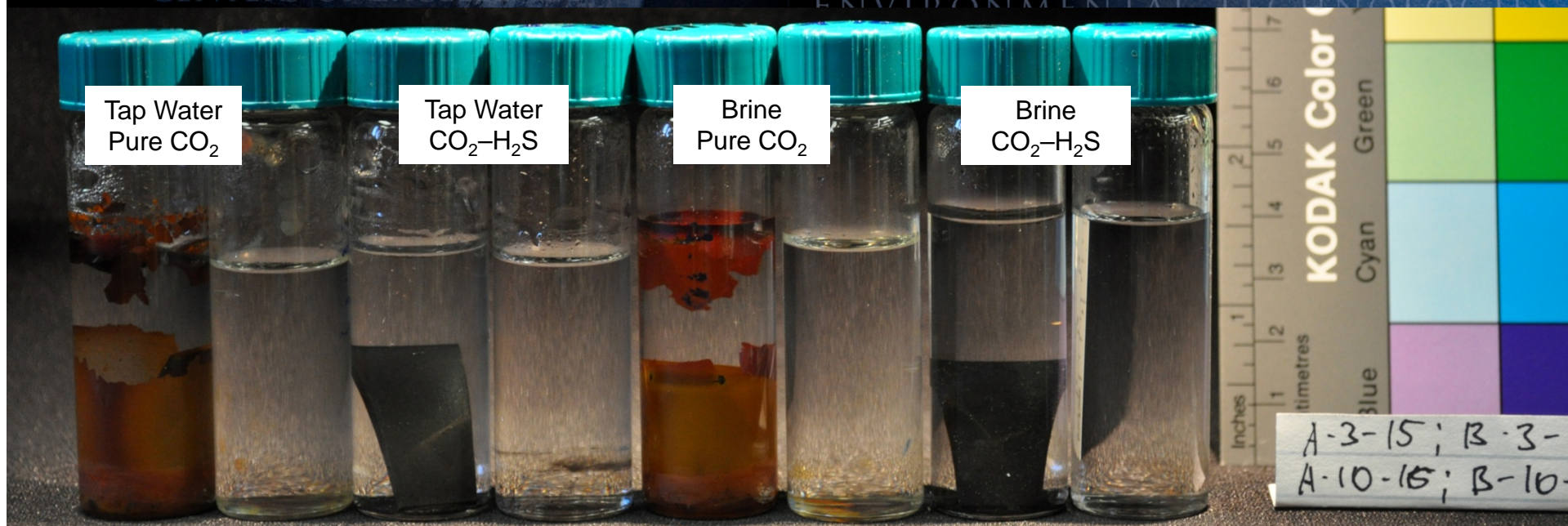


# J55 Fluid Analysis after Exposure

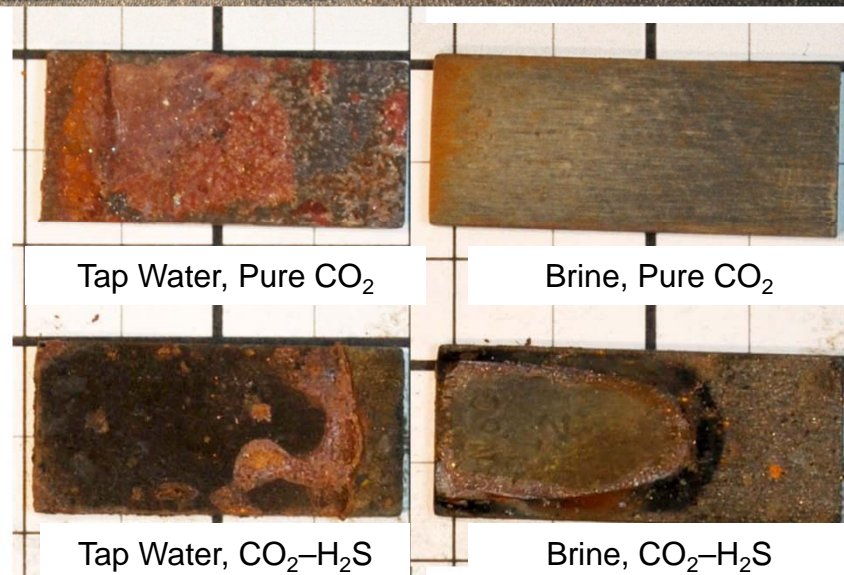
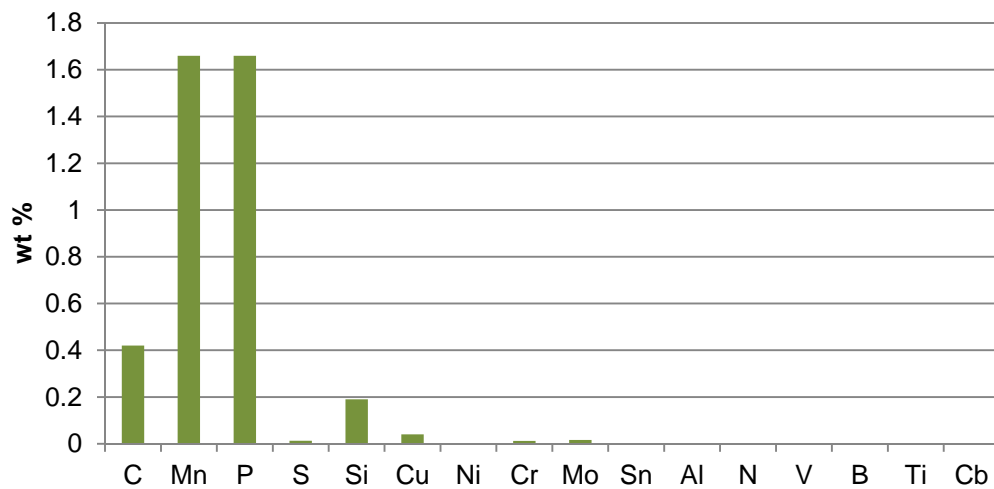


	Al	Cr	Fe	Mn	Ni	P	Si	V	S	Na
Tap + CO <sub>2</sub>	1	0	38	14	1	1	14	0	116	11
Tap + H <sub>2</sub> S	1	0	2	29	17	1	20	0	3730	11
Brine + CO <sub>2</sub>	5	0	114	13	1	1	13	0	896	47,600
Brine + H <sub>2</sub> S	1	0	2	32	0	2	19	0	2720	37,600

# Steel N80



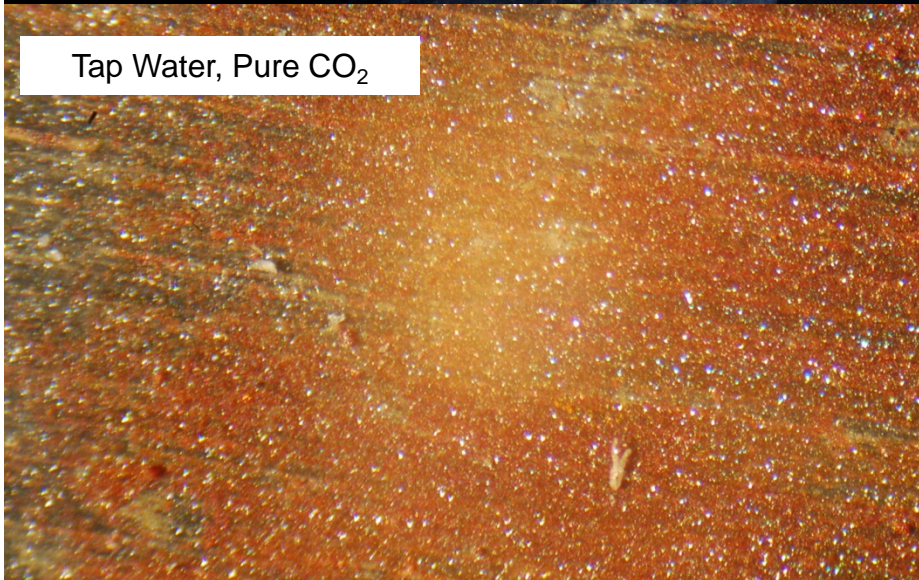
Original Chemical Composition of N80 Steel (Fe is in balance)



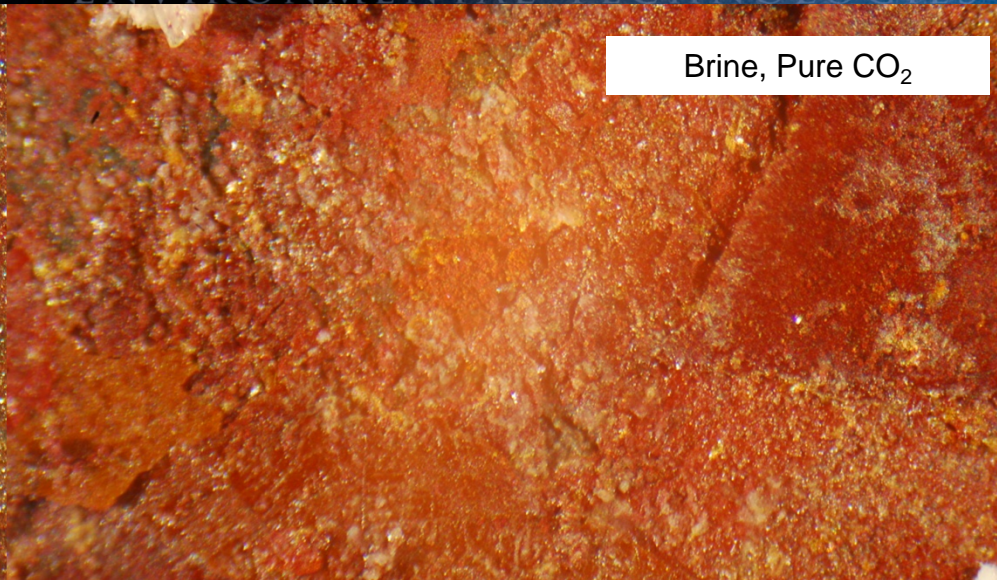


# Steel N80 (x400) after Exposure

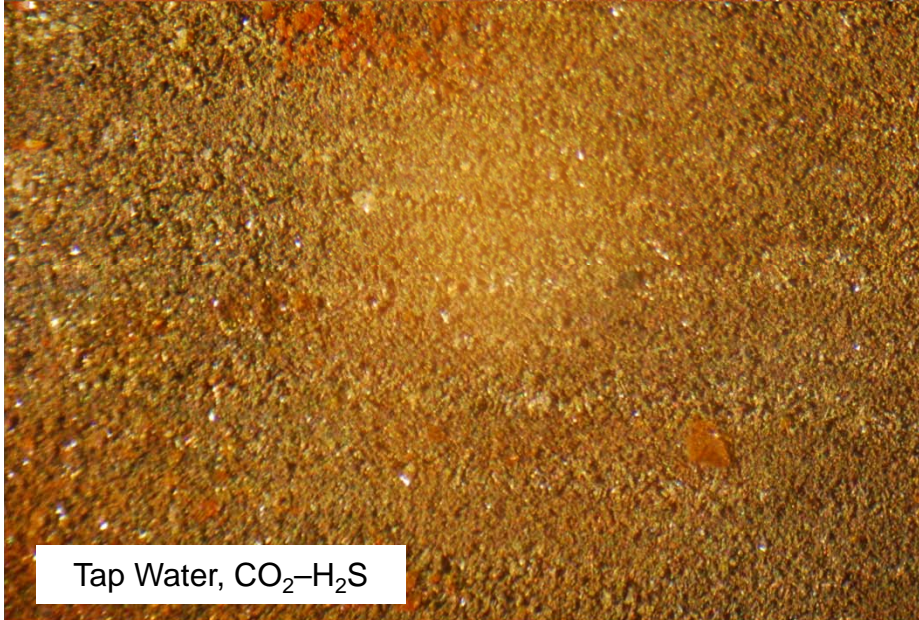
Tap Water, Pure CO<sub>2</sub>



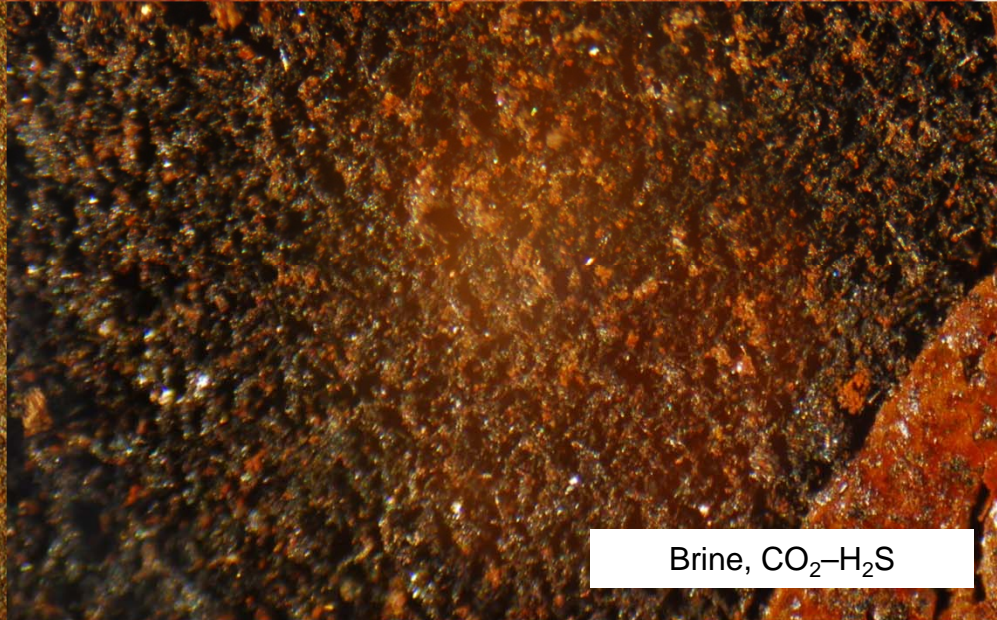
Brine, Pure CO<sub>2</sub>



Tap Water, CO<sub>2</sub>-H<sub>2</sub>S

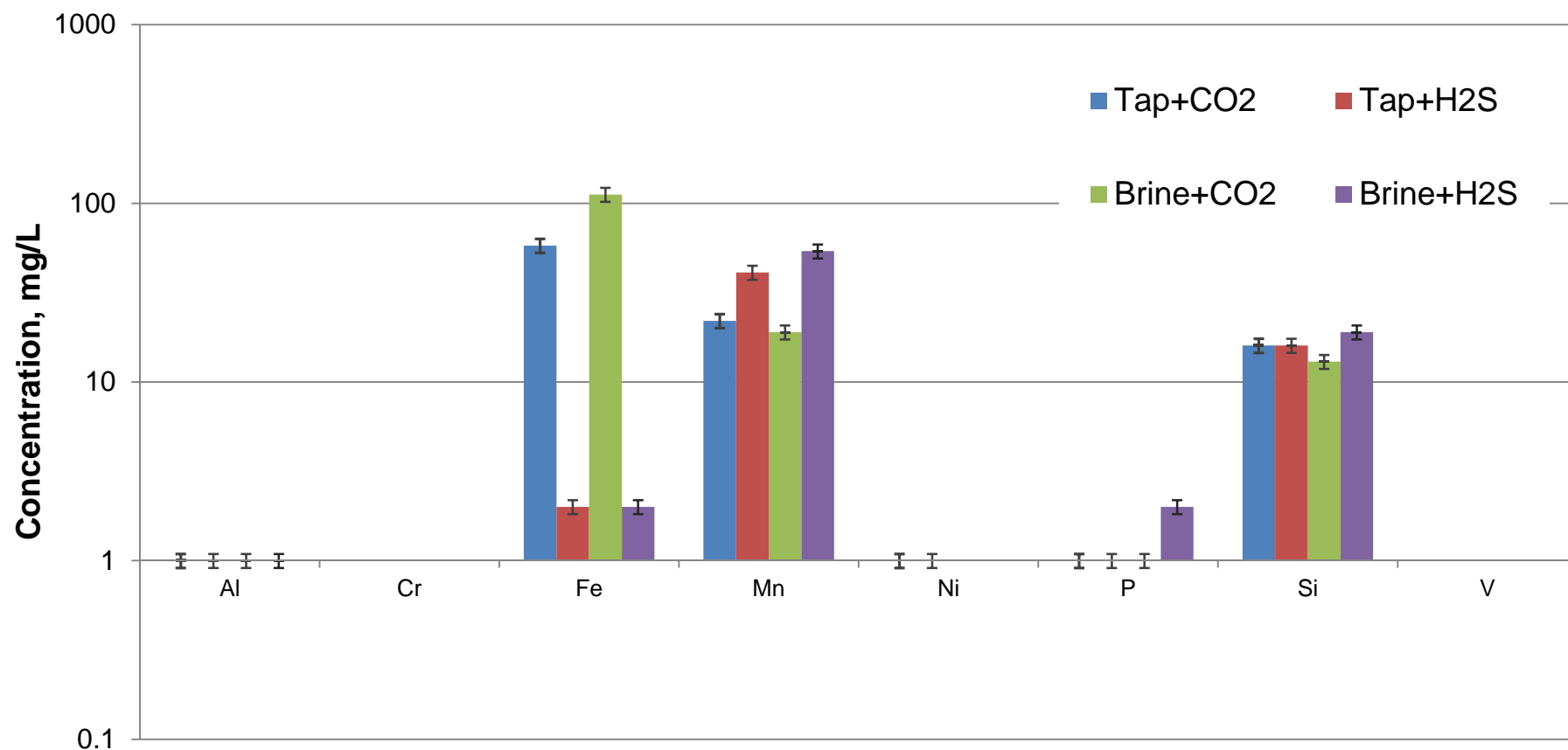


Brine, CO<sub>2</sub>-H<sub>2</sub>S





# N80 Fluid Analysis after Exposure

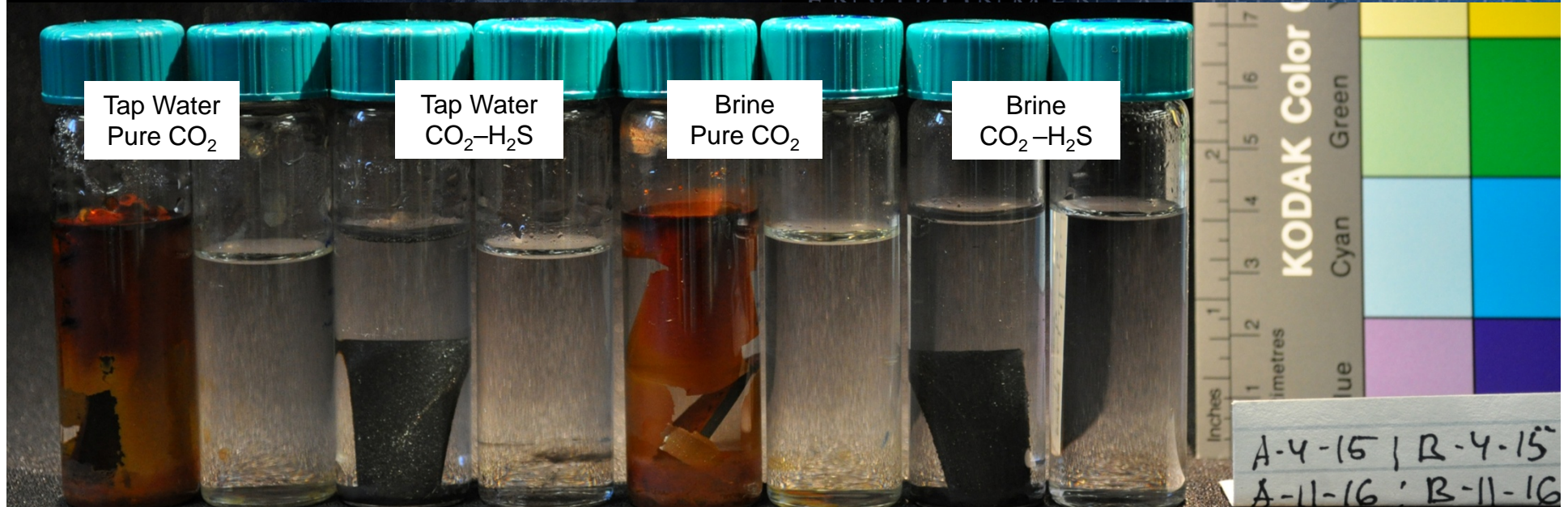


	Al	Cr	Fe	Mn	Ni	P	Si	V	S	Na
Tap + CO <sub>2</sub>	1	0	58	22	1	1	16	0	55	11
Tap + H <sub>2</sub> S	1	0	2	41	1	1	16	0	444	10
Brine + CO <sub>2</sub>	1	0	112	19	0	1	13	0	576	42,000
Brine + H <sub>2</sub> S	1	0	2	54	0	2	19	0	262	44,600

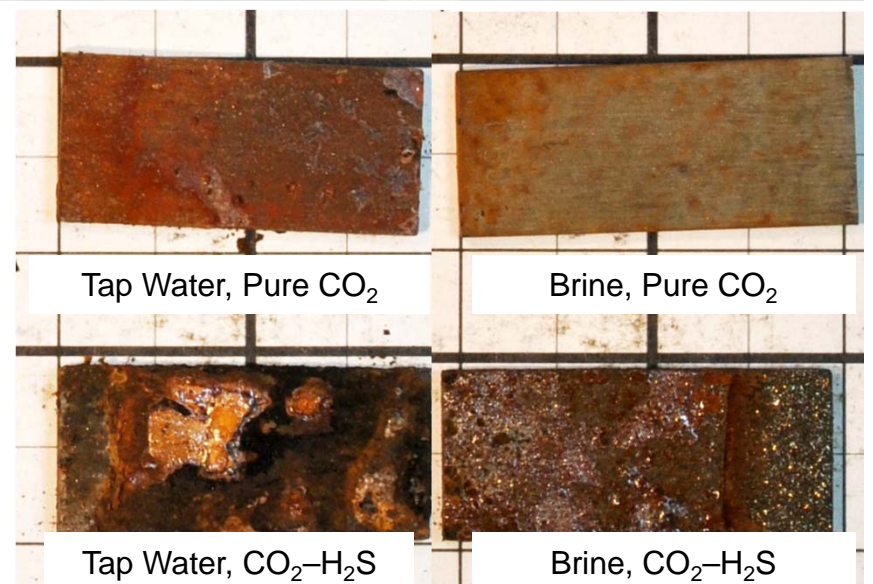
RESEARCH AND DEVELOPMENT  
PROGRAMS, OPPORTUNITIES FOR  
TECHNOLOGY COMMERCIALIZATION  
WORLD-CLASS  
CENTERS OF EXCELLENCE

# Steel C90

RESEARCH AND DEVELOPMENT  
PROGRAMS, OPPORTUNITIES FOR  
TECHNOLOGY COMMERCIALIZATION  
WORLD-CLASS  
CENTERS OF EXCELLENCE  
ENVIRONMENTAL TECHNOLOGIES



Original chemical composition  
data not available.

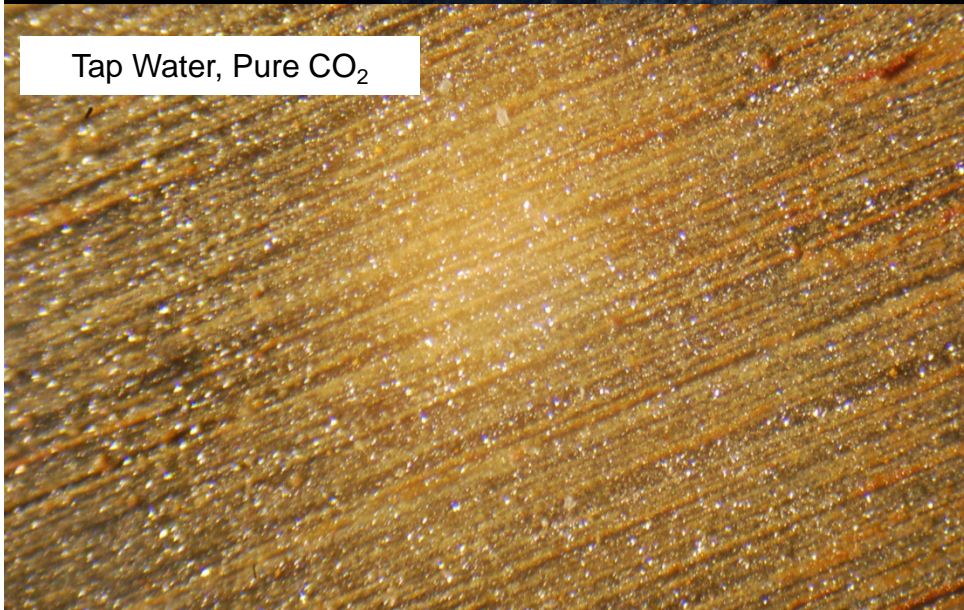




RESEARCH AND DEVELOPMENT PROGRAMS, OPPORTUNITIES FOR TECHNOLOGY COMMERCIALIZATION  
WORLD CLASS CENTERS OF EXCELLENCE  
ENVIRONMENTAL TECHNOLOGIES

# Steel C90 (x400) after Exposure

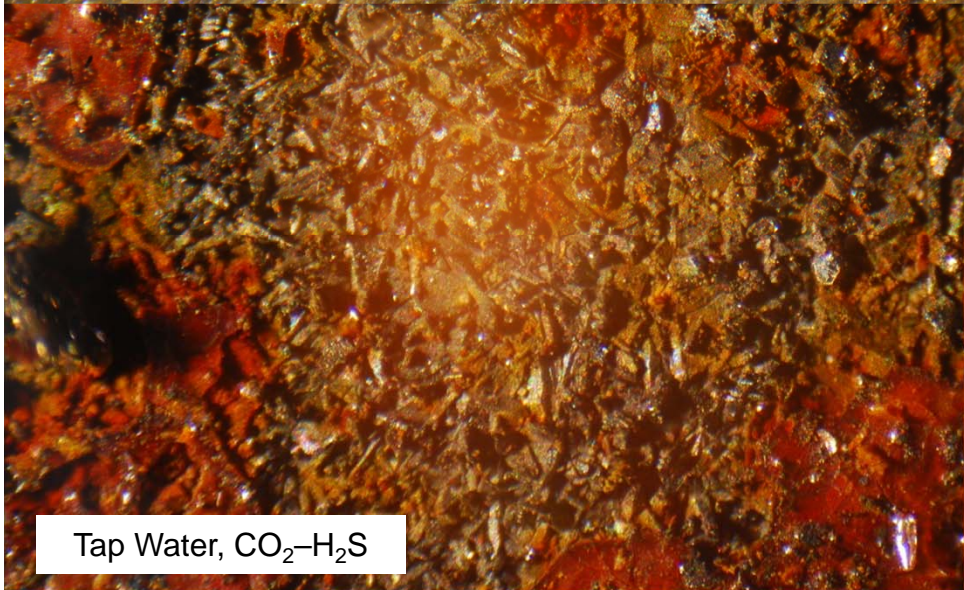
Tap Water, Pure CO<sub>2</sub>



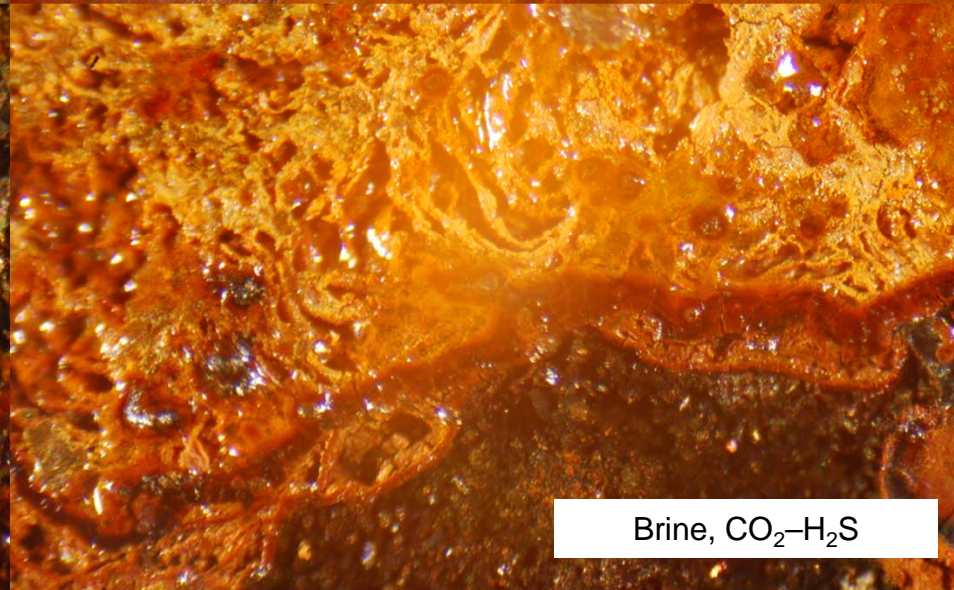
Brine, Pure CO<sub>2</sub>



Tap Water, CO<sub>2</sub>-H<sub>2</sub>S

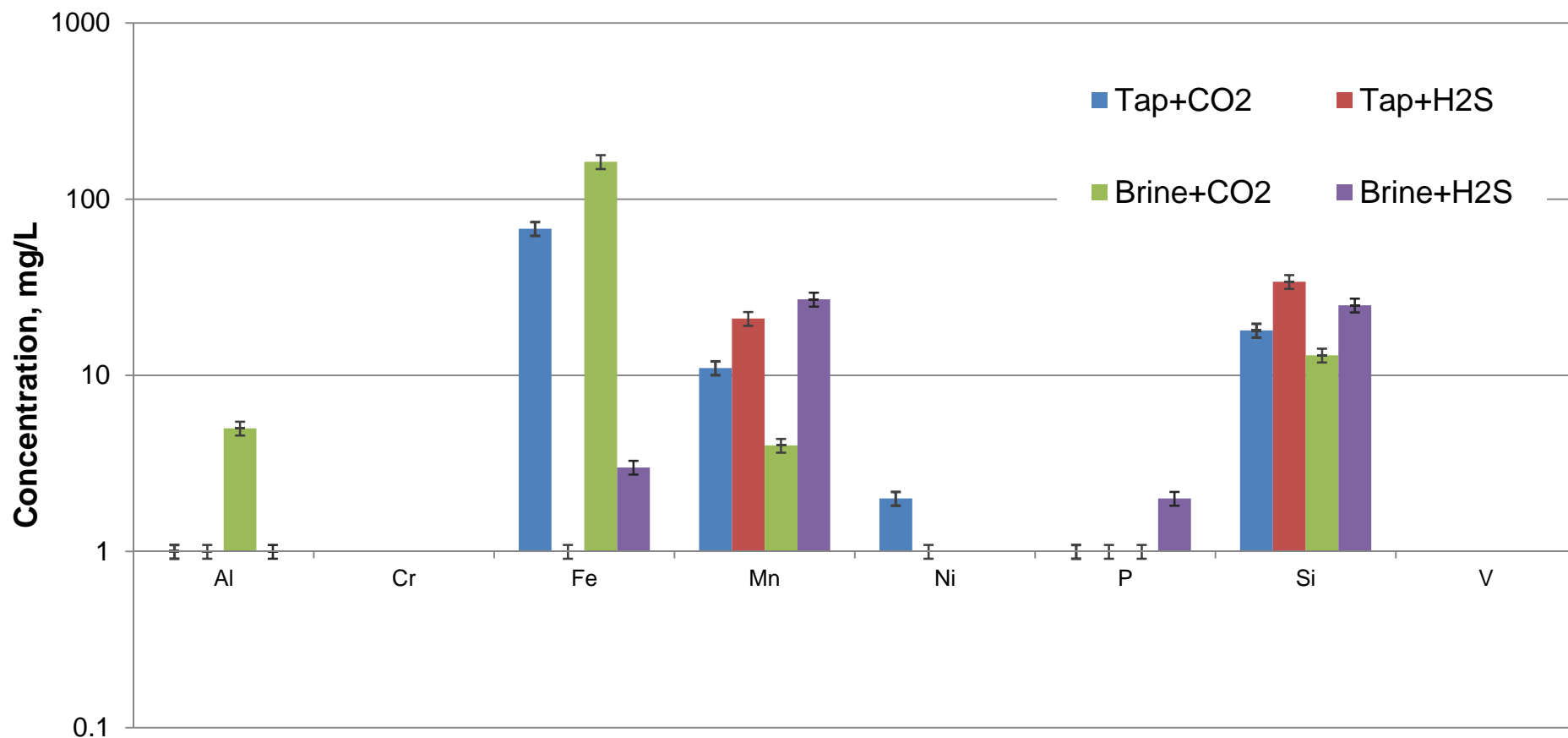


Brine, CO<sub>2</sub>-H<sub>2</sub>S



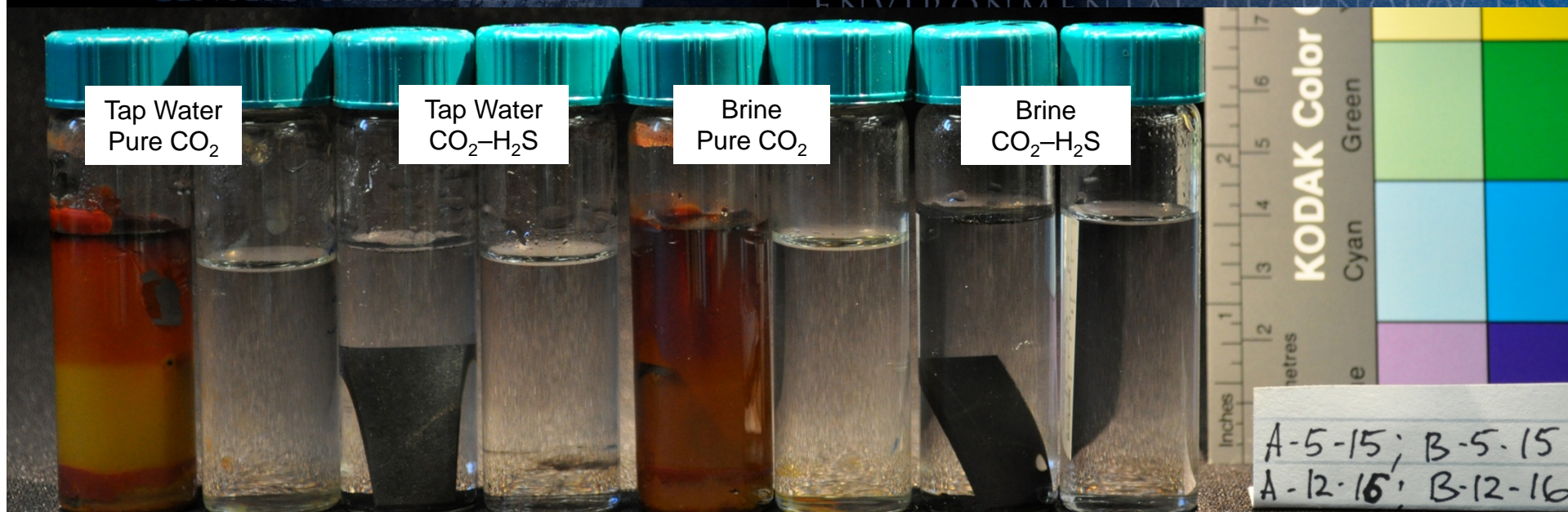


# C90 Fluid Analysis after Exposure

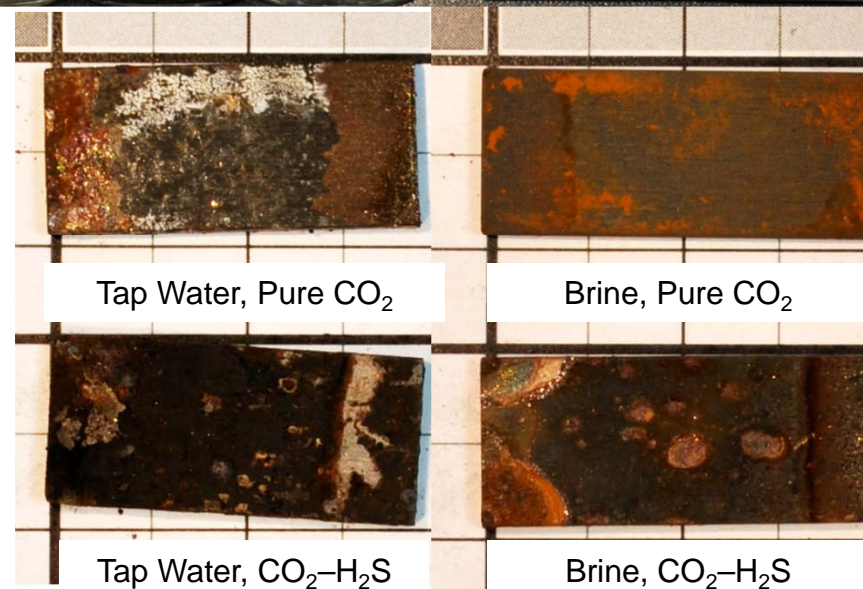
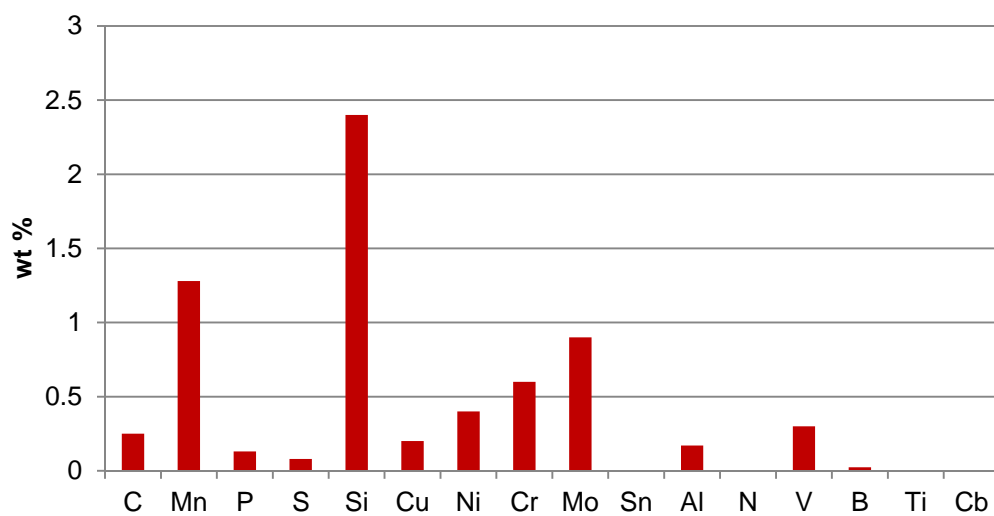


	Al	Cr	Fe	Mn	Ni	P	Si	V	S	Na
Tap + CO <sub>2</sub>	1	0	68	11	2	1	18	0	33	11
Tap + H <sub>2</sub> S	1	0	1	21	1	1	34	0	5880	16
Brine + CO <sub>2</sub>	5	0	163	4	0	1	13	0	384	40,800
Brine + H <sub>2</sub> S	1	0	3	27	0	2	25	0	2320	42,600

# Steel C95



Original Chemical Composition of C95 Steel (Fe is in balance)

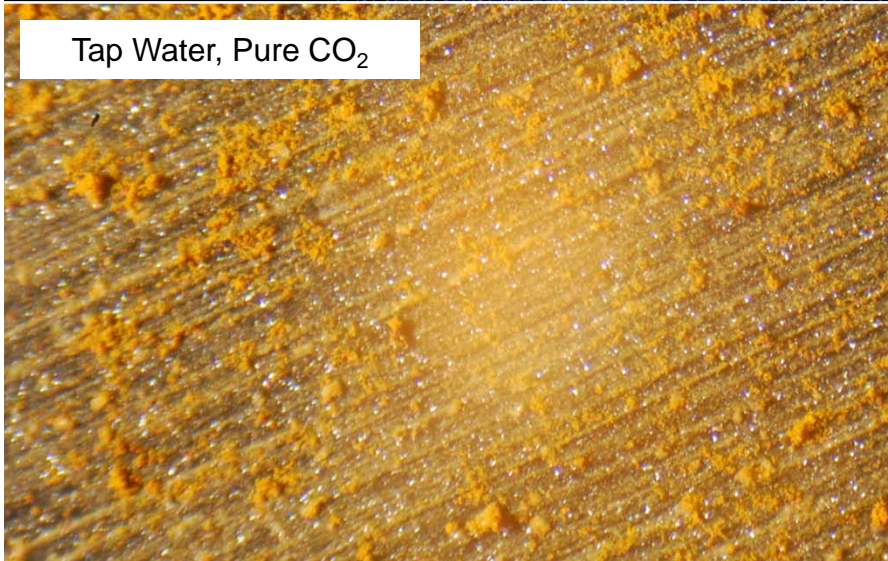




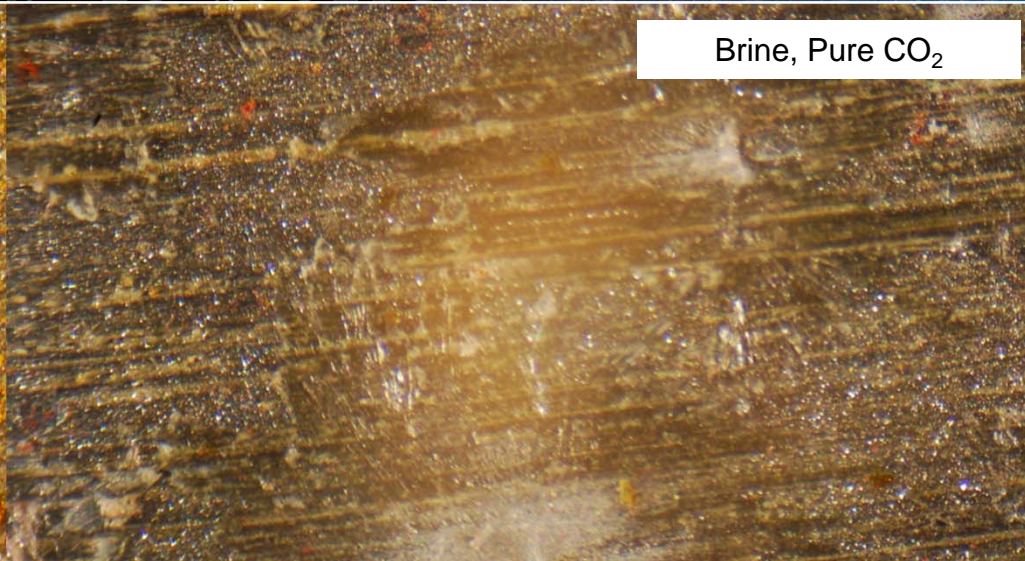
RESEARCH AND DEVELOPMENT PROGRAMS, OPPORTUNITIES FOR TECHNOLOGY COMMERCIALIZATION  
WORLD CLASS CENTERS OF EXCELLENCE  
ENVIRONMENTAL TECHNOLOGIES

# Steel C95 (x400) after Exposure

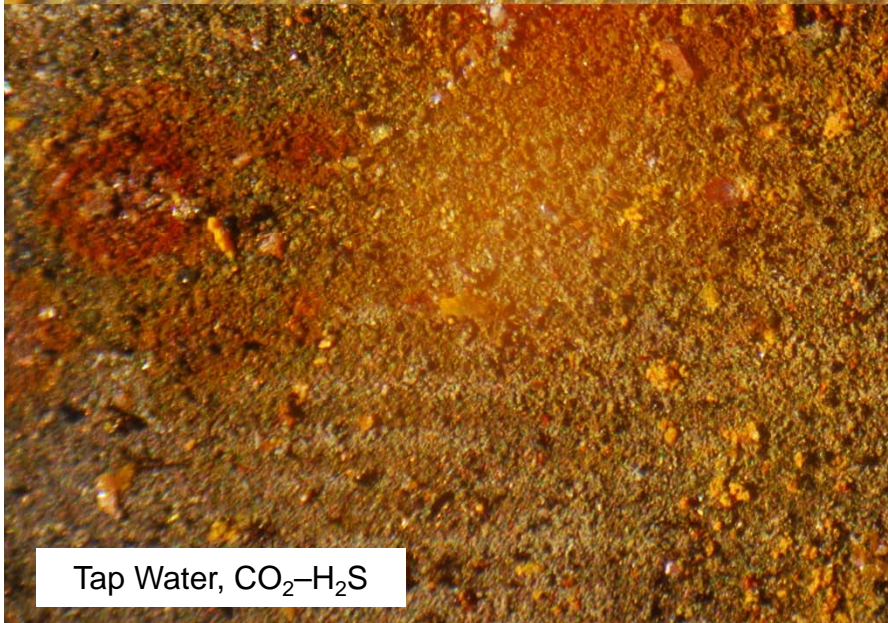
Tap Water, Pure CO<sub>2</sub>



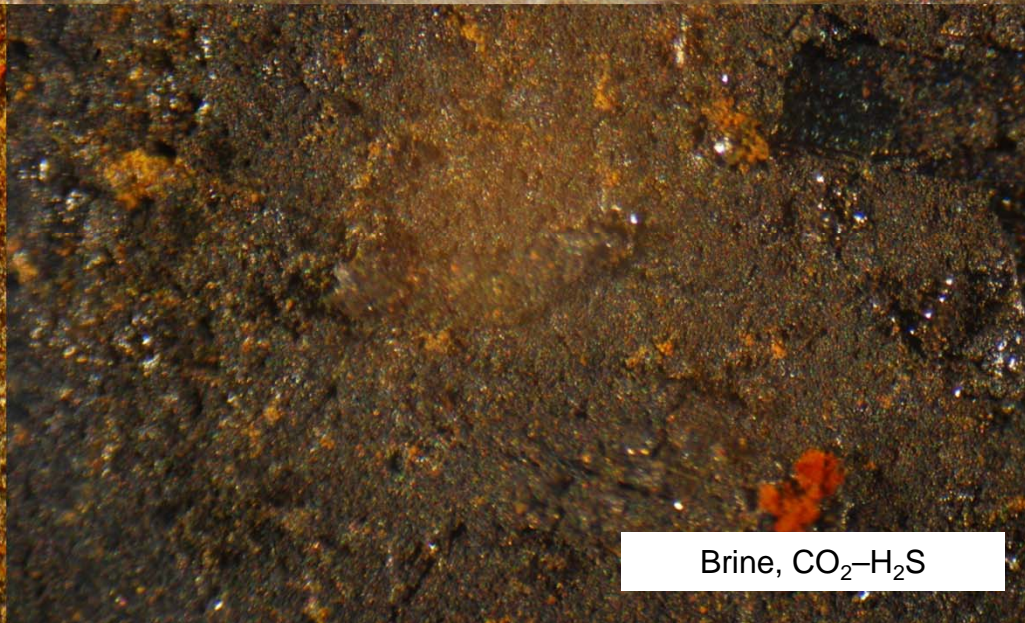
Brine, Pure CO<sub>2</sub>



Tap Water, CO<sub>2</sub>-H<sub>2</sub>S

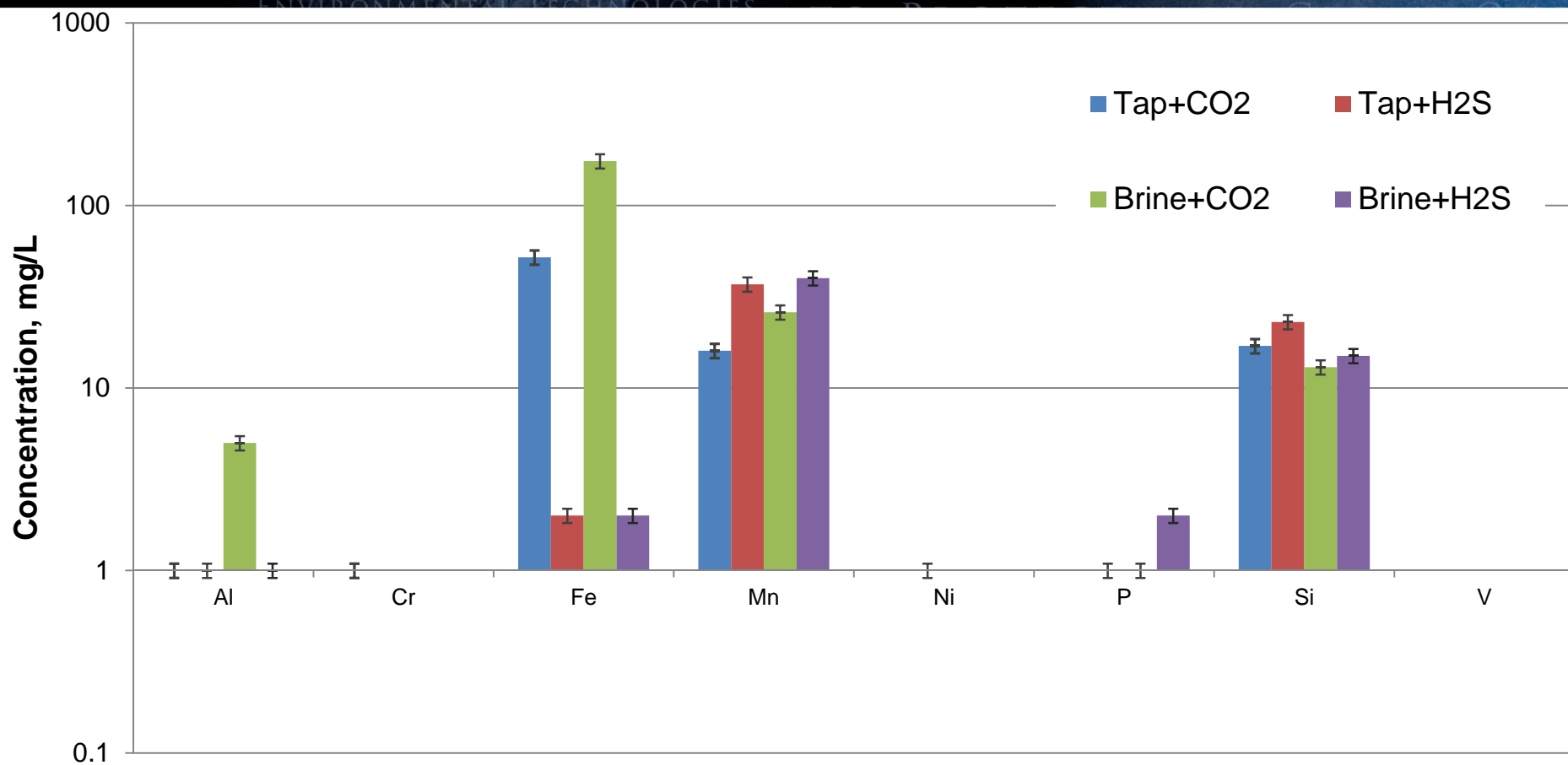


Brine, CO<sub>2</sub>-H<sub>2</sub>S





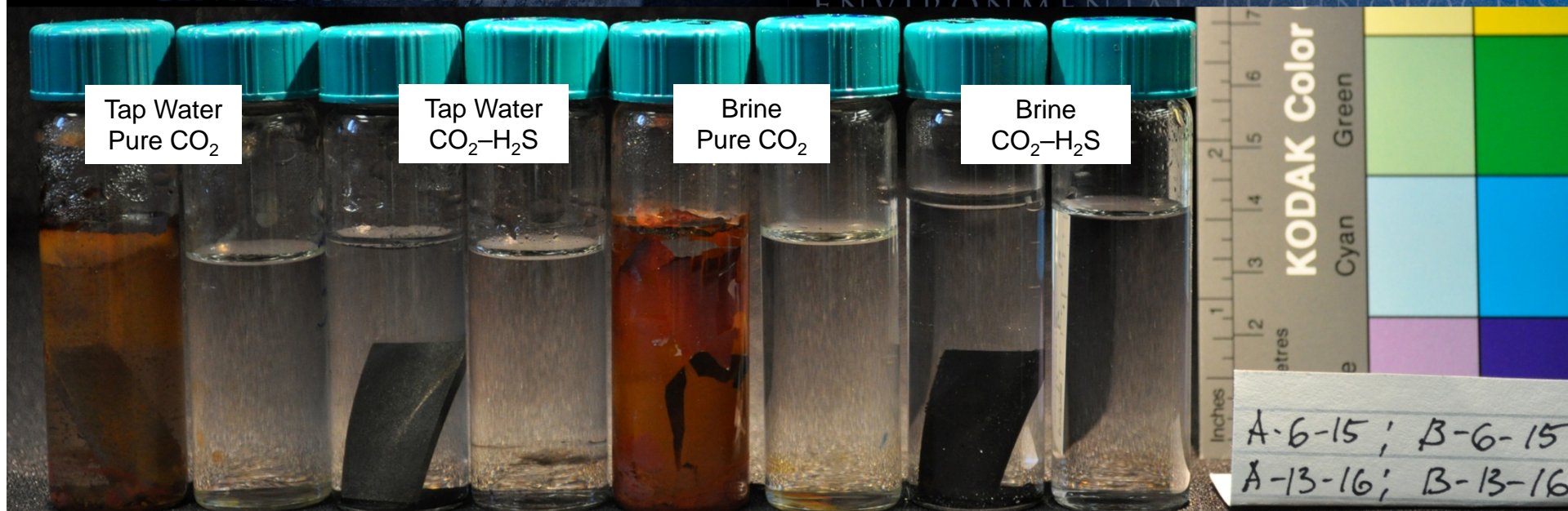
# C95 Fluid Analysis after Exposure



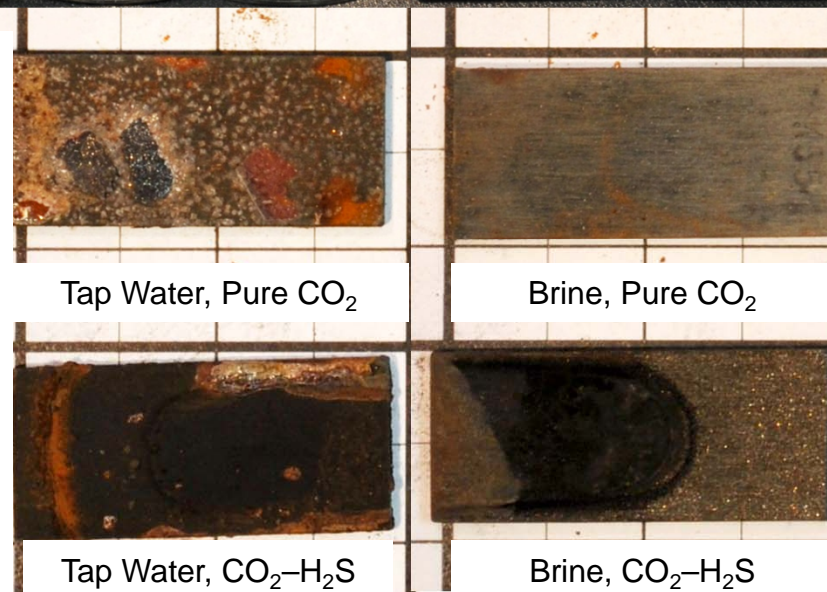
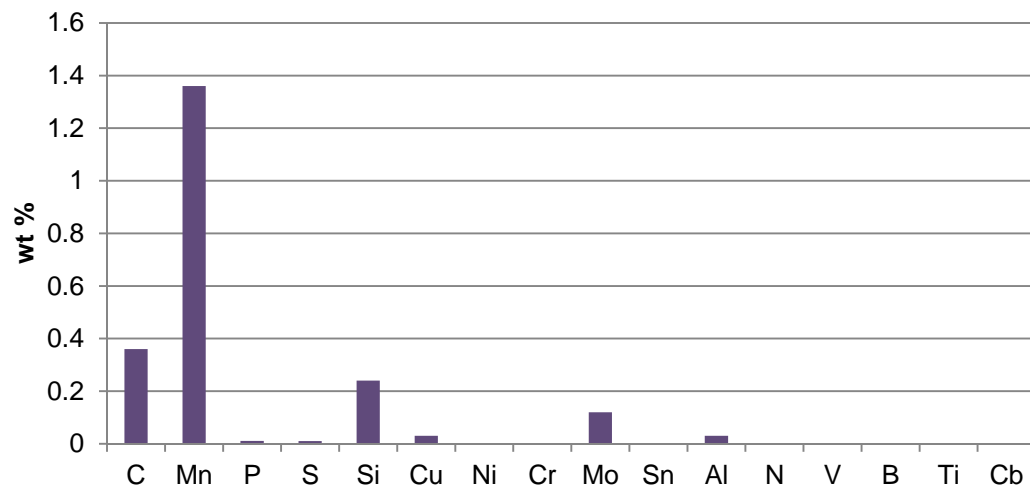
	Al	Cr	Fe	Mn	Ni	P	Si	V	S	Na
Tap + CO <sub>2</sub>	1	1	52	16	0	0	17	0	19	11
Tap + H <sub>2</sub> S	1	0	2	37	1	1	23	0	6160	16
Brine + CO <sub>2</sub>	5	0	175	26	0	1	13	0	306	44,200
Brine + H <sub>2</sub> S	1	0	2	40	0	2	15	0	3120	38,400



# Steel K55



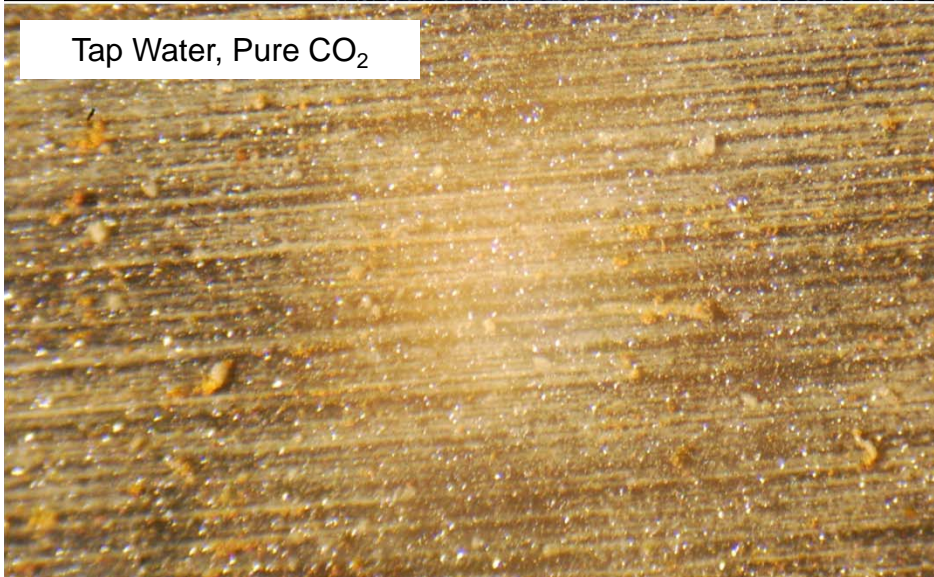
Original Chemical Composition of K55 Steel (Fe is in balance)



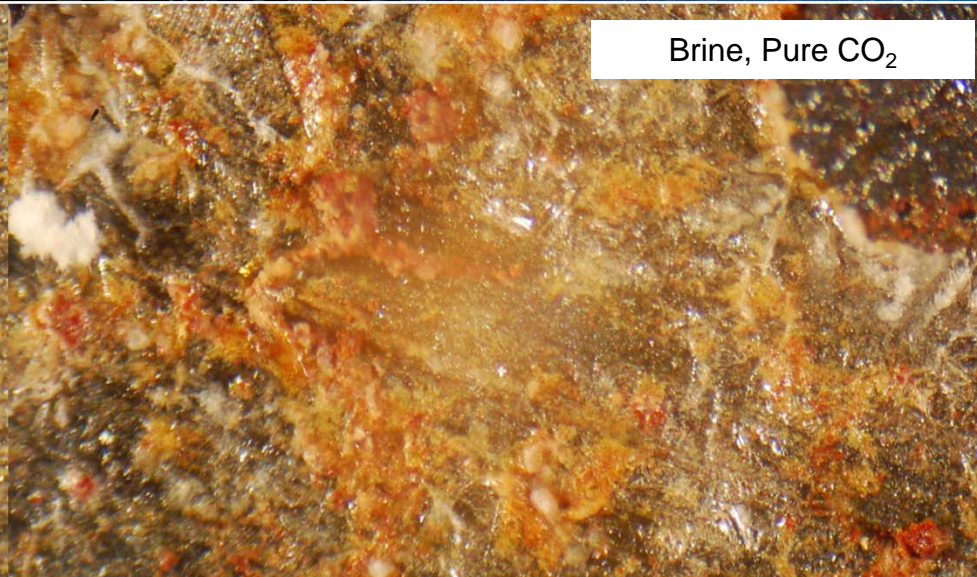


# Steel K55 (x400) after Exposure

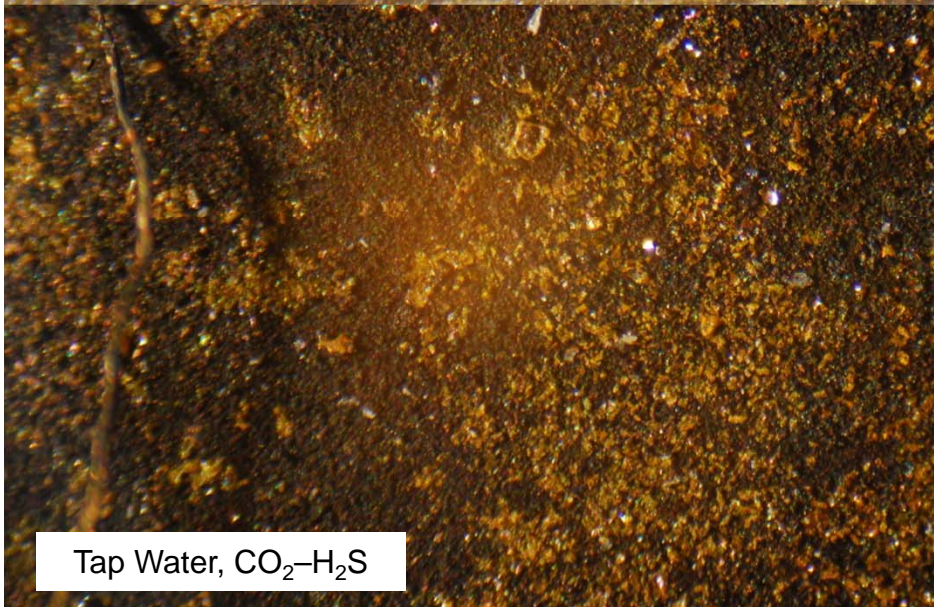
Tap Water, Pure CO<sub>2</sub>



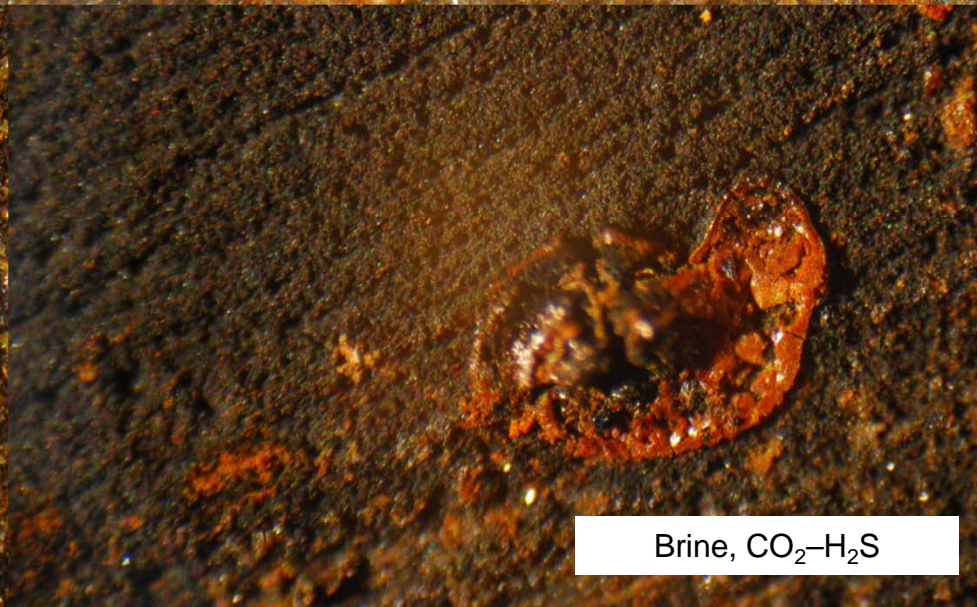
Brine, Pure CO<sub>2</sub>



Tap Water, CO<sub>2</sub>-H<sub>2</sub>S

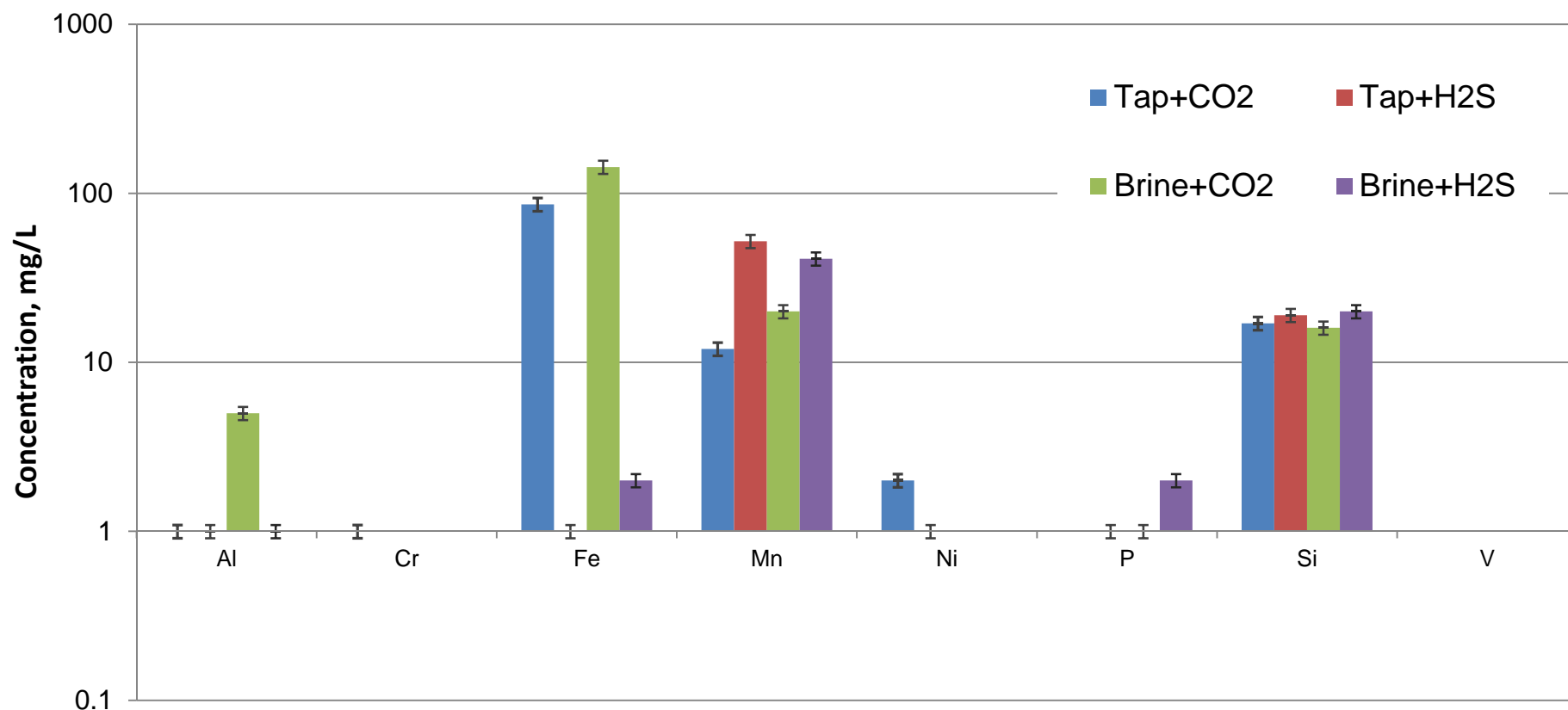


Brine, CO<sub>2</sub>-H<sub>2</sub>S



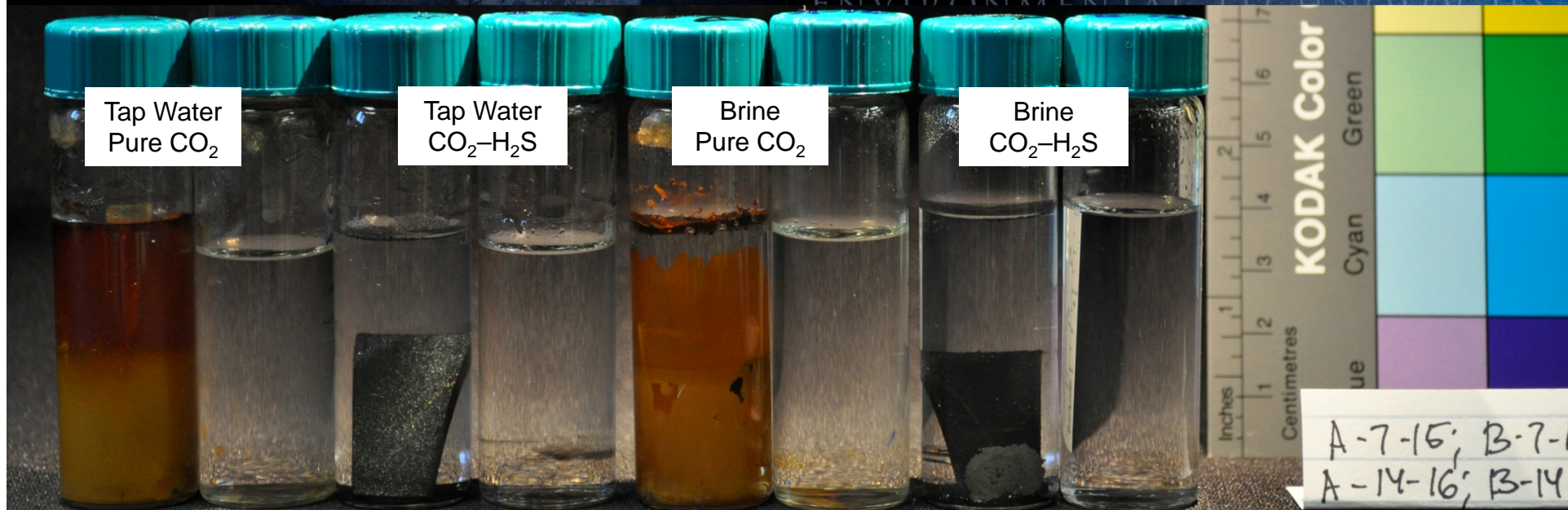


# K55 Fluid Analysis after Exposure

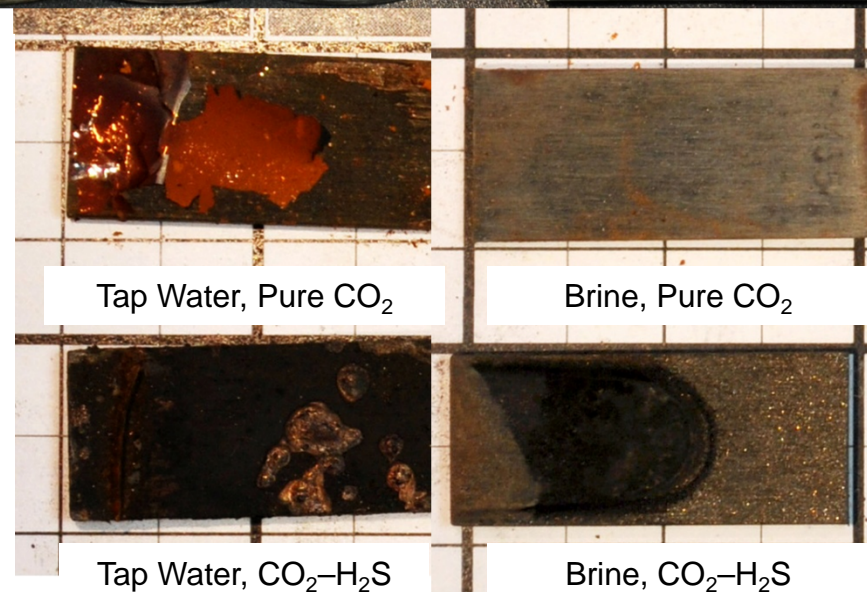
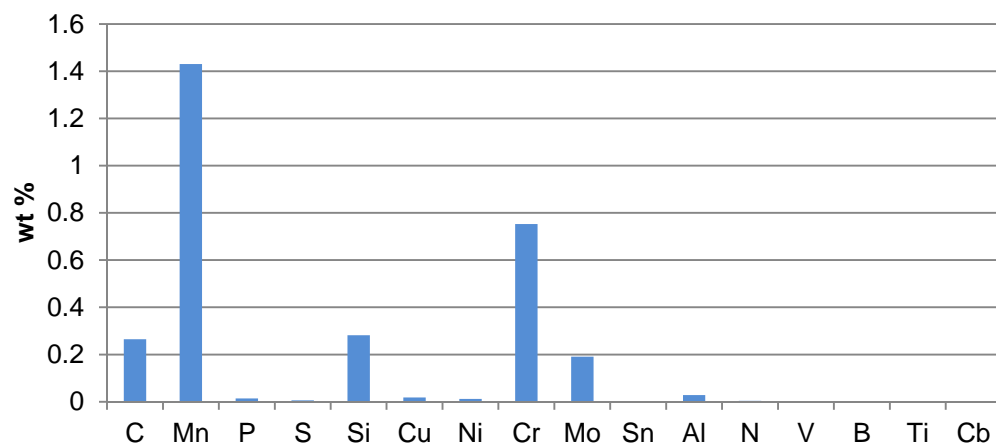


	Al	Cr	Fe	Mn	Ni	P	Si	V	S	Na
Tap + CO <sub>2</sub>	1	1	86	12	2	0	17	0	18	11
Tap + H <sub>2</sub> S	1	0	1	52	1	1	19	0	3440	10
Brine + CO <sub>2</sub>	5	0	143	20	0	1	16	0	246	40,000
Brine + H <sub>2</sub> S	1	0	2	41	0	2	20	0	3800	38,400

# Steel P110



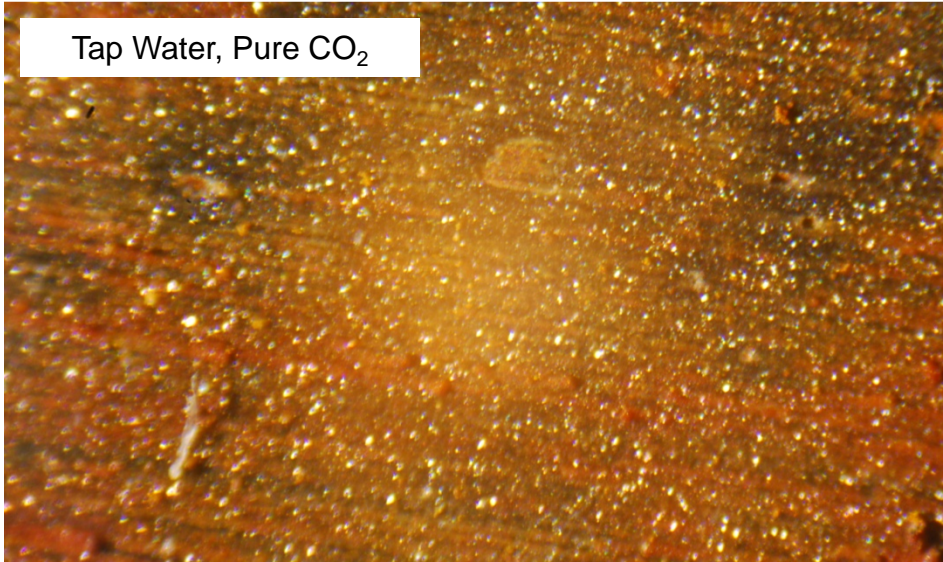
**Original Chemical Composition of P110 Steel  
(Fe is in balance)**



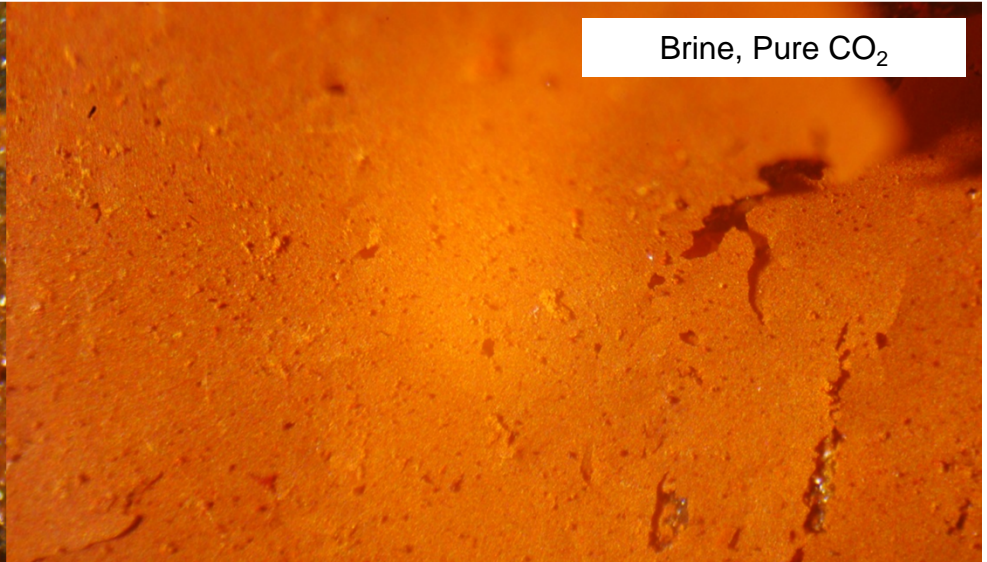


# Steel P110 (x400) after Exposure

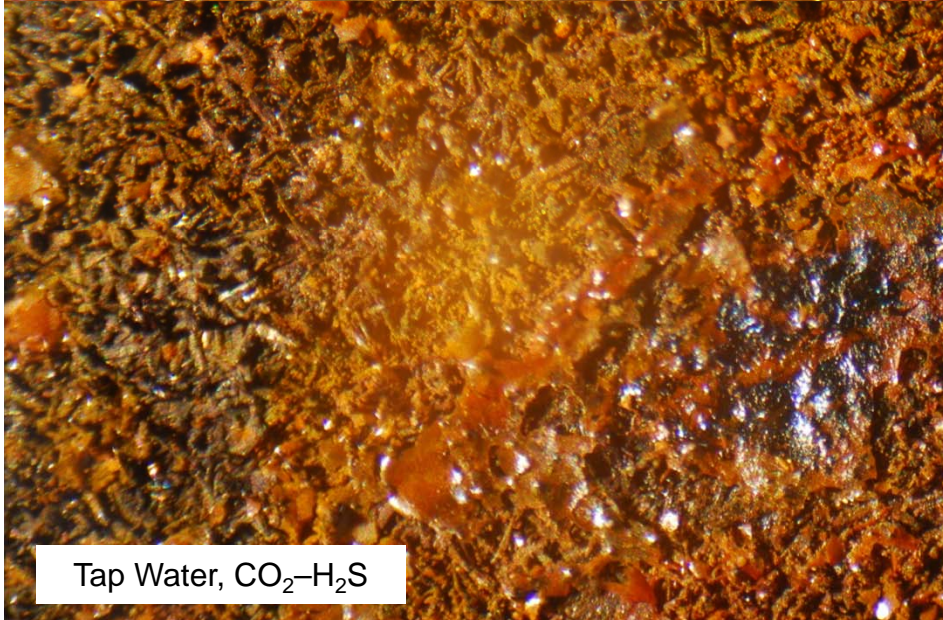
Tap Water, Pure CO<sub>2</sub>



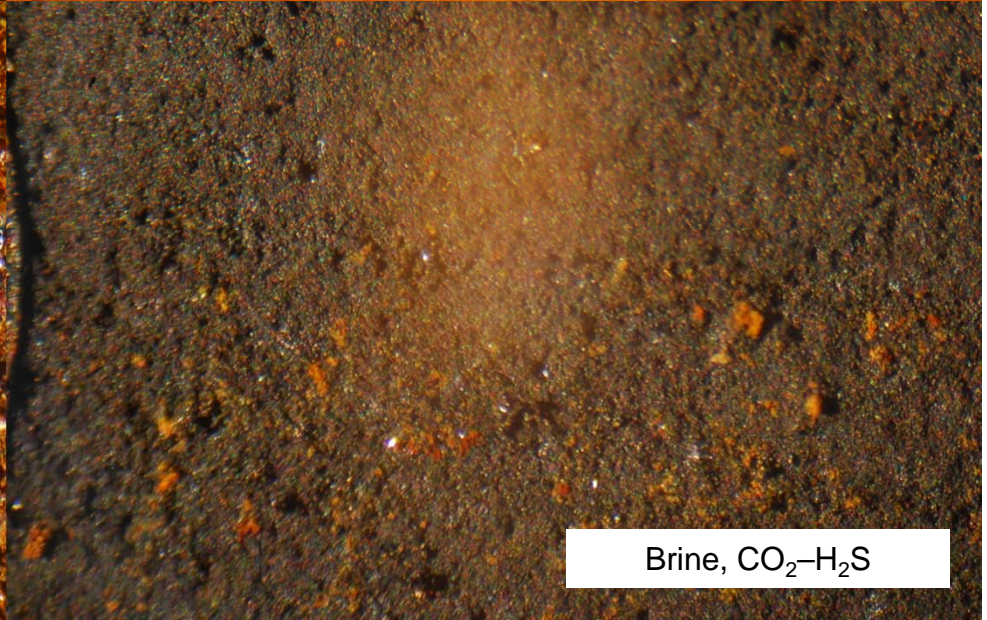
Brine, Pure CO<sub>2</sub>



Tap Water, CO<sub>2</sub>-H<sub>2</sub>S

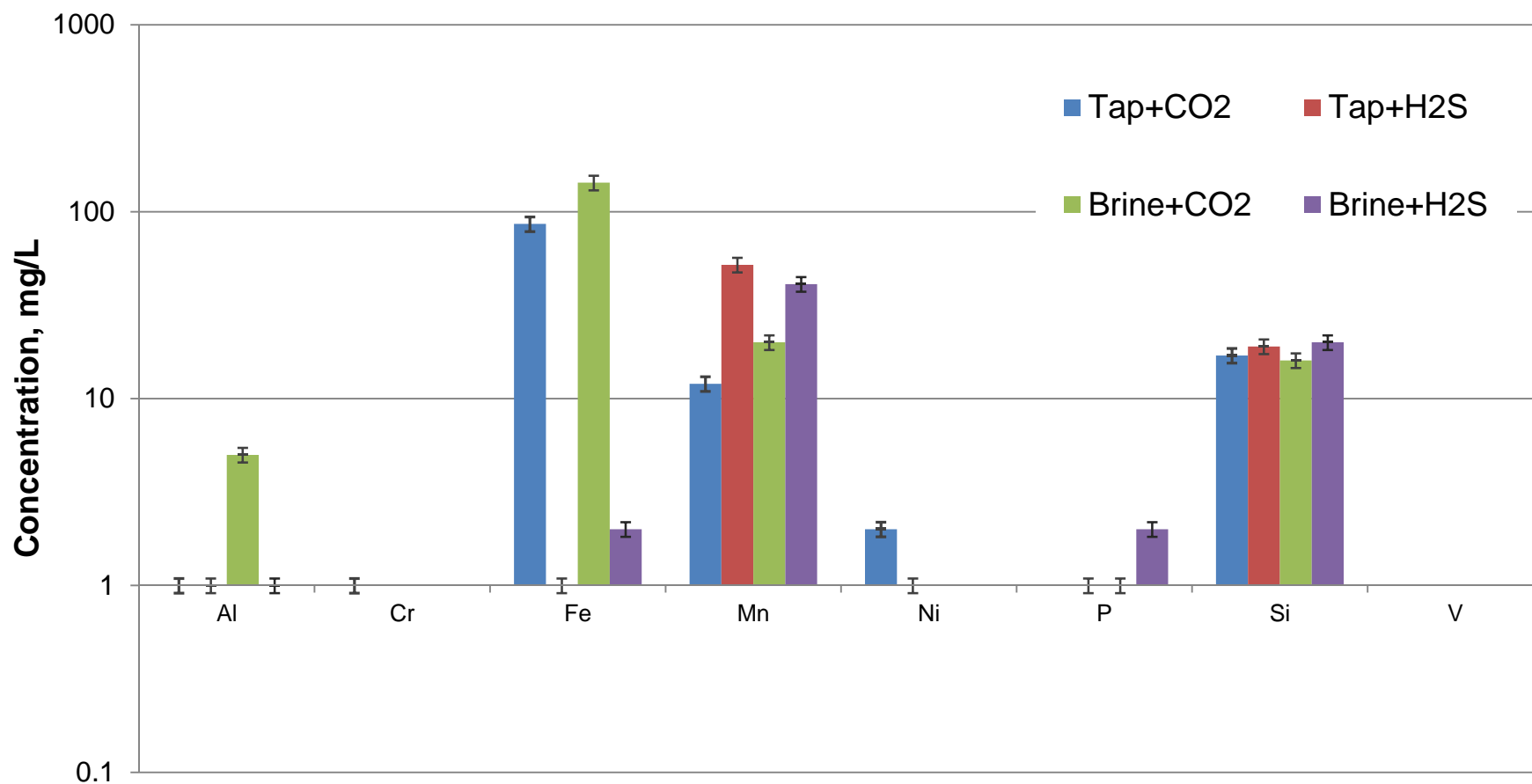


Brine, CO<sub>2</sub>-H<sub>2</sub>S





# P110 Fluid Analysis after Exposure



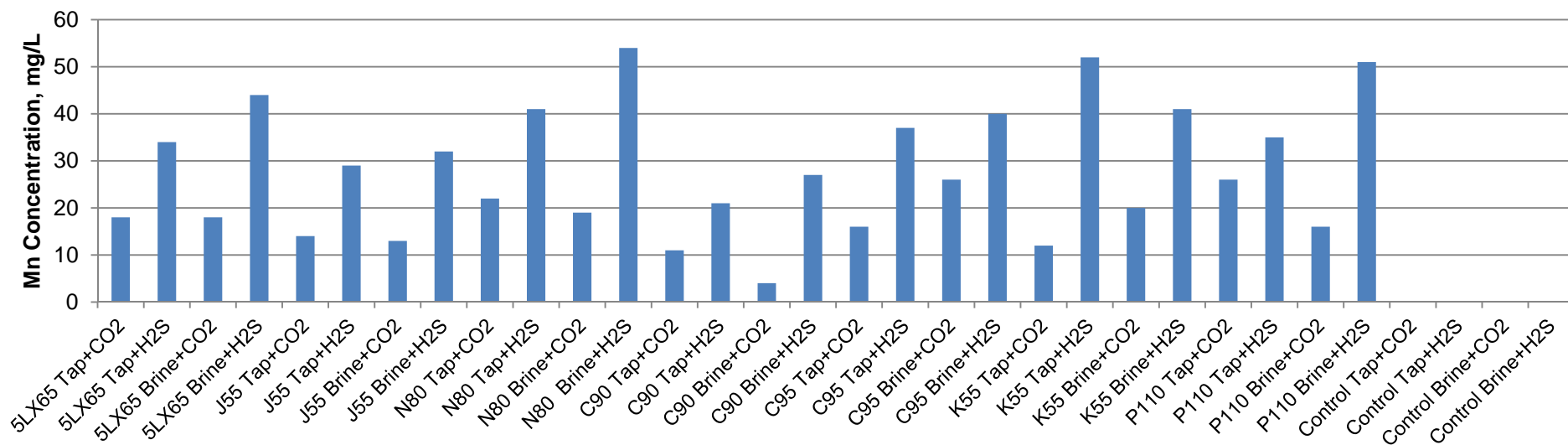
	Al	Cr	Fe	Mn	Ni	P	Si	V	S	Na
Tap + CO <sub>2</sub>	1	1	35	26	1	0	14	0	17	14
Tap + H <sub>2</sub> S	1	0	2	535	1	1	18	0	4720	10
Brine + CO <sub>2</sub>	5	1	155	16	0	1	11	0	210	41,600
Brine + H <sub>2</sub> S	1	0	2	51	0	2	20	0	2980	41,400

	Al	Cr	Fe	Mn	Ni	P	Si	V	S	Na
5LX65 Tap + CO <sub>2</sub>	2	0	21	18	13	0	15	0	668	12
5LX65 Tap + H <sub>2</sub> S	1	24	2	34	0	1	17	0	2310	11
5LX65 Brine + CO <sub>2</sub>	5	0	147	18	4	1	13	0	2960	5200
5LX65 Brine + H <sub>2</sub> S	5	0	2	44	0	2	18	0	2880	4040
J55 Tap + CO <sub>2</sub>	1	0	38	14	1	1	14	0	116	11
J55 Tap + H <sub>2</sub> S	1	0	2	29	17	1	20	0	3730	11
J55 Brine + CO <sub>2</sub>	5	0	114	13	1	1	13	0	896	47,600
J55 Brine + H <sub>2</sub> S	1	0	2	32	0	2	19	0	2720	37,600
N80 Tap + CO <sub>2</sub>	1	0	58	22	1	1	16	0	55	11
N80 Tap + H <sub>2</sub> S	1	0	2	41	1	1	16	0	444	10
N80 Brine + CO <sub>2</sub>	1	0	112	19	0	1	13	0	576	42,000
N80 Brine + H <sub>2</sub> S	1	0	2	54	0	2	19	0	262	44,600
C90 Tap + CO <sub>2</sub>	1	0	68	11	2	1	18	0	33	11
C90 Tap + H <sub>2</sub> S	1	0	1	21	1	1	34	0	5880	16
C90 Brine + CO <sub>2</sub>	5	0	163	4	0	1	13	0	384	40,800
C90 Brine + H <sub>2</sub> S	1	0	3	27	0	2	25	0	2320	42,600
C95 Tap + CO <sub>2</sub>	1	1	52	16	0	0	17	0	19	11
C95 Tap + H <sub>2</sub> S	1	0	2	37	1	1	23	0	6160	16
C95 Brine + CO <sub>2</sub>	5	0	175	26	0	1	13	0	306	44200
C95 Brine + H <sub>2</sub> S	1	0	2	40	0	2	15	0	3120	38,400
K55 Tap + CO <sub>2</sub>	1	1	86	12	2	0	17	0	18	11
K55 Tap + H <sub>2</sub> S	1	0	1	52	1	1	19	0	3440	10
K55 Brine + CO <sub>2</sub>	5	0	143	20	0	1	16	0	246	40,000
K55 Brine + H <sub>2</sub> S	1	0	2	41	0	2	20	0	3800	38,400
P110 Tap + CO <sub>2</sub>	1	1	35	26	1	0	14	0	17	14
P110 Tap + H <sub>2</sub> S	1	0	2	35	1	1	18	0	4720	10
P110 Brine + CO <sub>2</sub>	5	1	155	16	0	1	11	0	210	41,600
P110 Brine + H <sub>2</sub> S	1	0	2	51	0	2	20	0	2980	41,400
Control Tap + CO <sub>2</sub>	1	0	0	0	0	0	13	0	0	9
Control Tap + H <sub>2</sub> S	0	0	0	0	0	0	16	0	6760	16
Control Brine + CO <sub>2</sub>	1	0	1	0	0	0	10	0	180	38,200
Control Brine + H <sub>2</sub> S	1	0	0	0	0	0	10	0	6000	42,000

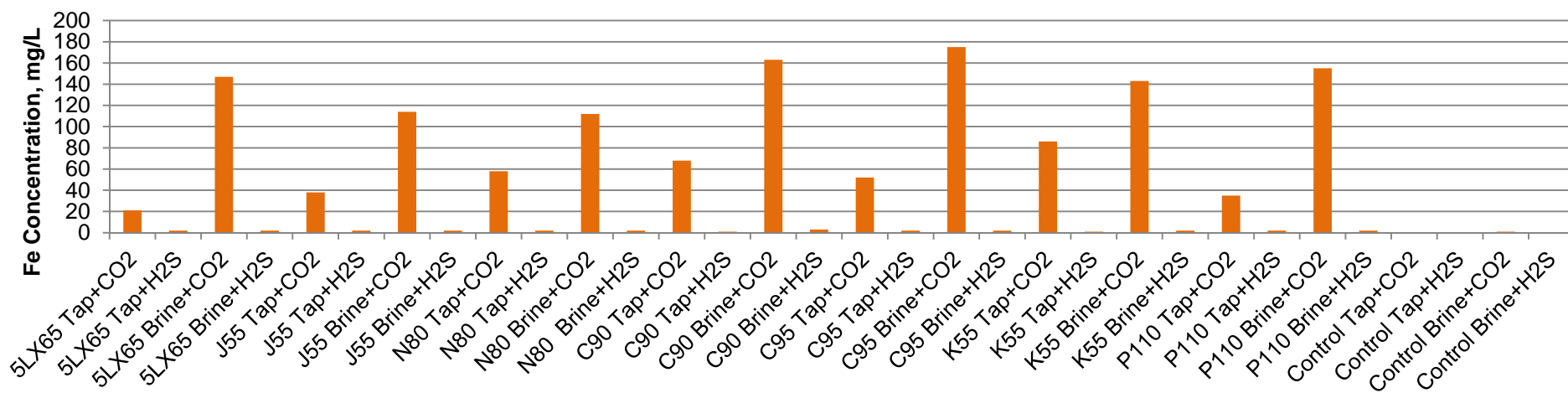


# Elements in Brine after Exposure

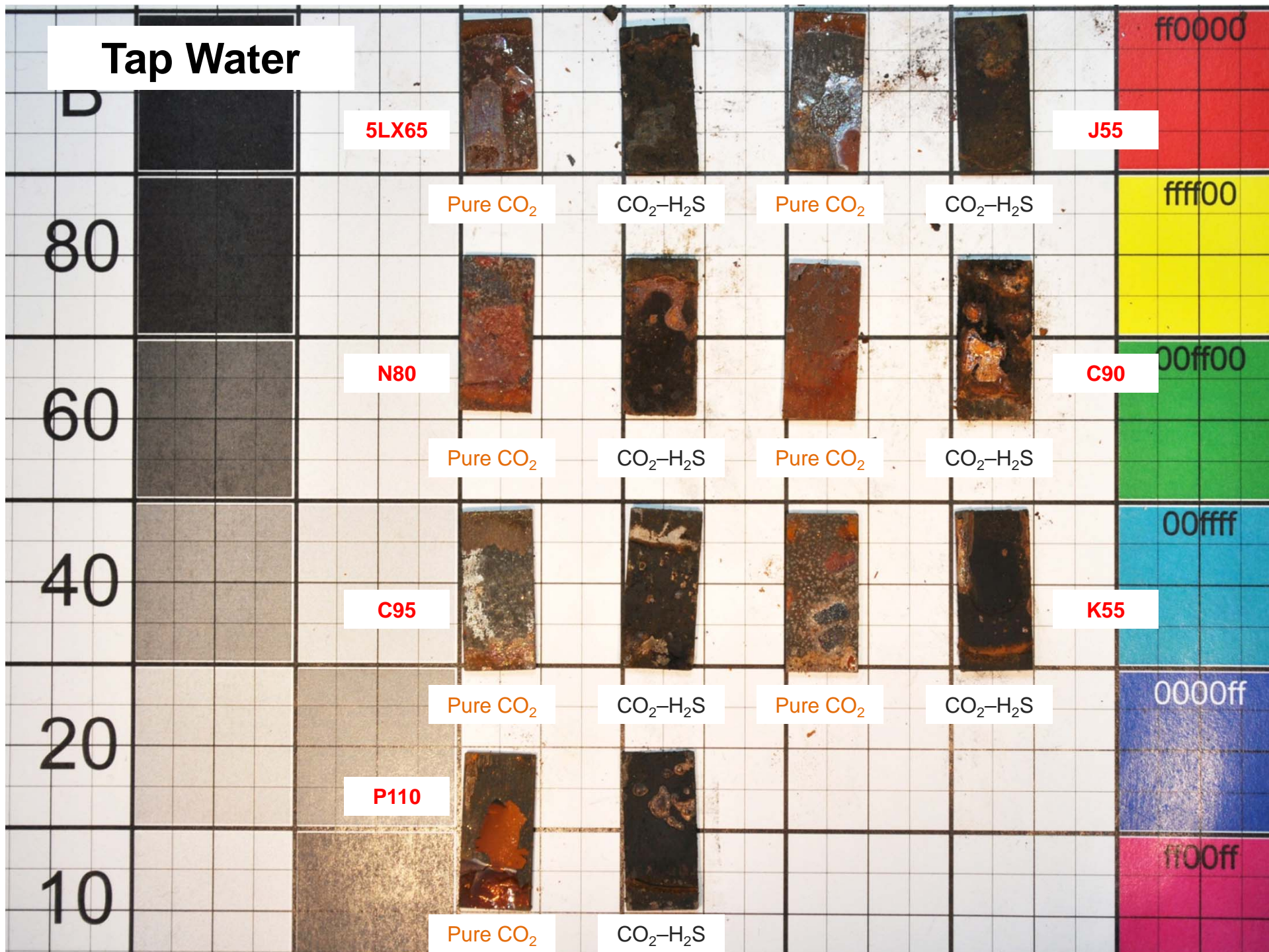
## Mn Concentration



## Fe Concentration



# Tap Water





# Brine

5LX65

J55

ff0000

Pure CO<sub>2</sub>

CO<sub>2</sub>-H<sub>2</sub>S

Pure CO<sub>2</sub>

CO<sub>2</sub>-H<sub>2</sub>S

ffff00

80

N80

C90

00ff00

Pure CO<sub>2</sub>

CO<sub>2</sub>-H<sub>2</sub>S

Pure CO<sub>2</sub>

CO<sub>2</sub>-H<sub>2</sub>S

60

C95

K55

00ffff

Pure CO<sub>2</sub>

CO<sub>2</sub>-H<sub>2</sub>S

Pure CO<sub>2</sub>

CO<sub>2</sub>-H<sub>2</sub>S

40

P110

0000ff

Pure CO<sub>2</sub>

CO<sub>2</sub>-H<sub>2</sub>S

ff00ff

20

10

# ANALYTICAL RESEARCH LAB - Final Results

April 30, 2013

<b>Set Number:</b> 52856	<b>Request Date:</b> Monday, July 11, 2011
<b>Fund#:</b> 15416	<b>Due Date:</b> Monday, July 25, 2011
<b>PI:</b> Steve Smith	<b>Set Description:</b> Zama core plugs saturated with two types of fluids exposed to pure CO2
<b>Contact Person:</b> Blaise Mibeck	

Sample	Parameter	Result
<b>52856-01</b>	<b>A-1 1633-025-01 NaCl brine</b>	
	Aluminum	< 2 mg/L
	Barium	< 0.03 mg/L
	Calcium	363 mg/L
	Iron	< 0.2 mg/L
	Magnesium	9.30 mg/L
	Manganese	< 0.2 mg/L
	Potassium	3 mg/L
	Sodium	66.3 mg/L
	Strontium	1.02 mg/L
	Sulfate	41 mg/L
	Total Dissolved Solids	580 mg/L
<b>52856-02</b>	<b>A-2 1633-025-02 pure water</b>	
	Aluminum	< 10 mg/L
	Barium	< 0.2 mg/L
	Calcium	424 mg/L
	Iron	< 1 mg/L
	Magnesium	10.5 mg/L
	Manganese	< 1 mg/L
	Potassium	< 20 mg/L
	Sodium	63600 mg/L
	Strontium	1.56 mg/L
	Sulfate	86 mg/L
	Total Dissolved Solids	178000 mg/L
<b>52856-03</b>	<b>B-1 1633-025-05 pure water</b>	
	Aluminum	< 2 mg/L
	Barium	< 0.03 mg/L

Distribution \_\_\_\_\_ Date \_\_\_\_\_



# ANALYTICAL RESEARCH LAB - Final Results

April 30, 2013

**Set Number:** 52856

**Request Date:** Monday, July 11, 2011

**Fund#:** 15416

**Due Date:** Monday, July 25, 2011

**PI:** Steve Smith

**Set Description:** Zama core plugs saturated with two types  
of fluids exposed to pure CO2

**Contact Person:** Blaise Mibeck

Sample	Parameter	Result
52856-03	<b>B-1 1633-025-05 pure water</b>	
	Calcium	342 mg/L
	Iron	< 0.2 mg/L
	Magnesium	22.6 mg/L
	Manganese	< 0.2 mg/L
	Potassium	20 mg/L
	Sodium	99.9 mg/L
	Strontium	1.48 mg/L
	Sulfate	155 mg/L
	Total Dissolved Solids	900 mg/L
52856-04	<b>B-2 1633-025-06 NaCl brine</b>	
	Aluminum	< 10 mg/L
	Barium	3.12 mg/L
	Calcium	376 mg/L
	Iron	< 1 mg/L
	Magnesium	21.2 mg/L
	Manganese	< 1 mg/L
	Potassium	< 20 mg/L
	Sodium	64800 mg/L
	Strontium	3.08 mg/L
	Sulfate	183 mg/L
	Total Dissolved Solids	172000 mg/L
52856-05	<b>C-1 1633-025-09 pure water</b>	
	Aluminum	< 2 mg/L
	Barium	0.060 mg/L
	Calcium	516 mg/L
	Iron	< 0.2 mg/L
	Magnesium	15.5 mg/L
	Manganese	< 0.2 mg/L
	Potassium	3.3 mg/L
	Sodium	60.0 mg/L
	Strontium	2.24 mg/L

Distribution \_\_\_\_\_ Date \_\_\_\_\_

# ANALYTICAL RESEARCH LAB - Final Results

April 30, 2013

**Set Number:** 52856

**Request Date:** Monday, July 11, 2011

**Fund#:** 15416

**Due Date:** Monday, July 25, 2011

**PI:** Steve Smith

**Set Description:** Zama core plugs saturated with two types  
of fluids exposed to pure CO2

**Contact Person:** Blaise Mibeck

Sample	Parameter	Result
52856-05	<b>C-1 1633-025-09 pure water</b>	
	Sulfate	80.5 mg/L
	Total Dissolved Solids	800 mg/L
52856-06	<b>C-2 1633-025-10 NaCl brine</b>	
	Aluminum	< 10 mg/L
	Barium	7.36 mg/L
	Calcium	462 mg/L
	Iron	< 1 mg/L
	Magnesium	26.0 mg/L
	Manganese	< 1 mg/L
	Potassium	< 20 mg/L
	Sodium	67600 mg/L
	Strontium	4.68 mg/L
	Sulfate	99 mg/L
	Total Dissolved Solids	176000 mg/L
52856-07	<b>D-1 1633-025-13 pure water</b>	
	Aluminum	< 2 mg/L
	Barium	0.033 mg/L
	Calcium	354 mg/L
	Iron	< 0.2 mg/L
	Magnesium	27.4 mg/L
	Manganese	< 0.2 mg/L
	Potassium	4.1 mg/L
	Sodium	71.4 mg/L
	Strontium	1.85 mg/L
	Sulfate	128 mg/L
52856-08	<b>D-2 1633-025-14 NaCl brine</b>	
	Aluminum	< 10 mg/L
	Barium	< 0.2 mg/L
	Calcium	374 mg/L

Distribution \_\_\_\_\_ Date \_\_\_\_\_

# ANALYTICAL RESEARCH LAB - Final Results

April 30, 2013

**Set Number:** 52856

**Request Date:** Monday, July 11, 2011

**Fund#:** 15416

**Due Date:** Monday, July 25, 2011

**PI:** Steve Smith

**Set Description:** Zama core plugs saturated with two types  
of fluids exposed to pure CO2

**Contact Person:** Blaise Mibeck

Sample	Parameter	Result
52856-08	<b>D-2 1633-025-14 NaCl brine</b>	
	Iron	< 1 mg/L
	Magnesium	14.7 mg/L
	Manganese	< 1 mg/L
	Potassium	< 20 mg/L
	Sodium	62400 mg/L
	Strontium	1.94 mg/L
	Sulfate	138 mg/L
	Total Dissolved Solids	179000 mg/L
52856-09	<b>E-1 1633-025-17 pure water</b>	
	Aluminum	< 2 mg/L
	Barium	0.13 mg/L
	Calcium	312 mg/L
	Iron	< 0.2 mg/L
	Magnesium	16.6 mg/L
	Manganese	< 0.2 mg/L
	Potassium	3.8 mg/L
	Sodium	46.2 mg/L
	Strontium	2.3 mg/L
	Sulfate	59.0 mg/L
	Total Dissolved Solids	540 mg/L
52856-10	<b>E-2 1633-025-18 NaCl brine</b>	
	Aluminum	< 10 mg/L
	Barium	< 0.2 mg/L
	Calcium	360 mg/L
	Iron	< 1 mg/L
	Magnesium	22.8 mg/L
	Manganese	< 1 mg/L
	Potassium	< 20 mg/L
	Sodium	65200 mg/L
	Strontium	2.88 mg/L
	Sulfate	76 mg/L

Distribution \_\_\_\_\_ Date \_\_\_\_\_

# ANALYTICAL RESEARCH LAB - Final Results

April 30, 2013

**Set Number:** 52856

**Request Date:** Monday, July 11, 2011

**Fund#:** 15416

**Due Date:** Monday, July 25, 2011

**PI:** Steve Smith

**Set Description:** Zama core plugs saturated with two types  
of fluids exposed to pure CO2

**Contact Person:** Blaise Mibeck

Sample	Parameter	Result
52856-10	<b>E-2 1633-025-18 NaCl brine</b>	
	Total Dissolved Solids	176000 mg/L
52856-11	<b>F-1 1633-025-21 pure water</b>	
	Aluminum	< 2 mg/L
	Barium	0.063 mg/L
	Calcium	318 mg/L
	Iron	< 0.2 mg/L
	Magnesium	16.6 mg/L
	Manganese	< 0.2 mg/L
	Potassium	< 3 mg/L
	Sodium	29 mg/L
	Strontium	1.64 mg/L
	Sulfate	67.0 mg/L
	Total Dissolved Solids	420 mg/L
52856-12	<b>F-2 1633-025-22 NaCl brine</b>	
	Aluminum	< 10 mg/L
	Barium	9.02 mg/L
	Calcium	376 mg/L
	Iron	< 1 mg/L
	Magnesium	21.0 mg/L
	Manganese	< 1 mg/L
	Potassium	< 20 mg/L
	Sodium	68000 mg/L
	Strontium	2.5 mg/L
	Sulfate	65 mg/L
	Total Dissolved Solids	177000 mg/L
52856-13	<b>G-1 1633-025-25 pure water</b>	
	Aluminum	< 2 mg/L
	Barium	< 0.03 mg/L
	Calcium	717 mg/L
	Iron	< 0.2 mg/L

Distribution \_\_\_\_\_ Date \_\_\_\_\_



# ANALYTICAL RESEARCH LAB - Final Results

April 30, 2013

**Set Number:** 52856

**Request Date:** Monday, July 11, 2011

**Fund#:** 15416

**Due Date:** Monday, July 25, 2011

**PI:** Steve Smith

**Set Description:** Zama core plugs saturated with two types  
of fluids exposed to pure CO2

**Contact Person:** Blaise Mibeck

Sample	Parameter	Result
52856-13	<b>G-1 1633-025-25 pure water</b>	
	Magnesium	89.7 mg/L
	Manganese	< 0.2 mg/L
	Potassium	79.8 mg/L
	Sodium	85.8 mg/L
	Strontium	8.58 mg/L
	Sulfate	1560 mg/L
	Total Dissolved Solids	3500 mg/L
52856-14	<b>G-2 1633-025-26 NaCl brine</b>	
	Aluminum	< 10 mg/L
	Barium	< 0.2 mg/L
	Calcium	546 mg/L
	Iron	< 1 mg/L
	Magnesium	72.2 mg/L
	Manganese	< 1 mg/L
	Potassium	83 mg/L
	Sodium	64000 mg/L
	Strontium	9.66 mg/L
	Sulfate	929 mg/L
	Total Dissolved Solids	176000 mg/L
52856-15	<b>H-1 brine standard</b>	
	Aluminum	< 2 mg/L
	Barium	< 0.03 mg/L
	Calcium	2.93 mg/L
	Iron	0.24 mg/L
	Magnesium	< 0.09 mg/L
	Manganese	< 0.2 mg/L
	Potassium	< 3 mg/L
	Sodium	27 mg/L
	Strontium	< 0.006 mg/L
	Sulfate	25 mg/L
	Total Dissolved Solids	120 mg/L

Distribution \_\_\_\_\_ Date \_\_\_\_\_

# ANALYTICAL RESEARCH LAB - Final Results

April 30, 2013

**Set Number:** 52856

**Request Date:** Monday, July 11, 2011

**Fund#:** 15416

**Due Date:** Monday, July 25, 2011

**PI:** Steve Smith

**Set Description:** Zama core plugs saturated with two types  
of fluids exposed to pure CO2

**Contact Person:** Blaise Mibeck

Sample	Parameter	Result
52856-15	H-1 brine standard	
52856-16	H-2 water standard	
	Aluminum	< 10 mg/L
	Barium	< 0.2 mg/L
	Calcium	14 mg/L
	Iron	< 1 mg/L
	Magnesium	< 0.6 mg/L
	Manganese	< 1 mg/L
	Potassium	< 20 mg/L
	Sodium	66800 mg/L
	Strontium	< 0.04 mg/L
	Sulfate	30 mg/L
	Total Dissolved Solids	178000 mg/L

Distribution \_\_\_\_\_ Date \_\_\_\_\_

# ANALYTICAL RESEARCH LAB - Final Results

April 30, 2013

**Set Number:** 52857      **Request Date:** Monday, July 11, 2011  
**Fund#:** 15416      **Due Date:** Monday, July 25, 2011  
**PI:** Steve Smith      **Set Description:** Zama core plugs saturated with two types  
 of fluids exposed to CO<sub>2</sub> and H<sub>2</sub>S  
**Contact Person:** Blaise Mibeck

Sample	Parameter	Result
<b>52857-01</b>	<b>A-3 1663-025-03 NaCl brine</b>	
	Aluminum	< 2 mg/L
	Barium	0.069 mg/L
	Calcium	203 mg/L
	Iron	< 0.2 mg/L
	Magnesium	17.2 mg/L
	Manganese	< 0.2 mg/L
	Potassium	< 3 mg/L
	Sodium	66.9 mg/L
	Strontium	1.15 mg/L
	Sulfate	20 mg/L
	Total Dissolved Solids	880 mg/L
<b>52857-02</b>	<b>A-4 1663-025-04 pure water</b>	
	Aluminum	< 10 mg/L
	Barium	0.74 mg/L
	Calcium	314 mg/L
	Iron	< 1 mg/L
	Magnesium	9.64 mg/L
	Manganese	1.3 mg/L
	Potassium	< 20 mg/L
	Sodium	58800 mg/L
	Strontium	1.8 mg/L
	Sulfate	35 mg/L
	Total Dissolved Solids	166000 mg/L
<b>52857-03</b>	<b>B-3 1663-025-07 pure water</b>	
	Aluminum	< 2 mg/L
	Barium	0.078 mg/L

Distribution \_\_\_\_\_ Date \_\_\_\_\_

# ANALYTICAL RESEARCH LAB - Final Results

April 30, 2013

**Set Number:** 52857

**Request Date:** Monday, July 11, 2011

**Fund#:** 15416

**Due Date:** Monday, July 25, 2011

**PI:** Steve Smith

**Set Description:** Zama core plugs saturated with two types  
of fluids exposed to CO2 and H2S

**Contact Person:** Blaise Mibeck

Sample	Parameter	Result
<b>52857-03 B-3 1663-025-07 pure water</b>		
	Calcium	378 mg/L
	Iron	< 0.2 mg/L
	Magnesium	37.5 mg/L
	Manganese	< 0.2 mg/L
	Potassium	7.5 mg/L
	Sodium	27 mg/L
	Strontium	1.65 mg/L
	Sulfate	57.5 mg/L
	Total Dissolved Solids	920 mg/L
<b>52857-04 B-4 1663-025-08 NaCl brine</b>		
	Aluminum	< 10 mg/L
	Barium	0.36 mg/L
	Calcium	264 mg/L
	Iron	< 1 mg/L
	Magnesium	29.0 mg/L
	Manganese	< 1 mg/L
	Potassium	22 mg/L
	Sodium	59600 mg/L
	Strontium	2.28 mg/L
	Sulfate	110 mg/L
	Total Dissolved Solids	163000 mg/L
<b>52857-05 C-3 1663-025-11 pure water</b>		
	Aluminum	< 2 mg/L
	Barium	0.32 mg/L
	Calcium	297 mg/L
	Iron	< 0.2 mg/L
	Magnesium	17.5 mg/L
	Manganese	< 0.2 mg/L
	Potassium	< 3 mg/L
	Sodium	17 mg/L
	Strontium	1.89 mg/L

Distribution \_\_\_\_\_ Date \_\_\_\_\_



# ANALYTICAL RESEARCH LAB - Final Results

April 30, 2013

**Set Number:** 52857

**Request Date:** Monday, July 11, 2011

**Fund#:** 15416

**Due Date:** Monday, July 25, 2011

**PI:** Steve Smith

**Set Description:** Zama core plugs saturated with two types  
of fluids exposed to CO<sub>2</sub> and H<sub>2</sub>S

**Contact Person:** Blaise Mibeck

Sample	Parameter	Result
52857-05	<b>C-3 1663-025-11 pure water</b>	
	Sulfate	28 mg/L
	Total Dissolved Solids	900 mg/L
52857-06	<b>C-4 1663-025-12 NaCl brine</b>	
	Aluminum	< 10 mg/L
	Barium	< 0.2 mg/L
	Calcium	172 mg/L
	Iron	< 1 mg/L
	Magnesium	25.4 mg/L
	Manganese	< 1 mg/L
	Potassium	< 20 mg/L
	Sodium	56400 mg/L
	Strontium	3.3 mg/L
	Sulfate	67 mg/L
	Total Dissolved Solids	170000 mg/L
52857-07	<b>D-3 1663-025-15 pure water</b>	
	Aluminum	< 2 mg/L
	Barium	0.066 mg/L
	Calcium	282 mg/L
	Iron	< 0.2 mg/L
	Magnesium	21.6 mg/L
	Manganese	< 0.2 mg/L
	Potassium	< 3 mg/L
	Sodium	17 mg/L
	Strontium	1.49 mg/L
	Sulfate	39 mg/L
	Total Dissolved Solids	640 mg/L
52857-08	<b>D-4 1663-025-16 NaCl brine</b>	
	Aluminum	< 10 mg/L
	Barium	< 0.2 mg/L
	Calcium	181 mg/L

Distribution \_\_\_\_\_ Date \_\_\_\_\_

# ANALYTICAL RESEARCH LAB - Final Results

April 30, 2013

**Set Number:** 52857

**Request Date:** Monday, July 11, 2011

**Fund#:** 15416

**Due Date:** Monday, July 25, 2011

**PI:** Steve Smith

**Set Description:** Zama core plugs saturated with two types  
of fluids exposed to CO2 and H2S

**Contact Person:** Blaise Mibeck

Sample	Parameter	Result
52857-08	<b>D-4 1663-025-16 NaCl brine</b>	
	Iron	< 1 mg/L
	Magnesium	17.2 mg/L
	Manganese	< 1 mg/L
	Potassium	< 20 mg/L
	Sodium	70000 mg/L
	Strontium	1.64 mg/L
	Sulfate	30 mg/L
	Total Dissolved Solids	170000 mg/L
52857-09	<b>E-3 1663-025-19 pure water</b>	
	Aluminum	< 2 mg/L
	Barium	0.099 mg/L
	Calcium	321 mg/L
	Iron	< 0.2 mg/L
	Magnesium	21.2 mg/L
	Manganese	< 0.2 mg/L
	Potassium	< 3 mg/L
	Sodium	16 mg/L
	Strontium	2.35 mg/L
	Sulfate	37 mg/L
	Total Dissolved Solids	980 mg/L
52857-10	<b>E-4 1663-025-20 NaCl brine</b>	
	Aluminum	< 10 mg/L
	Barium	0.54 mg/L
	Calcium	94.4 mg/L
	Iron	< 1 mg/L
	Magnesium	26.8 mg/L
	Manganese	8.0 mg/L
	Potassium	< 20 mg/L
	Sodium	71200 mg/L
	Strontium	3.80 mg/L
	Sulfate	58 mg/L

Distribution \_\_\_\_\_ Date \_\_\_\_\_

# ANALYTICAL RESEARCH LAB - Final Results

April 30, 2013

**Set Number:** 52857

**Request Date:** Monday, July 11, 2011

**Fund#:** 15416

**Due Date:** Monday, July 25, 2011

**PI:** Steve Smith

**Set Description:** Zama core plugs saturated with two types  
of fluids exposed to CO<sub>2</sub> and H<sub>2</sub>S

**Contact Person:** Blaise Mibeck

Sample	Parameter	Result
<b>52857-10</b>	<b>E-4 1663-025-20 NaCl brine</b>	
	Total Dissolved Solids	171000 mg/L
<b>52857-11</b>	<b>F-3 1663-025-23 pure water</b>	
	Aluminum	< 2 mg/L
	Barium	0.723 mg/L
	Calcium	266 mg/L
	Iron	< 0.2 mg/L
	Magnesium	23.1 mg/L
	Manganese	< 0.2 mg/L
	Potassium	< 3 mg/L
	Sodium	10 mg/L
	Strontium	1.60 mg/L
	Sulfate	21 mg/L
	Total Dissolved Solids	560 mg/L
<b>52857-12</b>	<b>F-4 1663-025-24 NaCl brine</b>	
	Aluminum	< 10 mg/L
	Barium	< 0.2 mg/L
	Calcium	181 mg/L
	Iron	< 1 mg/L
	Magnesium	22.4 mg/L
	Manganese	< 1 mg/L
	Potassium	< 20 mg/L
	Sodium	69200 mg/L
	Strontium	2.24 mg/L
	Sulfate	42 mg/L
	Total Dissolved Solids	171000 mg/L
<b>52857-13</b>	<b>G-3 1663-025-27 pure water</b>	
	Aluminum	< 2 mg/L
	Barium	0.060 mg/L
	Calcium	345 mg/L
	Iron	< 0.2 mg/L

Distribution \_\_\_\_\_ Date \_\_\_\_\_

# ANALYTICAL RESEARCH LAB - Final Results

April 30, 2013

**Set Number:** 52857

**Request Date:** Monday, July 11, 2011

**Fund#:** 15416

**Due Date:** Monday, July 25, 2011

**PI:** Steve Smith

**Set Description:** Zama core plugs saturated with two types  
of fluids exposed to CO2 and H2S

**Contact Person:** Blaise Mibeck

Sample	Parameter	Result
52857-13	<b>G-3 1663-025-27 pure water</b>	
	Magnesium	74.4 mg/L
	Manganese	< 0.2 mg/L
	Potassium	60.6 mg/L
	Sodium	37.5 mg/L
	Strontium	7.65 mg/L
	Sulfate	267 mg/L
	Total Dissolved Solids	2360 mg/L
52857-14	<b>G-4 1663-025-28 NaCl brine</b>	
	Aluminum	< 10 mg/L
	Barium	0.2 mg/L
	Calcium	280 mg/L
	Iron	< 1 mg/L
	Magnesium	50.0 mg/L
	Manganese	< 1 mg/L
	Potassium	63 mg/L
	Sodium	62400 mg/L
	Strontium	7.28 mg/L
	Sulfate	362 mg/L
	Total Dissolved Solids	168000 mg/L
52857-15	<b>H-3 brine standard</b>	
	Aluminum	< 2 mg/L
	Barium	< 0.03 mg/L
	Calcium	1.7 mg/L
	Iron	< 0.2 mg/L
	Magnesium	< 0.09 mg/L
	Manganese	< 0.2 mg/L
	Potassium	< 3 mg/L
	Sodium	6.0 mg/L
	Strontium	< 0.006 mg/L
	Sulfate	19 mg/L
	Total Dissolved Solids	< 10 mg/L

Distribution \_\_\_\_\_ Date \_\_\_\_\_



# ANALYTICAL RESEARCH LAB - Final Results

April 30, 2013

**Set Number:** 52857

**Request Date:** Monday, July 11, 2011

**Fund#:** 15416

**Due Date:** Monday, July 25, 2011

**PI:** Steve Smith

**Set Description:** Zama core plugs saturated with two types  
of fluids exposed to CO<sub>2</sub> and H<sub>2</sub>S

**Contact Person:** Blaise Mibeck

Sample	Parameter	Result
52857-15	H-3 brine standard	
52857-16	H-4 water standard	
	Aluminum	< 10 mg/L
	Barium	< 0.2 mg/L
	Calcium	< 2 mg/L
	Iron	< 1 mg/L
	Magnesium	< 0.6 mg/L
	Manganese	< 1 mg/L
	Potassium	< 20 mg/L
	Sodium	65600 mg/L
	Strontium	< 0.04 mg/L
	Sulfate	30 mg/L
	Total Dissolved Solids	169000 mg/L

Distribution \_\_\_\_\_ Date \_\_\_\_\_